



ADVANCING PD-CATALYZED STEREOSELECTIVE ALLYLIC SUBSTITUTION REACTIONS

Jianing Xie

ADVERTIMENT. L'accés als continguts d'aquesta tesi doctoral i la seva utilització ha de respectar els drets de la persona autora. Pot ser utilitzada per a consulta o estudi personal, així com en activitats o materials d'investigació i docència en els termes establerts a l'art. 32 del Text Refós de la Llei de Propietat Intel·lectual (RDL 1/1996). Per altres utilitzacions es requereix l'autorització prèvia i expressa de la persona autora. En qualsevol cas, en la utilització dels seus continguts caldrà indicar de forma clara el nom i cognoms de la persona autora i el títol de la tesi doctoral. No s'autoritza la seva reproducció o altres formes d'explotació efectuades amb finalitats de lucre ni la seva comunicació pública des d'un lloc aliè al servei TDX. Tampoc s'autoritza la presentació del seu contingut en una finestra o marc aliè a TDX (framing). Aquesta reserva de drets afecta tant als continguts de la tesi com als seus resums i índexs.

ADVERTENCIA. El acceso a los contenidos de esta tesis doctoral y su utilización debe respetar los derechos de la persona autora. Puede ser utilizada para consulta o estudio personal, así como en actividades o materiales de investigación y docencia en los términos establecidos en el art. 32 del Texto Refundido de la Ley de Propiedad Intelectual (RDL 1/1996). Para otros usos se requiere la autorización previa y expresa de la persona autora. En cualquier caso, en la utilización de sus contenidos se deberá indicar de forma clara el nombre y apellidos de la persona autora y el título de la tesis doctoral. No se autoriza su reproducción u otras formas de explotación efectuadas con fines lucrativos ni su comunicación pública desde un sitio ajeno al servicio TDR. Tampoco se autoriza la presentación de su contenido en una ventana o marco ajeno a TDR (framing). Esta reserva de derechos afecta tanto al contenido de la tesis como a sus resúmenes e índices.

WARNING. Access to the contents of this doctoral thesis and its use must respect the rights of the author. It can be used for reference or private study, as well as research and learning activities or materials in the terms established by the 32nd article of the Spanish Consolidated Copyright Act (RDL 1/1996). Express and previous authorization of the author is required for any other uses. In any case, when using its content, full name of the author and title of the thesis must be clearly indicated. Reproduction or other forms of for profit use or public communication from outside TDX service is not allowed. Presentation of its content in a window or frame external to TDX (framing) is not authorized either. These rights affect both the content of the thesis and its abstracts and indexes.



UNIVERSITAT
ROVIRA i VIRGILI

Advancing Pd-catalyzed Stereoselective Allylic Substitution Reactions

Jianing Xie



DOCTORAL THESIS
2020

DOCTORAL THESIS

Advancing Pd-catalyzed Stereoselective Allylic Substitution Reactions

Jianing Xie

Supervised by:

Prof. Dr. Arjan W. Kleij

ICIQ-URV



UNIVERSITAT
ROVIRA I VIRGILI

Tarragona

2020



UNIVERSITAT
ROVIRA I VIRGILI

Av. Països Catalans 16
43007 Tarragona
Tel: +34-977920847
E-mail: akleij@iciq.es

Prof. Dr. Arjan W. Kleij, Group Leader at the Institute of Chemical Research of Catalonia (ICIQ) and Research Professor of the Catalan Institution for Research and Advanced Studies (ICREA):

I hereby state that the present study, entitled “*Advancing Pd-catalyzed Stereoselective Allylic Substitution Reactions*”, presented by Jianing Xie for the award of the degree of Doctor, has been carried out under my supervision at the Institute of Chemical Research of Catalonia (ICIQ).

Tarragona, October 2020

Doctoral Thesis Supervisor

Prof. Dr. Arjan W. Kleij

List of publications

At the submission of this thesis, the following publications have been communicated:

1. “*Pd-catalyzed Stereoselective Tandem Ring-opening Amination/cyclization of Vinyl γ -lactones: Access to Caprolactam Diversity*”
J. Xie, X. Li, A. W. Kleij, *Chem. Sci.* **2020**, *11*, 8839-8845.
2. “*Pd-Catalyzed Stereodivergent Allylic Amination of α -Tertiary Allylic Alcohols towards α,β -Unsaturated γ -Amino Acids*”
J. Xie, C. Qiao, M. Martínez Belmonte, E. C. Escudero-Adán, A. W. Kleij, *ChemSusChem* **2019**, *12*, 3152-3158.
3. “*Domino Synthesis of α,β -Unsaturated γ -Lactams via Stereoselective Amination of α -Tertiary Allylic Alcohols*”
J. Xie, S. Xue, E. C. Escudero-Adán, A. W. Kleij, *Angew. Chem. Int. Ed.* **2018**, *57*, 16727-16731.
4. “*Catalytic Transformations of Functionalized Cyclic Organic Carbonates*”
W. Guo, J. E. Gómez, À. Cristòfol, **J. Xie**, A. W. Kleij, *Angew. Chem. Int. Ed.* **2018**, *57*, 13735-13747. (Review article)
5. “*Pd-Catalyzed Enantio- and Regioselective Formation of Allylic Aryl Ethers*”
J. Xie, W. Guo, A. Cai, E. C. Escudero-Adán, A. W. Kleij, *Org. Lett.* **2017**, *19*, 6388-6391.

The following article does not form part of the current thesis:

6. “*Asymmetric Synthesis of α,α -Disubstituted Allylic Amines through Palladium-Catalyzed Allylic Substitution*”
W. Guo, A. Cai, **J. Xie**, A. W. Kleij, *Angew. Chem. Int. Ed.* **2017**, *56*, 11797-11801.

Previous contributions from the PhD candidate:

7. “*One-pot Stepwise Synthesis of Cyclic Carbonates by Oxidative Carboxylation of Olefins with CO_2* ”
J. Xie, Z.-F. Diao, C. Qiao, R. Ma, L.-N. He, *J. CO₂ Util.* **2016**, *16*, 313-317.
8. “*Copper(I)/phosphine-catalyzed Tandem Carboxylation/Annulation of Terminal Alkynes under Ambient Pressure of CO_2 : One-pot access to 3a-*

hydroxyisoxazolo[3,2a]isoindol-8(3aH)-ones

J. Xie, B. Yu, C.-X. Guo, L.-N. He, *Green Chem.* **2015**, *17*, 4061-4067.

9. “*Copper(I)-catalyzed Carboxylation of Terminal Alkynes with CO₂ at Atmospheric Pressure*”

B. Yu, **J. Xie**, C.-L. Zhong, W. Li, L.-N. He, *ACS Catal.* **2015**, *5*, 3940-3944.

10. “*Copper(I)-based Ionic Liquid-catalyzed Carboxylation of Terminal Alkynes with CO₂ at Atmospheric Pressure*”

J. Xie, B. Yu, Z.-H. Zhou, H.-C. Fu, N. Wang, L.-N. He, *Tetrahedron Lett.* **2015**, *56*, 7059-7062.

11. “*Silver Tungstate: a Single-component Bifunctional Catalyst for Carboxylation of Terminal Alkynes with CO₂ in Ambient Conditions*”

C.-X. Guo, B. Yu, **J. Xie**, L.-N. He, *Green Chem.* **2015**, *17*, 474-479.

Curriculum Vitae

Jianing Xie was born on the 31th of July in 1989 in Hebei province, China. He started studying chemistry at Qingdao University of Science and Technology and obtained his BSc degree in July 2012. Then he moved to Nankai University in Tianjin, where he received his MSc degree in 2016 with a major in organic chemistry under the supervision of Prof. Liang-Nian He. During the MSc, his research was mainly focused on carboxylation of terminal alkynes and (cyclic) carbonate synthesis based on the catalytic transformation of CO₂. Hereafter, supported by Prof. Arjan W. Kleij, he successfully applied for a predoctoral fellowship awarded by the Chinese Scholarship Council (CSC). From December 2016 until October 2020 he carried out the work described in this thesis in the group of Prof. Dr. Arjan W. Kleij at the Institute of Chemical Research of Catalonia (ICIQ). His PhD research focus was on stereo/enantioselective Pd-catalyzed C–N/C–O bond formations applied to novel domino processes leading to heterocyclic products. Part of this PhD research was communicated as a poster or oral presentation at the German-Spanish Symposium and ICIQ-Summer School in Tarragona (2017), at the XXVII Reunión Bienal de Química Orgánica in Santiago (2018), at the ICIQ-INTECAT School in Costa Dorada-Tarragona (2018), and at the 2nd Trans Pyrenean Meeting in Catalysis (TrapCat2) in Tarragona (2018).

Acknowledgements

Time has passed quickly since I arrived at Tarragona for the first time in December of 2016. This is a very special moment for me to look back and think over my experiences from the past four years. There is no doubt that I could not have achieved such a doctoral thesis without the support and participation of other people.

First and foremost, I would like to express my sincerest gratitude to my supervisor, Professor **Arjan W. Kleij**, for allowing me to conduct this research under his supervision. I am especially grateful for his constant confidence, guidance and the freedom he gave me in at all stages to accomplish this work. In our daily communication, his words can always trigger our independent and critical thinking and deliver valuable knowledge and experience to us. He has often pointed out the incompleteness of my projects and helped me to improve my understanding of each challenge. The incalculable things that I have learned from Arjan, undoubtedly, will be always be a guide to me for the near and distant future.

I would also like to thank **Ingrid** for all the administrative support and ordering chemicals, which allowed me to focus on my research more efficiently. I will never forget that you offered me my first cup of coffee here at the cafeteria of the URV.

Many thanks also to all the former and present members of the Kleij group with whom I had the pleasure to spend all these years: **Nicole, Claudia, Sara, Christian, Antonella, Michela, Mariachiara (Mery), Leticia, Victor, Jeroen, Sergio, Cristina, Kun, Alèria, Nicola, Alba, Pè, Jixiang** and **Debasish**; it has been a pleasure to work around you guys, thanks for the deep conversations and the advice you have given to me. I'll never forget the many wonderful dinners and fun activities we've had together. I would particularly like to thank **Wusheng**, it was an extraordinary experience to work with you. Thanks for passing on your knowledge. During the year we worked together, I benefited a lot from your many insightful suggestions and our discussions, and I also miss the table tennis time we had. **Rui**, it was a pleasant time to share the apartment with you in the first months after I arrived here. Thanks for facilitating me to start a new life in Tarragona. Thank you for your inspiration in chemistry through sharing your research experience with me. **Aijie**, I cannot forget the first reaction I set up here with your help, thank you for sharing a fume hood with me, supporting me to adapt to the lab work and starting my own project. It was a real pleasure to collaborate with you in two projects, which inspired me a lot. I will not

forget the time we spent together in Spain and wish you all the best with your postdoctoral research work in the US. **Kike**, thanks for sharing many of your interesting ideas and giving me constructive advice. I really enjoyed talking chemistry with you. And also, thanks for your kind help looking for an apartment and helping me out with Spanish phone calls. **Àlex**, being among the first-moment colleagues, thank you for helping me solving language issues so many times and I wish you all best with your research and thesis. **Francesco**, thanks for sharing me your experience when applying for a postdoc position, it was and is very valuable to me. Also, thanks for teaching me to patiently set up polymerization reactions, which was of great value to me. **Bart**, you are wise, multi-skilled and full of humor. Your passion in life always inspires me, and I am glad to have had you around.

I am also profoundly grateful for the hard work of my co-authors and their substantial contribution to uplift the studies presented in this thesis. **Sijing**, you are always pleasant and positive, which is contagious. Thanks for sharing your chemistry knowledge with me. **Chang**, you are very thoughtful and considerate of others. I am glad to have been able to work with you again after working with you at Professor He' group during my master studies. **Xuetong**, thanks for joining my last project at the end of my thesis period which enabled me to complete my PhD research in time. Lovely girls, best wishes for your personal life and PhD work.

I would also like to thank many colleagues at ICIQ, especially the ICIQ Research Support team for their help during my PhD period. Without this support, it would have been much harder for me to complete my PhD assignment.

I would like to express my gratitude for the financial support from the CSC (China Scholarship Council), as well as the meticulous work of the education group in Spain.

Last, but not least, I would like to express my deepest gratitude to my family for all their love and encouragement. For my parents who raised me with full support and their trust in me regarding all my pursuits. Especially, my wife **Yandi** has been extremely supportive of me throughout the entire process. Because of your company, my life is filled with sunshine and happiness, allowing me to actively face the challenges every day. Without your inspiration, thoughtfulness and sacrifice, undoubtedly, I could not have reached what I intended to strive for. I look forward to our future with full confidence.

Jianing Xie, 2020

Table of Contents

List of abbreviations	1
Chapter 1. General Introduction	3
1.1 Selectivity in Organic Synthesis	5
1.2 Pd-catalyzed Allylic Substitution Reactions	5
1.2.1 General Aspects	5
1.2.2 Catalytic Cycle	7
1.2.3 π - σ - π Isomerization	8
1.2.4 Regioselectivity	9
1.2.5 Allylic Precursors with Different Leaving Group	10
1.3 Thesis Aim and Scope	17
Chapter 2. Pd-Catalyzed Enantio- and Regioselective Formation of Allylic Aryl Ethers	19
2.1 Introduction	21
2.1.1 Chiral Tertiary Aryl Ethers	21
2.1.2 TM-catalyzed Asymmetric Synthesis of Secondary Allylic Aryl Ethers ..	23
2.1.3 Pd-catalyzed Asymmetric Synthesis of Tertiary Allylic Aryl Ethers	29
2.1.4 Aim of the Work presented in this Chapter	31
2.2 Results and Discussion	33
2.2.1 Screening Studies	33
2.2.2 Scope of Substrates	36
2.2.3 Z-Stereoselective Formation of the Linear Allylic Aryl Ethers	39
2.3 Conclusions	41
2.4 Experimental Section	42
2.4.1 General Considerations	42
2.4.2 General Procedure for the Synthesis of VCCs	42
2.4.3 Typical Procedure for the Formation of Branched Aryl Ethers	43
2.4.4 Typical Procedure for the Formation of Linear Aryl Ethers	43
2.4.5 Typical Procedure for the Formation of 2a.1 at a 1.1 mmol Scale	44
2.4.6 X-ray Crystallographic Studies	44
2.4.7 Analytical Data for All Compounds	46
Chapter 3. Domino Synthesis of α,β-Unsaturated γ-Lactams via Stereo-selective Amination of α-Tertiary Allylic Alcohols	59
3.1 Introduction	61

3.1.1	Lactams.....	61
3.1.2	α,β -Unsaturated γ -Lactams	61
3.1.3	Allylic Alcohols as Precursors in Allylic Substitution Reactions	63
3.1.4	Pd-catalyzed Allylic Amination of Allylic Alcohols	64
3.1.5	Aim of the Work presented in this Chapter.....	69
3.2	Results and Discussion	71
3.2.1	Screening Studies	71
3.2.2	Scope of Substrates.....	73
3.2.3	Mechanistic Control Reactions.....	76
3.2.4	Synthetic Transformations.....	78
3.3	Conclusions	80
3.4	Experimental Section.....	81
3.4.1	General Considerations.....	81
3.4.2	General Procedure for the Synthesis of Vinyl Glycolic Acids.....	81
3.4.3	Typical Procedure for the Formation of Unsaturated γ -Lactams	83
3.4.4	Typical Procedure for the Formation of Decarboxylation/aza-Michael Addition Reaction Product	84
3.4.5	Post-synthetic Potential of the α,β -Unsaturated γ -Lactam Scaffolds.....	84
3.4.6	X-ray Crystallographic Studies	86
3.4.7	Analytical Data for All Compounds.....	89
Chapter 4. Pd-Catalyzed Stereodivergent Allylic Amination of α-Tertiary Allylic Alcohols towards α,β-Unsaturated γ-Amino Acids		107
4.1	Introduction	109
4.1.1	α,β -Unsaturated γ -Amino Acids.....	109
4.1.2	Stereoselective Olefin Synthesis	109
4.1.3	Aim of the Work presented in this Chapter.....	114
4.2	Results and Discussion	115
4.2.1	Screening Studies	115
4.2.2	Scope of Substrates.....	118
4.2.3	Proposed Stereocontrolled Manifold.....	122
4.3	Conclusions	124
4.4	Experimental Section.....	125
4.4.1	General Considerations.....	125
4.4.2	Typical Procedure for the <i>Z</i> -Selective Allylic Aminations	125
4.4.3	Typical Procedure for the <i>E</i> -Selective Allylic Aminations	126

4.4.4	X-ray Crystallographic Studies	126
4.4.5	Analytical Data for All Compounds	128
Chapter 5. Pd-Catalyzed Stereoselective Tandem Ring-opening Amination /cyclization of Vinyl γ-Lactones: Access to Caprolactam Diversity		
5.1	Introduction	139
5.1.1	Caprolactam	139
5.1.2	Catalytic Ring-opening of γ -Lactones	141
5.1.3	Ring-opening of γ -Lactones in Allylic Substitution Reactions	144
5.1.4	Aim of the Work presented in this Chapter	146
5.2	Results and Discussion	147
5.2.1	Screening Studies	147
5.2.2	Scope of Substrates	151
5.2.3	Mechanistic Control Reactions	155
5.2.4	Synthetic Transformations	156
5.3	Conclusions	158
5.4	Experimental Section	159
5.4.1	General Considerations	159
5.4.2	Procedure for the Preparation of Vinyl γ -Lactones	159
5.4.3	Procedure for the Preparation of Phosphoramidite Ligands	161
5.4.4	Procedure for the Screening Phase in the Preparation of Caprolactam ...	162
5.4.5	Typical Procedure for the Preparation of Caprolactams	163
5.4.6	Post-synthetic Potential of the Caprolactam Scaffolds	163
5.4.7	X-ray Crystallographic Studies	168
5.4.8	Analytical Data for All Compounds	169
Summary and General Conclusions		197

List of abbreviations

In this doctoral thesis, the abbreviations and acronyms most commonly used in organic chemistry are based on the recommendations of the ACS “Guidelines for authors” which can be found at:

http://pubs.acs.org/paragonplus/submission/joceah/joceah_abbreviations.pdf

Chapter 1.

General Introduction

Sections of this chapter have been adapted from:

W. Guo, J. E. Gómez, À. Cristòfol, J. Xie, A. W. Kleij, *Angew. Chem. Int. Ed.* **2018**, *57*, 13735-13747.

1.1 Selectivity in Organic Synthesis

Organic synthesis is extremely important for many facets of our daily life. Economic production of chemicals in sufficiently large amounts is necessary to maintain a healthy growth of modern civilization. Catalysis offers a unique possibility for efficient and selective synthesis of desired chemical compounds while minimizing the energy requirements of the process and reducing waste streams. In this context, a key challenge for catalytic synthesis is to control the process selectivity, i.e. the capacity to prepare only one of the possible products. Four major types of selectivity can be identified in modern organic synthesis, including chemo-, regio-, enantio- and diastereo-selectivity.

A general term that usually combines both enantioselectivity and diastereoselectivity is “stereoselectivity”, and it is used to indicate the selective formation of one of the possible stereoisomers. The most common stereo-elements are chiral centers and double-bonds such as in *cis*- or *trans*-configured alkenes. Because different stereoisomers of a molecule often have distinct biological activity, the development of methodologies for the preparation of stereo-pure compounds has received much attention from the chemical community as a result of its high value for the pharmaceutical, pesticide, cosmetic and fine-chemical industry.

1.2 Pd-catalyzed Allylic Substitution Reactions

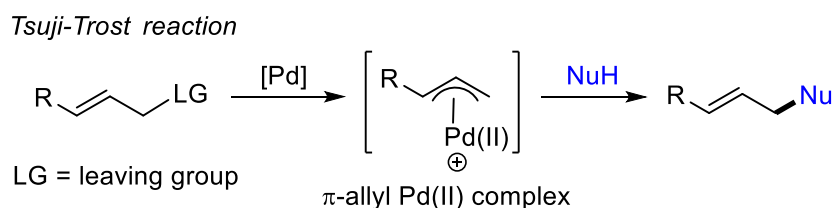
1.2.1 General Aspects

Transition metal (TM) catalysis has become an important tool in organic synthesis attributed to its ability towards the activation of organic substrates and promoting new types of connections. A rapid progress in the study of organometallic and coordination compounds has led to the development and successful industrial application of catalytic processes based on use of TM complexes as catalysts.¹ The major advantage of organometallic catalysis and its widespread adoption by industry is that it allows to selectively produce target products in high yield.

TM-catalyzed allylic substitution is one of the most versatile reactions in modern synthetic organic chemistry, and has received extensive attention to promote the

(1) a) Masters, C.; *Homogeneous Transition-metal Catalysis: a Gentle Art*, Chapman and Hall: New York, **1981**; b) Cornils, B.; Hermann, W.A.; *Applied Homogeneous Catalysis with Organometallic Compounds*, Weinheim: New York, **1996**.

construction of C–C and C–X (X stands for heteroatom) bonds. In 1965, Tsuji *et al.* reported the first examples of Pd-mediated, stoichiometric allylic substitution reactions.² In this work, ethyl malonate, acetoacetate and an enamine derived from cyclohexanone react smoothly with dimeric π -allyl palladium chloride to afford allylated products. After the disclosure of a catalytic version in 1970,³ Trost *et al.* reported the first Pd-catalyzed asymmetric allylic substitution reaction with a stabilized nucleophile in 1977.⁴ Since these pioneering works, the reaction commonly known as the “Tsuji–Trost reaction” (Scheme 1.1, Nu stand for nucleophile), has been significantly developed in many respects including the development of improved ligands, a better mechanistic understanding and designing applications that allow to prepare bioactive compounds using allylic alkylation as a key step. Moreover, in addition to Pd, catalysts derived from other TMs including those based on Ir,⁵ Rh,⁶ Ru,⁷ Pt,⁸ Ni,⁹ Cu,¹⁰ Mo,¹¹ W,¹² and Co¹³ have been documented as efficient catalysts with promising regio- and stereoselective control.

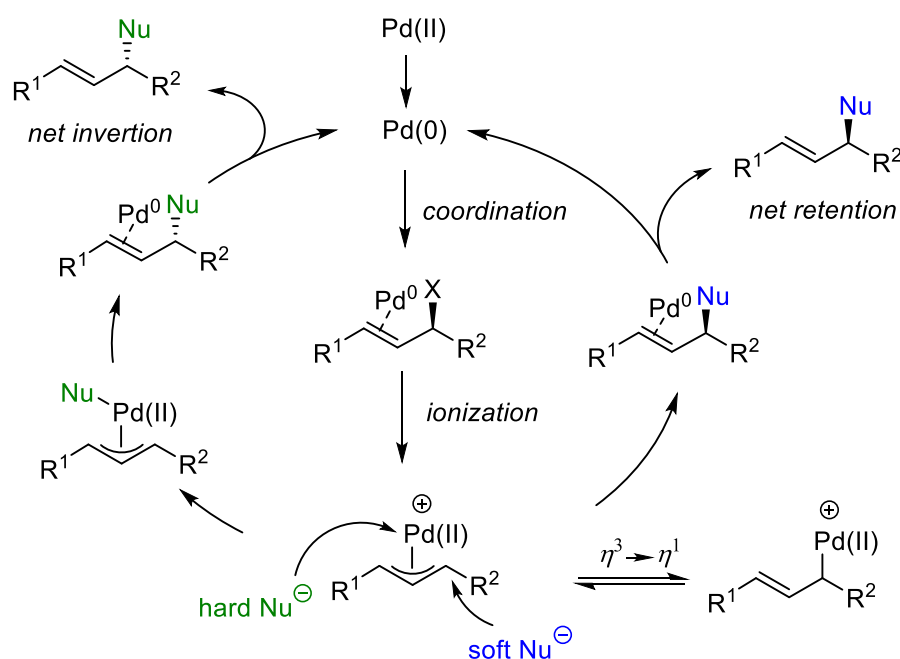


Scheme 1.1 General depiction of the Tsuji–Trost reaction.

- (2) J. Tsuji, H. Takahashi, M. Morikawa, *Tetrahedron Lett.* **1965**, 6, 4387.
- (3) a) K. E. Atkins, W. E. Walker, R. M. Manyik, *Tetrahedron Lett.* **1970**, 11, 3821; b) G. Hata, K. Takahashi, A. Miyake, *J. Chem. Soc., Chem. Commun.* **1970**, 1392.
- (4) B. M. Trost, P. E. Strege, *J. Am. Chem. Soc.* **1977**, 99, 1649.
- (5) Q. Cheng, H.-F. Tu, C. Zheng, J.-P. Qu, G. Helmchen, S.-L. You, *Chem. Rev.* **2019**, 119, 1855.
- (6) D. K. Leahy, P. A. Evans, *In Modern Rhodium-Catalyzed Organic Reactions*; P. A. Evans, Ed.; John Wiley & Sons, Inc.: New York, **2005**; pp 191.
- (7) a) Y. Matsushima, K. Onitsuka, T. Kondo, T. Mitsudo, S. Takahashi, *J. Am. Chem. Soc.* **2001**, 123, 10405; b) B. M. Trost, M. Rao, A. P. Dieskau, *J. Am. Chem. Soc.* **2013**, 135, 18697.
- (8) T. Ohshima, Y. Miyamoto, J. Ipposhi, Y. Nakahara, M. Utsunomiya, K. Mashima, *J. Am. Chem. Soc.* **2009**, 131, 14317.
- (9) a) Y. Bernhard, B. Thomson, V. Ferey, M. Sauthier, *Angew. Chem. Int. Ed.* **2017**, 56, 7460; b) Y. Kita, R. D. Kavthe, H. Oda, K. Mashima, *Angew. Chem. Int. Ed.* **2016**, 55, 1098.
- (10) a) H. Yorimitsu, K. Oshima, *Angew. Chem. Int. Ed.*, **2005**, 44, 4435; b) Y. Shi, B. Jung, S. Torker, A. H. Hoveyda, *J. Am. Chem. Soc.* **2015**, 137, 8948.
- (11) a) O. Belda, C. Moberg, *Acc. Chem. Res.* **2004**, 37, 159; b) C. Moberg, *Org. React.* **2014**, 84, 1; c) B. M. Trost, Y. Zhang, *Chem. Eur. J.* **2011**, 17, 2916.
- (12) G. C. Lloyd-Jones, A. Pfaltz, *Angew. Chem. Int. Ed. Engl.* **1995**, 34, 462.
- (13) a) J.-M. Begouin, J. E. M. N. Klein, D. Weickmann, B. Plietker, *Top. Organomet. Chem.* **2011**, 38, 269; b) K. Takizawa, T. Sekino, S. Sato, T. Yoshino, M. Kojima, S. Matsunaga, *Angew. Chem. Int. Ed.* **2019**, 58, 9199.

1.2.2 Catalytic Cycle

Pd-catalyzed allylic substitution is one of the widest studied reactions in organic chemistry and also considered a benchmark reaction to test new (chiral) ligands. The generally accepted mechanism for “soft” nucleophiles ($pK_a < 25$) starts from the coordination of a low valent and electron-rich Pd(0) species to the double bond of an allylic precursor. Subsequent oxidative addition affords the η^3 - π -allyl Pd(II) intermediate through a heterolytic cleavage of a C–X allylic bond, and can be in equilibrium with an isomeric η^1 -allyl Pd(II) complex. This process is regarded as an “ionization” pathway as the transiently generated η^3 -allyl intermediate is typically an ionic species. Following attack onto the cationic complex by a nucleophile (typically opposite to where the TM and its supporting ligands reside), dissociation of the product then regenerates the active catalyst. In this scenario, bond breaking and making events occur outside the coordination sphere of the metal. However, “hard(er)” nucleophiles ($pK_a > 25$) normally affect such reactions by initial coordination of the nucleophile to the metal followed by a reductive elimination step leading to an overall inversion of the stereochemistry.¹⁴ Consequently, “soft” nucleophiles tend to lead to net retention of configuration, and “hard” nucleophiles to formal inversion (Scheme 1.2).

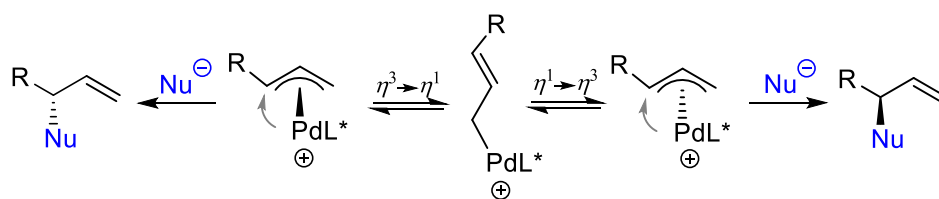


Scheme 1.2 Catalytic cycle for Pd-catalyzed allylic substitution reactions.

(14) H. Matsushita, E. Negishi, *J. Chem. Soc., Chem. Commun.* **1982**, 160.

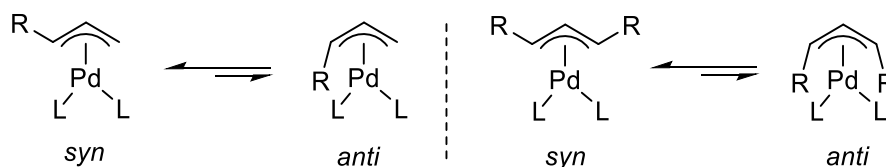
1.2.3 π - σ - π Isomerization

It is well-known that substituted η^3 - π -allyl Pd(II) complexes can undergo π - σ - π isomerization under ambient conditions,¹⁵ which is accomplished via a η^3 to η^1 rearrangement followed by C–Pd bond or/and C–C rotation. Finally, the η^3 - π -allyl Pd(II) complex is regenerated via η^1 to η^3 interconversion. In asymmetric allylic substitution reactions, a suitable chiral palladium catalyst can realize enantioface exchange by π - σ - π interconversion allowing for preferential nucleophilic attack onto a (sterically) favored diastereomeric π -allyl complex (Scheme 1.3).



Scheme 1.3 Pd-catalyzed enantioselective allylic substitution reaction.

The *syn/anti* isomerization of a π -allyl complex is another important feature in “allylic chemistry”. For a mono-substituted allylic complex, there are two possible geometric isomers, the *syn* and the *anti* isomer (see also chapter 4). Undoubtedly, the preferred geometry is the *syn* one. A di-substituted π -allyl Pd(II) complex favors the *syn/syn* geometry, and for an even more substituted allyl complex, the geometrical preference is based on the steric requirements of the substituents involved (Scheme 1.4). It should be noted that under certain circumstances, the isomeric forms are able to interconvert in the presence of a proper ligand or chelating function.¹⁶



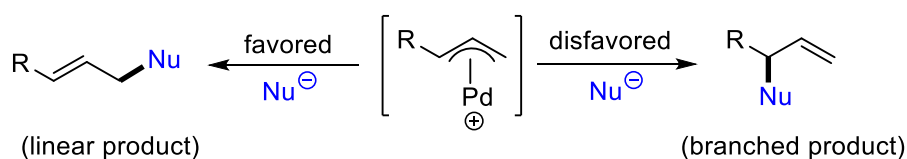
Scheme 1.4 The *syn* and *anti* geometries of π -allyl Pd(II) complexes.

(15) B. M. Trost, C. Lee, *In Catalytic Asymmetric Synthesis*; I. Ojima, Ed.; Wiley-VCH: New York, **2000**; p 593.

(16) B. Akemark, S. Hansson, A. Vitagliano, *J. Am. Chem. Soc.* **1990**, *112*, 4587.

1.2.4 Regioselectivity

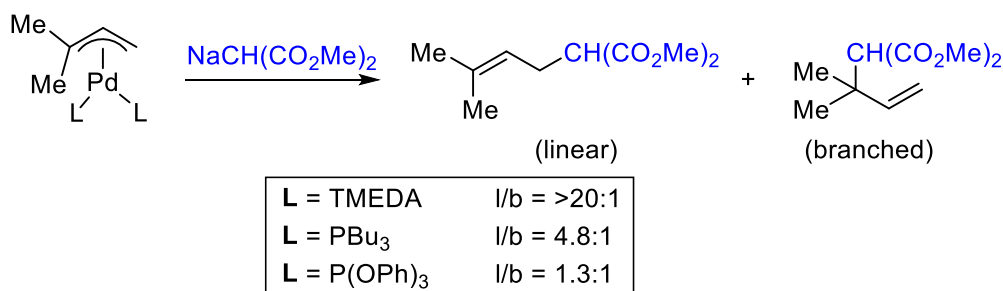
Control over the regioselectivity in Pd-mediated allylic substitution reactions remains one of the most difficult and challenging problems.¹⁷ In general, linear allylation products are preferentially generated as the result of a favorable nucleophilic attack onto the least substituted carbon terminus of the allyl Pd(II) unit (Scheme 1.5). Despite this significant hurdle, significant achievements in Pd-catalyzed branched-selective allylic substitution reactions have been accomplished by tuning the steric and electronic effects of the substrates, nucleophiles, ligands and bases.



Scheme 1.5 Regioselectivity in allylic substitution reactions.

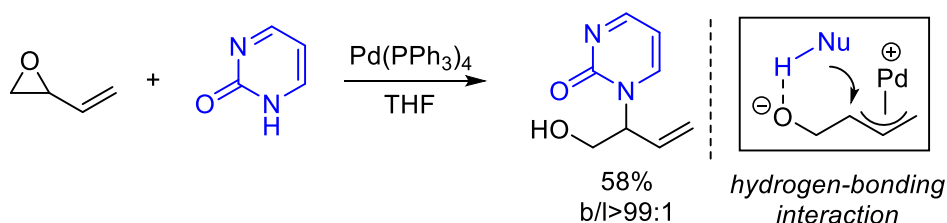
For example, a stronger π -acceptor ligand creates more positive charge in the allyl Pd(II) unit, and consequently the more substituted terminus would be more reactive to an incoming nucleophile. In this context, high linear regioselectivity was detected in the case of TMEDA as ligand, while more of the branched regioisomer resulting from attack at the more substituted terminus was observed when a π -acceptor ligand such as triphenylphosphite was employed (Scheme 1.6). Therefore, in the latter case intrinsically the attack of the nucleophile at the more substituted allylic terminus is favored for electronic reasons, whereas an increase of steric bulk in the allyl unit proportionally increases the preference for the linear product. Another design factor for supporting ligands should be considered: donor ligands are necessary to give access to sufficiently electron-rich Pd(0) species to promote the initial oxidation addition step. Therefore, suitable donor ligands are those that allow for fast turnovers in allylic substitution reactions.

(17) B. Akerman, B. Krakenberger, S. Hansson, A. Vitagliano, *Organometallics* **1987**, *6*, 620.



Scheme 1.6 Ligand effects on the regioselectivity of nucleophilic attack onto allyl Pd(II) complexes: l stands for “linear”, b for “branched”.

In the 1980s, pioneering work from Trost *et al.* illustrated that hydrogen-bonding interactions between amine nucleophiles and an oxygen anion in the π -allyl Pd(II) intermediate can switch the regiocontrol from linear to branched. By using vinyl epoxide as allylic precursor, an unexpected selective branched aminated product was generated (Scheme 1.7).¹⁸ Subsequent research by the same group revealed a hydrogen-bonding directing mode to explain the origin of this reversed regioselectivity.¹⁹ Hereafter, various strategies capitalizing on hydrogen bonding, electrostatic and/or coordination interactions were disclosed to enable a rather challenging branched selectivity in allylic substitution reactions.²⁰



Scheme 1.7 Pioneering work to achieve branched-selective Pd-catalyzed allylic amination enabled by a hydrogen-bond interaction.

1.2.5 Allylic Precursors with Different Leaving Group

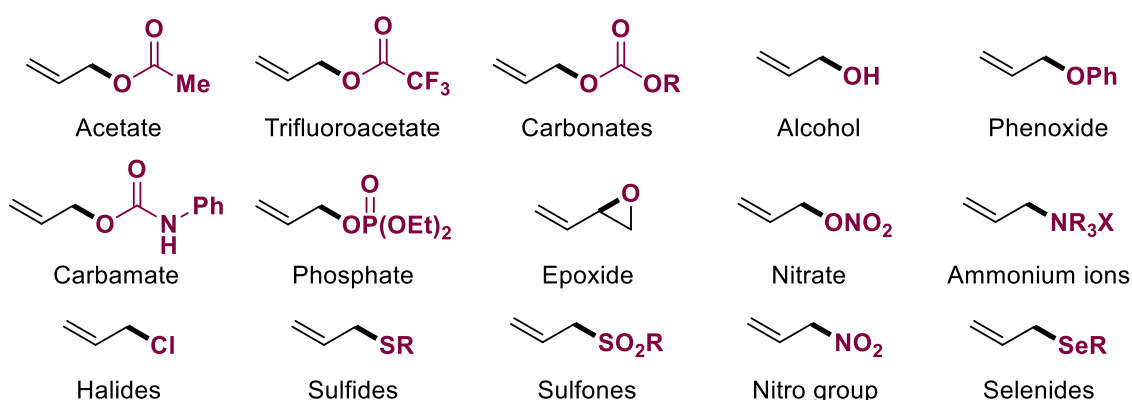
A large variety of allylic precursors containing C–X allylic bonds (with X being a suitable leaving group, LG) have been utilized over the years (Scheme 1.8). Importantly, the nature of the LG has a dramatic influence on the position of the pre-equilibrium and therefore on the whole substitution process. In principle, the better the LG the better the

(18) B. M. Trost, G.-H. Kuo, T. Benneche, *J. Am. Chem. Soc.* **1988**, *110*, 621.

(19) B. M. Trost, R. C. Bunt, R. C. Lemoine, T. L. Calkins, *J. Am. Chem. Soc.* **2000**, *122*, 5968.

(20) Y.-N. Wang, L.-Q. Lu, W.-J. Xiao, *Chem. Asian J.* **2018**, *13*, 2174.

inhibition of ion-pair recombination and hence the faster the turnover. Allylic acetates are the most widely used allylic precursors, and oxidative addition to a Pd(0) complex was firstly demonstrated in 1981 by Yamamoto and coworkers, who successfully isolated and characterized the corresponding η^3 -allyl(acetato)palladium intermediate.²¹ Formation of the π -allyl Pd(II) complex from allylic acetate and Pd(0) is reversible and the equilibrium predominantly favors the reformation of Pd(0) and allylic acetate.²² On the other hand, the oxidative addition of allylic trifluoroacetate to Pd(dba)₂ leads to quantitative formation of the corresponding π -allyl complex,²³ since trifluoroacetate is less strongly coordinating than acetate and acts thus as a superior LG.



Scheme 1.8 Classical allylic precursors with the different LGs highlighted.

Allylic carbonate is an efficient allylating agent and was firstly reported by Tsuji *et al.* in 1982.²⁴ η^3 -Allyl palladium alkoxy carbonate complexes can be isolated without showing spontaneous decarboxylation²⁵ and their reaction with an acidic substrate generates the corresponding hydrogen carbonate complex, which may decarboxylate at this stage. Allylic alcohols are attractive substrates from an atom-economical point of view. Although they were used as early as 1970 by Atkins,²⁶ their widespread use and reaction development has been hampered by the poor leaving ability of the hydroxyl group, and thus finding ways to efficiently convert allylic alcohols is still under active investigation (see also chapter 3). Apart from these classical substrates, allylic phenoxides,

- (21) T. Yamamoto, O. Saito, A. Yamamoto, *J. Am. Chem. Soc.* **1981**, *103*, 5600.
 (22) C. Amatore, A. A. Bahoun, A. Jutand, L. Mensah, G. Meyer, L. Ricard, *Organometallics* **2005**, *24*, 1569; b) C. Amatore, A. Jutand, G. Meyer, L. Mottier, *Chem. Eur. J.* **1999**, *5*, 466.
 (23) A. Vitagliano, B. Aakermark, S. Hansson, *Organometallics* **1991**, *10*, 2592.
 (24) a) J. Tsuji, I. Shimizu, I. Minami, Y. Ohashi, *Tetrahedron Lett.* **1982**, *23*, 4809; b) J. Tsuji, I. Shimizu, I. Minami, Y. Ohashi, T. Sugiura, K. Takahashi, *J. Org. Chem.* **1985**, *50*, 1523.
 (25) F. Ozawa, T. Son, S. Ebina, K. Osakada, A. Yamamoto, *Organometallics* **1992**, *11*, 171.
 (26) K. E. Atkins, W. E. Walker, R. M. Manyik, *Tetrahedron Lett.* **1970**, *23*, 3821.

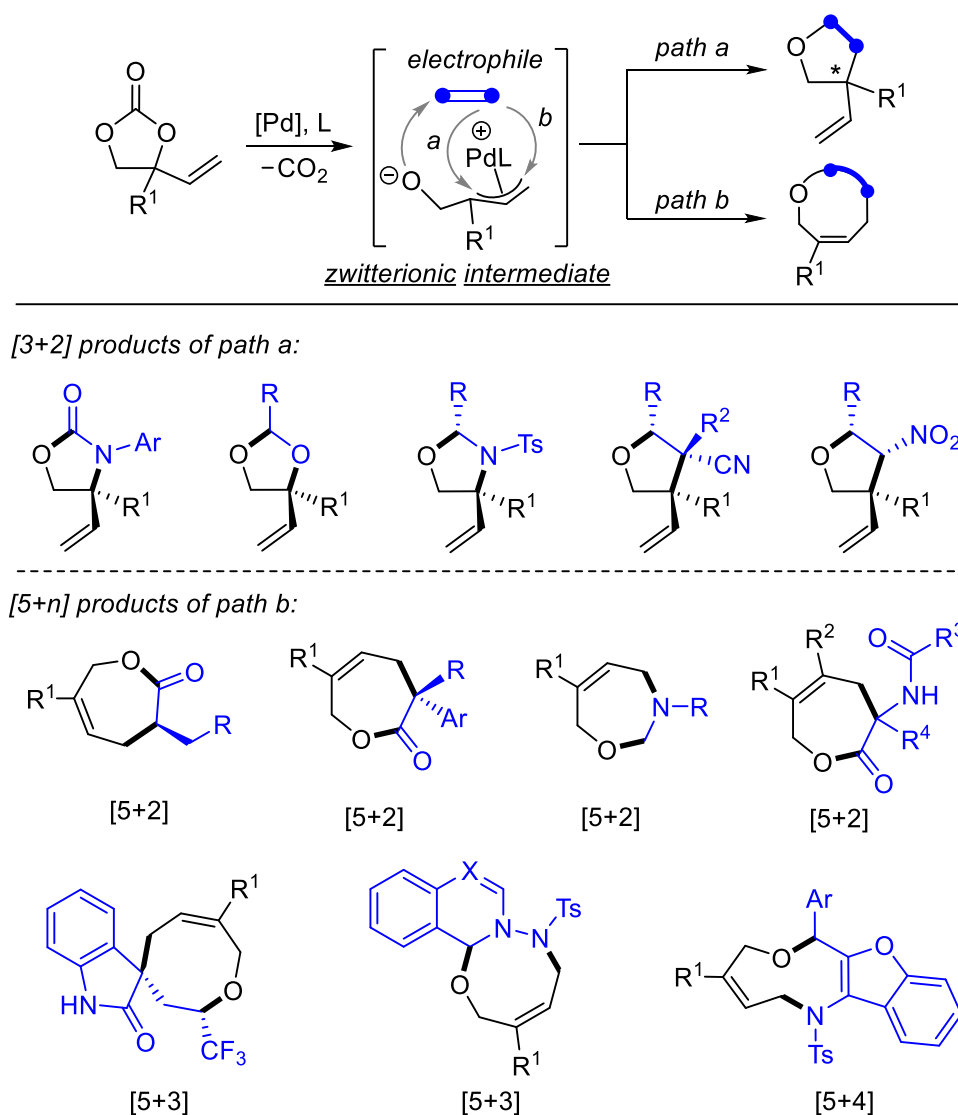
carbamates, phosphates, nitrates, ammonium ions, halides, sulfides, sulfones, nitrites and selenides have also been used as π -allyl precursors (Scheme 1.8).

Vinyl epoxides have likewise been successfully explored as allylic precursors with the cyclic ether thus acting as a LG.²⁷ Reaction of a vinyl epoxide with Pd(0) complex results into a π -allyl Pd(II) complex with a free pending alcohol, which was isolated and characterized by the group of Szabó.²⁸ Compared with vinyl epoxide, the reactivity of vinyl cyclic carbonates (VCCs) has proven to be markedly different in certain cases. Substituted VCCs are synthetically more easily accessible and highly modular: these cyclic carbonate precursors are easily prepared from ubiquitous α -hydroxy ketone precursors. Decarboxylation of five-membered VCCs in the presence of a Pd(0) precursor generates a presumed “zwitterionic intermediate” featuring a nucleophilic alkoxide and an electrophilic π -allyl Pd(II) site. This reactive zwitterionic species can serve as 1,3- or 1,5-dipole and its ambivalent character has been exploited significantly over the last five years (*vide infra* for a selection).

The first decarboxylative cyclization of six-membered VCCs and isocyanate electrophiles was reported by Tamaru *et al.* in 1994 to stereoselectively furnish cyclic carbamates.²⁹ In the following decade, cycloaddition reactions of VCCs with a variety of different electrophiles was enormously boosted. For instance, Zhang and co-workers utilized this concept to develop the asymmetric synthesis of various five-membered heterocycles by [3+2] cycloaddition reactions using five-membered VCCs and different electrophiles such as imines, isocyanates, formaldehyde, and Michael acceptors (Scheme 1.9, *path a*).³⁰ Recently, the Zhao group reported that similar π -allyl Pd(II) species can serve as 1,5-dipoles in [5+4] annulation reactions to form nine-membered heterocycles using 1,3-azadienes as electrophiles.³¹ Since then, the decarboxylative formation of

-
- (27) a) B. M. Trost, J. R. Granja, *Tetrahedron Lett.* **1991**, 32, 2193; b) R. Mizojiri, Y. Kobayashi, *J. Chem. Soc. Perkin Trans. I*, **1995**, 2073.
- (28) J. Kjellgren, J. Aydin, O. A. Wallner, I. V. Saltanova, K. J. Szabó, *Chem. Eur. J.* **2005**, 11, 5260.
- (29) T. Bando, H. Harayama, Y. Fukazawa, M. Shiro, K. Fugami, S. Tanaka, Y. Tamaru, *J. Org. Chem.* **1994**, 59, 1465.
- (30) a) L. Yang, A. Khan, R. Zheng, L. Y. Jin, Y. J. Zhang, *Org. Lett.* **2015**, 17, 6230; b) A. Khan, J. Xing, J. Zhao, Y. Kan, W. Zhang, Y. J. Zhang, *Chem. Eur. J.* **2015**, 21, 120; c) A. Khan, R. Zheng, Y. Kan, J. Ye, J. Xing, Y. J. Zhang, *Angew. Chem. Int. Ed.* **2014**, 53, 6439; d) A. Khan, L. Yang, J. Xu, L. Y. Jin, Y. J. Zhang, *Angew. Chem. Int. Ed.* **2014**, 53, 11257; e) K. Liu, I. Khan, J. Cheng, Y. J. Hsueh, Y. J. Zhang, *ACS Catal.* **2018**, 8, 11600.
- (31) a) L.-C. Yang, Z.-Q. Rong, Y.-N. Wang, Z. Y. Tan, M. Wang, Y. Zhao, *Angew. Chem. Int. Ed.* **2017**, 56, 2927; b) Z.-Q. Rong, L.-C. Yang, S. Liu, Z. Yu, Y.-N. Wang, Z. Y. Tan, R.-Z. Huang, Y. Lan, Y. Zhao, *J. Am. Chem. Soc.* **2017**, 139, 15304.

various medium sized heterocycles through Pd-catalyzed [5 + 2],³² [5 + 3]³³ or [5 + 4]³⁴ annulation reactions has been achieved by different research groups (Scheme 1.9, *path b*).



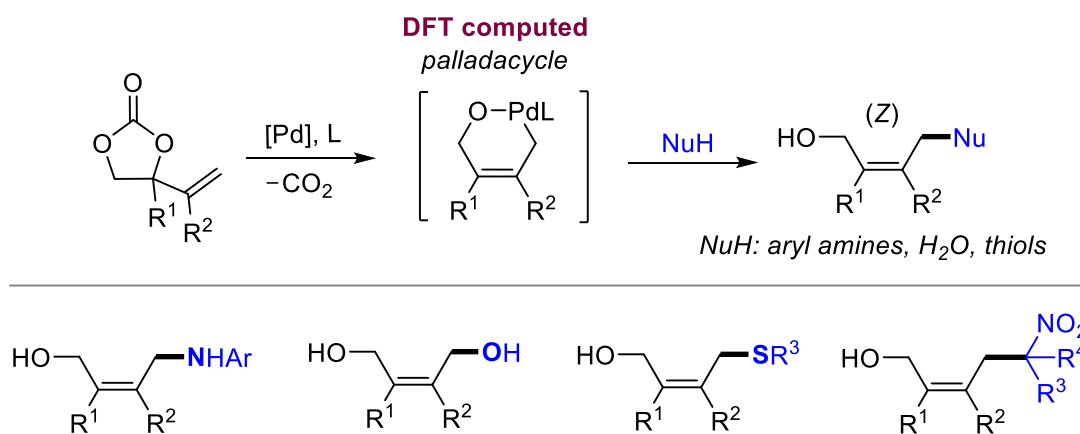
Scheme 1.9 Pd-catalyzed decarboxylative annulation reactions of VCCs with various electrophiles.

Unlike the cyclization process mentioned above that focus on the coupling of VCCs in the presence of electrophiles, the TM-catalyzed transformations of VCCs in the

- (32) a) S. Singha, T. Patra, C. G. Daniliuc, F. Glorius, *J. Am. Chem. Soc.* **2018**, *140*, 3551; b) Y. Wei, S. Liu, M.-M. Li, Y. Li, Y. Lan, L.-Q. Lu, W.-J. Xiao, *J. Am. Chem. Soc.* **2019**, *141*, 133; c) H.-W. Zhao, J. Du, J.-M. Guo, N.-N. Feng, L.-R. Wang, W.-Q. Ding, X.-Q. Song, *Chem. Commun.* **2018**, *54*, 9178; Y. Yang, W. Yang, *Chem. Commun.* **2018**, *54*, 12182.
- (33) a) C. Yuan, Y. Wu, D. Wang, Z. Zhang, C. Wang, L. Zhou, C. Zhang, B. Song, H. Guo, *Adv. Synth. Catal.* **2018**, *360*, 652; b) B. Niu, X.-Y. Wu, Y. Wei, M. Shi, *Org. Lett.* **2019**, *21*, 4859; c) H.-W. Zhao, L.-R. Wang, J.-M. Guo, W.-Q. Ding, X.-Q. Song, H.-H. Wu, Z. Tang, X.-Z. Fan, X.-F. Bi, *Adv. Synth. Catal.* **2019**, *361*, 4761.
- (34) P. Das, S. Gondo, P. Nagender, H. Uno, E. Tokunaga, N. Shibata, *Chem. Sci.* **2018**, *9*, 3276.

presence of nucleophiles also proved to be feasible and was initially investigated in the 1990s.³⁵

Recently, the Pd-catalyzed decarboxylative coupling of external nucleophiles and VCCs was extensively examined by our group towards the stereoselective synthesis of a range of highly functional allylic compounds through C–N, C–O, C–S and C–C bond formation reactions (Scheme 1.10).³⁶ DFT (Density Functional Theory) studies suggested that in the presence of a suitable palladium precursor, the formation of a six-membered palladacyclic intermediate (acting thus as the origin for more reactive, ring-opened species) rationalizes the experimentally observed exclusive stereocontrol affording *Z*-configured highly substituted allylic derivatives. Since then, various other nucleophiles were demonstrated to be efficient reaction partners in the stereoselective syntheses of a large number of allylic scaffolds.³⁷

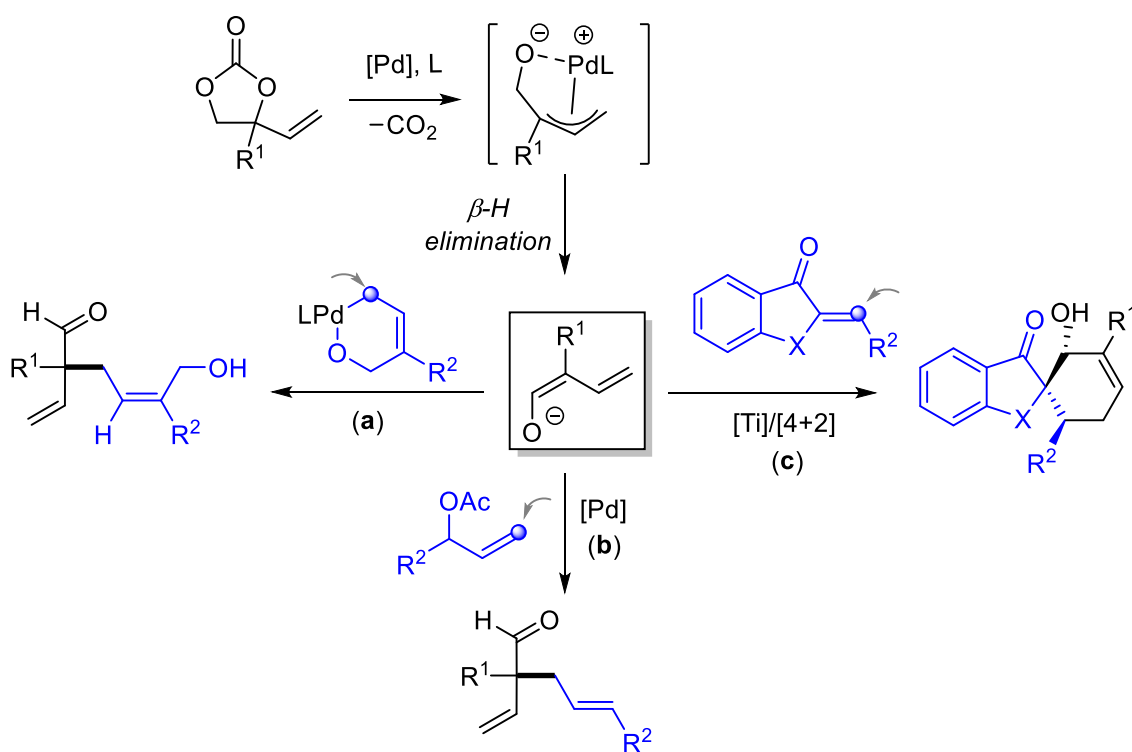


Scheme 1.10 Pd-catalyzed stereoselective allylic substitution with various nucleophiles based on VCCs and a DFT computed key palladacyclic intermediate.

Apart from externally added nucleophiles, a recent contribution from our group showed that under appropriate reaction conditions the VCC itself can *in situ* produce a pro-nucleophilic dienolate species by a formal umpolung of the π -allyl zwitterionic

- (35) a) B. M. Trost, J. R. Granja, *Tetrahedron Lett.* **1991**, 32, 2193; b) S.-K. Rang, S.-G. Kim, J.-S. Lee, *Tetrahedron: Asymmetry* **1992**, 3, 1139.
- (36) a) W. Guo, L. Martínez-Rodríguez, R. Kuniyil, E. Martín, E. C. Escudero-Adán, F. Maseras, A. W. Kleij, *J. Am. Chem. Soc.* **2016**, 138, 11970; b) W. Guo, L. Martínez-Rodríguez, E. Martín, E. C. Escudero-Adán, A. W. Kleij, *Angew. Chem. Int. Ed.* **2016**, 55, 11037; c) J. E. Gómez, W. Guo, A. W. Kleij, *Org. Lett.* **2016**, 18, 6042; d) À. Cristófol, E. C. Escudero-Adán, A. W. Kleij, *J. Org. Chem.* **2018**, 83, 9978.
- (37) a) L. Deng, A. W. Kleij, W. Yang, *Chem. Eur. J.* **2018**, 24, 19156; b) L. Shi, Y. He, J. Gong, Z. Yang, *Asian J. Org. Chem.* **2019**, 8, 823; c) M. Ke, G. Huang, L. Ding, J. Fang, F.-E. Chen, *ChemCatChem* **2019**, 11, 4720.

species through a β -H elimination. This VCC based pronucleophile then engages with a second decarboxylated VCC to form a highly functionalized, challenging quaternary carbon center (Scheme 1.11, a).³⁸ Shortly after, Zhai *et al.* found that this method could be extended by using allylic acetate as the electrophile in the presence of a sterically demanding Pd(*t*Bu₃P)₂ pre-catalyst (Scheme 1.11, b).³⁹ Later, this umpolung strategy was further developed by Zhao and coworkers,⁴⁰ and allowed for novel annulation processes using aurones (a type of flavonoid) and VCCs as starting materials in the presence of a dual palladium/titanium relay catalyst. In this case, [6,5] spiro-heterocycles were generated bearing three contiguous stereocenters with excellent diastereoselectivity (Scheme 1.11, c).



Scheme 1.11 Pd-catalyzed decarboxylative umpolung reactivity of VCCs.

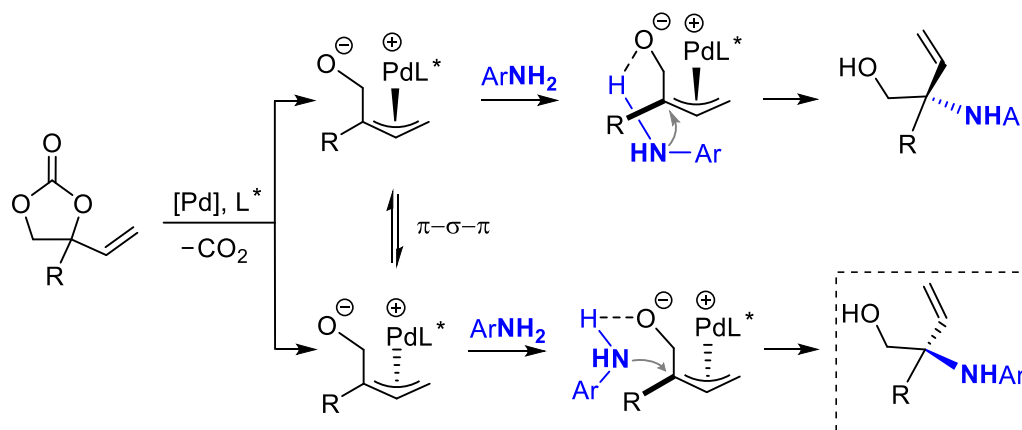
By a judicious choice of the ligand and palladium precursor, a dynamic kinetic asymmetric transformation of VCCs is feasible when the π - σ - π interconversion occurs faster than the subsequent nucleophilic attack. Our group recently demonstrated that the regiochemistry of the nucleophilic attack could be switched to the sterically more

(38) W. Guo, R. Kuniyil, J. E. Gómez, F. Maseras, A. W. Kleij, *J. Am. Chem. Soc.* **2018**, *140*, 3981.

(39) H. Wang, S. Qiu, S. Wang, H. Zhai, *ACS Catal.* **2018**, *8*, 11960.

(40) L.-C. Yang, Z. Y. Tan, Z.-Q. Rong, R. Liu, Y.-N. Wang, Y. Zhao, *Angew. Chem. Int. Ed.* **2018**, *57*, 7860.

hindered carbon of the palladium allyl intermediate allowing the asymmetric synthesis of challenging chiral α,α -disubstituted allylic aryl amines in the presence of a phosphoramidite ligand (Scheme 1.12).⁴¹ Thereafter, a mechanistic study was conducted by Huang, Kleij and coworkers revealing that after oxidative addition/ CO_2 extrusion the nucleophilic attack leading to branched allylic amine product proceeds through a novel type of inner-sphere pathway comprising of a η^2 -aryl coordination of the aromatic group of the amine to the Pd center.⁴²



Scheme 1.12 Pd-catalyzed decarboxylative amination of VCCs affording enantioenriched branched allylic amines.

Zhang and co-workers developed a protocol allowing to construct chiral allylic 1,2-diols and alkyl ethers by directing the attack of the oxygen nucleophile using an organoboron compound as co-catalyst.⁴³ Very recently, Kleij and coworkers demonstrated that allylic sulfones featuring quaternary stereocenters can be obtained from linear carbonates and sulfinate salts,⁴⁴ shortly followed by a contribution from Khan and coworkers who reported the asymmetric synthesis of similar α,α -disubstituted allylic sulfones based on Pd-catalyzed sulfonylation of VCCs with sodium sulfonates acting as nucleophiles.

(41) A. Cai, W. Guo, L. Martínez-Rodríguez, A. W. Kleij, *J. Am. Chem. Soc.* **2016**, *138*, 14194.

(42) L. Hu, A. Cai, Z. Wu, A. W. Kleij, G. Huang, *Angew. Chem. Int. Ed.* **2019**, *58*, 14694.

(43) A. Khan, S. Khan, I. Khan, C. Zhao, Y. Mao, Y. Chen, Y. J. Zhang, *J. Am. Chem. Soc.* **2017**, *139*, 10733.

(44) a) A. Cai, A. W. Kleij, *Angew. Chem. Int. Ed.* **2019**, *58*, 14944; b) A. Khan, H. Zhao, M. Zhang, S. Khan, D. Zhao, *Angew. Chem. Int. Ed.* **2020**, *59*, 1340.

1.3 Thesis Aim and Scope

Over the last 50 years, remarkable progress has been made in TM-catalyzed allylic substitution reactions testified by the significant potential in the rapid and cost-effective synthesis of natural products, pharmaceuticals, and functional materials. Current research in the area of “allylic chemistry” is mainly focused on maturing the regio-, stereo-, and enantio-selective features combined with the development of new ligands, allylic precursors, advancing mechanistic studies and more elaborate synthetic applications. Despite these significant advances, there remain underdeveloped aspects in Pd-catalyzed allylic substitution reactions, including:

- (1) the asymmetric construction of sterically congested quaternary stereocenters;
- (2) the use of allylic substitution as a key step in the rapid construction (through stereoselective cascade/tandem processes) of pharmaceutically relevant heterocyclic products;
- (3) and the design of greener processes by novel activation modes for allylic alcohols.

Based on the previous knowledge attained in our group in allylic substitution reactions enabled by ligand engineering and careful substrate design, the **General Objective** of this doctoral thesis is *the development of novel catalytic (domino) synthesis methods based on Pd-catalyzed allylic substitution for the stereoselective synthesis of functional small molecules and heterocycles utilizing a detailed ligand engineering approach.*

With this general aim in mind, the scope of this thesis is organized into five chapters. In the current **first chapter**, an introduction on the general aspects of “allylic chemistry” is provided together with the development of using VCCs as privileged substrates. This puts the results reported in chapters 2-5 into the appropriate context.

In **chapter 2**, the first general method for the preparation of enantioenriched tertiary allylic aryl ethers is presented through a Pd-mediated regio- and enantioselective transformation of VCCs in the presence of phenolic nucleophiles. A mechanistic model for the regio-control in this protocol is also put forward.

In **chapter 3**, a novel domino synthesis route towards the formation of unsaturated γ -lactam is described that takes advantage of a newly designed substrate that allows for ambient activation of the allylic alcohol unit enabled by Pd-catalysis. In the presence of suitable ligands, this method provides a stereoselective manifold giving Z-configured

unsaturated γ -amino acid intermediates (derived from primary amines) that easily cyclize towards the targeted α,β -unsaturated γ -lactams.

In **chapter 4**, a stereodivergent approach for the synthesis of either *Z*- or *E*-configured unsaturated γ -amino acids derived from tertiary allylic alcohols and secondary amines is illustrated with a crucial role for the ancillary (phosphine) ligand. The role of the bite angle of the diphosphine ligands is discussed and its effect on the isomerization rate of the Pd(allyl) intermediate.

In the **last chapter (five)**, a process for the allylic amination of vinyl γ -lactones is reported that combines simultaneous control over the regio-, stereo- and chemoselectivity of this cascade transformation. The intermediate ϵ -amino acids are easily cyclized to afford a library of functional caprolactam building blocks and post-synthetic derivatives of value in synthetic chemistry.

Chapter 2.

Pd-Catalyzed Enantio- and Regioselective Formation of Allylic Aryl Ethers

This chapter has been published in:

J. Xie, W. Guo, A. Cai, E. C. Escudero-Adán, A. W. Kleij, *Org. Lett.* **2017**, *19*, 6388-6391.

2.1 Introduction

2.1.1 Chiral Tertiary Aryl Ethers

Enantiomerically enriched tertiary aryl ethers are valuable building blocks, as these substructures are present in numerous ether-containing natural products and biologically active compounds such as GPR₁₁₉ agonist,⁴⁵ Ustiloxin D,⁴⁶ Vitamin E⁴⁷ and products known as peroxisome proliferator-activated receptor γ (PPAR γ) modulators⁴⁸ (Figure 2.1).

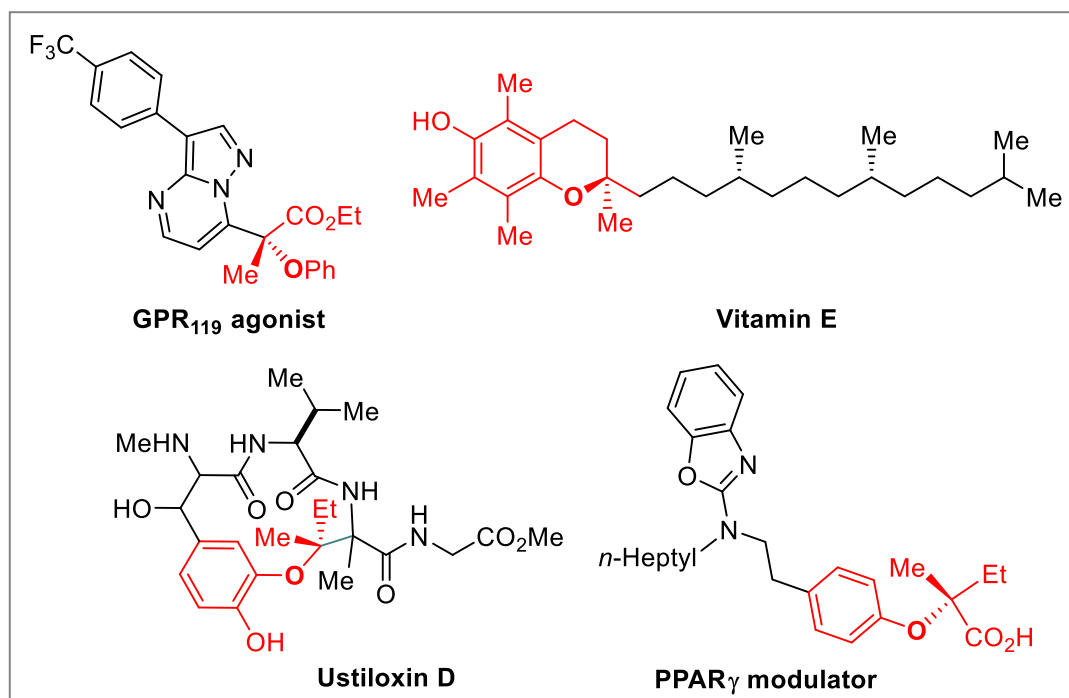
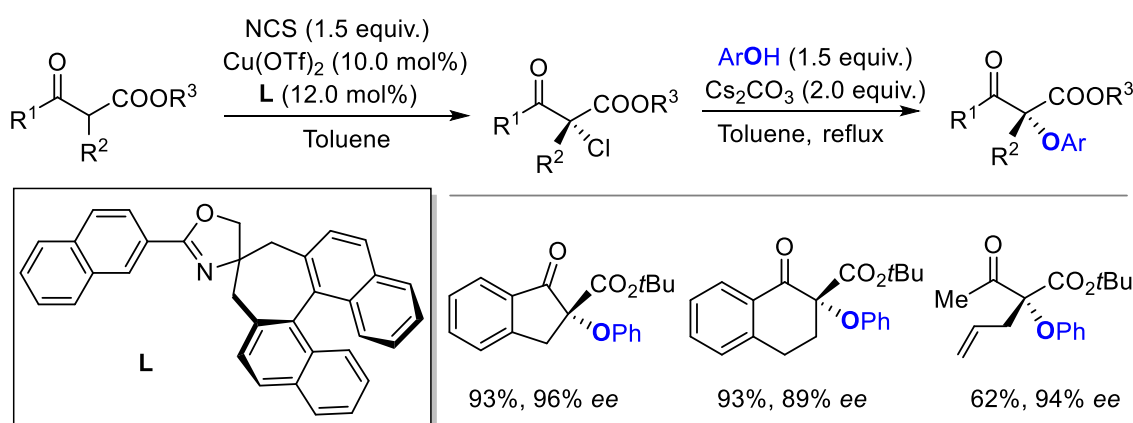


Figure 2.1 Representative biologically active compounds with a chiral tertiary aryl ether moiety.

Over the last decades, numerous synthetic methodologies for the enantioselective formation of tertiary aryl ethers have been reported. One approach concerns S_N2 displacement reactions of chiral tertiary centers with phenol nucleophiles that form the

- (45) A. Phillip, A. Mihai, C. Christopher, E. Robert, L. Gerald, M. Daniel, N. Victor, PCT Int. Appl. (2011), WO 2011014520 A2 20110203.
- (46) For the total synthesis of Ustiloxin D using an allylic tertiary aryl ether as intermediate: a) A. M. Sawayama, H. Tanaka, T. J. Wandless, *J. Org. Chem.* **2004**, *69*, 8810. Also see: b) B. Cao, H. Park, M. M. Joullié, *J. Am. Chem. Soc.* **2002**, *124*, 520; c) H. Tanaka, A. M. Sawayama, T. J. Wandless, *J. Am. Chem. Soc.* **2003**, *125*, 6864.
- (47) a) B. M. Trost, F. D. Toste, *J. Am. Chem. Soc.* **1998**, *120*, 9074; b) B. M. Trost, N. Asakawa, *Synthesis* **1999**, 1491; c) B. M. Trost, *J. Org. Chem.* **2004**, *69*, 5813; d) E. Mizuguchi, K. Achiwa, *Chem. Pharm. Bull.* **1997**, *45*, 1209.
- (48) G. Pochetti, N. Mitro, A. Lavecchia, F. Gilardi, N. Besker, E. Scotti, M. Aschi, N. Re, G. Fracchiolla, A. Laghezza, P. Tortorella, R. Montanari, E. Novellino, F. Mazza, M. Crestani, F. Loiodice, *J. Med. Chem.* **2010**, *53*, 4354.

chirality-inverted substituted products.⁴⁹ For example, Shi and coworkers described a stereospecific synthesis of chiral tertiary alkyl-aryl ethers in about 50% chemical yield via a Mitsunobu reaction with complete inversion of configuration.⁵⁰ In 2004, Mukaiyama *et al.* realized the etherification of chiral tertiary alcohols with inversion of their configurations through the preparation of chiral tertiary aryl ethers using an oxidation-reduction process.⁵¹ Recently, Shibatomi and Iwasa reported the enantioselective synthesis of α -aryloxy- β -keto esters by a Williamson ether synthesis method through the sequential chlorination of β -keto esters and nucleophilic substitution of the chlorine atoms by (substituted) phenols (Scheme 2.1).⁵² However, these traditional stereospecific approaches leading to chiral tertiary aryl ethers rely on pre-functionalized and chiral tertiary alcohols or halogen reagents, for which multistep synthetic sequences and/or the use of large amount of coupling reagents are inevitable, while the scope of the tertiary aryl ethers also remains relatively narrow.



Scheme 2.1 Preparation of chiral tertiary aryl ethers by a Williamson ether synthesis.

Asymmetric epoxidation of 1,1-disubstituted alkenes provides yet another pathway to access chiral tertiary aryl ethers, however, the enantioselectivity of the process is challenged by the requisite of having efficient enantiofacial discrimination between the two substituents flanking the carbon-carbon double bond.⁵³ Thus, the development of more general, attractive catalytic methods for assembling tertiary aryl ethers has and

(49) N. L. Dirlam, B. S. Moore, F. J. Urban, *J. Org. Chem.* **1987**, *52*, 3587.

(50) Y.-J. Shi, D. L. Hughes, J. M. McNamara, *Tetrahedron Lett.* **2003**, *44*, 3609.

(51) T. Shintou, T. Mukaiyama, *J. Am. Chem. Soc.* **2004**, *126*, 7359.

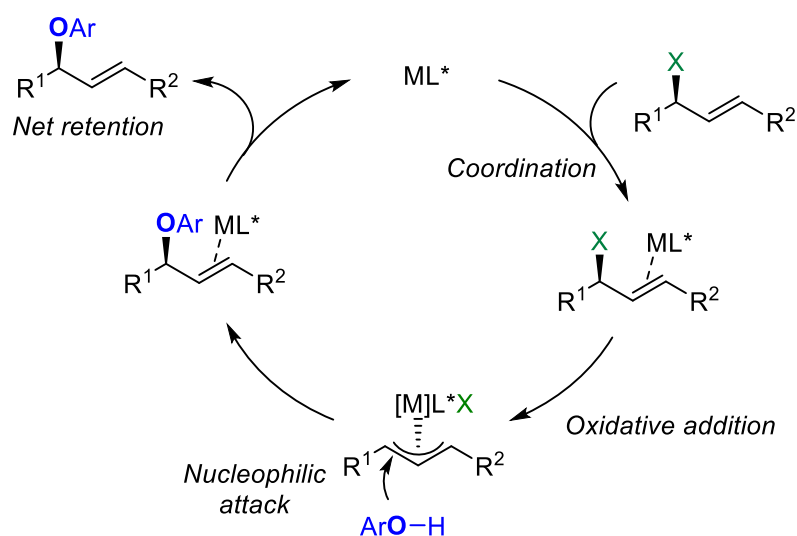
(52) K. Shibatomi, M. Kotozaki, N. Sasaki, I. Fujisawa, S. Iwasa, *Chem. Eur. J.* **2015**, *21*, 14095.

(53) For reviews, see: a) O. A. Wong, Y. Shi, *Chem. Rev.* **2008**, *108*, 3958; b) T. Katsuki, *Adv. Synth. Catal.* **2002**, *344*, 131; c) R. A. Johnson, K. B. Sharpless, in *Catalytic Asymmetric Synthesis*, 2nd ed.; I. Ojima, Ed.; WILEY-VCH: New York, **2000**; p 231.

continues to attract the attention from both academia and industry.

2.1.2 TM-catalyzed Asymmetric Synthesis of Secondary Allylic Aryl Ethers

Allylic aryl ethers are useful intermediates towards biologically active natural compounds.⁵⁴ Moreover, recent work on aryl-Claisen [3,3]-sigmatropic rearrangements⁵⁵ and Friedel-Crafts type cyclizations of aryl allyl ethers further attest the importance of aryl allyl ethers in organic synthesis. The TM-catalyzed allylic substitution using phenolic nucleophiles provides a versatile and straightforward approach to access allylic aryl ethers. These kinds of substitution reactions generally occur at ambient temperature and facilitates the introduction of a new stereogenic center. Over the past decades, considerable progress has been achieved in catalytic (asymmetric) allylic etherification with phenol (pro)nucleophiles, with the main challenge in these reactions being to control the reaction performance including stereo-, regio-, and enantio-selectivity features. Asymmetric allylic substitution methods to access secondary allylic aryl ethers have been reported using primarily Pd(0), Ir(I), Ru(II) or Rh(I) catalysts.

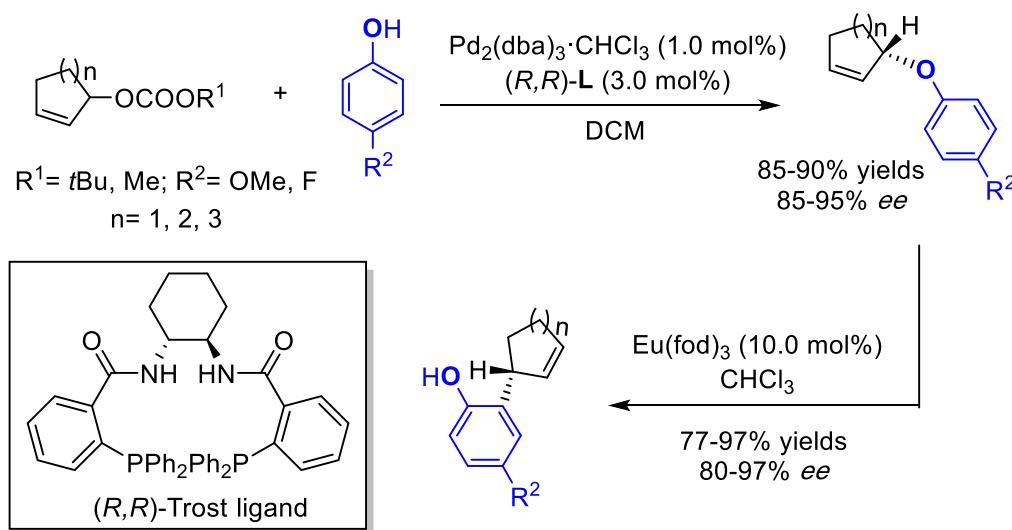


Scheme 2.2 Typical catalytic cycle for TM-catalyzed allylic etherification reactions.

- (54) a) B. M. Trost, M. L. Crawley, *Chem. Rev.* **2003**, *103*, 2921. Also see: b) B. M. Trost, F. D. Toste, *J. Am. Chem. Soc.* **2000**, *122*, 11262; c) B. M. Trost, J. L. Gunzner, O. Dirat, Y. H. Rhee, *J. Am. Chem. Soc.* **2002**, *124*, 10397; d) B. M. Trost, O. R. Thiel, H.-C. Tsui, *J. Am. Chem. Soc.* **2002**, *124*, 11616; e) B. M. Trost, F. D. Toste, *J. Am. Chem. Soc.* **1999**, *121*, 3543; f) B. M. Trost, M. L. Crawley, *J. Am. Chem. Soc.* **2002**, *124*, 9328.
- (55) a) *The Claisen Rearrangement: Methods and Applications*; M. Hiersemann, U. Nubbemeyer, Eds.; Wiley-VCH: Weinheim, Germany, **2007**; b) E. A. Ilardi, C. E. Stivala, A. Zakarian, *Chem. Soc. Rev.* **2010**, *38*, 3133; c) A. M. Martin Castro, *Chem. Rev.* **2004**, *104*, 2939.

A typical catalytic cycle occurs via oxidative addition of an allyl electrophile to a low-valent TM complex to form a π -allyl metal intermediate. This step is followed by the attack of the phenol (pro)nucleophile onto the cationic π -allyl species from the *rear*-face, and finally dissociation of the product regenerates the catalyst (Scheme 2.2).

To realize chirality transfer from an allylic aryl ether precursor through aromatic Claisen rearrangement, Trost and co-workers disclosed a method involving the first Pd-catalyzed asymmetric allylic etherification of a cyclic substrate using a phenol nucleophile, followed by diastereoselective Claisen rearrangement mediated by a lanthanide catalyst (*fod*, 6,6,7,7,8,8,8-heptafluoro-2,2-dimethyl-3,5-octanedionato).⁵⁶ The first step was successfully accomplished by using the (*R,R*)-Troost ligand ((*R,R*)-DACH-phenyl Trost ligand) providing high yields and enantioselectivities. Five-, six-, and seven-membered ring cyclic allyl carbonates were tolerated in this protocol, which permitted to access a wide scope of aryl ether intermediates and chiral rearranged products (Scheme 2.3).

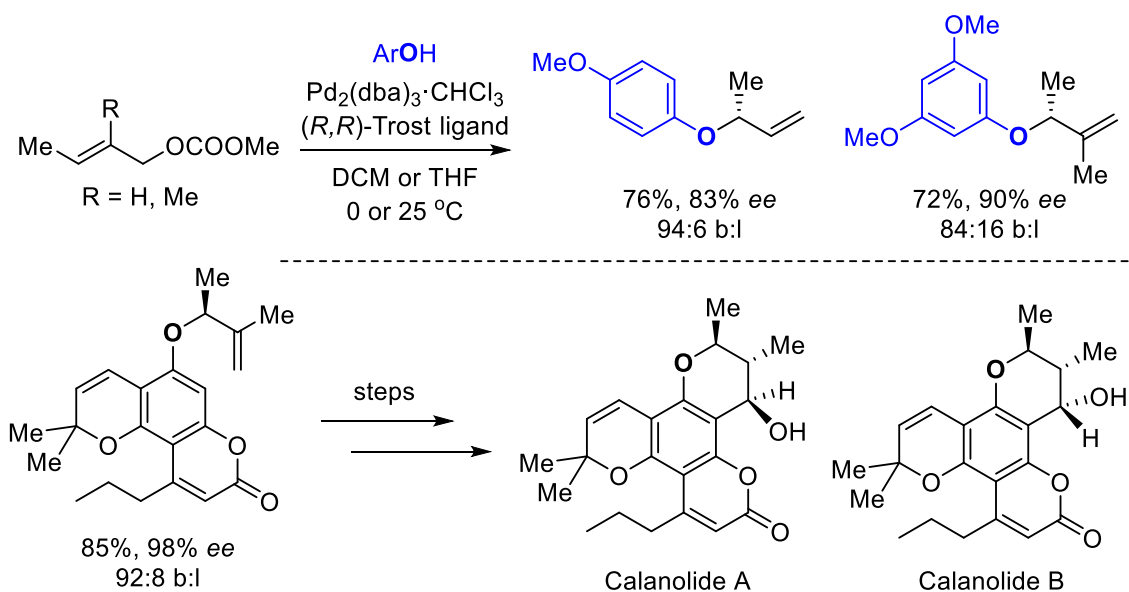


Scheme 2.3 Pd-catalyzed asymmetric allylic etherification of cyclic allylic precursors.

Compared to symmetrical π -allyl complexes ($R^1 = R^2$, Scheme 2.2), the development of allylic substitutions involving unsymmetrical intermediates ($R^1 \neq R^2$, Scheme 2.2) is much more interesting and challenging, because both regio- and enantioselectivity aspects must be controlled simultaneously. Several factors determine the regioselectivity of the nucleophilic attack on a monosubstituted intermediate. Steric factors will direct this attack to the less sterically demanding carbon center, while electronic factors tend to favor

(56) B. M. Trost, F. D. Toste, *J. Am. Chem. Soc.* **1998**, *120*, 815.

attack at the more electropositive secondary (internal) carbon atom. Additionally, for unsymmetrical allyl Pd(II) species, a propensity for attack at the less sterically hindered primary carbon was observed by using an achiral ligand and phenol type nucleophiles. To overcome this challenge, the Trost group developed an asymmetric regioselective allylic etherification process using crotyl (or tiglyl) methyl carbonate as substrate under Pd/(*R,R*)-Trost ligand catalysis (Scheme 2.4).⁵⁷ Furthermore, this efficient methodology could be applied to the enantioselective synthesis of chromans and chromanols, which culminated into a total synthesis of Calanolides A and B.



Scheme 2.4 Pd-catalyzed asymmetric allylic etherification of unsymmetrical allylic precursors.

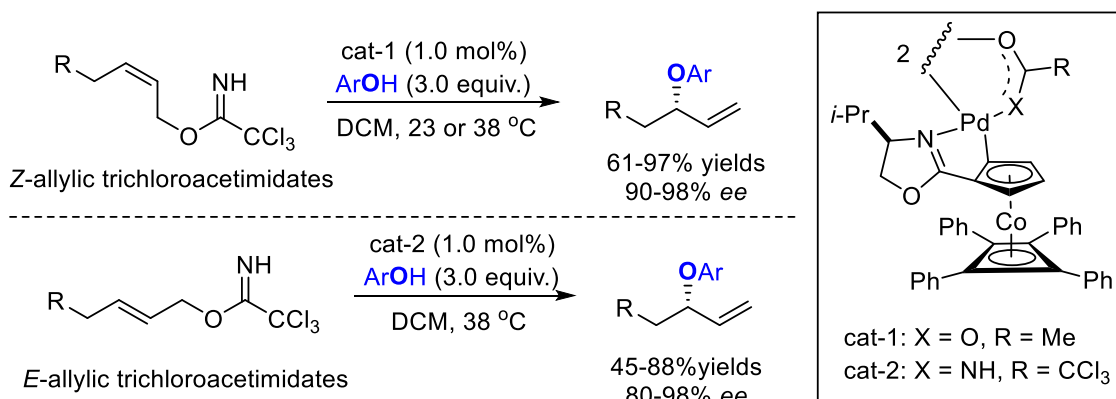
In 2007, Overman and coworkers discovered that the commercially available Pd(II) complex [COP-OAc]₂ (COP, cobalt oxazoline palladacycle) could act as an efficient pre-catalyst for the formation of enantioenriched secondary allylic aryl ethers starting from *Z*-allylic trichloroacetimidates and phenolic nucleophiles.⁵⁸ Afterwards, to overcome the limitations of competitive [3,3] sigmatropic rearrangements for the *E*-configured substrate, they developed a new type of COP catalyst. As a result, *E*-allylic trichloroacetimidates could be successfully transformed into the desired branched products in appreciable yields and high enantioselectivities (Scheme 2.5).⁵⁹ Mechanistic

(57) B. M. Trost, F. D. Toste, *J. Am. Chem. Soc.* **1998**, *120*, 9074.

(58) S. F. Kirsch, L. E. Overman, N. S. White, *Org. Lett.* **2007**, *9*, 911.

(59) A. C. Olson, L. E. Overman, H. F. Sneddon, J. W. Ziller, *Adv. Synth. Catal.* **2009**, *351*, 3186.

studies revealed that the reaction proceeds through nucleopalladation/deoxypalladation in a formal S_N2' process rather than via η^3 -allyl Pd(II) intermediates.⁶⁰

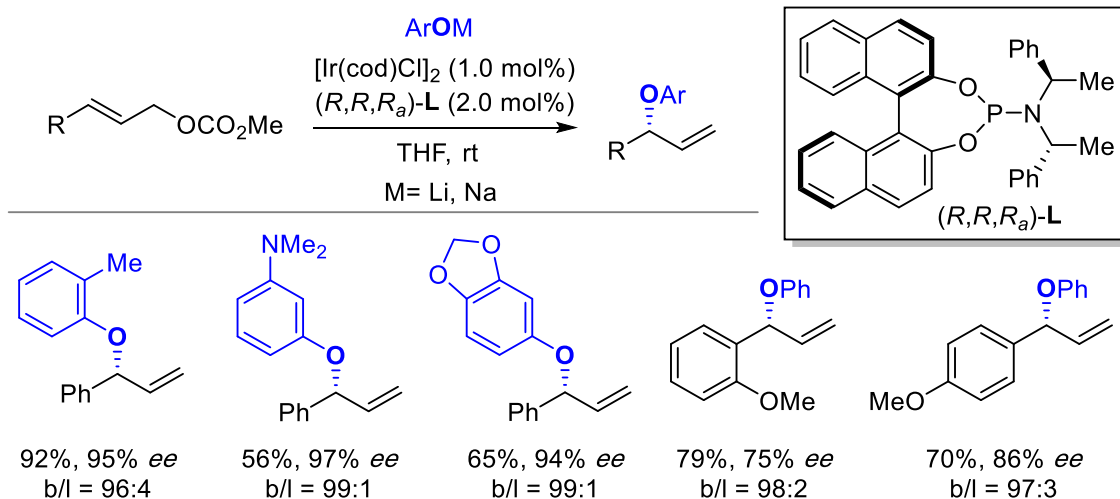


Scheme 2.5 Pd-catalyzed secondary allylic aryl ethers synthesis from allylic trichloroacetimidates and phenols.

Although Pd catalysts have played a dominant role in this area, other metal complexes have also been found to catalyze allylic etherification reactions often providing complementary stereochemical outcomes. Compared with Pd catalysis, Ir catalysts normally furnish branched products with excellent regio- and enantioselectivities, which may be attributed to the efficiency typically induced by chiral phosphoramidite ligands. Hartwig and coworkers reported in 2003 the first Ir-catalyzed enantioselective etherification of allylic carbonates using phenolic reagents (Scheme 2.6).⁶¹ The *in situ* generated phenoxide nucleophile derived from phenol by treatment with *n*-BuLi or NaH proved to be efficient nucleophiles. A wide range of allyl aryl ethers were obtained in high yields (up to 93%) and enantioselectivities (up to 97% *ee*). They also proved that the process is reversible, as a decrease of both enantioselectivity and regioselectivity was observed after prolonged reaction times.

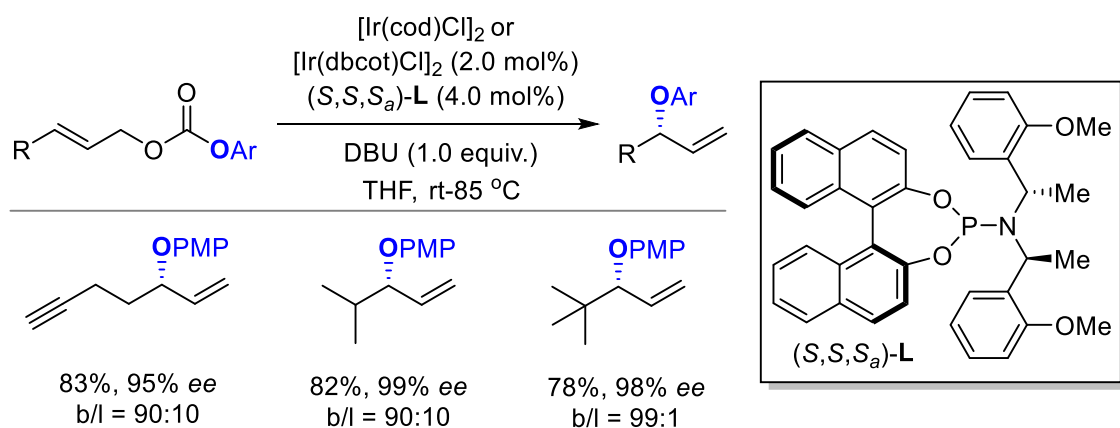
(60) J. S. Cannon, S. F. Kirsch, L. E. Overman, H. F. Sneddon, *J. Am. Chem. Soc.* **2010**, *132*, 15192.

(61) F. Lopez, T. Ohmura, J. F. Hartwig, *J. Am. Chem. Soc.* **2003**, *125*, 3426.



Scheme 2.6 Ir-catalyzed asymmetric allylic etherification using phenoxide nucleophiles.

Ir-catalyzed allylic etherification reactions with phenols usually require preformation of a suitable phenoxide salt, and they display lower selectivities when alkyl-substituted allylic substrates are used. In this context, Han developed a decarboxylative allylic etherification process for the asymmetric synthesis of allylic ethers with a wide product scope featuring the conversion of several alkyl allylic substrates ($R = \text{alkyl}$).⁶² The method could be further expanded to bulky alkyl groups by using $[\text{Ir}(\text{dbcot})\text{Cl}]_2$ (dbcot, dibenzo[*a,e*]cyclooctatetraene) as an Ir(I) precursor (Scheme 2.7).

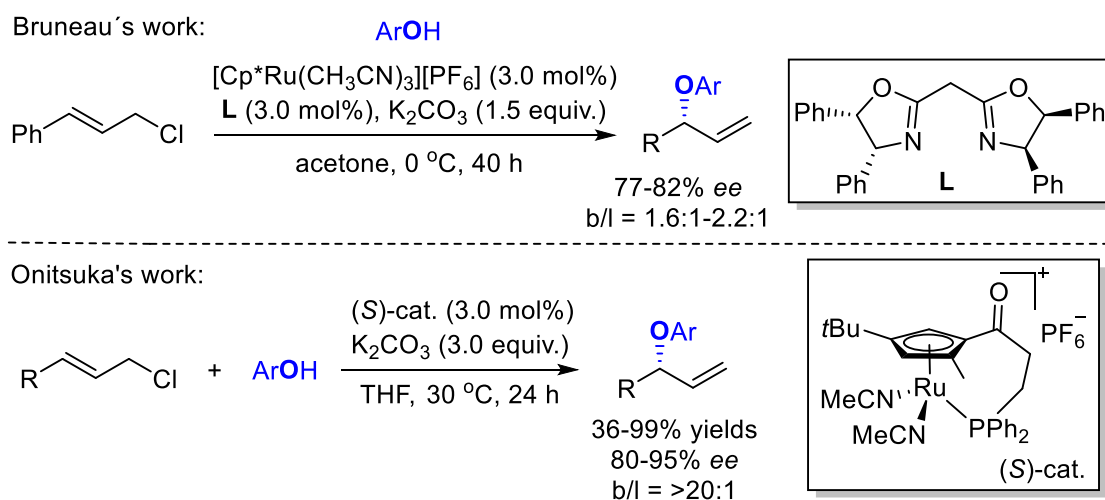


Scheme 2.7 Ir-catalyzed asymmetric decarboxylative allylic etherification of aryl allyl carbonates.

Ru catalysts are known to promote the regioselective formation of chiral branched compounds via allylic substitution from unsymmetrical precursors. Ru-catalyzed enantioselective etherification of allylic chlorides with phenols was first presented by

(62) D. Kim, S. Reddy, O. V. Singh, J. S. Lee, S. B. Kong, H. Han, *Org. Lett.* **2013**, *15*, 512.

Bruneau *et al.* in 2004.⁶³ Good enantioselectivities (up to 82% *ee*) and moderate regioselectivities was obtained utilizing a (pentamethylcyclopentadienyl) ruthenium precursor and a chiral bisoxazoline ligand. Later, Onitsuka and coworkers described the highly regio- and enantioselective allylic etherification of substituted cinnamyl chlorides.⁶⁴ The reaction proceeded smoothly giving the branched allylic ethers by switching to a planar-chiral Cp*Ru based complex (Scheme 2.8). Compared to the work from Bruneau, the conversion of crotyl chloride produced the branched allylic ether in 36% yield and with 80% *ee*.



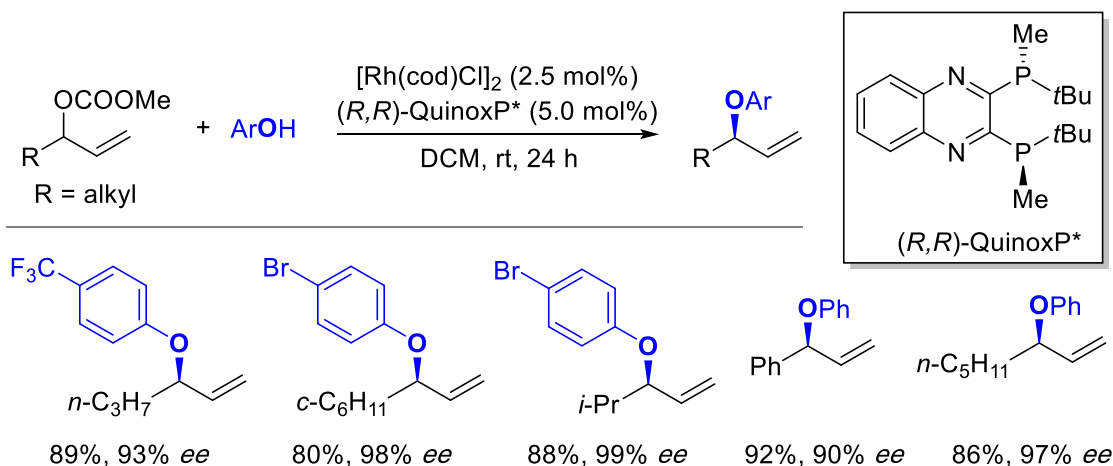
Scheme 2.8 Ru-catalyzed enantioselective etherification of allylic chlorides with phenols.

Rh-catalyzed allylic substitution is also known for providing high branched regioselectivity in contrast to Pd catalysis. Recently, Breit *et al.* reported a Rh-catalyzed dynamic kinetic asymmetric allylic etherification reaction using a Rh complex derived from the chiral and electron-rich ligand (*R,R*)-QuinoxP* giving the allylic aryl ethers in high regio- and enantioselectivities (Scheme 2.9).⁶⁵ This method proved to be efficient for a series of alkyl-substituted allylic carbonates, and thus complements known Ir- and Ru-catalyzed (intermolecular) allylic substitution reactions. Furthermore, compared to branched allylic substrates, the corresponding linear allylic substrates show lower reactivity in the presence of this Rh catalyst.

(63) M. D. Mbaye, J.-L. Renaud, B. Demerseman, C. Bruneau, *Chem. Commun.* **2004**, 1870.

(64) K. Onitsuka, H. Okuda, H. Sasai, *Angew. Chem. Int. Ed.* **2008**, *47*, 1454.

(65) C. Li, B. Breit, *Chem. Eur. J.* **2016**, *22*, 14655.



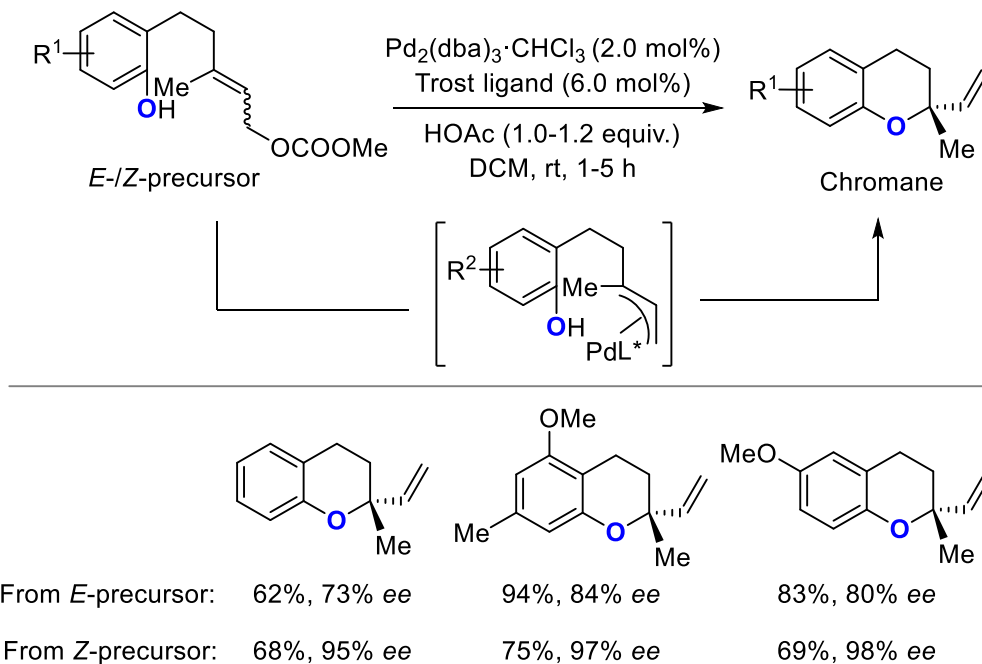
Scheme 2.9 Rh-catalyzed allylic etherification yielding chiral secondary allylic aryl ethers.

2.1.3 Pd-catalyzed Asymmetric Synthesis of Tertiary Allylic Aryl Ethers

Although TM-catalyzed allylic substitution has been well developed to provide secondary chiral allylic aryl ether products, regioselective synthesis of sterically more congested *tertiary* allylic aryl ethers featuring a quaternary stereocenter through allylic substitution from 1,1- or 3,3-disubstituted allylic precursors is still a huge challenge. Due to the inherently fast rate of bond formation in intramolecular reactions, seminal work from the Trost group illustrated the use of an intramolecular strategy to give rise to the desired aryl ethers by using suitable tethers thereby avoiding the formation of regioisomers.⁶⁶ The enantioselectivity of this Pd-catalyzed intramolecular allylic etherification process is presumably governed by the π - σ - π equilibration of diastereoisomeric allyl Pd(II) complexes (Curtin-Hammett conditions). They found that *Z*-configured trisubstituted olefins gave excellent *ee* (95-97%) by using (*S,S*)-Trost ligand when forming chromane products, being significantly higher than those obtained using their *E*-configured counterparts by using (*R,R*)-Trost ligand. These results were rationalized assuming that large *anti*-substituents are better accommodated by the chiral ligand than large *syn*-substituents (Scheme 2.10). Furthermore, this methodology was applied to the synthesis

(66) a) B. M. Trost, H. C. Shen, L. Dong, J.-P. Surivet, *J. Am. Chem. Soc.* **2003**, *125*, 9276; b) B. M. Trost, H. C. Shen, L. Dong, J.-P. Surivet, C. Sylvain, *J. Am. Chem. Soc.* **2004**, *126*, 11966; c) B. Cao, H. Park, M. M. Joullié, *J. Am. Chem. Soc.* **2002**, *124*, 520.

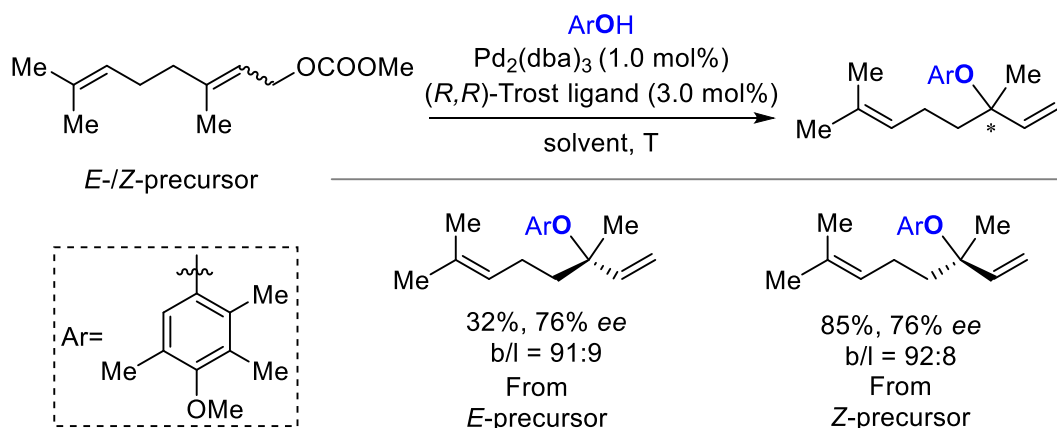
of some bioactive compounds such as the core unit of vitamin E, (+)-clusifoliol, (-)-siccadin and an advanced intermediate towards (+)-rhododaurichromanic acid A.



Scheme 2.10 Intramolecular allylic etherification for tertiary allylic aryl ether synthesis.

Compared with the well-developed intramolecular process for chiral tertiary allylic aryl ether synthesis, intermolecular processes of this kind are much more challenging and quite limited due to regioselectivity issues. Based on the results obtained in the preparation of secondary allylic aryl ethers, Trost and co-workers presented Pd-catalyzed allylic substitution for tertiary branched product synthesis using (*R,R*)-Trost ligand with good regioselectivity though moderately high enantioselectivity (Scheme 2.11).⁶⁷ The reported product scope was, however, narrow and the different stereoisomeric forms of the precursors gave opposite product enantiomers.

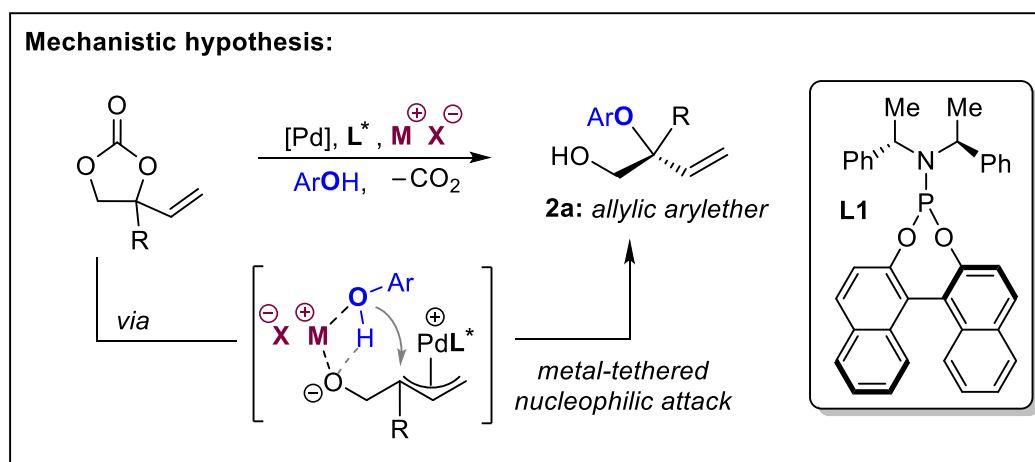
(67) For an additional example see: A. M. Sawayama, H. Tanaka, T. J. Wandless, *J. Org. Chem.* **2004**, *69*, 8810.



Scheme 2.11 Intermolecular allylic etherification producing tertiary allylic aryl ethers.

2.1.4 Aim of the Work presented in this Chapter

Despite the fact that a series of TM complexes have been studied for the asymmetric synthesis of allylic aryl ethers in the past decades, a general methodology that allows to access allylic aryl ethers featuring a quaternary stereocenters is still a challenging yet inspiring synthetic problem.



Scheme 2.12 Envisioned Pd-catalyzed asymmetric synthesis of allylic aryl ethers featuring quaternary stereocenters using VCCs.

Our group recently reported the first regio- and enantioselective synthesis of α,α -disubstituted allylic *N*-aryl amines based on a Pd-catalyzed conversion of cyclic carbonate **A** through a zwitterionic intermediate in presence of phosphoramidite ligand **L1** (Scheme 2.12).⁶⁸ Based on this previous research, we hypothesized the synthesis of enantioenriched tertiary aryl ethers of type **2a** would be feasible by using phenols as

(68) A. Cai, W. Guo, L. Martínez-Rodríguez, A. W. Kleij, *J. Am. Chem. Soc.* **2016**, *138*, 14194.

(pro)nucleophile. Additionally, considering the strong interaction between oxygen donors and alkali metal cationic species,⁶⁹ we envisaged that in the presence of a phosphoramidite ligand, the presence of suitable metal cations could help to direct the nucleophilic attack toward the internal carbon center of the Pd-allyl intermediate rather than the less hindered terminal one (Scheme 2.12). In this chapter, we disclose the first general method for regio- and enantioselective synthesis of allylic aryl ethers featuring quaternary stereocenters, which is based on a Pd-catalyzed allylic substitution using VCCs and phenol (pro)nucleophiles as reaction partners.

(69) a) N. Kumar, I. Leray, A. Depauw, *Coord. Chem. Rev.* **2016**, *310*, 1; b) M. R. Awual, T. Yaita, Y. Miyazaki, D. Matsumura, H. Shiwaku, T. Taguchi, *Sci. Rep.* **2016**, 19937.

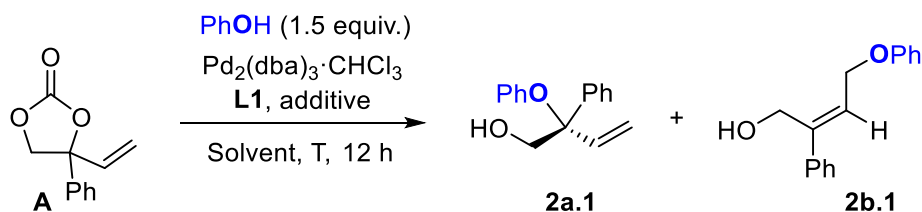
2.2 Results and Discussion

2.2.1 Screening Studies

Based on our previous research on asymmetric synthesis of α,α -disubstituted allylic *N*-aryl amines, we expected that the synthesis of enantioenriched tertiary aryl ether **2a.1** would be feasible by changing the nucleophile from aniline to phenol under similar reaction conditions. Thus, the reaction of carbonate **A** and phenol was performed, but unfortunately only 25% of the aryl ether **2a.1** was isolated. Notably, under these conditions a substantial amount of undesired linear product (**2b.1**) was formed (Table 2.1, entry 1).

In order to check our working hypothesis, Cs₂CO₃ was first examined as the metal cation source with the use of **L1**. We were pleased to find that the addition of three equiv. (equivalents) of Cs₂CO₃ led to appreciable product formation (**2a.1**; 56% yield) with an *er* of 87:13 and 76:24 b/l ratio (entries 2–4). The control reaction in the absence of Cs₂CO₃ only gave rise to 10% of product, pointing at a crucial role of the Cs salt towards regio- and enantiocontrol (entry 5). The reactions performed at lower concentration gave a slightly higher *er* and lower yield (entry 6). The use of other solvents/potassium salts did not improve the results significantly (entries 7–10). No reaction was observed in the presence of DBU suggesting that basicity is probably not a key parameter (entry 11). The use of CsF (entry 12) showed a similar outcome (*cf.*, entry 3) further confirming the key role of the Cs cation in this reaction. Lowering the reaction temperature to 0 °C significantly improved the yield (76%), enantioselectivity (*er* = 94.5:5.5) and regioselectivity (entries 12–13; b/l = 88:12) despite the requirement of longer reaction times.

Table 2.1: Optimization of the reaction conditions towards enantioenriched aryl ether **2a.1**^a



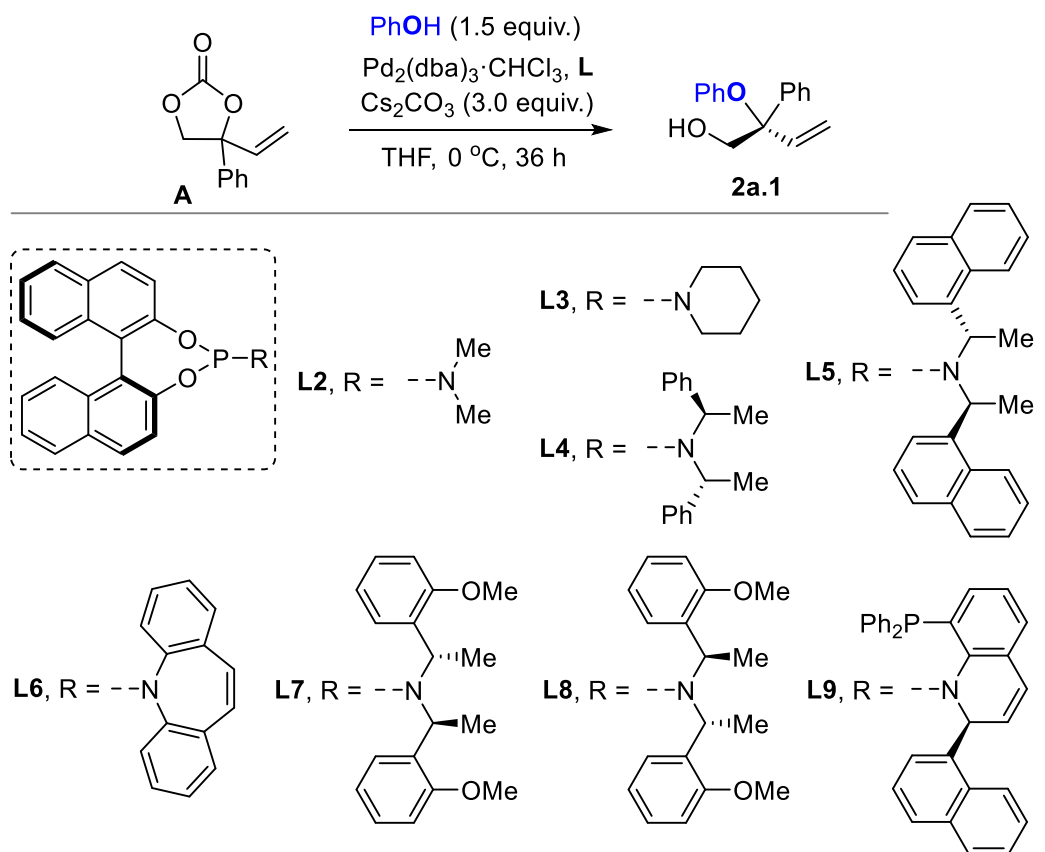
Entry	Solvent	T [°C]	Additive [equiv.]	b/l ^b	Yield of 2a.1 [%] ^c	<i>er</i> [%] ^d
1	THF	0	–	–	25	–
2	THF	25	Cs ₂ CO ₃ (1)	26:74	19	67.5:32.5
3	THF	25	Cs ₂ CO ₃ (2)	56:44	44	76:24
4	THF	25	Cs ₂ CO ₃ (3)	76:24	56	87:13
5	THF	25	–	–	10	–
6 ^e	THF	25	Cs ₂ CO ₃ (3)	75:25	53	88.5:11.5
7	DCM	25	Cs ₂ CO ₃ (3)	–	0	–
8	Toluene	25	Cs ₂ CO ₃ (3)	–	0	–
9	THF	25	K ₃ PO ₄ (3)	0:100	0	–
10	THF	25	K ₂ CO ₃ (3)	38:62	36	74:26
11	THF	25	DBU (3)	–	0	–
12	THF	25	CsF (3)	70:30	50	74.5:25.5
13	THF	10	Cs ₂ CO ₃ (3)	82:18	73	91:9
14 ^f	THF	0	Cs ₂ CO ₃ (3)	88:12	76	94.5:5.5

^aReaction conditions: carbonate **A** (0.20 mmol, 1.0 equiv.), phenol (1.5 equiv.), Pd₂(dba)₃·CHCl₃ (2.0 mol%), **L1** (8.0 mol%), solvent (0.20 mL), additive, 12 h, open to air.

^bDetermined by ¹H NMR. ^cIsolated yield of **2a.1**. ^dDetermined by HPLC. ^eUsing 0.30 mL of THF. ^f36 h.

Attempts to improve the enantioselectivity with other phosphoramidite ligands **L2–L9** was not successful (Table 2.2, entries 2–9). The presence of **L5**, **L7** and **L8** was beneficial for the yield of **2a.1**, however, lower enantiomeric excess were observed. A lower amount of phenol (entry 10) or catalyst loading (entry 11) gave slightly inferior results. Performing the reaction under diluted conditions gave **2a.1** in 85% yield with an *er* of 95:5 (entry 12), and these optimized reaction conditions were subsequently applied to investigate the product scope of these allylic etherifications.

Table 2.2: Effect of ligands towards the enantioenriched aryl ether **2a.1**^a



Entry	Ligand	T [°C]	Yield of 2a.1 [%] ^b	<i>er</i> [%] ^c
1	L1	0	76	94.5:95.5
2	L2	0	0	–
3	L3	0	0	–
4	L4	0	65	86:14
5	L5	0	81	78:22
6	L6	0	0	–
7	L7	0	88	85:15
8	L8	0	85	23:77
9	L9	0	0	–
10 ^d	L1	0	74	94:6
11 ^e	L1	0	74	94:6
12 ^f	L1	0	85	95:5

^aReaction conditions: carbonate **A** (0.20 mmol, 1.0 equiv.), phenol (1.5 equiv.), $\text{Pd}_2(\text{dba})_3 \cdot \text{CHCl}_3$ (2.0 mol%), **L** (8.0 mol%), THF (0.20 mL), C_2CO_3 (3.0 equiv.), open to air. ^bIsolated yield of **2a.1**. ^cDetermined by HPLC. ^dPhenol (1.2 equiv.). ^e $\text{Pd}_2(\text{dba})_3 \cdot \text{CHCl}_3$ (1.25 mol%), **L1** (5.0 mol%). ^fTHF (0.30 mL).

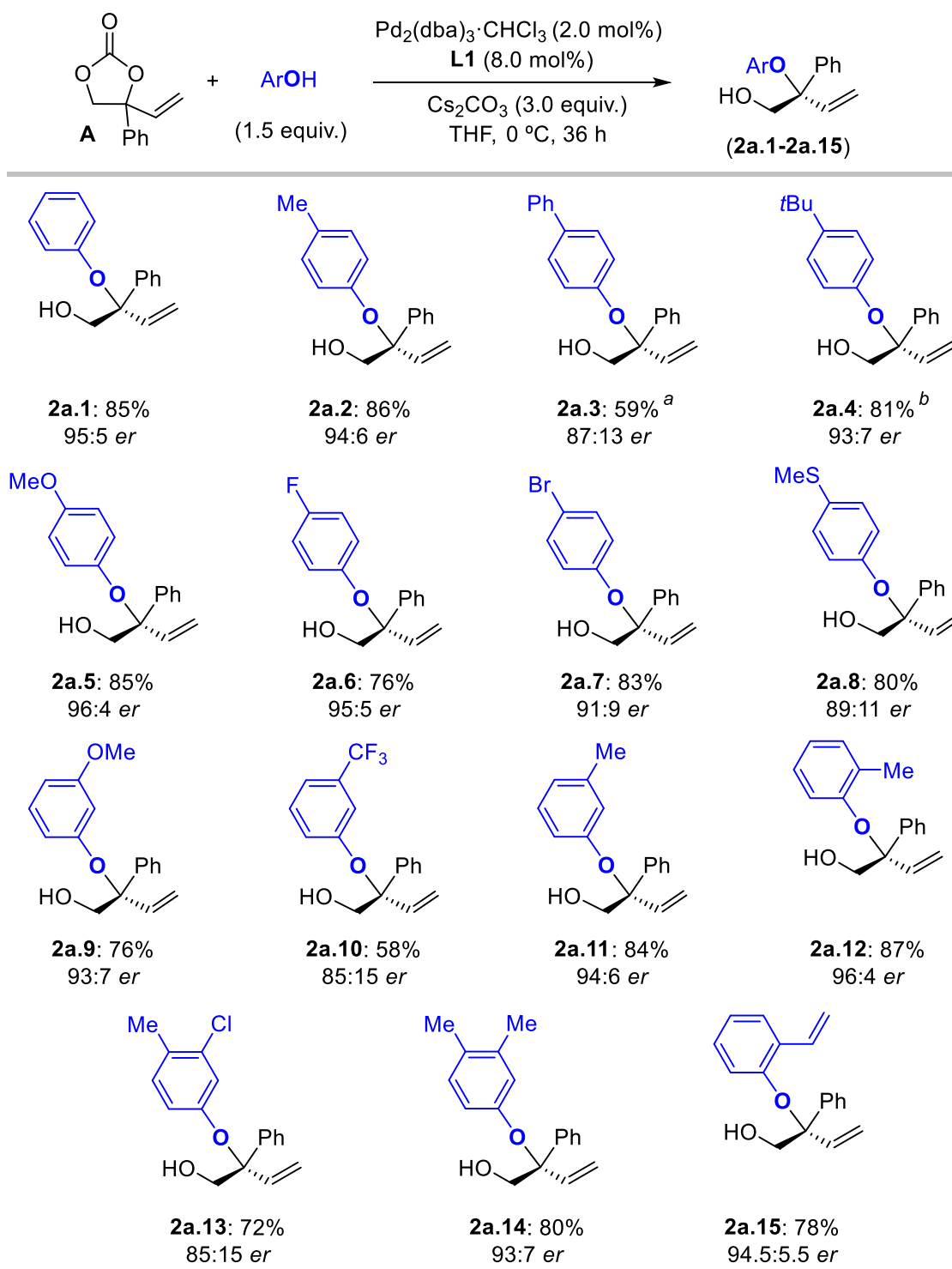
2.2.2 Scope of Substrates

With the optimized conditions of entry 12 in Table 2.2, we then set out to examine the scope of this method. Various substituted phenols proved to be suitable reaction partners to produce a range of allylic tertiary aryl ethers (Scheme 2.13) in good yields and appreciable enantioinduction (generally *er* >90:10). Various *para*-substitutions on the phenol reagents including electron -withdrawing and -donating groups were endorsed, and *meta*- (**2a.9–2a.11**), *ortho*- (**2a.12** and **2a.15**) and di-substituted phenols (**2a.13** and **2a.14**) also showed good reactivity. It is worth noting that the introduction of two vinyl fragments in the aryl ether product is feasible as exemplified by the successful isolation of product **2a.15**; this kind of product has potential in the synthesis of highly functionalized enantioenriched chromanes, which are important fragments in many drugs and natural products such as vitamin E, Clusifoliol, Siccanin and Calanolide A.

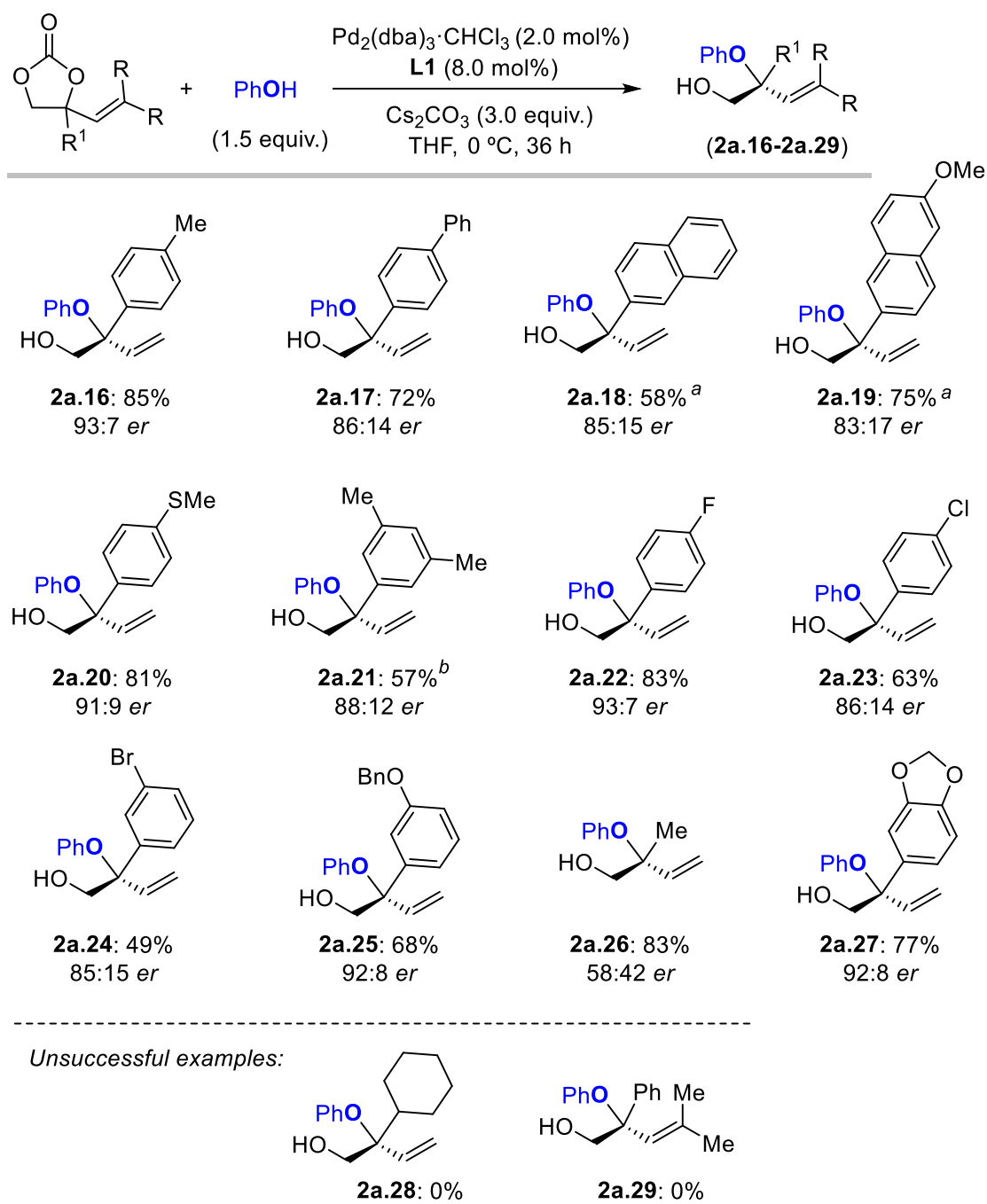
In order to further amplify the scope of this transformation, we then systematically varied the cyclic carbonate partner (Scheme 2.14). Various aromatic substituents in the VCC, including those having *para*- or *meta*-substitutions, were tolerated. The sulfur-containing substrate allowed to produce compound **2a.20** without noticeable deactivation of the palladium catalyst (see also product **2a.8**).⁷⁰ The aryl ethers with a bulky naphthyl group (**2a.18** and **2a.19**) could be obtained by using longer reaction times. The methyl-substituted cyclic carbonate also proved to be reactive albeit though a lack of enantio-discrimination was noted (**2a.26**), while the bulky cyclohexyl-substituted carbonate showed no reactivity at all (**2a.28**). The installation of a heterocycle in the aryl ether was feasible (**2a.27**),⁷¹ whereas attempts to install substituents on the vinyl group failed (**2a.29**). The absolute configuration of tertiary aryl ether **2a.20** (*S*) was deduced by the X-ray diffraction studies (see section 2.4.6, Figure 2.2).

(70) The sulfur-containing substrates have the potential to poison the Pd-catalyst and typically require higher reaction temperatures.

(71) Enantioenriched compounds with 1,3-benzodioxole fragments are of interest in pharmaceutical development, see: J. D. Bloom, M. D. Dutia, B. D. Johnson, A. Wissner, M. G. Burns, E. E. Largis, J. A. Dolan, T. H. Claus, *J. Med. Chem.* **1992**, *35*, 3081.



Scheme 2.13 The scope in phenolic reagents. Reaction conditions unless stated otherwise: all reactions were performed under the optimized conditions (Table 2.2, entry 12). Isolated yields are reported. ^a60 h. ^b45 h.



Scheme 2.14 The scope in VCCs. Reaction conditions unless stated otherwise: all reactions were performed under the optimized conditions (Table 2.2, entry 12). Isolated yields are reported. ^a60 h. ^bUsing 0.20 mL of THF.

2.2.3 Z-Stereoselective Formation of the Linear Allylic Aryl Ethers

Table 2.3: Optimization of the reaction conditions towards the formation of Z-linear allylic aryl ethers^a

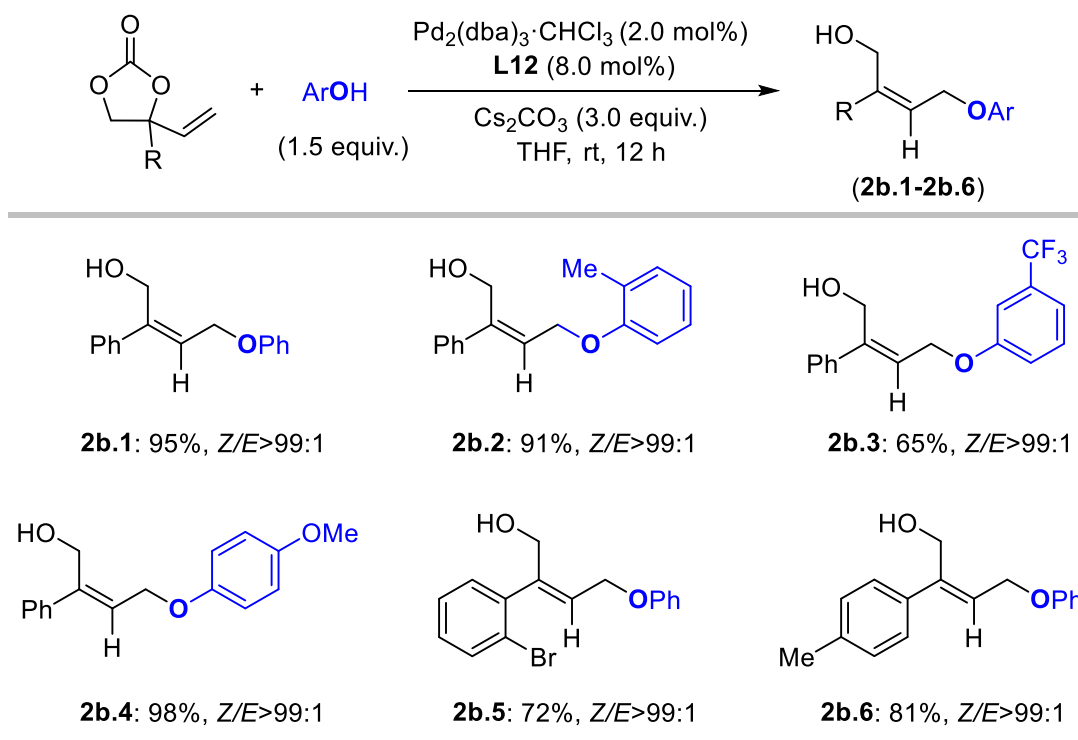
Entry	Ligand	Additive (equiv.)	Yield of 2b.1 [%] ^b	1/b ^c	Z/E ^c
1	L10	–	57	>99:1	>99:1
2	L11	–	69	99:1	>99:1
3	L12	–	88	91:9	>99:1
4	L13	–	79	>99:1	>99:1
5	L14	–	82	>99:1	>99:1
6	L12	Cs ₂ CO ₃ (3)	98	>99:1	>99:1

^aReaction conditions: carbonate **A** (0.20 mmol, 1.0 equiv.), phenol (1.5 equiv.), Pd₂(dba)₃·CHCl₃ (2.0 mol%), monodentate ligand (8.0 mol%) or bidentate ligand (4.0 mol%), THF (0.20 mL), rt, open to air. ^bDetermined by ¹H NMR using toluene as an internal standard. ^cDetermined by ¹H NMR.

Encouraged by our previous success in Z-stereoselective synthesis of linear allylic products,⁷² we also probed the regio- and stereoselective synthesis of highly functionalized linear allylic aryl ethers through an *in situ* formed six-membered palladacyclic intermediate in the presence of suitable ligand. We first selected the reaction between phenol and cyclic carbonate **A** in THF at rt as a model system (Table 2.3). The use of **L10** led to an appreciable yield of the linear product **2b.1** (57%) while the branched product **2b.1** was not observed. Further screening of ligands (**L11–L14**) suggested that **L12** is the best ligand among the series tested for the selective formation of linear allylic aryl ether **2b.1** (88%). In contrast, only a small amount of the branched product **2a.1** (<9%)

(72) a) W. Guo, L. Martínez-Rodríguez, R. Kuniyil, E. Martín, E. C. Escudero-Adán, F. Maseras, A. W. Kleij, *J. Am. Chem. Soc.* **2016**, *138*, 11970; b) W. Guo, L. Martínez-Rodríguez, E. Martín, E. C. Escudero-Adán, A. W. Kleij, *Angew. Chem. Int. Ed.* **2016**, *55*, 11037; c) J. E. Gómez, W. Guo, A. W. Kleij, *Org. Lett.* **2016**, *18*, 6042.

was observed suggesting that a judicious choice of the ligand is crucial to control the regioselectivity. Interestingly, the formation of branched product was further suppressed by the addition of Cs₂CO₃ and the yield of the linear product was improved to 98% indicating a subtle role of Cs₂CO₃ in this ligand-governed process. It is worth noting that the use of ligands **L10–L14** gave rise to product **2b.1** with excellent stereoselectivity (*Z/E*>99:1).



Scheme 2.15 Preparation of linear allylic aryl ethers. Reaction conditions unless stated otherwise: optimized conditions from Table 2.3, entry 6. Isolated yields.

With the conditions optimized, the formation of linear allylic aryl ethers **2b.1–2b.6** was then investigated (Scheme 2.15) and showed in all cases good yields and excellent stereoselectivity. The *Z*-configuration of all the linear products was supported by ¹H-selective 1D NOESY NMR analysis.

2.3 Conclusions

Significant progress has been observed in recent years in the synthesis of allylic aryl ethers, which are valuable building blocks in synthetic chemistry. Although the regio- and enantioselective construction of secondary allylic aryl ether from phenols (or phenoxides) and prochiral allylic precursors has been well developed using Pd, Rh, Ru, or Ir catalysts, the asymmetric construction of sterically more demanding tertiary allylic aryl ether products has proven to be very challenging and quite limited.

In this chapter, we present a general method for the synthesis of such enantioenriched tertiary allylic aryl ethers through a Pd-catalyzed decarboxylative allylic substitution reaction that employs modular VCCs and phenol type nucleophiles with a readily available phosphoramidite ligand (**L1**). The addition of Cs₂CO₃ proved to be crucial toward the formation of sterically hindered branched products using **L1**. A judicious choice of the ligand (i.e., **L12**) switches the regioselectivity toward the *Z*-stereoselective formation of highly functionalized linear products and the Cs additive then suppresses the formation of the branched regioisomer. This mild protocol is characterized by a fair scope in reaction partners, overall good yields and either appreciably high enantio-induction (for the branched products) or high stereoselectivity (for the linear congeners).

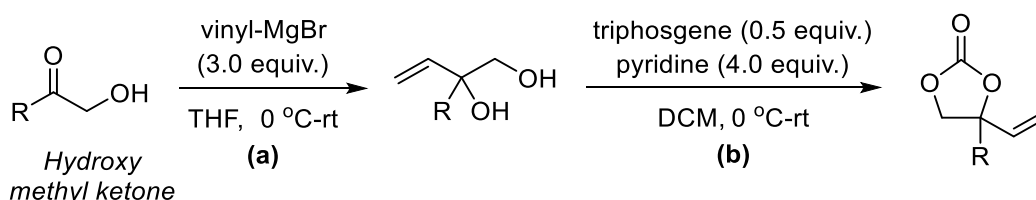
2.4 Experimental Section

2.4.1 General Considerations

Commercially available phenols and solvents were purchased from Aldrich or TCI, and used without further purification. The palladium precursors and bases were purchased from Aldrich. Phosphoramidites **L1**, **L3–L6**, **L8–L12** were purchased from Aldrich or Strem; **L2**⁷³ and **L7**⁷⁴ were prepared according to previously reported procedures. All racemic allylic aryl ethers compounds were made using (*rac*)-**L1**. ¹H NMR, ¹³C NMR, ¹⁹F NMR spectra were recorded at room temperature on a Bruker AV-400 or AV-500 spectrometer and referenced to the residual deuterated solvent signals. All reported NMR values are given in parts per million (ppm). FT-IR measurements were carried out on a Bruker Optics FTIR Alpha spectrometer. Chiral high-performance liquid chromatography (HPLC) analysis, Mass spectrometric analyses and X-ray diffraction studies were performed by the Research Support Group at ICIQ. Note: EA stands for ethyl acetate.

2.4.2 General Procedure for the Synthesis of VCCs

The vinyl-carbonates can be easily prepared according to a previous reported procedure with minor modifications (Scheme 2.16).⁷⁵



Step (a): To a solution of the respective hydroxy methyl ketone (5.0 mmol, 1.0 equiv.) in THF (20 mL) was added vinyl magnesium bromide (1.0 M in THF, 2.5 equiv.) at 0 °C. The reaction was stirred under an N₂ atmosphere at room temperature for 2 h. The reaction mixture was then quenched with saturated aqueous NH₄Cl, and extracted with EtOAc (ethyl acetate). The combined organic layers were dried over anhydrous Na₂SO₄, filtered

(73) C. R. Smith, D. J. Mans, T. V. RajanBabu, *Org. Synth.* **2008**, *85*, 238.

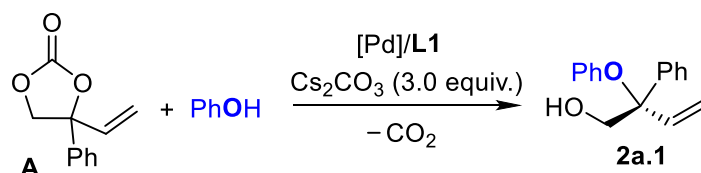
(74) D. Polet, A. Alexakis, K. Tissot-Croset, C. Corminboeuf, K. Ditrach, *Chem. Eur. J.* **2006**, *12*, 3596.

(75) a) A. Khan, R. Zheng, Y. Kan, J. Ye, J. Xing, Y. J. Zhang, *Angew. Chem. Int. Ed.* **2014**, *53*, 6439;
 b) A. Khan, L. Yang, J. Xu, L. Y. Jin, Y. J. Zhang, *Angew. Chem. Int. Ed.* **2014**, *53*, 11257.

and concentrated affording the diol product as a light yellow oil, which was directly used in next step.

Step (b): To a solution of the diol (1.0 equiv.) in DCM (30 mL) was added pyridine (20.0 mmol, 4.0 equiv.) and triphosgene (2.5 mmol, 0.5 equiv.) at 0 °C. The reaction was stirred under an N₂ atmosphere at room temperature for 2 h. The reaction mixture was then quenched with saturated aqueous NH₄Cl, washed with H₂O, and extracted with DCM. The combined organic layers were dried over anhydrous Na₂SO₄, filtered and concentrated. The residue was purified by flash chromatography on silica to afford the corresponding carbonate.

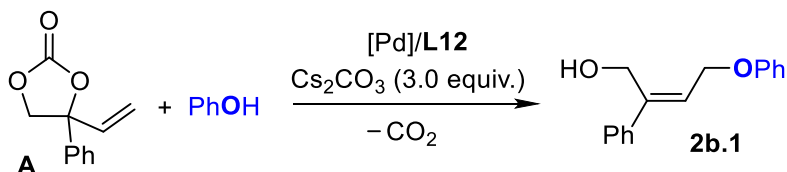
2.4.3 Typical Procedure for the Formation of Branched Aryl Ethers



Representative case:

Carbonate **A** (0.20 mmol, 0.0380 g, 1.0 equiv.) was combined with Pd₂(dba)₃·CHCl₃ (0.0041 g, 2.0 mol%), **L1** (0.0086 g, 8.0 mol%) and phenol (0.0282 g, 1.5 equiv.) in THF (0.30 mL) at room temperature in air. The reaction mixture was stirred at 0 °C for 36 h, after which the reaction mixture was mixed with 15 mL DCM and then washed with NaOH (0.1 N, 2 × 5 mL), brine (10 mL), dried (MgSO₄), filtered and the solvent was removed in vacuum. The residue was subjected to flash column chromatography and the pure product **2a.1** was isolated (40.8 mg, 85%) (Hexane/EtOAc = 50:1, R_f = 0.15). The *er* values were determined by HPLC equipped with a chiral column.

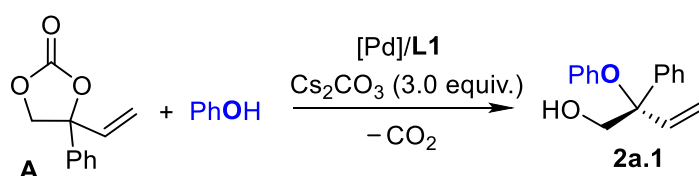
2.4.4 Typical Procedure for the Formation of Linear Aryl Ethers



Representative case:

Carbonate **A** (0.20 mmol, 0.0380 g, 1.0 equiv.) was combined with Pd₂(dba)₃·CHCl₃ (0.0041 g, 2.0 mol%), **L12** (0.0043 g, 8.0 mol%) and phenol (0.0282 g, 1.5 equiv.) in THF (0.20 mL) at room temperature in air. The reaction mixture was stirred at room temperature for 12 h. Once the reaction had finished, the reaction mixture was purified by flash column chromatography (Hexane/EtOAc = 10:1, *R_f* = 0.20) and the pure product **2b.1** was isolated (45.5 mg, 95%).

2.4.5 Typical Procedure for the Formation of **2a.1** at a 1.1 mmol Scale



Carbonate **A** (1.1 mmol, 0.2090 g, 1.0 equiv.) was combined with Pd₂(dba)₃·CHCl₃ (0.0226 g, 2.0 mol%), **L1** (0.0473 g, 8.0 mol%) and phenol (0.1551 g, 1.5 equiv.) in THF (1.65 mL) at room temperature open to air. The reaction mixture was stirred at 0 °C for 36 h, after which the reaction mixture was mixed with 30 mL of DCM and then washed with NaOH (0.1 M, 2 × 10 mL), brine (10 mL), dried over MgSO₄ and filtered. The solvent was removed in vacuo. The residue was subjected to flash column chromatography (Hexane/EtOAc = 50:1, *R_f* = 0.15), and the pure product **2a.1** was isolated (0.2135 g, 81%) with an *er* of 95:5 as determined by HPLC equipped with a chiral column).

2.4.6 X-ray Crystallographic Studies

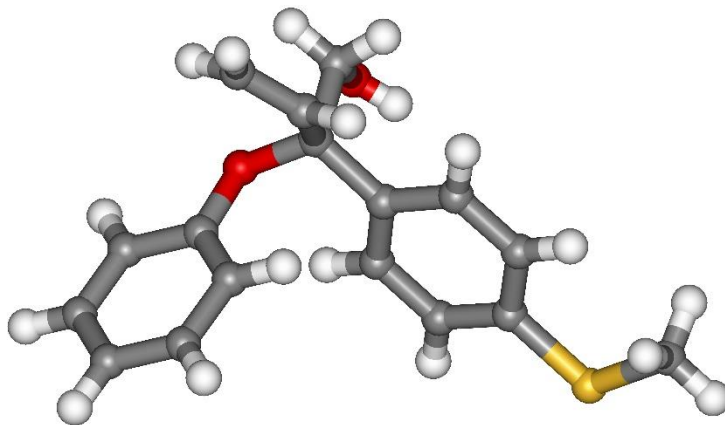


Figure 2.2 X-ray analysis of (*S*)-tertiary aryl ether **2a.20**.

General procedure:

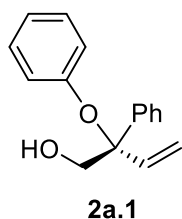
The measured crystal of **2a.20** was stable under atmospheric conditions; nevertheless, they were treated under inert conditions immersed in perfluoro-polyether as protecting oil for manipulation. Data Collection: measurements were made on a Bruker-Nonius diffractometer equipped with an APPEX II 4K CCD area detector, a FR591 rotating anode with Mo K α radiation, Montel mirrors and a Kryoflex low temperature device (T = -173 °C). Full-sphere data collection was used with ω and φ scans. Programs used: Data collection Apex2 V2011.3 (Bruker-Nonius 2008), data reduction Saint+Version 7.60A (Bruker AXS 2008) and absorption correction SADABS V. 2008-1 (2008). Structure Solution: SHELXTL Version 6.10 (Sheldrick, 2000) was used.⁷⁶ Structure Refinement: SHELXTL-97-UNIX VERSION.

Crystal data for 2a.20:

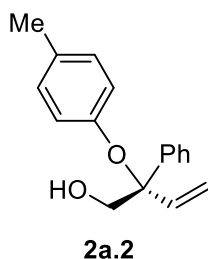
C₁₇H₁₈O₂S, Mr = 286.37, monoclinic, C2, $a = 19.4127(5)$ Å, $b = 5.7269(2)$ Å, $c = 13.0858(6)$ Å, $\alpha = 90^\circ$, $\beta = 92.163(3)^\circ$, $\gamma = 90^\circ$, $V = 1453.77(9)$ Å³, $Z = 4$, $\rho = 1.308$ mg·M⁻³, $\mu = 0.221$ mm⁻¹, $\lambda = 0.71073$ Å, T = 100(2) K, $F(000) = 608$, crystal size = 0.20 × 0.04 × 0.02 mm³, $\theta(\text{min}) = 2.100^\circ$, $\theta(\text{max}) = 34.573^\circ$, 21979 reflections collected, 5905 reflections unique ($R_{\text{int}} = 0.0422$), GoF = 1.062, $R_1 = 0.0368$ and $wR_2 = 0.0955$ [$I > 2\sigma(I)$], $R_1 = 0.0423$ and $wR_2 = 0.0975$ (all indices), min/max residual density = -0.268/0.433 [e·Å⁻³], $x = -0.03(3)$. Completeness to $\theta(34.573^\circ) = 97.5\%$.

(76) G. M. Sheldrick, *SHELXTL Crystallographic System*, version 6.10; Bruker AXS, Inc.: Madison, WI, 2000.

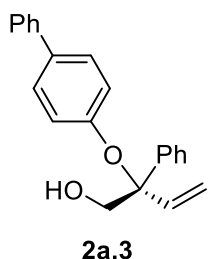
2.4.7 Analytical Data for All Compounds



Scale: 0.20 mmol; isolated 40.8 mg (85% yield), light yellow oil, Hexane : EA = 50 : 1, $R_f = 0.15$. $^1\text{H NMR}$ (400 MHz, CDCl_3) δ 7.50 – 7.43 (m, 2H), 7.40 – 7.33 (m, 2H), 7.33 – 7.27 (m, 1H), 7.17 – 7.07 (m, 2H), 6.88 (t, $J = 7.4$ Hz, 1H), 6.39 (dd, $J = 17.5, 11.1$ Hz, 1H), 5.51 (dd, $J = 11.2, 1.0$ Hz, 1H), 5.44 (dd, $J = 17.5, 1.0$ Hz, 1H), 3.97 – 3.81 (m, 2H), 2.06 (dd, $J = 7.5, 6.3$ Hz, 1H) ppm. $^{13}\text{C NMR}$ (101 MHz, CDCl_3) δ 155.15, 139.86, 135.57, 128.86, 128.68, 127.97, 126.88, 121.44, 119.82, 119.67, 84.90, 70.48 ppm. **IR** (neat): ν (cm^{-1}) = 3282, 3058, 2927, 2852, 1597, 1503, 1446, 1338, 995, 748, 692. **HRMS** (ESI+, MeOH): m/z calcd. 263.1043 ($\text{M} + \text{Na}$)⁺, found: 263.1043. **HPLC** conditions: Chiralpak IA 250 \times 4.6 mm, 5 μm , Hex/MTBE = 80 : 20, 1 mL/min; 95:5 *er*; $[\alpha]_{\text{D}}^{25} = -56.03$ ($c = 0.12$, CHCl_3). Hex = hexane, MTBE = methyl *tert*-butyl ether.

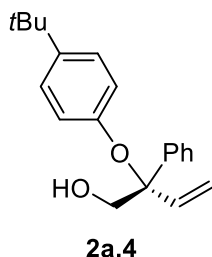


Scale: 0.20 mmol; isolated 43.5 mg (86% yield), light yellow oil, Hexane : EA = 50 : 1, $R_f = 0.15$. $^1\text{H NMR}$ (400 MHz, CDCl_3) δ 7.49 – 7.43 (m, 2H), 7.39 – 7.33 (m, 2H), 7.33 – 7.27 (m, 1H), 6.92 (d, $J = 8.7$ Hz, 2H), 6.64 (d, $J = 8.6$ Hz, 2H), 6.35 (dd, $J = 17.5, 11.1$ Hz, 1H), 5.49 (d, $J = 11.1$ Hz, 1H), 5.43 (d, $J = 17.5$ Hz, 1H), 3.96 – 3.82 (m, 2H), 2.22 (s, 3H), 2.08 (t, $J = 6.8$ Hz, 1H) ppm. $^{13}\text{C NMR}$ (101 MHz, CDCl_3) δ 152.84, 140.06, 135.88, 130.85, 129.38, 128.62, 127.90, 126.92, 119.81, 119.49, 84.77, 70.15, 20.62 ppm. **IR** (neat): ν (cm^{-1}) = 3371, 3027, 2922, 2855, 1610, 1506, 1447, 1222, 1050, 927, 813, 700. **HRMS** (ESI+, MeOH): m/z calcd. 277.1199 ($\text{M} + \text{Na}$)⁺, found: 277.1197. **HPLC** conditions: Chiralpak IC 250 \times 4.6 mm, 5 μm , Hex/MTBE = 80 : 20, 1 mL/min; 94:6 *er*; $[\alpha]_{\text{D}}^{25} = -46.21$ ($c = 0.11$, CHCl_3).

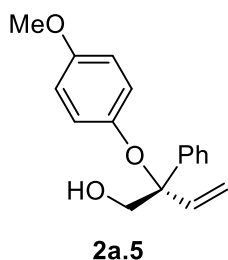


Scale: 0.20 mmol; isolated 37.0 mg (59% yield), light yellow solid, Hexane : EA = 50 : 1, $R_f = 0.15$. $^1\text{H NMR}$ (400 MHz, CDCl_3) δ 7.53 – 7.46 (m, 4H), 7.43 – 7.36 (m, 5H), 7.36 – 7.26 (m, 3H), 6.88 – 6.76 (m, 2H), 6.44 (dd, $J = 17.5, 11.1$ Hz, 1H), 5.55 (dd, $J = 11.2, 1.0$ Hz, 1H), 5.50 (dd, $J = 17.5, 1.0$ Hz, 1H), 4.00 – 3.85 (m, 2H), 2.12 (s, 1H) ppm. $^{13}\text{C NMR}$ (101 MHz, CDCl_3) δ 154.73, 140.74, 139.76, 135.45, 134.30, 128.78, 128.73, 128.02, 127.49, 126.87, 126.82, 126.80, 119.94, 119.81, 85.04, 70.56 ppm. **IR** (neat): ν (cm^{-1}) = 3393, 2984, 2925, 2856, 1594, 1490, 1374, 1227, 1059, 926, 757, 696. **HRMS**

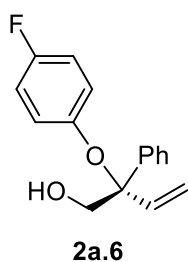
(ESI+, MeOH): m/z calcd. 339.1356 ($M + Na$)⁺, found: 339.1365. **HPLC** conditions: Chiralpak IC 250 × 4.6 mm, 5 μm, Hex/MTBE = 80 : 20, 1 mL/min; 87:13 *er*; $[\alpha]_D^{25} = -44.09$ ($c = 0.10$, CHCl₃).



Scale: 0.20 mmol; isolated 47.9 mg (81% yield), light yellow oil, Hexane : EA = 50 : 1, $R_f = 0.15$. **¹H NMR** (400 MHz, CDCl₃) δ 7.50 – 7.45 (m, 2H), 7.39 – 7.34 (m, 2H), 7.33 – 7.28 (m, 1H), 7.15 – 7.09 (m, 2H), 6.69 – 6.63 (m, 2H), 6.35 (dd, $J = 17.5, 11.2$ Hz, 1H), 5.49 (dd, $J = 11.1, 1.0$ Hz, 1H), 5.44 (dd, $J = 17.5, 1.1$ Hz, 1H), 3.98 – 3.81 (m, 2H), 1.24 (s, 9H) ppm. **¹³C NMR** (101 MHz, CDCl₃) δ 152.70, 144.14, 140.20, 135.97, 128.62, 127.87, 126.90, 125.68, 119.45, 119.24, 84.70, 70.06, 34.19, 31.59 ppm. **IR** (neat): ν (cm⁻¹) = 2959, 2866, 1606, 1508, 1447, 1363, 1232, 1182, 829, 760, 701. **HRMS** (ESI+, MeOH): m/z calcd. 319.1669 ($M + Na$)⁺, found: 319.1668. **HPLC** conditions: Chiralpak IA 250 × 4.6 mm, 5 μm, Hex/MTBE = 80 : 20, 1 mL/min; 93:7 *er*; $[\alpha]_D^{25} = -31.72$ ($c = 0.10$, CHCl₃).

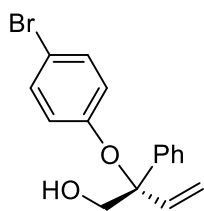


Scale: 0.20 mmol; isolated 45.5 mg (85% yield), light yellow oil, Hexane : EA = 50 : 1, $R_f = 0.15$. **¹H NMR** (400 MHz, CDCl₃) δ 7.52 – 7.43 (m, 2H), 7.40 – 7.28 (m, 3H), 6.75 – 6.63 (m, 4H), 6.27 (dd, $J = 17.6, 11.1$ Hz, 1H), 5.48 (dd, $J = 11.1, 1.1$ Hz, 1H), 5.42 (dd, $J = 17.6, 1.1$ Hz, 1H), 3.99 – 3.81 (m, 2H), 3.72 (s, 3H), 2.04 (t, $J = 6.7$ Hz, 1H) ppm. **¹³C NMR** (101 MHz, CDCl₃) δ 154.58, 148.75, 140.14, 136.36, 128.59, 127.96, 127.07, 121.47, 119.33, 114.02, 84.98, 69.27, 55.64 ppm. **IR** (neat): ν (cm⁻¹) = 3057, 2929, 2833, 1601, 1503, 1446, 1210, 1034, 927, 826, 773, 701. **HRMS** (ESI+, MeOH): m/z calcd. 293.1148 ($M + Na$)⁺, found: 293.1155. **HPLC** conditions: Chiralpak IA 250 × 4.6 mm, 5 μm, Hex/IPA = 98 : 2, 1 mL/min; 96:4 *er*; $[\alpha]_D^{25} = -39.25$ ($c = 0.11$, CHCl₃).



Scale: 0.20 mmol; isolated 39.0 mg (76% yield), light yellow oil, Hexane : EA = 50 : 1, $R_f = 0.15$. **¹H NMR** (400 MHz, CDCl₃) δ 7.48 – 7.42 (m, 2H), 7.40 – 7.34 (m, 2H), 7.34 – 7.29 (m, 1H), 6.84 – 6.77 (m, 2H), 6.73 – 6.66 (m, 2H), 6.31 (dd, $J = 17.5, 11.1$ Hz, 1H), 5.51 (dd, $J = 11.1, 1.0$ Hz, 1H), 5.43 (dd, $J = 17.5, 1.0$ Hz, 1H), 3.98 – 3.80 (m, 2H),

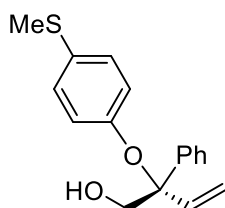
2.02 (s, 1H) ppm. ^{13}C NMR (101 MHz, CDCl_3) δ 158.98, 156.60, 151.06, 151.03, 139.60, 135.67, 128.72, 128.13, 126.98, 121.30, 121.22, 119.74, 115.43, 115.20, 85.24, 69.80 ppm. ^{19}F NMR (376 MHz, CDCl_3) δ -122.74 ppm. IR (neat): ν (cm^{-1}) = 3413, 3059, 2925, 1600, 1499, 1447, 1200, 1051, 1008, 929, 828, 785, 757, 701. HRMS (ESI+, MeOH): m/z calcd. 281.0948 ($\text{M} + \text{Na}$) $^+$, found: 281.0942. HPLC conditions: Chiralpak IC 250 \times 4.6 mm, 5 μm , Hex/MTBE = 80 : 20, 1 mL/min; 95:5 *er*; $[\alpha]_{\text{D}}^{25} = -44.70$ ($c = 0.10$, CHCl_3).



2a.7

Scale: 0.20 mmol; isolated 52.7 mg (83% yield), light yellow oil, Hexane : EA = 50 : 1, $R_f = 0.15$. ^1H NMR (400 MHz, CDCl_3) δ 7.44 – 7.40 (m, 2H), 7.39 – 7.34 (m, 2H), 7.34 – 7.29 (m, 1H), 7.23 – 7.17 (m, 2H), 6.68 – 6.54 (m, 2H), 6.38 (dd, $J = 17.5, 11.2$ Hz, 1H), 5.53 (dd, $J = 11.1, 0.9$ Hz, 1H), 5.43 (dd, $J = 17.5, 0.9$ Hz, 1H), 3.94 – 3.78 (m, 2H), 2.01 (s, 1H) ppm.

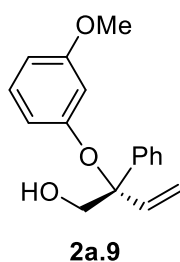
^{13}C NMR (101 MHz, CDCl_3) δ 154.30, 139.20, 134.93, 131.72, 128.81, 128.18, 126.81, 121.42, 120.04, 113.79, 85.25, 70.60 ppm. IR (neat): ν (cm^{-1}) = 2923, 1586, 1483, 1477, 1278, 1228, 1170, 1070, 1004, 929, 821, 760, 700, 504. HRMS (ESI+, MeOH): m/z calcd. 341.0148 ($\text{M} + \text{Na}$) $^+$, found: 341.0145. HPLC conditions: Chiralpak IC 250 \times 4.6 mm, 5 μm , Hex/MTBE = 80 : 20, 1 mL/min; 91:9 *er*; $[\alpha]_{\text{D}}^{25} = -40.73$ ($c = 0.09$, CHCl_3).



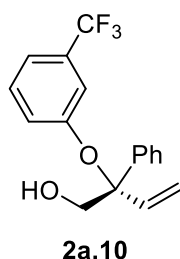
2a.8

Scale: 0.20 mmol; isolated 45.7 mg (80% yield), light yellow solid, Hexane : EA = 50 : 1, $R_f = 0.15$. ^1H NMR (400 MHz, CDCl_3) δ 7.46 – 7.42 (m, 2H), 7.39 – 7.34 (m, 2H), 7.33 – 7.28 (m, 1H), 7.09 – 7.04 (m, 2H), 6.70 – 6.65 (m, 2H), 6.37 (dd, $J = 17.5, 11.1$ Hz, 1H), 5.51 (dd, $J = 11.1, 1.0$ Hz, 1H), 5.43 (dd, $J = 17.5, 1.0$ Hz, 1H), 3.96 – 3.80 (m, 2H), 2.39 (s, 3H), 2.10 (s, 1H) ppm.

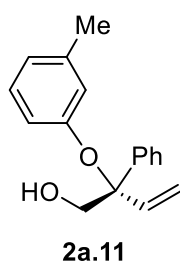
^{13}C NMR (101 MHz, CDCl_3) δ 153.41, 139.61, 135.39, 129.86, 128.69, 128.68, 128.02, 126.85, 120.43, 119.75, 85.04, 70.34, 17.38 ppm. IR (neat): ν (cm^{-1}) = 3353, 3026, 2918, 1591, 1488, 1446, 1273, 1227, 1175, 1069, 1007, 820, 762, 701. HRMS (ESI+, MeOH): m/z calcd. 309.0920 ($\text{M} + \text{Na}$) $^+$, found: 309.0921. HPLC conditions: Chiralpak IA 250 \times 4.6 mm, 5 μm , Hex/MTBE = 70 : 30, 1 mL/min; 89:11 *er*; $[\alpha]_{\text{D}}^{25} = -33.99$ ($c = 0.12$, CHCl_3).



Scale: 0.20 mmol; isolated 41 mg (76% yield), light yellow oil, Hexane : EA = 50 : 1, $R_f = 0.15$. **$^1\text{H NMR}$** (400 MHz, CDCl_3) δ 7.45 (m, 2H), 7.39 – 7.33 (m, 2H), 7.33 – 7.27 (m, 1H), 6.99 (t, $J = 8.2$ Hz, 1H), 6.47 – 6.27 (m, 4H), 5.52 (dd, $J = 11.1, 1.0$ Hz, 1H), 5.46 (dd, $J = 17.5, 1.0$ Hz, 1H), 3.98 – 3.80 (m, 2H), 3.66 (s, 3H), 2.08 (t, $J = 6.9$ Hz, 1H) ppm. **$^{13}\text{C NMR}$** (101 MHz, CDCl_3) δ 160.22, 156.35, 139.82, 135.51, 129.14, 128.69, 127.99, 126.83, 119.62, 112.20, 107.13, 105.88, 85.04, 70.50, 55.27 ppm. **IR** (neat): ν (cm^{-1}) = 3424, 3027, 2933, 2834, 1598, 1488, 1447, 1261, 1196, 1146, 1041, 1007, 842, 759, 701. **HRMS** (ESI+, MeOH): m/z calcd. 293.1157 ($\text{M} + \text{Na}$)⁺, found: 293.1148. **HPLC** conditions: Chiralpak IC 250 \times 4.6 mm, 5 μm , Hex/MTBE = 70 : 30, 1 mL/min; 93:7 *er*; $[\alpha]_{\text{D}}^{25} = -38.13$ ($c = 0.10$, CHCl_3).

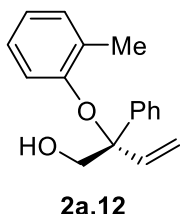


Scale: 0.20 mmol; isolated 35.7 mg (58% yield), light yellow oil, Hexane : EA = 50 : 1, $R_f = 0.15$. **$^1\text{H NMR}$** (400 MHz, CDCl_3) δ 7.43 (m, 2H), 7.40 – 7.35 (m, 2H), 7.34 – 7.29 (m, 1H), 7.18 (t, $J = 7.9$ Hz, 1H), 7.12 (d, $J = 7.7$ Hz, 1H), 7.05 (s, 1H), 6.81 (d, $J = 9.6$ Hz, 1H), 6.42 (dd, $J = 17.5, 11.1$ Hz, 1H), 5.55 (dd, $J = 11.1, 0.9$ Hz, 1H), 5.45 (dd, $J = 17.5, 0.9$ Hz, 1H), 3.99 – 3.80 (m, 2H), 2.02 (s, 1H) ppm. **$^{13}\text{C NMR}$** (101 MHz, CDCl_3) δ 155.41, 138.90, 134.74, 131.40 (q, $J = 32.32$ Hz), 129.18, 128.89, 128.30, 126.79, 122.72, 120.24, 117.94 (q, $J = 4.04$ Hz), 116.63 (q, $J = 4.04$ Hz), 85.57, 70.69 ppm. **$^{19}\text{F NMR}$** (376 MHz, CDCl_3) δ -62.92 ppm. **IR** (neat): ν (cm^{-1}) = 2925, 2870, 1592, 1491, 1448, 1223, 1166, 1065, 940, 788, 757, 698. **HRMS** (ESI+, MeOH): m/z calcd. 331.0916 ($\text{M} + \text{Na}$)⁺, found: 331.0922. **HPLC** conditions: Chiralpak IA 250 \times 4.6 mm, 5 μm , Hex/MTBE = 80 : 20, 1 mL/min; 85:15 *er*; $[\alpha]_{\text{D}}^{25} = -43.10$ ($c = 0.11$, CHCl_3).

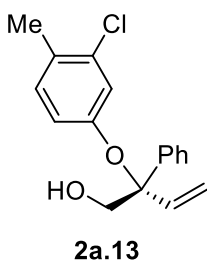


Scale: 0.20 mmol; isolated 42.6 mg (84% yield), light yellow oil, Hexane : EA = 50 : 1, $R_f = 0.15$. **$^1\text{H NMR}$** (400 MHz, CDCl_3) δ 7.49 – 7.44 (m, 2H), 7.40 – 7.34 (m, 2H), 7.33 – 7.28 (m, 1H), 6.97 (t, $J = 7.9$ Hz, 1H), 6.71 (m, 1H), 6.66 (t, $J = 2.0$ Hz, 1H), 6.47 (dd, $J = 8.2, 2.4$ Hz, 1H), 6.38 (dd, $J = 17.5, 11.1$ Hz, 1H), 5.50 (dd, $J = 11.1, 1.0$ Hz, 1H), 5.44 (dd, $J = 17.5, 1.0$ Hz, 1H), 3.97 – 3.82 (m, 2H), 2.23 (s, 3H), 2.09 (s, 1H) ppm. **$^{13}\text{C NMR}$** (101 MHz, CDCl_3) δ 155.09, 140.00, 138.99, 135.76, 128.62, 128.42, 127.90, 126.86, 122.34, 120.59, 119.50, 116.82, 84.80, 70.34, 21.54 ppm. **IR** (neat): ν (cm^{-1}) = 3569, 3429, 3028, 2921, 2854, 1601, 1582, 1487, 1447, 1286, 1253, 1153, 1050, 940, 770, 700. **HRMS**

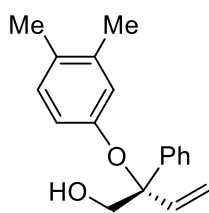
(ESI+, MeOH): m/z calcd. 277.1199 ($M + Na$)⁺, found: 277.1186. **HPLC** conditions: Chiralpak IA 250 × 4.6 mm, 5 μm, Hex/MTBE = 70 : 30, 1 mL/min; 94:6 *er*; $[\alpha]_D^{25} = -40.14$ ($c = 0.11$, CHCl₃).



Scale: 0.20 mmol; isolated 44.2 mg (87% yield), light yellow oil, Hexane : EA = 50 : 1, $R_f = 0.15$. **¹H NMR** (400 MHz, CDCl₃) δ 7.47 – 7.42 (m, 2H), 7.37 (m, 2H), 7.33 – 7.28 (m, 1H), 7.17 – 7.11 (m, 1H), 6.85 – 6.75 (m, 2H), 6.44 – 6.32 (m, 2H), 5.50 (dd, $J = 11.1, 1.0$ Hz, 1H), 5.44 (dd, $J = 17.5, 1.0$ Hz, 1H), 4.03 – 3.85 (m, 2H), 2.36 (s, 3H), 2.06 (t, $J = 5.6$ Hz, 1H) ppm. **¹³C NMR** (101 MHz, CDCl₃) δ 153.12, 140.10, 135.64, 130.89, 128.67, 128.44, 127.91, 126.76, 125.71, 120.98, 119.46, 118.53, 84.83, 70.90, 17.19 ppm. **IR** (neat): ν (cm⁻¹) = 3589, 3398, 3026, 2954, 2923, 2857, 1599, 1489, 1447, 1378, 1234, 1185, 1117, 1048, 927, 751, 700. **HRMS** (ESI+, MeOH): m/z calcd. 277.1199 ($M + Na$)⁺, found: 277.1199. **HPLC** conditions: Chiralpak IC 250 × 4.6 mm, 5 μm, Hex/MTBE = 80 : 20, 1 mL/min; 96:4 *er*; $[\alpha]_D^{25} = -41.26$ ($c = 0.10$, CHCl₃).

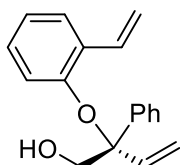


Scale: 0.20 mmol; isolated 41.0 mg (72% yield), light yellow solid, Hexane : EA = 50 : 1, $R_f = 0.15$. **¹H NMR** (400 MHz, CDCl₃) δ 7.46 – 7.41 (m, 2H), 7.37 (m, 2H), 7.34 – 7.29 (m, 1H), 6.92 (d, $J = 8.4$ Hz, 1H), 6.81 (d, $J = 2.5$ Hz, 1H), 6.50 (dd, $J = 8.4, 2.5$ Hz, 1H), 6.36 (dd, $J = 17.5, 11.1$ Hz, 1H), 5.52 (dd, $J = 11.1, 1.0$ Hz, 1H), 5.43 (dd, $J = 17.5, 1.0$ Hz, 1H), 3.96 – 3.77 (m, 2H), 2.23 (s, 3H), 2.03 (s, 1H) ppm. **¹³C NMR** (101 MHz, CDCl₃) δ 153.75, 139.40, 135.26, 134.01, 130.51, 128.85, 128.75, 128.13, 126.84, 120.51, 119.90, 118.23, 85.27, 70.31, 19.19 ppm. **IR** (neat): ν (cm⁻¹) = 3570, 3390, 3027, 2923, 2854, 1604, 1567, 1489, 1447, 1278, 1233, 1195, 1042, 997, 938, 757, 700. **HRMS** (ESI+, MeOH): m/z calcd. 311.0809 ($M + Na$)⁺, found: 311.0801. **HPLC** conditions: Chiralpak IA 250 × 4.6 mm, 5 μm, Hex/MTBE = 80 : 20, 1 mL/min; 85:15 *er*; $[\alpha]_D^{25} = -43.90$ ($c = 0.13$, CHCl₃).



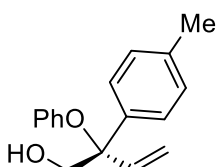
2a.14

Scale: 0.20 mmol; isolated 42.8 mg (80% yield), light yellow oil, Hexane : EA = 50 : 1, R_f = 0.15. **$^1\text{H NMR}$** (400 MHz, CDCl_3) δ 7.50 – 7.44 (m, 2H), 7.40 – 7.34 (m, 2H), 7.33 – 7.28 (m, 1H), 6.84 (d, J = 8.3 Hz, 1H), 6.66 (d, J = 2.7 Hz, 1H), 6.43 – 6.28 (m, 2H), 5.49 (dd, J = 11.1, 1.1 Hz, 1H), 5.44 (dd, J = 17.5, 1.1 Hz, 1H), 3.97 – 3.82 (m, 2H), 2.14 (d, J = 2.1 Hz, 6H), 2.09 (t, J = 6.8 Hz, 1H) ppm. **$^{13}\text{C NMR}$** (101 MHz, CDCl_3) δ 153.04, 140.21, 137.31, 136.03, 129.60, 128.59, 127.85, 126.90, 121.28, 119.36, 117.15, 84.66, 70.05, 20.05, 18.93 ppm. **IR** (neat): ν (cm^{-1}) = 3373, 3023, 2956, 2922, 2858, 1608, 1497, 1447, 1293, 1249, 1203, 1158, 1004, 809, 757, 700. **HRMS** (ESI+, MeOH): m/z calcd. 291.1356 ($\text{M} + \text{Na}$)⁺, found: 291.1355. **HPLC** conditions: Chiralpak IA 250 \times 4.6 mm, 5 μm , Hex/MTBE = 80 : 20, 1 mL/min; 93:7 *er*; $[\alpha]_{\text{D}}^{25}$ = -39.95 (c = 0.12, CHCl_3).



2a.15

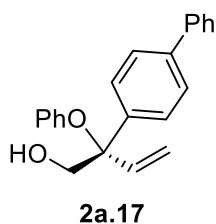
Scale: 0.20 mmol; isolated 43.7 mg (78% yield), light yellow oil, Hexane : EA = 50 : 1, R_f = 0.15. **$^1\text{H NMR}$** (400 MHz, CDCl_3) δ 7.46 – 7.41 (m, 2H), 7.39 – 7.28 (m, 3H), 7.16 (dd, J = 6.8, 2.4 Hz, 1H), 6.90 – 6.75 (m, 2H), 6.43 (dd, J = 17.5, 11.2 Hz, 1H), 6.34 (dd, J = 7.6, 1.8 Hz, 1H), 6.11 (ddt, J = 15.7, 11.0, 6.3 Hz, 1H), 5.51 (dd, J = 11.2, 1.0 Hz, 1H), 5.44 (dd, J = 17.5, 1.0 Hz, 1H), 5.21 – 5.03 (m, 2H), 3.98 – 3.82 (m, 2H), 3.62 – 3.47 (m, 2H), 2.22 (s, 1H) ppm. **$^{13}\text{C NMR}$** (101 MHz, CDCl_3) δ 152.76, 139.82, 137.69, 135.20, 130.42, 129.68, 128.67, 127.90, 126.69, 126.27, 120.89, 119.63, 118.44, 115.52, 84.83, 71.31, 35.66 ppm. **IR** (neat): ν (cm^{-1}) = 3553, 3060, 3026, 2923, 2856, 1637, 1598, 1585, 1487, 1448, 1232, 1046, 996, 913, 752, 700. **HRMS** (ESI+, MeOH): m/z calcd. 303.1356 ($\text{M} + \text{Na}$)⁺, found: 303.1352. **HPLC** conditions: Chiralpak IC 250 \times 4.6 mm, 5 μm , Hex/MTBE = 80 : 20, 1 mL/min; 94.5:5.5 *er*; $[\alpha]_{\text{D}}^{25}$ = -70.28 (c = 0.12, CHCl_3).



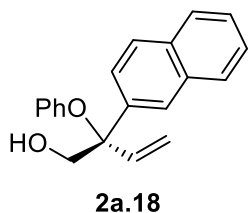
2a.16

Scale: 0.20 mmol; isolated 43.2 mg (85% yield), light yellow solid, Hexane : EA = 50 : 1, R_f = 0.15. **$^1\text{H NMR}$** (400 MHz, CDCl_3) δ 7.37 – 7.31 (m, 2H), 7.19 – 7.15 (m, 2H), 7.14 – 7.09 (m, 2H), 6.88 (t, J = 7.3 Hz, 1H), 6.79 – 6.69 (m, 2H), 6.38 (dd, J = 17.5, 11.1 Hz, 1H), 5.50 (dd, J = 11.1, 1.0 Hz, 1H), 5.44 (dd, J = 17.5, 1.1 Hz, 1H), 3.87 (m, 2H), 2.34 (s, 3H), 2.08 (s, 1H) ppm. **$^{13}\text{C NMR}$** (101 MHz, CDCl_3) δ 155.22, 137.68, 136.74, 135.61, 129.39, 128.81, 126.77, 121.30, 119.74, 119.49, 84.81, 70.57, 21.19 ppm. **IR** (neat): ν (cm^{-1}) = 3356, 3026, 2922, 2867, 1595, 1489, 1412, 1223, 1048, 928, 812, 752, 692. **HRMS** (ESI+, MeOH): m/z calcd. 277.1199 ($\text{M} + \text{Na}$)⁺, found: 277.1193.

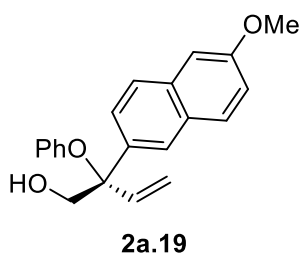
HPLC conditions: Chiralpak IC 250 × 4.6 mm, 5 μm, Hex/MTBE = 70 : 30, 1 mL/min; 93:7 *er*; $[\alpha]_D^{25} = -38.01$ ($c = 0.12$, CHCl₃).



Scale: 0.20 mmol; isolated 45.5 mg (72% yield), yellow solid, Hexane : EA = 50 : 1, $R_f = 0.15$. **¹H NMR** (400 MHz, CDCl₃) δ 7.61 – 7.58 (m, 4H), 7.52 (d, $J = 8.6$ Hz, 2H), 7.46 – 7.41 (m, 2H), 7.35 (t, $J = 7.3$ Hz, 1H), 7.14 (m, 2H), 6.90 (t, $J = 7.9$ Hz, 1H), 6.78 (m, 2H), 6.42 (dd, $J = 17.5, 11.1$ Hz, 1H), 5.53 (dd, $J = 11.2, 1.0$ Hz, 1H), 5.47 (dd, $J = 17.5, 1.0$ Hz, 1H), 4.01 – 3.86 (m, 2H), 2.12 (d, $J = 6.9$ Hz, 1H) ppm. **¹³C NMR** (101 MHz, CDCl₃) δ 155.15, 140.75, 140.55, 138.87, 135.57, 128.94, 128.92, 127.60, 127.34, 127.20, 121.51, 119.85, 119.74, 84.82, 70.50 ppm. **IR** (neat): ν (cm⁻¹) = 3595, 3436, 3030, 2924, 2870, 1595, 1487, 1409, 1229, 1074, 1007, 936, 834, 752, 694. **HRMS** (ESI+, MeOH): m/z calcd. 339.1356 (M + Na)⁺, found: 339.1363. **HPLC** conditions: Chiralpak IC 250 × 4.6 mm, 5 μm, Hex/MTBE = 70 : 30, 1 mL/min; 86:14 *er*; $[\alpha]_D^{25} = -29.27$ ($c = 0.11$, CHCl₃).

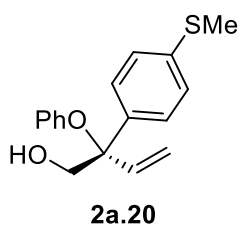


Scale: 0.20 mmol; isolated 33.6 mg (58% yield), light yellow solid, Hexane : EA = 50 : 1, $R_f = 0.15$. **¹H NMR** (400 MHz, CDCl₃) δ 7.94 (d, $J = 1.8$ Hz, 1H), 7.84 (m, 3H), 7.57 (m, 1H), 7.50 (m, 2H), 7.10 (m, 2H), 6.90 – 6.84 (m, 1H), 6.82 – 6.76 (m, 2H), 6.49 (dd, $J = 17.5, 11.1$ Hz, 1H), 5.57 (dd, $J = 11.1, 1.0$ Hz, 1H), 5.51 (dd, $J = 17.5, 1.0$ Hz, 1H), 4.09 – 3.90 (m, 2H), 2.11 (s, 1H) ppm. **¹³C NMR** (126 MHz, CDCl₃) δ 155.20, 137.58, 135.64, 133.23, 132.95, 128.94, 128.51, 128.40, 127.73, 126.52, 126.46, 125.99, 124.75, 121.58, 119.88, 119.82, 85.03, 70.22 ppm. **IR** (neat): ν (cm⁻¹) = 3315, 3057, 2919, 2853, 1594, 1485, 1221, 1074, 936, 859, 817, 748, 690. **HRMS** (ESI+, MeOH): m/z calcd. 313.1199 (M + Na)⁺, found: 313.1202. **HPLC** conditions: Chiralpak IC 250 × 4.6 mm, 5 μm, Hex/MTBE = 70 : 30, 1 mL/min; 85:15 *er*; $[\alpha]_D^{25} = -51.92$ ($c = 0.12$, CHCl₃).

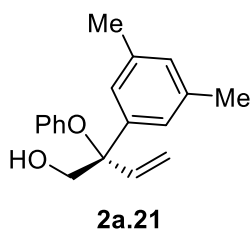


Scale: 0.20 mmol; isolated 48.0 mg (75% yield), light yellow solid, Hexane : EA = 20 : 1, $R_f = 0.15$. **¹H NMR** (400 MHz, CDCl₃) δ 7.85 (d, $J = 1.7$ Hz, 1H), 7.72 (m, 2H), 7.53 (m, 1H), 7.19 – 7.06 (m, 4H), 6.87 (t, $J = 7.4$ Hz, 1H), 6.78 (m, 2H), 6.47 (dd, $J = 17.5, 11.1$ Hz, 1H), 5.55 (dd, $J = 11.1, 1.0$ Hz, 1H), 5.50

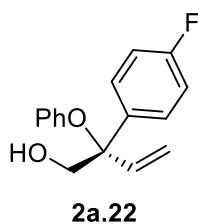
(dd, $J = 17.5, 1.0$ Hz, 1H), 4.07 – 3.87 (m, 5H), 2.10 (t, $J = 6.9$ Hz, 1H) ppm. $^{13}\text{C NMR}$ (101 MHz, CDCl_3) δ 158.24, 155.26, 135.72, 135.13, 134.15, 129.87, 128.91, 128.69, 127.36, 125.81, 125.30, 121.50, 119.89, 119.65, 119.31, 105.68, 85.01, 70.21, 55.50 ppm. **IR** (neat): ν (cm^{-1}) = 3570, 3060, 2936, 1632, 1596, 1487, 1389, 1266, 1221, 1164, 1028, 904, 853, 731, 693. **HRMS** (ESI+, MeOH): m/z calcd. 343.1305 ($\text{M} + \text{Na}$) $^+$, found: 343.1303. **HPLC** conditions: Chiralpak IC 250 \times 4.6 mm, 5 μm , Hex/MTBE = 70 : 30, 1 mL/min; 83:17 *er*; $[\alpha]_{\text{D}}^{25} = -55.49$ ($c = 0.11$, CHCl_3).



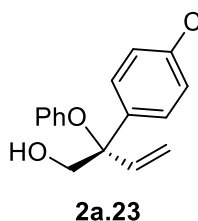
Scale: 0.20 mmol; isolated 46.3 mg (81% yield), light yellow solid, Hexane : EA = 50 : 1, $R_f = 0.15$. $^1\text{H NMR}$ (400 MHz, CDCl_3) δ 7.41 – 7.33 (m, 2H), 7.26 – 7.20 (m, 2H), 7.16 – 7.08 (m, 2H), 6.89 (t, $J = 7.4$ Hz, 1H), 6.74 (dd, $J = 8.7, 1.0$ Hz, 2H), 6.35 (dd, $J = 17.5, 11.1$ Hz, 1H), 5.50 (dd, $J = 11.1, 1.0$ Hz, 1H), 5.43 (dd, $J = 17.5, 1.0$ Hz, 1H), 3.93 – 3.79 (m, 2H), 2.47 (s, 3H), 2.09 (t, $J = 6.9$ Hz, 1H) ppm. $^{13}\text{C NMR}$ (101 MHz, CDCl_3) δ 155.06, 138.41, 136.52, 135.42, 128.89, 127.39, 126.44, 121.48, 119.79, 119.70, 84.65, 70.42, 15.63 ppm. **IR** (neat): ν (cm^{-1}) = 3514, 3065, 2959, 2921, 2904, 2854, 1595, 1489, 1403, 1226, 1076, 1043, 993, 919, 800, 747, 687. **HRMS** (ESI+, MeOH): m/z calcd. 309.0920 ($\text{M} + \text{Na}$) $^+$, found: 309.0917. **HPLC** conditions: Chiralpak IC 250 \times 4.6 mm, 5 μm , Hex/MTBE = 70 : 30, 1 mL/min; 90.5:9.5 *er*; $[\alpha]_{\text{D}}^{25} = -36.48$ ($c = 0.10$, CHCl_3).



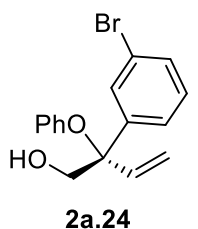
Scale: 0.20 mmol; isolated 30.5 mg (57% yield), yellow solid, Hexane : EA = 50 : 1, $R_f = 0.15$. $^1\text{H NMR}$ (500 MHz, CDCl_3) δ 7.15 – 7.10 (m, 2H), 7.06 (s, 2H), 6.94 (s, 1H), 6.91 – 6.86 (m, 1H), 6.79 – 6.73 (m, 2H), 6.34 (dd, $J = 17.6, 11.1$ Hz, 1H), 5.47 (dd, $J = 11.1, 1.0$ Hz, 1H), 5.41 (dd, $J = 17.6, 1.0$ Hz, 1H), 3.96 – 3.79 (m, 2H), 2.30 (s, 6H), 2.02 (s, 1H) ppm. $^{13}\text{C NMR}$ (126 MHz, CDCl_3) δ 155.28, 139.91, 138.18, 135.91, 129.65, 128.83, 124.56, 121.43, 119.97, 119.34, 84.88, 70.21, 21.66 ppm. **IR** (neat): ν (cm^{-1}) = 3411, 3036, 2919, 2855, 1597, 1490, 1377, 1223, 1029, 850, 752, 692. **HRMS** (ESI+, MeOH): m/z calcd. 291.1356 ($\text{M} + \text{Na}$) $^+$, found: 291.1361. **HPLC** conditions: Chiralpak IC 250 \times 4.6 mm, 5 μm , Hex/MTBE = 80 : 20, 1 mL/min; 88:12 *er*; $[\alpha]_{\text{D}}^{25} = +3.1$ ($c = 0.07$, CHCl_3).



Scale: 0.20 mmol; isolated 42.8 mg (83% yield), white solid, Hexane : EA = 50 : 1, R_f = 0.15. **$^1\text{H NMR}$** (400 MHz, CDCl_3) δ 7.46 – 7.39 (m, 2H), 7.16 – 7.10 (m, 2H), 7.08 – 7.01 (m, 2H), 6.90 (t, J = 7.4 Hz, 1H), 6.76 – 6.69 (m, 2H), 6.34 (dd, J = 17.5, 11.1 Hz, 1H), 5.54 – 5.41 (m, 2H), 3.94 – 3.81 (m, 2H), 2.08 (t, J = 6.9 Hz, 1H) ppm. **$^{13}\text{C NMR}$** (126 MHz, CDCl_3) δ 163.41, 161.44, 154.95, 135.68, 135.65, 135.52, 128.95, 128.79, 128.72, 121.71, 119.93, 119.83, 115.65, 115.48, 84.55, 70.30 ppm. **$^{19}\text{F NMR}$** (376 MHz, CDCl_3) δ -114.64 ppm. **IR** (neat): ν (cm^{-1}) = 3474, 3072, 2927, 2857, 1596, 1507, 1489, 1409, 1224, 1074, 1006, 920, 836, 750. **HRMS** (ESI+, MeOH): m/z calcd. 281.0948 ($\text{M} + \text{Na}$)⁺, found: 281.0957. **HPLC** conditions: Chiralpak IC 250 \times 4.6 mm, 5 μm , Hex/MTBE = 70 : 30, 1 mL/min; 93:7 *er*; $[\alpha]_{\text{D}}^{25}$ = -40.14 (c = 0.13, CHCl_3).

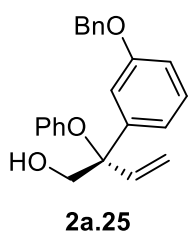


Scale: 0.20 mmol; isolated 34.5 mg (63% yield), light yellow oil, Hexane : EA = 50 : 1, R_f = 0.15. **$^1\text{H NMR}$** (400 MHz, CDCl_3) δ 7.42 – 7.37 (m, 2H), 7.36 – 7.30 (m, 2H), 7.17 – 7.10 (m, 2H), 6.93 – 6.88 (m, 1H), 6.75 – 6.68 (m, 2H), 6.33 (dd, J = 17.5, 11.1 Hz, 1H), 5.51 (dd, J = 11.1, 0.9 Hz, 1H), 5.43 (dd, J = 17.5, 0.9 Hz, 1H), 3.87 (qd, J = 11.6, 5.4 Hz, 2H), 2.09 (t, J = 6.9 Hz, 1H) ppm. **$^{13}\text{C NMR}$** (101 MHz, CDCl_3) δ 154.86, 138.53, 135.24, 133.94, 128.98, 128.84, 128.39, 121.74, 120.04, 119.84, 84.50, 70.34 ppm. **IR** (neat): ν (cm^{-1}) = 3579, 3417, 3061, 2923, 1595, 1488, 1398, 1221, 1092, 1074, 1011, 827, 753, 692. **HRMS** (ESI+, MeOH): m/z calcd. 297.0653 ($\text{M} + \text{Na}$)⁺, found: 297.0662. **HPLC** conditions: Chiralpak IC 250 \times 4.6 mm, 5 μm , Hex/MTBE = 70 : 30, 1 mL/min; 86:14 *er*; $[\alpha]_{\text{D}}^{25}$ = -38.00 (c = 0.09, CHCl_3).

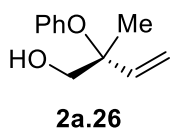


Scale: 0.20 mmol; isolated 31.1 mg (49% yield), yellow solid, Hexane : EA = 50 : 1, R_f = 0.15. **$^1\text{H NMR}$** (400 MHz, CDCl_3) δ 7.63 (t, J = 1.8 Hz, 1H), 7.45 (m, 1H), 7.39 (m, 1H), 7.23 (m, 1H), 7.19 – 7.10 (m, 2H), 6.92 (t, J = 7.4 Hz, 1H), 6.81 – 6.71 (m, 2H), 6.30 (dd, J = 17.5, 11.1 Hz, 1H), 5.51 (dd, J = 11.1, 0.9 Hz, 1H), 5.43 (dd, J = 17.5, 0.9 Hz, 1H), 3.88 (q, J = 8.4, 6.7 Hz, 2H), 2.05 (s, 1H) ppm. **$^{13}\text{C NMR}$** (101 MHz, CDCl_3) δ 154.78, 142.62, 135.23, 131.12, 130.20, 129.95, 129.03, 125.71, 122.90, 121.93, 120.15, 120.02, 84.44, 70.09 ppm. **IR** (neat): ν (cm^{-1}) = 3350, 3062, 2924, 1593, 1565, 1488, 1408, 1221, 1073, 996, 753, 692. **HRMS** (ESI+, MeOH): m/z calcd. 341.0148 ($\text{M} + \text{Na}$)⁺, found:

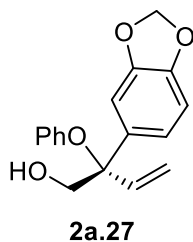
341.0143. **HPLC** conditions: Chiralpak IC 250 x 4.6 mm, 5 μ m, Hex/MTBE = 80 : 20, 1 mL/min; 85:15 *er*; $[\alpha]_D^{25} = -26.16$ ($c = 0.10$, CHCl_3).



Scale: 0.20 mmol; isolated 47.0 mg (68% yield), light yellow solid, Hexane : EA = 50 : 1, $R_f = 0.10$. **$^1\text{H NMR}$** (500 MHz, CDCl_3) δ 7.41 (m, 4H), 7.37 – 7.32 (m, 1H), 7.32 – 7.28 (m, 1H), 7.19 – 7.12 (m, 3H), 7.08 (d, $J = 7.8$ Hz, 1H), 6.98 – 6.90 (m, 2H), 6.77 (d, $J = 7.9$ Hz, 2H), 6.37 (dd, $J = 17.5, 11.1$ Hz, 1H), 5.52 (d, $J = 11.1$ Hz, 1H), 5.46 (d, $J = 17.5$ Hz, 1H), 5.05 (d, $J = 2.3$ Hz, 2H), 4.02 – 3.80 (m, 2H), 2.08 (s, 1H) ppm. **$^{13}\text{C NMR}$** (126 MHz, CDCl_3) δ 159.07, 155.12, 141.68, 136.89, 135.51, 129.74, 128.88, 128.72, 128.17, 127.74, 121.50, 119.82, 119.64, 119.46, 114.10, 114.05, 84.78, 70.33, 70.23 ppm. **IR** (neat): ν (cm^{-1}) = 3570, 3438, 3032, 2923, 2867, 1583, 1487, 1437, 1223, 1167, 1025, 752, 695. **HRMS** (ESI+, MeOH): m/z calcd. 369.1461 ($\text{M} + \text{Na}$)⁺, found: 369.1463. **HPLC** conditions: Chiralpak IC 250 \times 4.6 mm, 5 μ m, Hex/MTBE = 70 : 30, 1 mL/min; 92:8 *er*; $[\alpha]_D^{25} = -36.06$ ($c = 0.10$, CHCl_3).

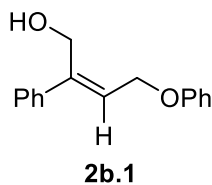


Scale: 0.20 mmol; isolated 29.5 mg (83% yield), light yellow oil, Hexane : EA = 50 : 1, $R_f = 0.15$. **$^1\text{H NMR}$** (400 MHz, CDCl_3) δ 7.25 (m, 2H), 7.01 (m, 3H), 6.12 (dd, $J = 17.6, 11.1$ Hz, 1H), 5.36 – 5.25 (m, 2H), 3.71 – 3.54 (m, 2H), 2.19 (s, 1H), 1.44 (s, 3H) ppm. **$^{13}\text{C NMR}$** (101 MHz, CDCl_3) δ 155.46, 140.50, 129.14, 122.67, 121.30, 116.96, 82.13, 70.23, 19.18 ppm. **IR** (neat): ν (cm^{-1}) = 3393, 3087, 2984, 2925, 2856, 1594, 1490, 1374, 1227, 1059, 926, 757, 696. **HRMS** (ESI+, MeOH): m/z calcd. 201.0886 ($\text{M} + \text{Na}$)⁺, found: 201.0883. **HPLC** conditions: Chiralpak IA 250 \times 4.6 mm, 5 μ m, Hex/MTBE = 80:20, 1 mL/min; 57.5:42.5 *er*; $[\alpha]_D^{25} = -1.22$ ($c = 0.09$, CHCl_3).

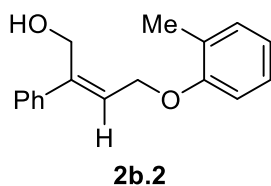


Scale: 0.20 mmol; isolated 43.7 mg (77% yield), light yellow solid, Hexane : EA = 50 : 1, $R_f = 0.15$. **$^1\text{H NMR}$** (400 MHz, CDCl_3) δ 7.13 (m, 2H), 6.96 – 6.86 (m, 3H), 6.81 – 6.73 (m, 3H), 6.32 (dd, $J = 17.5, 11.1$ Hz, 1H), 5.95 (q, $J = 1.4$ Hz, 2H), 5.49 (dd, $J = 11.1, 1.0$ Hz, 1H), 5.43 (dd, $J = 17.5, 1.0$ Hz, 1H), 3.95 – 3.77 (m, 2H), 2.08 (s, 1H) ppm. **$^{13}\text{C NMR}$** (101 MHz, CDCl_3) δ 155.07, 148.12, 147.34, 135.59, 133.82, 128.90, 121.53, 120.30, 119.82, 119.55, 108.29, 107.69, 101.35, 84.69, 70.35 ppm. **IR** (neat): ν (cm^{-1}) =

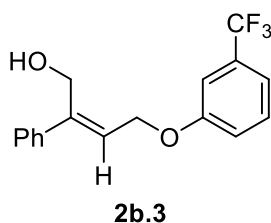
3554, 2917, 1585, 1483, 1435, 1222, 1075, 1029, 919, 746, 684. **HRMS** (ESI+, MeOH): m/z calcd. 307.0941 ($M + Na$)⁺, found: 307.0940. **HPLC** conditions: Chiralpak IC 250 × 4.6 mm, 5 μm, Hex/MTBE = 60 : 40, 1 mL/min; 92:8 *er*; $[\alpha]_D^{25} = -45.14$ ($c = 0.12$, CHCl₃).



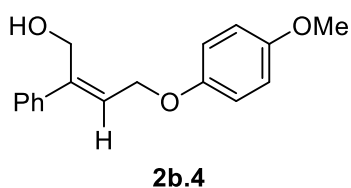
Scale: 0.20 mmol; isolated 45.5 mg (95% yield), $Z/E > 99:1$, light yellow oil, Hexane : EA = 10 : 1, $R_f = 0.20$. **¹H NMR** (500 MHz, CDCl₃) δ 7.51 – 7.47 (m, 2H), 7.40 – 7.35 (m, 2H), 7.34 – 7.29 (m, 3H), 7.01 – 6.95 (m, 3H), 6.18 (t, $J = 6.4$ Hz, 1H), 4.82 (d, $J = 6.4$ Hz, 2H), 4.64 (s, 2H), 1.79 (s, 1H) ppm. **¹³C NMR** (101 MHz, CDCl₃) δ 158.50, 143.43, 140.04, 129.72, 128.74, 128.05, 126.63, 126.35, 121.33, 114.97, 77.48, 77.16, 76.84, 64.58, 60.58 ppm. **IR** (neat): ν (cm⁻¹) = 3393, 3087, 2984, 2925, 2856, 1594, 1490, 1374, 1227, 1059, 926, 757, 696. **HRMS** (ESI+, MeOH): m/z calcd. 263.1043 ($M + Na$)⁺, found: 263.1042.



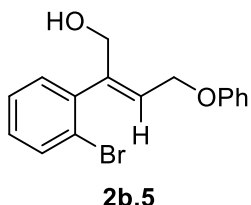
Scale: 0.20 mmol; isolated 46.2 mg (91% yield), $Z/E > 99:1$, light yellow liquid, Hexane : EA = 10 : 1, $R_f = 0.20$. **¹H NMR** (400 MHz, CDCl₃) δ 7.54 – 7.46 (m, 2H), 7.42 – 7.35 (m, 2H), 7.35 – 7.30 (m, 1H), 7.19 (t, $J = 7.0$ Hz, 2H), 6.97 – 6.87 (m, 2H), 6.20 (t, $J = 6.3$ Hz, 1H), 4.83 (d, $J = 6.3$ Hz, 2H), 4.64 (d, $J = 4.3$ Hz, 2H), 2.28 (s, 3H), 1.84 (t, $J = 5.5$ Hz, 1H) ppm. **¹³C NMR** (101 MHz, CDCl₃) δ 156.71, 142.97, 140.06, 130.99, 128.71, 127.98, 127.14, 126.95, 126.72, 126.61, 120.97, 111.69, 64.80, 60.48, 16.49 ppm. **IR** (neat): ν (cm⁻¹) = 3569, 3368, 3024, 2923, 1600, 1492, 1460, 1376, 1237, 1189, 1120, 1008, 749, 697. **HRMS** (ESI+, MeOH): m/z calcd. 277.1199 ($M + Na$)⁺, found: 277.1186.



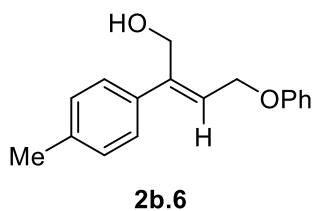
Scale: 0.20 mmol; isolated 40.0 mg (65% yield), $Z/E > 99:1$, yellow solid, Hexane : EA = 10 : 1, $R_f = 0.20$. **¹H NMR** (400 MHz, CDCl₃) δ 7.50 – 7.46 (m, 2H), 7.44 – 7.35 (m, 3H), 7.35 – 7.30 (m, 1H), 7.24 (d, $J = 7.7$ Hz, 1H), 7.20 (s, 1H), 7.13 (m, 1H), 6.13 (t, $J = 6.4$ Hz, 1H), 4.86 (d, $J = 6.4$ Hz, 2H), 4.66 (s, 2H), 1.65 (s, 1H) ppm. **¹³C NMR** (101 MHz, CDCl₃) δ 158.69, 143.71, 139.83, 132.1 (q, $J = 32.32$ Hz), 130.22, 128.80, 128.21, 126.67, 125.61, 118.41, 118.40, 117.94 (q, $J = 4.04$ Hz), 111.72 (q, $J = 4.04$ Hz), 64.93, 60.61 ppm. **¹⁹F NMR** (376 MHz, CDCl₃) δ -62.80 ppm. **IR** (neat): ν (cm⁻¹) = 3378, 3059, 2925, 1597, 1493, 1448, 1325, 1220, 1167, 1123, 1009, 752, 695. **HRMS** (ESI+, MeOH): m/z calcd. 331.0916 ($M + Na$)⁺, found: 331.0916.



Scale: 0.20 mmol; isolated 52.9 mg (98% yield), *Z/E*>99:1, white solid, Hexane : EA = 10 : 1, R_f = 0.20. **$^1\text{H NMR}$** (400 MHz, CDCl_3) δ 7.52 – 7.46 (m, 2H), 7.39 – 7.28 (m, 3H), 6.94 – 6.81 (m, 4H), 6.16 (t, J = 6.4 Hz, 1H), 4.76 (d, J = 6.4 Hz, 2H), 4.61 (d, J = 2.9 Hz, 2H), 3.78 (s, 3H), 1.80 (s, 1H) ppm. **$^{13}\text{C NMR}$** (101 MHz, CDCl_3) δ 154.35, 152.62, 143.43, 140.10, 128.72, 128.01, 126.61, 126.52, 116.12, 114.89, 65.44, 60.55, 55.88 ppm. **IR** (neat): ν (cm^{-1}) = 3433, 3036, 2920, 2836, 1506, 1439, 1375, 1287, 1230, 1031, 997, 822, 738, 689. **HRMS** (ESI+, MeOH): m/z calcd. 293.1148 ($\text{M} + \text{Na}$)⁺, found: 293.1137.



Scale: 0.20 mmol; isolated 45.8 mg (72% yield), *Z/E*>99:1, white solid, Hexane : EA = 10 : 1, R_f = 0.20. **$^1\text{H NMR}$** (400 MHz, CDCl_3) δ 7.58 (dd, J = 8.0, 1.2 Hz, 1H), 7.35 – 7.25 (m, 5H), 7.20 – 7.14 (m, 1H), 7.02 – 6.96 (m, 3H), 5.88 (t, J = 6.0 Hz, 1H), 4.87 (d, J = 6.1 Hz, 2H), 4.54 (s, 2H), 1.87 (s, 1H) ppm. **$^{13}\text{C NMR}$** (101 MHz, CDCl_3) δ 158.48, 143.81, 142.08, 132.79, 131.23, 129.76, 129.67, 129.23, 127.56, 122.49, 121.26, 115.02, 64.50, 61.64 ppm. **IR** (neat): ν (cm^{-1}) = 3382, 3059, 2926, 1597, 1493, 1448, 1379, 1325, 1219, 1168, 1123, 1009, 752, 694. **HRMS** (ESI+, MeOH): m/z calcd. 341.0148 ($\text{M} + \text{Na}$)⁺, found: 341.0133.



Scale: 0.20 mmol; isolated 41.1 mg (81% yield), *Z/E*>99:1, yellow oil, Hexane : EA = 10 : 1, R_f = 0.20. **$^1\text{H NMR}$** (400 MHz, CDCl_3) δ 7.41 – 7.37 (m, 2H), 7.34 – 7.28 (m, 2H), 7.18 (d, J = 7.8 Hz, 2H), 7.02 – 6.93 (m, 3H), 6.15 (t, J = 6.4 Hz, 1H), 4.80 (d, J = 6.4 Hz, 2H), 4.62 (s, 2H), 2.36 (s, 3H), 1.75 (s, 1H) ppm. **$^{13}\text{C NMR}$** (101 MHz, CDCl_3) δ 158.52, 143.28, 137.92, 137.02, 129.70, 129.44, 126.50, 125.42, 121.27, 114.96, 64.58, 60.48, 21.26 ppm. **IR** (neat): ν (cm^{-1}) = 3382, 3026, 2920, 1597, 1494, 1377, 1236, 1007, 753, 691. **HRMS** (ESI+, MeOH): m/z calcd. 277.1199 ($\text{M} + \text{Na}$)⁺, found: 277.1195.

Chapter 3.

Domino Synthesis of α,β -Unsaturated γ -Lactams via Stereoselective Amination of α -Tertiary Allylic Alcohols

This chapter has been published in:

J. Xie, S. Xue, A. Cai, E. C. Escudero-Adán, A. W. Kleij, *Angew. Chem. Int. Ed.* **2018**, *57*, 16727-16731.

3.1 Introduction

3.1.1 Lactams

Lactams, also known as cyclic amides, are an important class of compounds owing to their presence in numerous biologically active molecules of natural and unnatural origin. They are also highly versatile synthetic intermediates that can be elaborated into interesting compounds for material science and medicinal applications. Lactams are defined as β -lactams (four-atom ring), γ -lactams (five-atom ring), δ -lactams (six-atom ring) and ϵ -caprolactams (seven-atom ring) and so on according to the spatial nature between the “N” and “C=O” fragments. Classic approaches for the preparation of lactams are based on acid-catalyzed rearrangement of oximes in the Beckmann rearrangement,⁷⁷ the reaction between cyclic ketones and hydrazoic acid in the Schmidt reaction⁷⁸ and cyclization of amino acids or similar precursors.⁷⁹ Although lactams are relatively stable, especially γ - and δ -lactams, ring opening may occur at the amide carbon during hydrolysis, aminolysis, hydrogenolysis and ring-opening polymerization (ROP) reactions. The amide bond of lactam can be reduced to produce *N*-heterocyclic rings (such as azetidine, pyrrole, piperidine and azepane ring systems) that are ubiquitous and important motifs in organic compounds relevant to living organisms.

3.1.2 α,β -Unsaturated γ -Lactams

The γ -lactam moiety can be considered as one of the most important heterocyclic motifs used in chemistry.⁸⁰ α,β -Unsaturated γ -lactams (also referred to as 3-pyrrolin-2-ones, 1,5-dihydro-2*H*-pyrrol-2-ones or pyrrol-2-ones) are highly attractive synthesis scaffolds as

-
- (77) a) A. H. Blatt, *Chem. Rev.* **1933**, *12*, 215; b) J. L. Kenwright, W. R. J. D. Galloway, L. Wortmann, D. R. Spring, *Synth. Commun.* **2013**, 1508; c) X. Mo, T. D. R. Morgan, H. T. Ang, D. G. Hall, *J. Am. Chem. Soc.* **2018**, *140*, 5264; d) F. Rivas, T. Ling, *Org. Prep. Proced. Int.* **2016**, *48*, 254; e) J. Caruano, G. G. Muccioli, R. Robiette, *Org. Biomol. Chem.* **2016**, *14*, 10134; f) M. Negwer, H.-G. Scharnow, *Organic-Chemical Drugs and their Synonyms*, 8th ed.; Wiley-VCH: Weinheim, **2001**; g) D.-N. Zhou, C.-X. Wang, M.-L. Li, Z. Long, J.-B. Lan, *Chin. Chem. Lett.* **2018**, *29*, 191.
- (78) a) S. Lang, J. A. Murphy, *Chem. Soc. Rev.* **2006**, *35*, 146; b) A. Wroblewski, T. C. Coombs, C. W. Huh, S.-W. Li, J. Aubé, *Org. React.* **2012**, *78*, 1; c) H. Wolff, *Org. React.* **2011**, *77*, 307.
- (79) For some examples: a) C. Xie, J. Song, H. Wu, Y. Hu, H. Liu, Z. Zhang, P. Zhang, B. Chen, B. Han, *J. Am. Chem. Soc.* **2019**, *141*, 4002; b) J. Qi, C. Sun, Y. Tian, X. Wang, G. Li, Q. Xiao, D. Yin, *Org. Lett.* **2014**, *16*, 190; c) J. Escalante, M. A. González-Tototzin, J. Aviña, O. Muñoz-Muñiz, E. Juaristi, *Tetrahedron* **2011**, *57*, 1883; d) O. David, W. J. Meester, H. Bieraugel, H. E. Schoemaker, H. Hiemstra, J. H. van Maarseveen, *Angew. Chem. Int. Ed.* **2003**, *42*, 4373.
- (80) L.-W. Ye, C. Shu, F. Gagosz, *Org. Biomol. Chem.* **2018**, *16*, 6840.

these substructures are part of a wide range of bioactive compounds⁸¹ (Scheme 3.1) and are valuable precursors towards pyrroles, (saturated) γ -lactams and γ -amino acid derivatives.⁸²

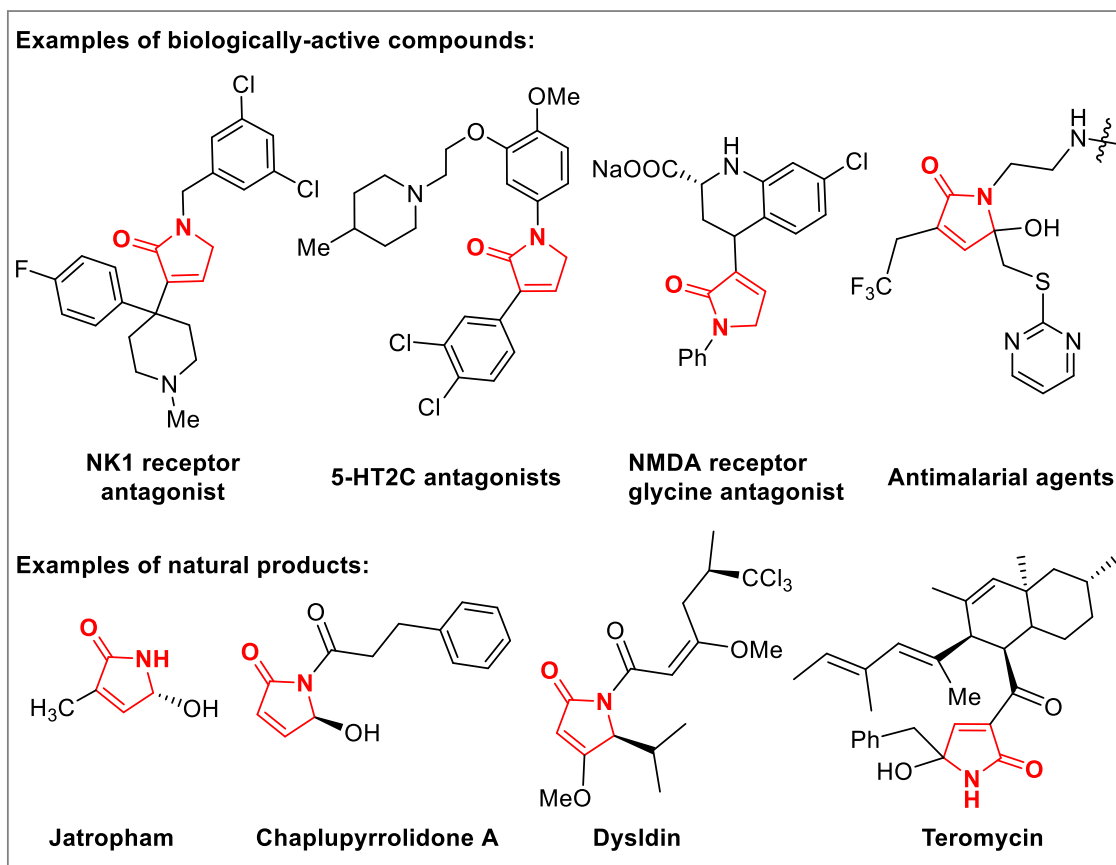
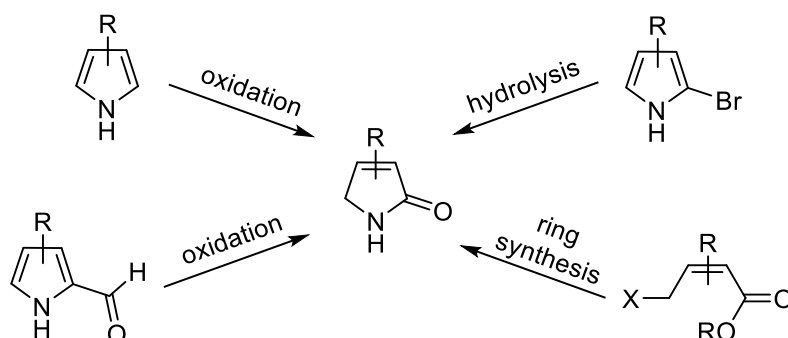


Figure 3.1 Selected examples of bioactive/natural compounds incorporating an unsaturated γ -lactam unit.

The first reported synthesis of the parent α,β -unsaturated γ -lactam and isomeric 4-pyrroloin-2-one can be traced back to 1951 and 1949, respectively.⁸³ Traditional synthetic approaches to α,β -unsaturated γ -lactams include: (1) the oxidation of pyrroles; (2) the oxidation of pyrrole-2-carboxaldehydes; (3) the hydrolysis of 2-bromopyrroles; and (4)

- (81) a) Z. Feng, F. Chu, Z. Guo, P. Sun, *Bioorg. Med. Chem. Lett.* **2009**, *19*, 2270; b) G.-Y. Zhu, G. Chen, L. Liu, L.-P. Bai, Z.-H. Jiang, *J. Nat. Prod.* **2014**, *77*, 983; c) F. Micheli, A. Pasquarello, G. Tedesco, D. Hamprecht, G. Bonanomi, A. Checchia, A. Jaxa-Chamiec, F. Damiani, S. Davalli, D. Donati, C. Gallotti, M. Petrone, M. Rinaldi, G. Riley, S. Terreni, *Bioorg. Med. Chem. Lett.* **2006**, *16*, 3906.
- (82) a) G. Hughes, M. Kimura, S. L. Buchwald, *J. Am. Chem. Soc.* **2003**, *125*, 11253; b) Y. Xie, Y. Zhao, B. Qian, L. Yang, C. Xia, H. Huang, *Angew. Chem. Int. Ed.* **2011**, *50*, 5682; c) C. Shao, H.-J. Yu, N.-Y. Wu, P. Tian, R. Wang, C.-G. Feng, G.-Q. Lin, *Org. Lett.* **2011**, *13*, 788.
- (83) a) C. A. Grob, P. Ankli, *Helv. Chim. Acta.* **1949**, *32*, 2010; b) W. Langenbeck, H. Boser, *Chem. Ber.* **1951**, *84*, 526.

procedures that involve ring-closing chemistry (Scheme 3.1). In this context, it has been a long-standing objective of the synthetic community to achieve efficient and selective methods for their synthesis, ideally in a catalytic and preferably waste-free manner.

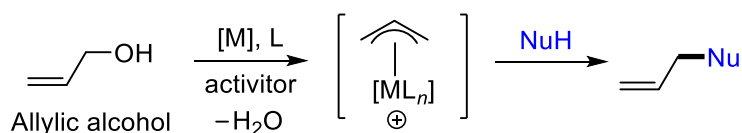


Scheme 3.1 Traditional approaches to α,β -unsaturated γ -lactams.

3.1.3 Allylic Alcohols as Precursors in Allylic Substitution Reactions

TM-catalyzed allylic substitution reactions have provided convenient access to more complex target (heterocyclic) molecules via C–C and C–X (X = N, O, S) bond formation reactions. These methods typically utilize an activated allylic substrate, such as an allylic alcohol protected by a carbonate or ester acting as a LG. However, these reagents require an additional synthetic step compared to the use of allylic alcohols and the conversion results in the formation of stoichiometric amounts of (salt) waste. More recent focus in this area has shifted towards allylic alcohols as relatively unactivated and more ubiquitous substrates as to increase both the atom- and step-economy of the allylic substitution process, with water as the sole generated side-product.⁸⁴ Therefore, allylic substitution reactions starting from these alcohols are attractive but the poor leaving group ability of the hydroxyl group renders the allylic substitution process more challenging (Scheme 3.2). As such, often the use of a protic solvent such as MeOH or water, the presence of stoichiometric or catalytic amount of Lewis/Brønsted acidic additives, the synthesis of specific catalysts, and/or elevated temperatures are required for efficient turnover.⁸⁵

- (84) For accounts on the use of allylic alcohols as substrates: a) M. Bandini, *Angew. Chem. Int. Ed.* **2011**, *50*, 994; b) B. Sundararaju, M. Achard, C. Bruneau, *Chem. Soc. Rev.* **2012**, *41*, 4467; c) M. Bandini, G. Cera, M. Chiarucci, *Synthesis* **2012**, *44*, 504; d) J. Muzart, *Tetrahedron* **2005**, *61*, 4179; e) Y. Tamaru, *Eur. J. Org. Chem.* **2005**, 2647; f) N. A. Butt, W. Zhang, *Chem. Soc. Rev.* **2015**, *44*, 7929.
- (85) For representative recent examples: a) X.-Q. Hu, Z. Hu, A. S. Trita, G. Zhang, L. J. Gooßen, *Chem. Sci.* **2018**, *9*, 5289; b) Y.-X. Li, Q.-Q. Xuan, L. Liu, D. Wang, Y.-J. Chen, C.-J. Li, *J. Am. Chem. Soc.* **2013**, *135*, 12536; c) H. Zhou, L. Zhang, C. Xu, S. Luo, *Angew. Chem. Int. Ed.* **2015**, *54*, 12645; d) D. Banerjee, R. V. Jagadeesh, K. Junge, H. Junge, M. Beller, *Angew. Chem. Int. Ed.* **2012**, *51*, 11556; e) H. Hikawa, Y. Yokoyama, *J. Org. Chem.* **2011**, *76*, 8433. For the α -allylation



Scheme 3.2 General pathway for TM-catalyzed allylic substitution reactions using allylic alcohols.

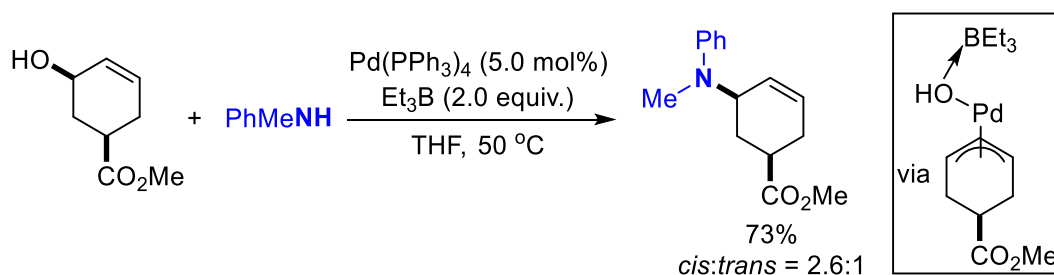
3.1.4 Pd-catalyzed Allylic Amination of Allylic Alcohols

Allylic amines are highly important building blocks for various bioactive compounds such as AchE inhibitor Huperzine A, the antifungal drug Naftifine and the calcium channel blocker Flunarizine.⁸⁶ They also serve as key intermediates for ring-closing metathesis,⁸⁷ asymmetric isomerization,⁸⁸ and in the total synthesis of natural products.⁸⁹ Pd-catalyzed allylic substitution with nitrogen nucleophiles is one of the most powerful and straightforward methods for the synthesis of allylic amines.⁹⁰ These reactions are known to proceed through a π -allyl Pd(II) intermediates generated by the oxidative addition of the allylic substrate to a Pd(0) species, followed by addition of the nitrogen nucleophile to form a new C–N bond in a regio-, stereo-, and enantio-selective manner. Over the past two decades, development of direct amination of allylic alcohols without prior derivatization has attracted much attention with respect to increasing the atom- and step-economy and thereby the environmental friendliness of the overall transformation.

Lewis acids are commonly used activators of allylic alcohols, particularly those based on boron. Tamaru *et al.* found that allylic alcohols can be *in situ* activated by

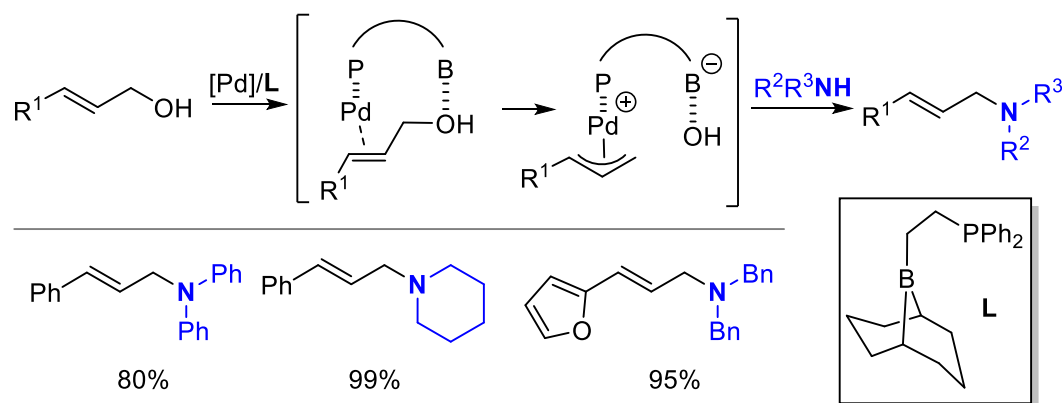
-
- of aldehydes and *N*-allylation using allylic alcohols as substrates in the presence of a Ni(0) catalyst: f) Y. Bernhard, B. Thomson, V. Ferey, M. Sauthier, *Angew. Chem. Int. Ed.* **2017**, *56*, 7460; g) M. Salah Azizi, Y. Edder, A. Karim, M. Sauthier, *Eur. J. Org. Chem.* **2016**, 3796; h) Y. Kayaki, T. Koda, T. Ikariya, *J. Org. Chem.* **2004**, *69*, 2595.
- (86) a) G. Petranyi, N. S. Ryder, A. Stutz, *Science* **1984**, *224*, 1239; b) H. Kanno, R. J. K. Taylor, *Tetrahedron Lett.* **2002**, *43*, 7337; c) J. Olesen, *J. Neurol.* **1991**, *238*, S23; d) E. M. Skoda, G. C. Davis, P. Wipf, *Org. Process Res. Dev.* **2012**, *16*, 26.
- (87) K. C. Nicolaou, P. G. Bulger, D. Sarlar, *Angew. Chem. Int. Ed.* **2005**, *44*, 4490.
- (88) S. Akutagawa, K. Tani, in: *Catalytic Asymmetric Synthesis, 2nd ed.* (Ed.: I Ojima), Wiley-VCH, New York, **2000**.
- (89) a) E. M. Skoda, G. C. Davis, P. Wipf, *Org. Process Res. Dev.* **2012**, *16*, 26; b) *Chiral Amine Synthesis* (Ed.: T. C. Nugent), Wiley-VCH, New York, **2008**; c) B. M. Trost, M. L. Crawley, *Chem. Rev.* **2003**, *103*, 2921.
- (90) a) M. Johansen, K. A. Jørgensen, *Chem. Rev.* **1998**, *98*, 1689. For original work: b) P. A. Evans, E. A. Clizbe, *J. Am. Chem. Soc.* **2009**, *131*, 8722; c) K.-Y. Ye, Q. Cheng, C.-X. Zhuo, L.-X. Dai, S.-L. You, *Angew. Chem. Int. Ed.* **2016**, *55*, 8113; d) I. Dubovyk, I. D. G. Watson, A. K. Yudin, *J. Am. Chem. Soc.* **2007**, *129*, 14172; e) B. M. Trost, D. R. Fandrick, T. Brodmann, D. T. Stiles, *Angew. Chem. Int. Ed.* **2007**, *46*, 6123; f) D. Banerjee, K. Junge, M. Beller, *Angew. Chem. Int. Ed.* **2014**, *53*, 13049.

stoichiometric or catalytic amounts of Et₃B and converted directly to the corresponding Pd(π -allyl) intermediates via oxidative addition to Pd(PPh₃)₄ (Scheme 3.3).⁹¹ This method is suitable for the bis-allylation of primary amines or mono-allylation of secondary aromatic and aliphatic amines.



Scheme 3.3 Amination of Et₃B-activated allylic alcohols.

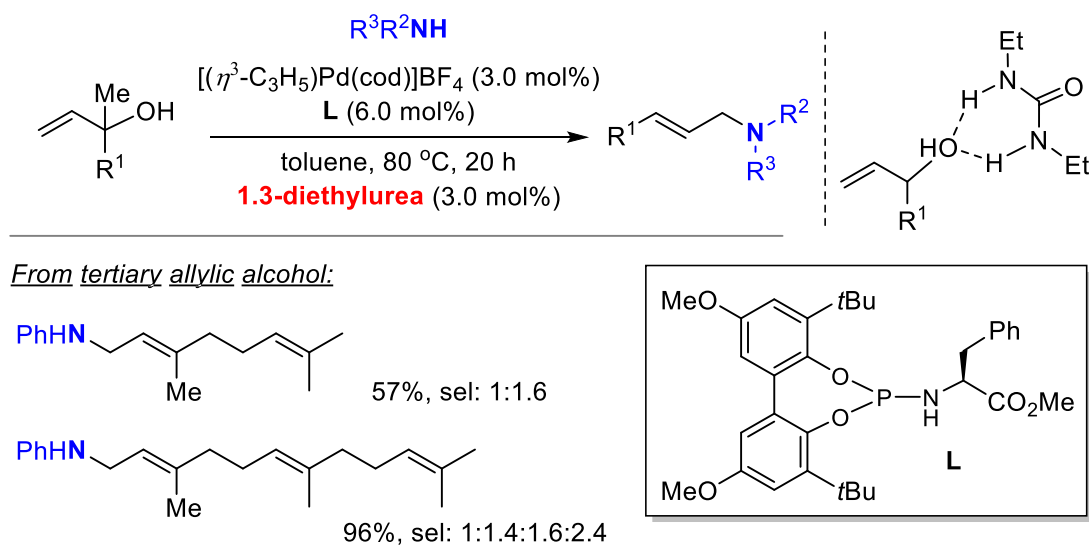
Afterwards, the same group employed a phosphine-borane ligand to the direct amination of the allylic alcohol.⁹² The Lewis acidic boryl group of the Pd/phosphine-borane catalyst activates the hydroxyl group and oxidative addition proceeds intramolecularly to give the corresponding allylic amines after nucleophilic attack on the π -allyl Pd(II) intermediate (Scheme 3.4). Additionally, other types of Lewis acids such as Ti(Oi-Pr)₄⁹³ and SnCl₂⁹⁴ could also be used as activator in this protocol.



Scheme 3.4 Pd/phosphine-borane catalyzed amination of allylic alcohols.

- (91) M. Kimura, M. Futamata, K. Shibata, Y. Tamaru, *Chem. Commun.* **2003**, 234.
 (92) G. Hirata, H. Satomura, H. Kumagai, A. Shimizu, G. Onodera, M. Kimura, *Org. Lett.* **2017**, *19*, 6148.
 (93) a) S.-C. Yang, C.-W. Hung, *J. Org. Chem.* **1999**, *64*, 5000; b) S.-C. Yang, Y.-C. Tsai, *Organometallics* **2001**, *20*, 763.
 (94) Y. Masuyama, M. Kagawa, Y. Kurusu, *Chem. Lett.* **1995**, 1121.

Supramolecular interactions are powerful to generate catalysts *in situ* by self-assembly of functionalized ligand building blocks, and often utilize hydrogen-bond interactions to modify the activity and selectivity of the catalyst. TM-catalyzed processes utilizing supramolecular interactions to activate allylic alcohols have gained prominence. In these approaches, the hydroxy function is made a better LG in the course of the allylic substitution reaction. Breit *et al.* developed an elegant self-assembled pyridone-phosphine ligand framework based on a complementary hydrogen bonding motif for allylation of indole derivatives and aniline nucleophiles.⁹⁵ Recently, a urea-based hydrogen-bonding strategy was disclosed by the Reek group,⁹⁶ and the presence of a functionalized monodentate phosphoramidite ligand (**L**) and 1,3-diethylurea was the key for the Pd mediated allylic amination process utilizing primary and secondary amines and allylic alcohols as substrates (Scheme 3.5). The phosphoramidite ligand with a phenyl alanine moiety has functional groups that allows for supramolecular interactions with the substrate. In terms of the scope of substrates containing a tertiary allylic alcohol, a mixture of stereoisomers were obtained in good yields.



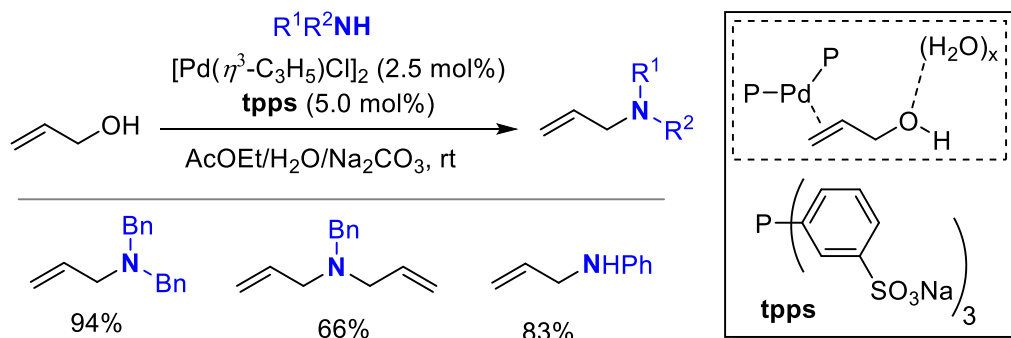
Scheme 3.5 Urea/phosphoramidite ligand-assisted amination of allylic alcohols.

A (protic) solvent as the hydrogen-bond donor can also effectively activate the hydroxyl group of an allylic alcohol to promote C–O bond cleavage and facilitate as such allylic amination with aryl and alkyl amines. Oshima and coworkers reported that hydrogen-bonding between water and allylic alcohols is key to reduce the activation

(95) I. Usui, S. Schmidt, M. Keller, B. Breit, *Org. Lett.* **2008**, *10*, 1207.

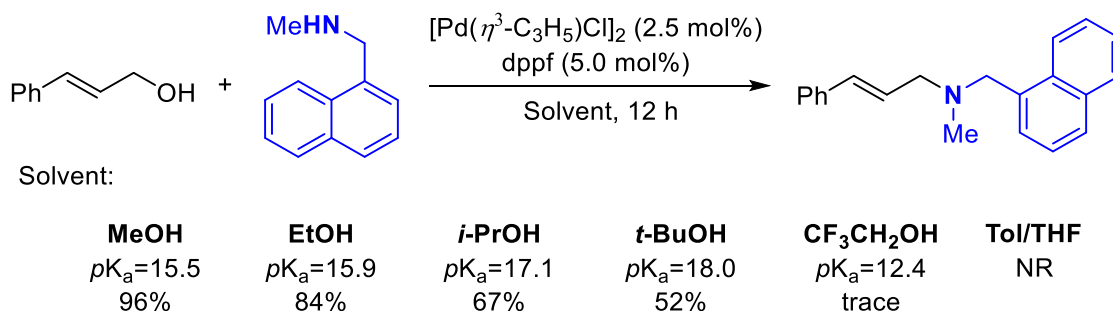
(96) Y. Gumrukcu, B. de Bruin, J. N. H. Reek, *ChemSusChem* **2014**, *7*, 890.

barrier for allylic amination (Scheme 3.6). This procedure has been realized with a catalyst system consisting of a suitable Pd precursor and *ttps* ligand (a sulfonated aryl phosphine) in the presence of a H₂O-based biphasic system. Theoretical calculations supported the importance of hydrogen-bonding between H₂O and the hydroxyl group of the allylic alcohol substrate to generate the Pd-allyl intermediate.⁹⁷



Scheme 3.6 Allylic alcohol activation by water to induce allylic amination.

Later, Zhang and coworkers found that MeOH is a suitable hydrogen-bond donor solvent for the activation of allylic alcohols, thus enabling the formation of the allyl Pd(II) intermediate by lowering the activation energy for the oxidative addition step (Scheme 3.7).⁹⁸ A series of protic solvents (MeOH, EtOH, *i*-PrOH, *t*-BuOH or CF₃CH₂OH) with different *pK_a* values were explored. The results indicated that MeOH (*pK_a* = 15.5) gives the best yield of allylic amine product, while the presence of much stronger acidic solvents (such as CF₃CH₂OH) or aprotic solvents such as toluene and THF resulted in much lower catalytic efficiencies.

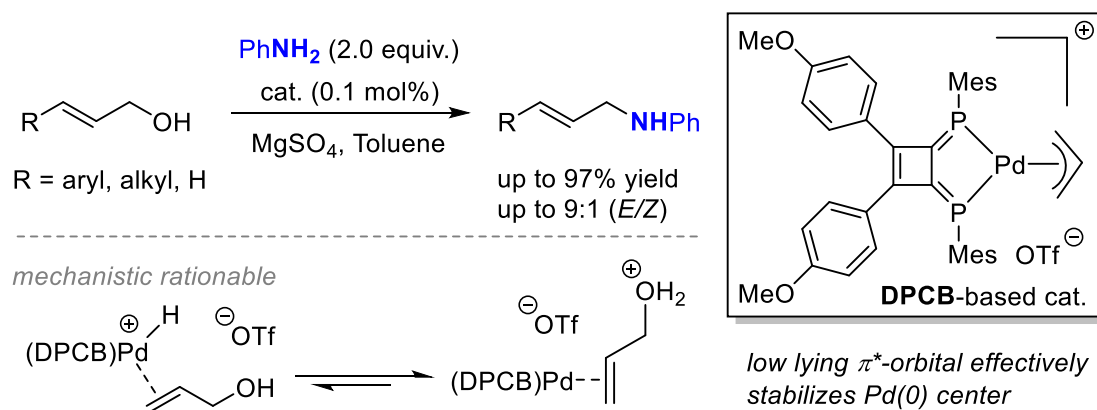


Scheme 3.7 Allylic alcohols activated by MeOH in allylic amination reactions.

(97) H. Kinoshita, H. Shinokubo, K. Oshima, *Org. Lett.* **2004**, *6*, 4085.

(98) J. Jing, X. Huo, J. Shen, J. Fu, Q. Meng, W. Zhang, *Chem. Commun.* **2017**, *53*, 5151.

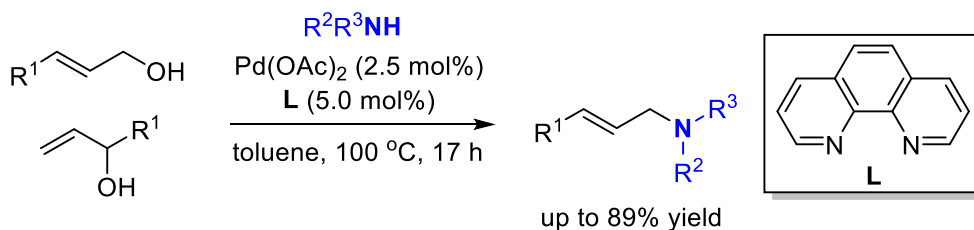
Another successful strategy proved to be the use of electron-deficient phosphorous-based ligands. Early work by Ozawa *et al.* demonstrated that a direct catalytic allylic amination of allyl alcohols by a (π -allyl)palladium complex bearing sp^2 -hybridized diphosphinocyclobutene ligand (DPCB) is feasible in the absence of external additives. DPCB (Scheme 3.8) as a low-coordinate phosphorus compound bears an extremely low-lying π^* -orbital which engages in significant Pd-to-phosphorus back-bonding favoring the formation of a protonated allylic alcohol-Pd(0) species over a cationic Pd(II) center, facilitating C–O bond cleavage (Scheme 3.8).⁹⁹ After that, Sarkar *et al.* reported a catalytic amination reaction of aryl-substituted allylic alcohols using aromatic amines by introducing a high π -acidity, bidentate phosphine ligand.¹⁰⁰ Recently, an effective Pd(BiPhePhos) based catalyst was reported by Samec *et al.* for a stereospecific allylic amination, and the authors suggested the intermediacy of a palladium hydride as a key species being responsible for the high reactivity.¹⁰¹



Scheme 3.8 Ligand promoted Pd-catalyzed amination of allylic alcohols.

Additionally, Beller and coworkers studied the reactivity of a series of nitrogen donor ligands, which are not commonly utilized in the amination of allylic alcohols. They found that the combination of $\text{Pd}(\text{OAc})_2$ and 1,10-phenanthroline allows for the successful conversion of a variety of aromatic and aliphatic allylic alcohols to their corresponding allylic amines by heating to 100 °C (Scheme 3.9). Moreover, the allylic amine yield was significantly suppressed when the reaction was carried out at lower temperature.¹⁰²

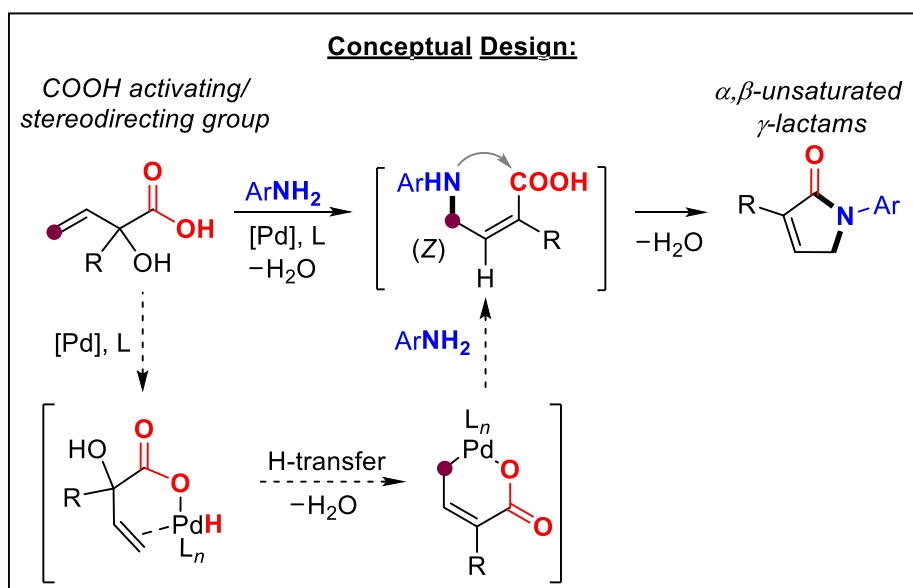
- (99) F. Ozawa, H. Okamoto, S. Kawagishi, S. Yamamoto, T. Minami, M. Yoshifuji, *J. Am. Chem. Soc.* **2002**, *124*, 10968.
 (100) R. Ghosh, A. Sarkar, *J. Org. Chem.* **2011**, *76*, 8508.
 (101) S. Akkarasamiyo, S. Sawadjoon, A. Orthaber, J. S. M. Samec, *Chem. Eur. J.* **2018**, *24*, 3488.
 (102) D. Banerjee, R. V. Jagadeesh, K. Junge, H. Junge, M. Beller, *ChemSusChem* **2012**, *5*, 2039.



Scheme 3.9 Phenanthroline promoted Pd-catalyzed amination of allylic alcohols.

3.1.5 Aim of the Work presented in this Chapter

Although allylic amination using allylic alcohol as substantially more economical substrates has been widely investigated, the reactions still require acidic activators or high reaction temperature to provide to promote C–O bond cleavage. We recently developed both stereo- as well as enantioselective protocols for challenging highly substituted allylic amines. Key to the success of these latter approaches was the presence of easy to activate LGs in the allylic precursor.



Scheme 3.10 Conceptual design towards a domino process converting α -tertiary allylic alcohols into an α, β -unsaturated γ -lactams under Pd catalysis.

Inspired by previous work on allylic amination from Ozawa¹⁰³ and Samec¹⁰⁴ revealing a transient Pd hydride species, we envisaged that an allylic alcohol substrate featuring a

- (103) a) F. Ozawa, T. Ishiyama, S. Yamamoto, S. Kawagishi, H. Murakami, *Organometallics* **2004**, *23*, 1698. b) F. Ozawa, H. Okamoto, S. Kawagishi, S. Yamamoto, T. Minami, M. Yoshifuji, *J. Am. Chem. Soc.* **2002**, *124*, 10968.
- (104) S. Sawadjoon, P. J. R. Sjöberg, A. Orthaber, O. Matsson, J. S. M. Samec, *Chem. Eur. J.* **2014**, *20*, 1520.

carboxylic acid group (Scheme 3.10) could generate a Pd hydride via oxidative addition to a suitable Pd(0) precursor.¹⁰⁵ This should allow for the formation of a palladacyclic intermediate that incorporates the requisite stereochemistry for efficient cyclization towards an α,β -unsaturated γ -lactams product¹⁰⁶ via amination of the terminal position of the allyl Pd(II) species.

A few challenges in this envisioned manifold need to be addressed, including the rarely developed stereocontrolled conversion of α -tertiary allylic alcohols,¹⁰⁷ and the use of mild reaction conditions to reduce the intrinsic risk of parasitic decarboxylative pathways. If successful, this method would represent a conceptually novel and practical approach for amination of allylic alcohols into valuable γ -lactam building blocks under ambient conditions without external additives. This envisioned catalytic transformation thus aims for the use of a carboxylic acid group acting as a hydrogen donor, stereodirecting and functional group to provide a wide series of pharma-relevant building blocks.

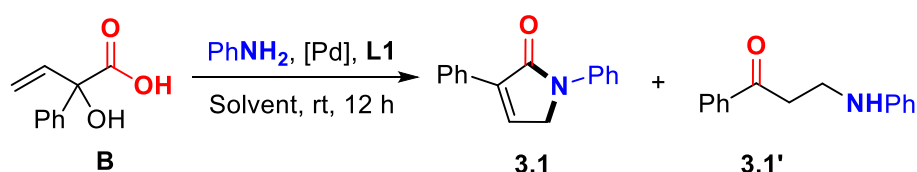
-
- (105) Initial oxidative addition of carboxylic acids to Pd(0) precursors to form metal carboxylates has been documented, see: a) N. Rodríguez, L. J. Gooßen, *Chem. Soc. Rev.* **2011**, *40*, 5030; b) L. J. Gooßen, N. Rodríguez, K. Gooßen, *Angew. Chem. Int. Ed.* **2008**, *47*, 3100.
- (106) a) J. Mathew, B. Alink, *J. Org. Chem.* **1990**, *55*, 3880; b) B. M. Trost, G. J. Roth, *Org. Lett.* **1999**, *1*, 67; c) X. del Corte, A. Maestro, J. Vicario, E. Martínez de Marigorta, F. Palacios, *Org. Lett.* **2018**, *20*, 317. Note that the *E*-isomers of the unsaturated γ -amino acids can be isolated and need to be hydrogenated first before cyclization to their γ -lactams can take place, see: d) C. Xia, J. Shen, D. Liu, W. Zhang, *Org. Lett.* **2017**, *19*, 4251.
- (107) Only very few contributions report on the use of these substrates though with important limitations in their substitution patterns, see: a) H. Hikawa, Y. Yokoyama, *Org. Biomol. Chem.* **2011**, *9*, 4044; b) T. Nishikata, B. H. Lipshutz, *Org. Lett.* **2009**, *11*, 2377. The use of a substrate with a mixed α,α -substitution in a Pd-catalyzed amination reaction of allylic alcohols was reported by Reek *et al.* (see ref. 96) albeit without stereocontrol.

3.2 Results and Discussion

3.2.1 Screening Studies

First, the required substrates were designed and these could be readily prepared from α -keto acids and vinyl Grignard reagents affording in good yields the desired vinyl glycolic acids. Allylic alcohol **B** was selected towards screening of appropriate reaction conditions and Pd/ligand combinations (Table 3.1) preferentially leading to the formation of γ -lactam **3.1**. The use of Pd(II) precursors (entries 1–2) proved to be rather unproductive.

Table 3.1: Optimization of the reaction conditions towards γ -lactam **3.1**^a



Entry	[Pd]	Solvent	Yield of 3.1 [%] ^b	3.1/3.1' ^c
1	Pd(OAc) ₂	CH ₃ CN	10	96:4
2	[allylPdCl] ₂	CH ₃ CN	0	–
3	Pd ₂ (dba) ₃ ·CHCl ₃	CH ₃ CN	45	98:2
4	Pd ₂ (dba) ₃ ·CHCl ₃	THF	14	76:24
5	Pd ₂ (dba) ₃ ·CHCl ₃	DMF	21	100:0
6	Pd ₂ (dba) ₃ ·CHCl ₃	DMSO	34	83:17
7	Pd ₂ (dba) ₃ ·CHCl ₃	MeOH	25	93:7
8	Pd ₂ (dba) ₃ ·CHCl ₃	DCM	30	99:1
9	Pd ₂ (dba) ₃ ·CHCl ₃	EtOAc	12	98:2
10	Pd ₂ (dba) ₃ ·CHCl ₃	Toluene	22	98:2

^aReaction conditions: allylic alcohol **B** (0.15 mmol), aniline (0.23 mmol, 1.5 equiv.), solvent (0.15 mL; 1.0 M), Pd₂(dba)₃·CHCl₃ (2.0 mol%), **L1**, DPEPhos (4.0 mol%), rt, 12 h. ^bDetermined by ¹H NMR (CDCl₃) using toluene as internal standard. ^cDetermined by ¹H NMR.

The use of a Pd(0) precursor and **L1** (DPEPhos) (entry 3) showed a significant improvement in the yield of **3.1** at only 25 °C, and the best solvent turned out to be acetonitrile (entry 3; 45% yield, **3.1:3.1'** = 98:2). The use of other solvents showed in several cases significant formation of **3.1'** that is formed after decarboxylation following an aza-Michael addition. Other ligands (**L2–L10**, Table 3.2, entries 1–10) were then probed, and the use of **L6** (dppf; entry 6) showed an encouraging increase in the yield of **3.1** to 79%.

Table 3.2: Further optimization of the reaction conditions towards γ -lactam **3.1**^a

B $\xrightarrow[\text{Solvent, rt, 12 h}]{\text{Pd}_2(\text{dba})_3 \cdot \text{CHCl}_3, \text{L}, \text{PhNH}_2 (1.5 \text{ equiv.})}$ **3.1** + **3.1'**

L1

L3: $n = 0$
L4: $n = 1$
L5: $n = 2$

L6: R = Ph
L7: R = *i*-Pr
L8: R = Cy

L2

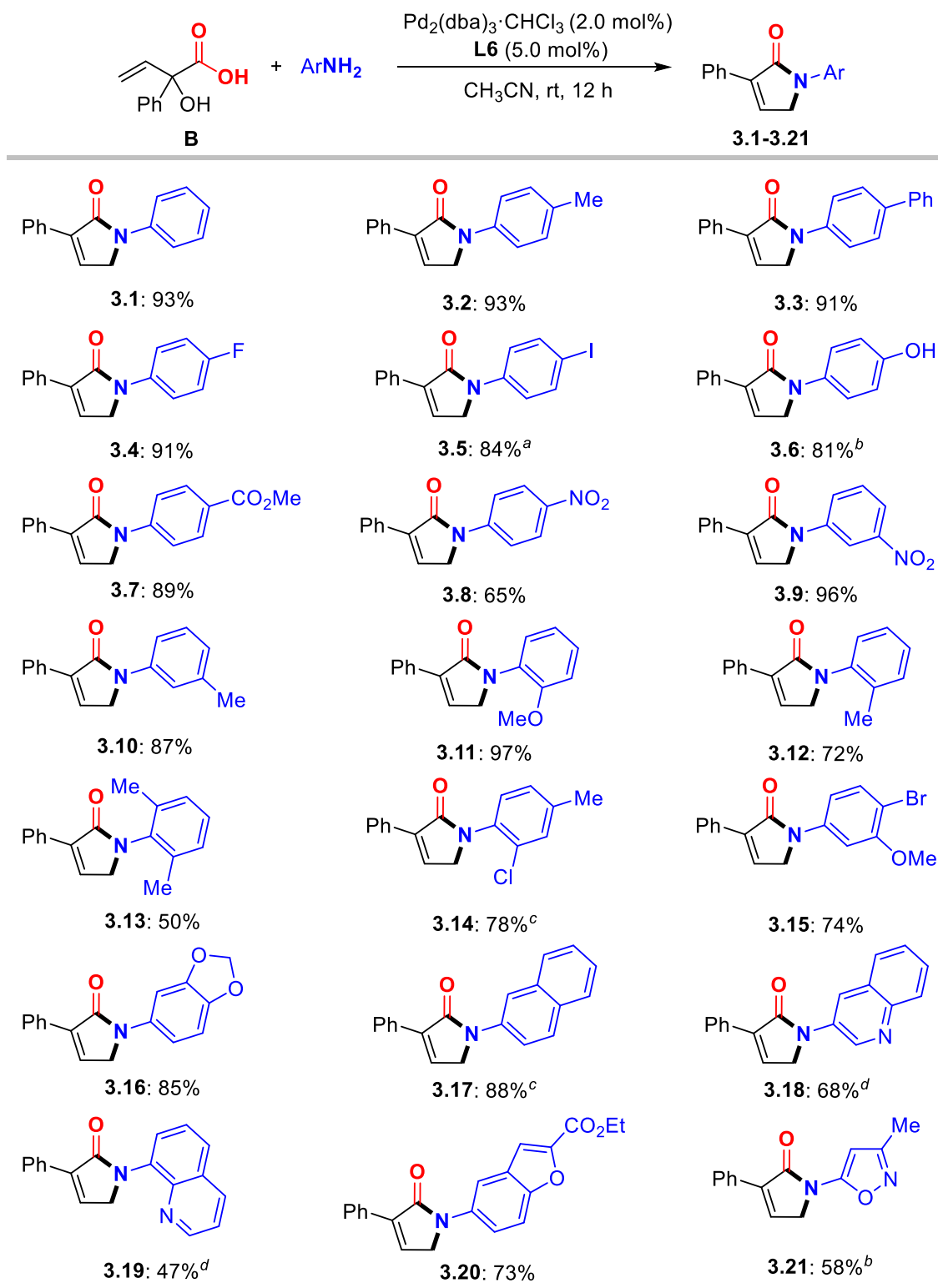
L9: R = Ph
L10: R = 2-furyl

Entry	Ligand	Solvent	Yield of 3.1 [%] ^b	3.1/3.1' ^c
1	L1	CH ₃ CN	45	98:2
2	L2	CH ₃ CN	5	–
3	L3	CH ₃ CN	trace	–
4	L4	CH ₃ CN	7	79:21
5	L5	CH ₃ CN	18	87:13
6	L6	CH ₃ CN	79	98:2
7	L7	CH ₃ CN	trace	–
8	L8	CH ₃ CN	trace	–
9	L9	CH ₃ CN	8	–
10	L10	CH ₃ CN	5	–
11 ^d	L6	CH ₃ CN	95	97:3
12 ^{d,e}	L6	CH ₃ CN	95	97:3
13 ^f	L6	CH ₃ CN	0	–

^aReaction conditions: allylic alcohol **B** (0.15 mmol), aniline (0.23 mmol, 1.5 equiv.), solvent (0.15 mL; 1.0 M), Pd₂(dba)₃·CHCl₃ (2.0 mol%), **L**, for monodentate ligand (8.0 mol%) or bidentate ligand (4.0 mol%), rt, 12 h. ^bDetermined by ¹H NMR (CDCl₃) using toluene as internal standard. ^cDetermined by ¹H NMR. ^d**L6** (5.0 mol%). ^eAniline (1.1 equiv.). ^fNo Pd precursor.

The optimized conditions for the formation of **3.1** were achieved by further increasing the amount of **L6** to 5.0 mol% and reducing the amount of aniline to 1.1 equiv. giving 93% isolated yield of **3.1** (entries 11–12). The presence of a Pd catalyst was crucial as no conversion of substrate **B** was noted in its absence (entry 13).

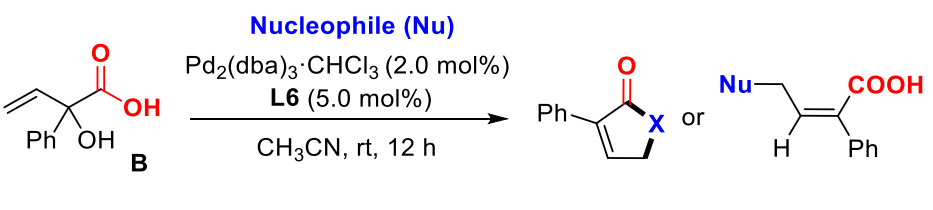
3.2.2 Scope of Substrates



Scheme 3.11 Variation of the aniline derivatives. Reaction conditions unless stated otherwise: all reactions were performed under the optimized conditions (Table 3.2, entry 12). Isolated yields are reported. ^a18 h. ^b26 h. ^cCH₃CN (0.30 mL). ^d50 °C, 24 h.

With the optimized conditions in hand, we then examined the scope in reaction partners and first varied the nature of the amine substrate (Scheme 3.11). Various anilines with *para*-, *meta*-, and *ortho*-substituents proved to be productive substrates giving clean access to the γ -lactam products (**3.1–3.15**) in typically appreciable to high isolated yields. The introduction of phenolic or aryl iodide groups in the lactam product is tolerated as exemplified by the successful isolation of product **3.5** and **3.6**, which have the potential for late stage modification towards the formation of biologically active compounds. Anilines with *para* electron-withdrawing groups or with a double *ortho*-substitution gave, as expected, somewhat lower yields (**3.8**; 65% and **3.13**; 50%). Interestingly, the developed protocol also tolerated the introduction of various other aromatic/heterocyclic fragments as illustrated by the synthesis of derivatives **3.16–3.21**, although in some of these latter cases a higher reaction temperature (50 °C) and/or longer reaction time was required. Product **3.19** incorporates a useful 8-quinolyl fragment, which is frequently utilized as a directing group in C–H functionalization.

Table 3.3: Examination of other nucleophiles^a

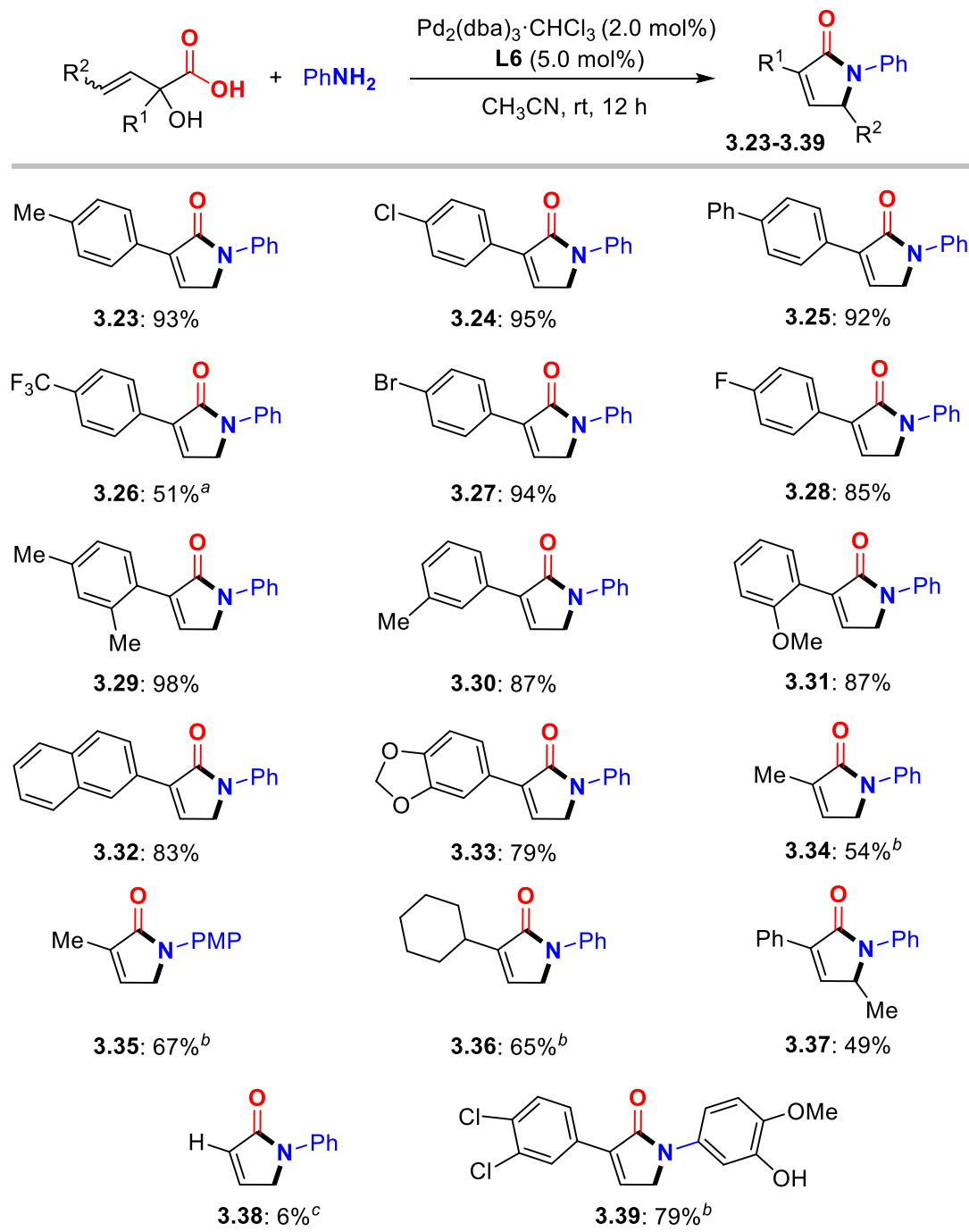


Entry	Nucleophile	Conv. ^b	Yield [%] ^b
1	PhCH ₂ NH ₂	100	24 ^c
2	MeOH	10	0
3	H ₂ O	9	0
4	TsNH ₂	5	0
5	PhCONH ₂	7	0
6	PhOH	14	0

^aReaction conditions: allylic alcohol **B** (0.15 mmol), nucleophile (1.1 equiv.), CH₃CN (0.15 mL), Pd₂(dba)₃·CHCl₃ (2.0 mol%), **L6** (5.0 mol%), rt, 12 h. ^bBy ¹H NMR (CDCl₃) using toluene as internal standard. ^c50.0 mol% CF₃COOH as additive, X = NCH₂Ph (product **3.22**), isolated yield.

Finally, we also attempted the use of alkyl amines, and while preliminary reactions showed that these easily become protonated and formation of the desired lactam is subsequently blocked, addition of sub-stoichiometric amounts of a Brønsted acid (CF₃COOH; **3.22**, 24%) allows for some product formation (Table 3.3, entry 1). A series of other potential nucleophiles (*O*- or *N*-based) were tested under the optimized

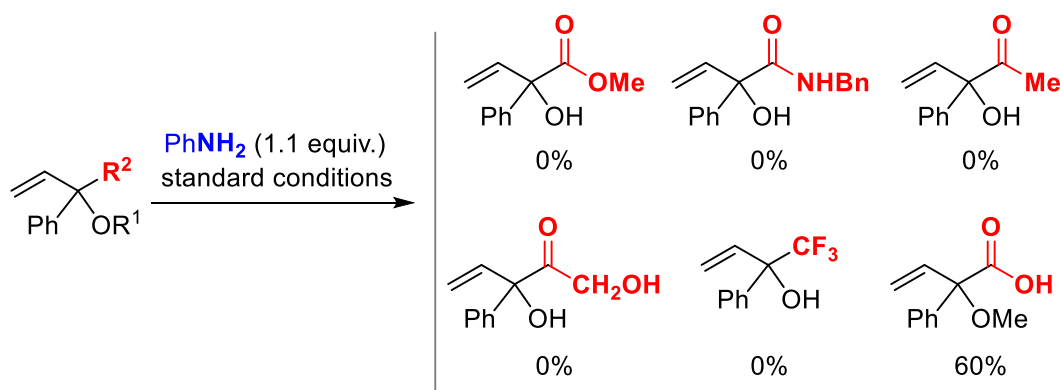
conditions. In the case of PhOH, H₂O, MeOH, TsNH₂ and PhC(O)NH₂ some conversion of **B** was noted but only decarboxylated product was detected (entries 2–6). The poor nucleophilic character of these compounds may explain these results.



Scheme 3.12 Variation of the α -tertiary allylic alcohols. Reaction conditions unless stated otherwise: all reactions were performed under the optimized conditions (Table 3.2, entry 12). Isolated yields are reported. ^a36 h. ^bUsing DMF (0.15 mL) as solvent at 70 °C. PMP = *p*-MeO-phenyl. ^c70 °C, 100% conversion, NMR yield of **3.38**.

Upon variation of the substituent of the α -tertiary allylic alcohol, a further amplification of lactam products could be easily realized (Scheme 3.12; products **3.23–3.39**). The installation of a bulky naphthyl group (**3.32**) or a heterocycle (**3.33**) in the lactam was feasible, while the conversion of the CF_3 -substituted allylic alcohol (*cf.*, synthesis of **3.26**) required a longer reaction time. In the case of the alkyl-substituted substrate congeners (*cf.*, preparation of **3.34–3.36**), the use of DMF at elevated temperature was required to maintain a homogeneous reaction medium. The use of a γ -substituted tertiary allylic alcohol also afforded the desired lactam product ($\text{R}^1 = \text{Ph}$, $\text{R}^2 = \text{Me}$; **3.37**, 49%) though the use of a secondary allylic alcohol ($\text{R}^1 = \text{R}^2 = \text{H}$; **3.38**) at room temperature showed no conversion. A higher reaction temperature was needed (70 °C), though a complex mixture was obtained and the lactam derivative was formed in only 6% yield. Lactam **3.39** could be isolated in 79% yield, which is a useful precursor for the 5-HT_{2C}-antagonist in Figure 3.1. The molecular structure of γ -lactam **3.1** was deduced by the X-ray diffraction studies (see section 3.4.6, Figure 3.2).

3.2.3 Mechanistic Control Reactions



Scheme 3.13 Different substituted allylic precursors subjected to the standard reaction conditions: substrate (0.15 mmol), aniline (1.1 equiv.), CH_3CN (0.15 mL), $\text{Pd}_2(\text{dba})_3 \cdot \text{CHCl}_3$ (2.0 mol%), **L6** (5.0 mol%), rt, 12 h. Yields determined by ^1H NMR using toluene as internal standard.

In order to support the mechanistic scenario displayed in Scheme 3.10, a number of control experiments were conducted. First, various substitutions were examined in the allylic substrate (Scheme 3.13), showing the crucial role of a free carboxyl group in allylic alcohol **B** to accommodate the conversion of the allylic substrate under ambient conditions. The replacement of the COOH for an ester, amide, methyl, alcohol or strong

electron-withdrawing CF₃ group did not lead to any observable conversion, whereas allylic alcohol protection (–OMe) still provided 60% yield of the lactam derivative **3.1**.

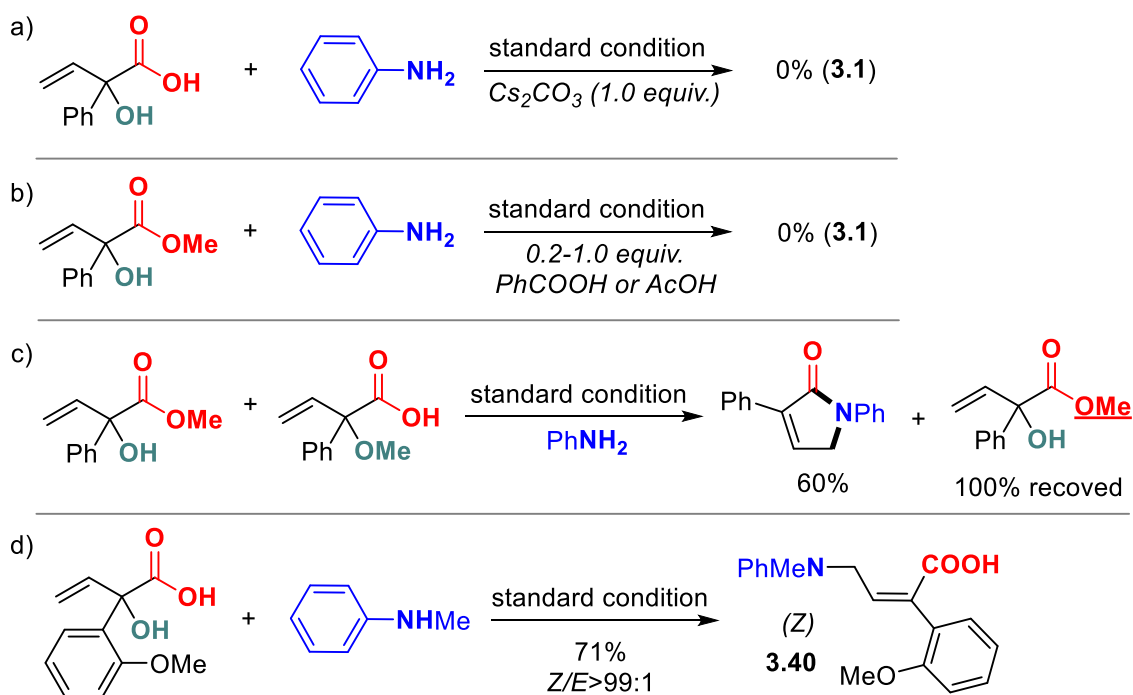
Further to this, in the presence of 1.0 equiv. of base (Scheme 3.14a; Cs₂CO₃) also no conversion of **B** could be achieved, further affirming the key role of the free carboxyl group within the substrate. The influence of the presence of (sub)stoichiometric amounts of a Brønsted acid (Scheme 3.14b) using methyl-ester **B**^{COOMe} was also examined. However, no conversion was noted in the presence of 0.5-2 equiv. HOAc as additive. An additional competition experiment involving a 1:1 mixture of the methyl-ester **B**^{COOMe} and the alcohol-protected substrate **B**^{OMe} showed only conversion of the latter: the ester derivative **B**^{COOMe} was quantitatively recovered (Scheme 3.14c). Both reactions illustrate that intermolecular COOH···OH hydrogen-bond activation does not seem to play any significant role in the conversion of the allylic substrate.¹⁰⁸

The X-ray analysis of allylic substrate **B** shows that the alcoholic OH group is involved in an intermolecular hydrogen bond with the carboxyl group of an adjacent molecule of **B**, with an O···H distance of 1.828 Å (O–H···O = 171.11°). Another intermolecular hydrogen bond was also detected between the carbonyl oxygen of a COOH group and the hydrogen of an OH fragment of a second molecule of **B**, with a distance of 1.926 Å (O–H···O = 153.86°). When examining intramolecular H-bonding, a hydrogen bond was found between the OH group and carbonyl oxygen of the COOH group with an O–H distance of 2.314 Å (O–H···O = 107.61°), which is similar to previously reported data for analogous compounds.¹⁰⁹ However, we did not detect any intramolecular hydrogen bond between the OH and COOH group (O–H distance of 4.149 Å) to account for an “OH activation model” (see section 3.4.6, Figure 3.3).

A conclusive confirmation of a possible HO···HO–C(O) interaction by ¹H NMR could not be obtained. However, the occurrence of some degree of requisite HO···HOOC hydrogen bonding in solution cannot be fully ruled out. Finally, a secondary aniline (Scheme 3.14d) was tested in the allylic amination of **B** providing in 71% yield the unsaturated γ -amino acid **Z-3.40** (for X-ray analysis see section 3.4.6, Figure 3.4) in support of the proposed mechanism presented in Scheme 10.

(108) Benzoic acid was previously reported to act as an activator in the amination of allylic alcohols, see: K. Kang, J. Kim, A. Lee, W. Y. Kim, H. Kim, *Org. Lett.* **2016**, *18*, 616.

(109) a) C. E. Blom, A. Bander, *J. Am. Chem. Soc.* **1982**, *104*, 2996; b) A. Borba, A. Gomez-Zavaglia, L. Lapinski, R. Fausto, *Phys. Chem. Chem. Phys.* **2004**, *6*, 2101.



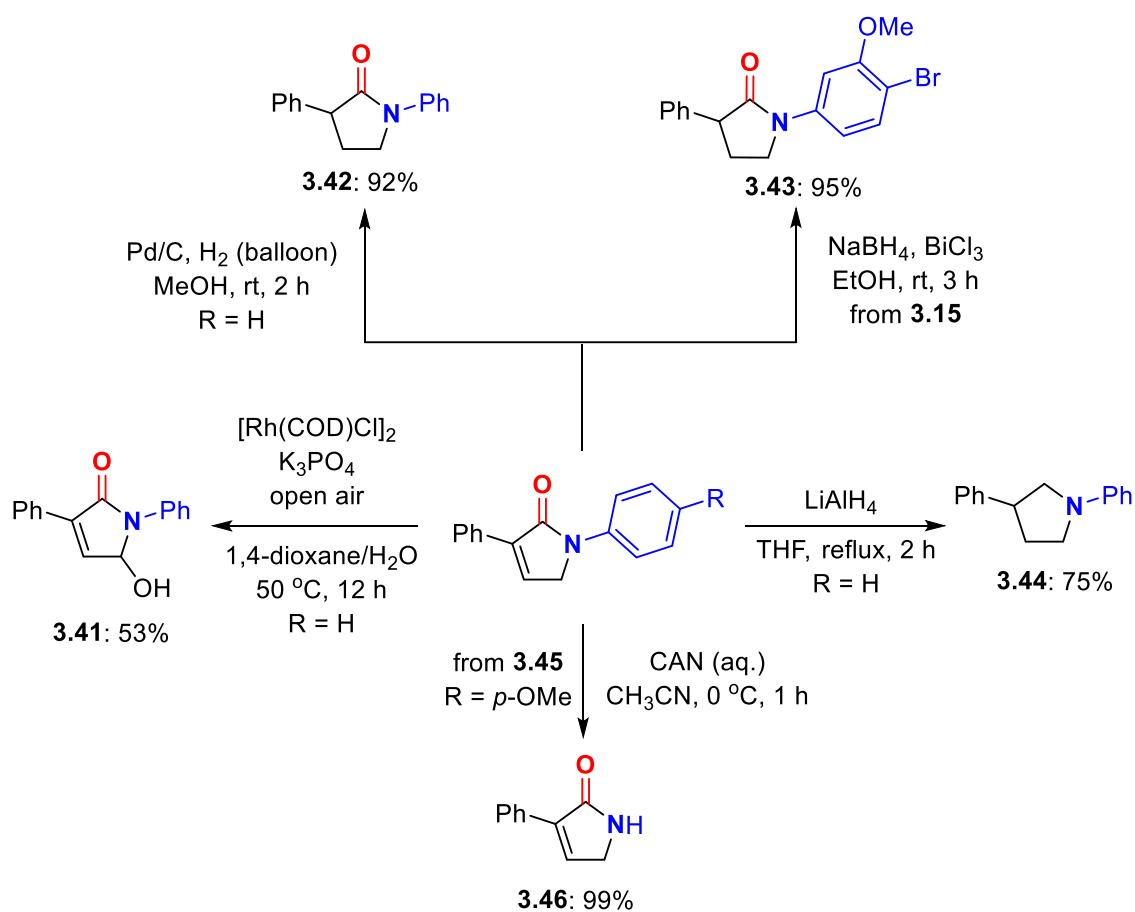
Scheme 3.14 Mechanistic control experiments to support the manifold proposed in Scheme 3.10. The standard conditions relate to entry 12 in Table 3.2.

3.2.4 Synthetic Transformations

We further explored the synthetic utility of these lactam compounds through a series of site-selective post-modifications (Scheme 3.15). A Rh-mediated oxidative C–H functionalization of **3.1** afforded **3.41** in 53% yield, and the identity of the product was unambiguously confirmed by X-ray analysis (see section 3.4.6, Figure 3.5). Hydrogenation of **3.1** using Pd/C as catalyst gave clean access to **3.42** (92%), while the use of a different reducing medium (NaBH₄/BiCl₃) for more functional lactam precursor **3.15** provided **3.43** in 95% yield. Pyrrolidine **3.44** could be prepared in 75% by reducing **3.1** in the presence of LiAlH₄, and finally deprotection of the *N*-PMP protected lactam **3.45** in the presence of cerium ammonium nitrate (CAN) gave the free lactam **3.46** in good yield. It should be further noted that products **3.35** and **3.43** are considered useful entries towards the formation of bioactive lactams Jatropham¹¹⁰ and therapeutic agents for neurological disorders,¹¹¹ respectively.

(110) L.-W. Liu, Z.-Z. Wang, H.-H. Zhang, W.-S. Wang, J.-Z. Zhang, Y. Tang, *Chem. Comm.* **2015**, 51, 9531.

(111) B. Blass, *ACS Med. Chem. Lett.* **2015**, 6, 1092.



Scheme 3.15 Post-synthetic potential of the α,β -unsaturated γ -lactam compounds.

3.3 Conclusions

Compared with procedures using “activated” allylic precursors in allylic substitution reactions, allylic alcohols have both economic and ecological advantages as their conversion would only produce water as by product. However, the addition of protic or Lewis acid additives and/or more forcing reaction conditions is typically required because of their lower reactivity, which may counterbalance the aforementioned advantages.

In this chapter, we disclose a user-friendly, mild and attractive protocol for direct and stereoselective amination of tertiary allylic alcohols in the absence of external additives. The *in situ* formed *Z*-configured γ -amino acid cyclizes to afford the synthetically useful α,β -unsaturated γ -lactams using readily available substrates. Key to the observed and unique reactivity is the presence of a free, carboxyl group in the substrate that allows for Pd-mediated activation of the allylic alcohol under ambient conditions. This new activation mode therefore holds great promise for a wider range of stereoselective allylic substitution reactions under sustainable reaction conditions.

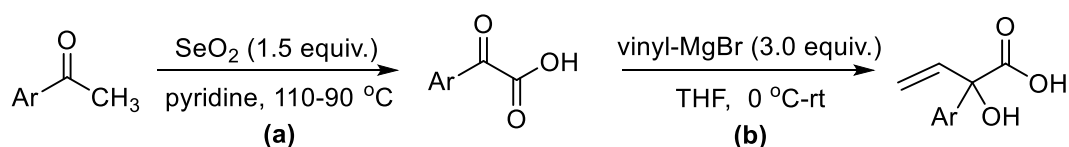
3.4 Experimental Section

3.4.1 General Considerations

Commercially available aryl methyl ketones, amines and solvents were purchased from Aldrich or TCI, and used without further purification. The palladium catalysts/precursors and ligands were purchased from Aldrich or TCI. ^1H NMR, ^{13}C NMR and ^{19}F NMR spectra were recorded at room temperature on a Bruker AV-400 or AV-500 spectrometer and referenced to the residual deuterated solvent signals. All reported NMR values are given in parts per million (ppm). FT-IR measurements were carried out on a Bruker Optics FTIR Alpha spectrometer. Mass spectrometric analyses and X-ray diffraction studies were performed by the Research Support Group at ICIQ. In the screening phase, the internal standard toluene (1.0 equiv.) was added after the reaction mixture was stirred at room temperature for 12 h, and then an aliquot of the mixture was taken for NMR analysis.

3.4.2 General Procedure for the Synthesis of Vinyl Glycolic Acids

The vinyl aryl glycolic acids can be easily prepared according to a reported procedure.¹¹²



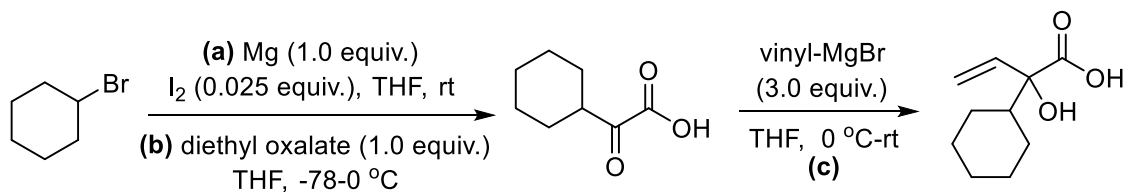
Step (a): To a round-bottom flask equipped with a stirring bar was added the aryl methyl ketone (10.0 mmol) and selenium dioxide (SeO_2 , 1.67 g, 15.0 mmol), then anhydrous pyridine (40 mL) was added quickly. The reaction was stirred and heated in an oil bath under an N_2 atmosphere to 110 $^\circ\text{C}$ for 1 h, and then the bath temperature was lowered and kept at 90 $^\circ\text{C}$ for another 4 h. The reaction mixture was filtered using a Büchner funnel, and the aqueous layer was washed with EtOAc (3×20 mL). The combined filtrate was treated with HCl (1.0 M) to about pH 1.5, and extracted with EtOAc (3×30 mL). The combined organic layers were dried over anhydrous Na_2SO_4 , filtered

(112) a) R. J. Adamski, J. G. Cannon, *J. Med. Chem.* **1965**, *8*, 444; b) L. J. Gooßen, F. Rudolphi, C. Oppel, N. Rodríguez, *Angew. Chem. Int. Ed.* **2008**, *47*, 3043; c) K. Wadhwa, C. Yang, P. R. West, K. C. Deming, S. R. Chemburkar, R. E. Reddy, *Synth. Commun.* **2008**, *38*, 4434.

and concentrated under reduced pressure. The crude aryl glyoxylic acid could be directly used in the next step (see below).

Step (b): Under an N₂ atmosphere, to a separate flame-dried round-bottom flask equipped with a stirring bar was added the crude aryl glyoxylic acid (8.0 mmol) and THF (16.0 mL). The solution was cooled down to 0 °C (ice/water), followed by dropwise addition of vinyl magnesium bromide in THF (1.0 M, 24.0 mL, 24.0 mmol). The reaction was allowed to stir under room temperature for 12 h. The reaction mixture was quenched with saturated aqueous NH₄Cl, then an excess of cold 50% (v/v) H₂SO₄ was added. The resulting organic layer was separated and the aqueous layer was washed with ether (4 × 30 mL). The combined organic layers were dried over anhydrous Na₂SO₄, filtered and concentrated. The residue was purified by flash chromatography on silica to afford the corresponding vinyl aryl glycolic acids.

The cyclohexyl vinyl glycolic acid can be prepared according to a previous reported procedure with minor modifications.¹¹³



Step (a): Magnesium turnings (10.0 mmol, 0.24 g) and I₂ (0.025 equiv.) were introduced into a well-dried Schlenk flask equipped with a stirring bar; the mixture was subjected to three cycles of vacuum/filling with N₂. After that, under protection of N₂, the flask was gently heated with a heat gun until the iodine had melted completely. The resultant mixture was stirred for 30 min at room temperature. Then dry THF (15 mL) was added affording a brown solution, to which cyclohexyl bromide (10.0 mmol, 1.63 g) was added in one portion. Upon stirring for 30 min at room temperature all the magnesium turnings had been consumed.

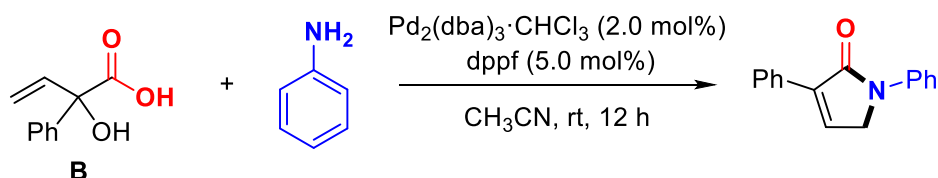
Step (b): This solution was then cooled down to -78 °C, followed by dropwise addition of a solution of diethyl oxalate (1.46 g, 10.0 mmol) in THF (40 mL). The reaction was allowed to warm to 0 °C and stirred for 10 min. The reaction mixture was quenched with

(113) W.-M. Cheng, R. Shang, H.-Z. Yu, Y. Fu, *Chem. Eur. J.* **2015**, *21*, 13191.

10% (v/v) HCl, then an excess of water was added. The resulting mixture was extracted by EtOAc (4 × 30 mL). The combined organic layers were dried over anhydrous Na₂SO₄, filtered and concentrated to give the crude ethyl 2-cyclohexyl-2-oxoacetate, which could be used directly. To a solution of ethyl 2-cyclohexyl-2-oxoacetate in MeOH (25 mL) was added water (60 mL) and NaOH (50.0 wt %, 20 mL) at room temperature. The reaction mixture was stirred at 60 °C for 6 h. After the reaction, the mixture was acidified with 15.0 % (v/v) HCl and extracted with EtOAc (2 × 50 mL). The extracts were dried over anhydrous Na₂SO₄, filtered and concentrated to give a white solid.

The following step (c) is similar with the second step of the general method and afforded the cyclohexyl vinyl glycolic acid as a white solid.

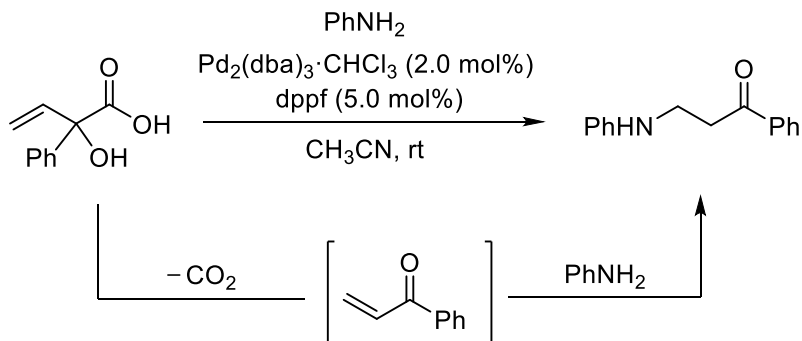
3.4.3 Typical Procedure for the Formation of Unsaturated γ -Lactams



Representative case:

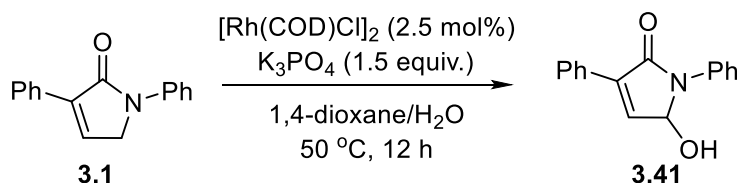
Vinyl glycolic acid **B** (0.0267 g, 0.15 mmol, 1.0 equiv.) was combined with Pd₂(dba)₃·CHCl₃ (0.0030 g, 2.0 mol%), dppf (0.0042 g, 5.0 mol%) and aniline (0.0153 g, 0.165 mmol, 1.1 equiv.) in CH₃CN (0.15 mL) at room temperature in air. The reaction mixture was stirred at room temperature for 12 h, after which the pure product was isolated by flash chromatography (32.8 mg, 93%, Hexane/EtOAc = 20:1, *R_f* = 0.15). All purified products were fully characterized by NMR (¹H, ¹³C, ¹⁹F), IR and HRMS. For some cases, it proved to be difficult to isolate the pure lactam by chromatography as small amounts of decarboxylated aza-Michael addition product remained. In those cases, additional recrystallization was needed from DCM/pentane.

3.4.4 Typical Procedure for the Formation of Decarboxylation/aza-Michael Addition Reaction Product



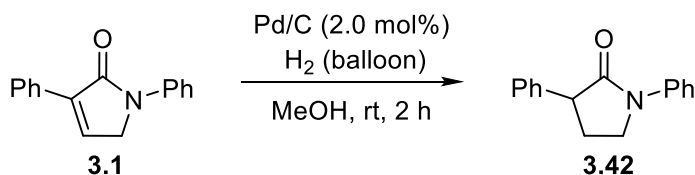
The by-product was detected in the presence of $\text{Pd}_2(\text{dba})_3 \cdot \text{CHCl}_3$ and dppf . The ^1H and ^{13}C NMR data is in agreement with previously reported data.¹¹⁴

3.4.5 Post-synthetic Potential of the α,β -Unsaturated γ -Lactam Scaffolds

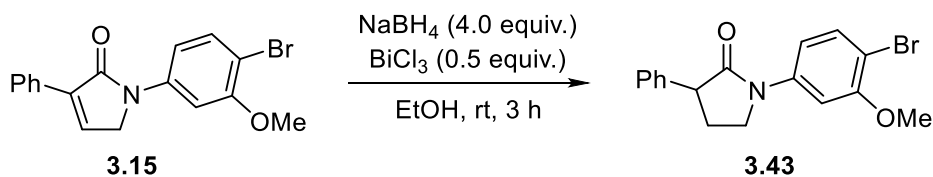


The γ -lactam **3.1** (39.8 mg, 0.15 mmol, 1.0 equiv.), $[\text{Rh}(\text{COD})\text{Cl}]_2$ (1.85 mg, 2.5 mol%) and K_3PO_4 (47.5 mg, 1.5 equiv.) were dissolved into 1,4-dioxane/ H_2O (5/1, v/v, 1.0 mL), and then the resultant mixture was stirred for 12 h at 50 °C under air, after which the pure product (**3.41**) was isolated by flash chromatography (19.9 mg, 53%) as a light yellow solid.

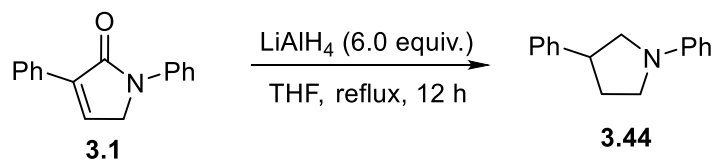
(114) D. Das, S. Pratihari, S. Roy, *J. Org. Chem.* **2013**, 78, 2430.



A Schlenk tube was charged with γ -lactam **3.1** (35.3 mg, 0.15 mmol, 1.0 equiv.) and Pd/C catalyst (3.2 mg, 10.0 wt % palladium on carbon), and then the reactor was evacuated/filled with H₂ (balloon) for three times. After that, MeOH (0.5 mL) was added and the reaction mixture was stirred under H₂ atmosphere (balloon) for 2 h at room temperature, and monitored by NMR. The reaction mixture was filtered through Celite. The solvent in the filtrate was evaporated under reduced pressure. The residue was purified by flash chromatography to afford the pure saturated γ -lactam **3.42** (32.7 mg, 92%) as a white solid. The ¹H and ¹³C NMR data is in agreement with those previously reported.¹¹⁵



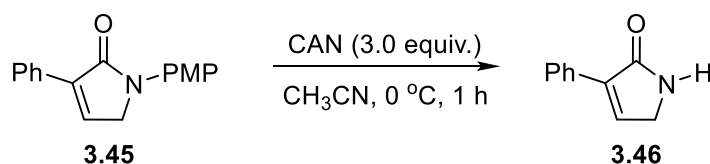
To a solution of the lactam **3.15** (0.1 mmol, 34.4 mg) in EtOH (0.6 mL), bismuth chloride (0.05 mmol, 15.7 mg) was added. After stirring for 10 min, NaBH₄ (0.4 mmol, 15.2 mg) was added at 0 °C, then the mixture was allowed to stir at room temperature for 3 h. After evaporation of the solvent, the residue was purified by flash chromatography to afford product **3.43** (32.9 mg, 95%) as a white oil.



To an oven-dried Schlenk tube was added γ -lactam **3.1** (35.3 mg, 0.15 mmol, 1.0 equiv.), and the reactor was evacuated/filled with N₂ for three times. After that, LiAlH₄ in THF (1.0 M, 0.9 mL, 6.0 equiv.) was added and the reaction mixture was heated to

(115) I. Sorribes, J. R. Cabrero-Antonino, C. Vicent, K. Junge, M. Beller, *J. Am. Chem. Soc.* **2015**, *137*, 13580.

reflux for 12 h. The reaction mixture was quenched with 10% NaOH (aq) and heated at reflux for another 1 h. The organic components were extracted with DCM (3×15 mL), the combined organic layers were washed with brine, dried over Na₂SO₄, filtered, and then concentrated under reduced pressure. The residue was purified by flash chromatography to afford the pure, reduced product **3.44** (25.1 mg, 75%) as a yellow oil.



The γ -lactam **3.45** (39.8 mg, 0.15 mmol, 1.0 equiv.) was dissolved into CH₃CN (0.8 mL), and a solution of CAN (240.0 mg, 0.45 mmol) in H₂O (1.2 mL) was added dropwise at 0 °C. The resultant solution was stirred for 1 h at 0 °C. Hereafter, saturated aqueous NaHCO₃ was added and the organic components were extracted with DCM (3×15 mL). Upon removal of the organic solvent, the crude product was purified by flash chromatography to afford the deprotected γ -lactam **3.46** (23.9 mg, 99%) as a white solid.

3.4.6 X-ray Crystallographic Studies

The experimental procedure for the X-ray analyses of compounds **3.1**, **3.40**, **3.41** and substrate **B** was the same as detailed in chapter 2.



Figure 3.2 X-ray molecular structure of γ -lactam **3.1**.

Crystal data for 3.1:

C_{9.5}H_{9.5}N_{0.5}OCl, *Mr* = 182.13, triclinic, *P*-1, *a* = 7.4617(13) Å, *b* = 11.272(2) Å, *c* = 11.3361(18) Å, α = 72.069(5)°, β = 77.994(5)°, γ = 78.711(5)°, *V* = 878.4(3) Å³, *Z* = 4, ρ = 1.377 mg·M⁻³, μ = 0.380 mm⁻¹, λ = 0.71073 Å, *T* = 100(2) K, *F*(000) = 380, crystal size = 0.10 × 0.05 × 0.03 mm³, θ (min) = 1.912°, θ (max) = 32.411°, 8818 reflections collected, 5094 reflections unique (*R*_{int} = 0.0353), *GoF* = 1.066, *R*₁ = 0.0616 and *wR*₂ =

0.1641 [$I > 2\sigma(I)$], $R_1 = 0.0964$ and $wR_2 = 0.1829$ (all indices), min/max residual density = $-0.449/0.427$ [$e \cdot \text{\AA}^{-3}$]. Completeness to $\theta(32.411^\circ) = 80.8\%$. For further details see CCDC number 1895597.

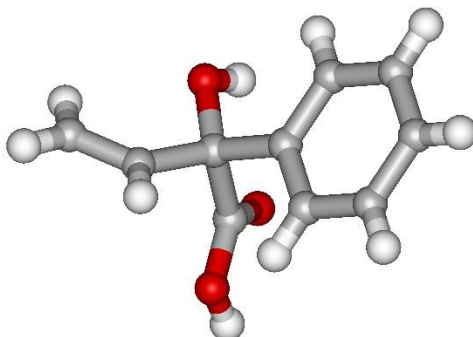


Figure 3.3 X-ray molecular structure of substrate **B**.

Crystal data for substrate **B**:

$C_{10}H_{10}O_3$, $M_r = 178.18$, monoclinic, $C2/1c$, $a = 20.6169(10)$ \AA , $b = 5.8027(3)$ \AA , $c = 16.2203(7)$ \AA , $\alpha = 90^\circ$, $\beta = 111.4952(12)^\circ$, $\gamma = 90^\circ$, $V = 1805.53(15)$ \AA^3 , $Z = 8$, $\rho = 1.311$ $\text{mg} \cdot \text{M}^{-3}$, $\mu = 0.097$ mm^{-1} , $\lambda = 0.71073$ \AA , $T = 100(2)$ K , $F(000) = 752$, crystal size = $0.50 \times 0.10 \times 0.10$ mm^3 , $\theta(\text{min}) = 2.699^\circ$, $\theta(\text{max}) = 30.597^\circ$, 6306 reflections collected, 2660 reflections unique ($R_{\text{int}} = 0.0229$), $\text{GoF} = 1.028$, $R_1 = 0.0380$ and $wR_2 = 0.0995$ [$I > 2\sigma(I)$], $R_1 = 0.0423$ and $wR_2 = 0.1029$ (all indices), min/max residual density = $-0.253/0.446$ [$e \cdot \text{\AA}^{-3}$]. Completeness to $\theta(30.597^\circ) = 95.6\%$. For further details see CCDC number 1865708.

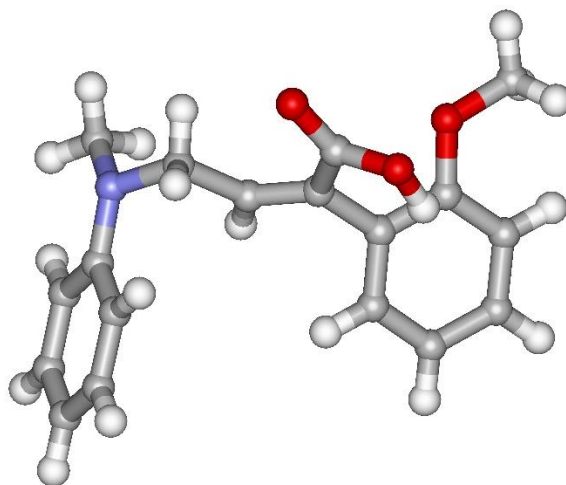


Figure 3.4 X-ray molecular structure of **3.40**.

Crystal data for 3.40:

$C_{18}H_{19}NO_3$, $M_r = 297.34$, monoclinic, $P2(1)/n$, $a = 10.908(3) \text{ \AA}$, $b = 7.824(2) \text{ \AA}$, $c = 18.575(5) \text{ \AA}$, $\alpha = 90^\circ$, $\beta = 100.740(7)^\circ$, $\gamma = 90^\circ$, $V = 1557.5(7) \text{ \AA}^3$, $Z = 4$, $\rho = 1.268 \text{ mg}\cdot\text{M}^{-3}$, $\mu = 0.086 \text{ mm}^{-1}$, $\lambda = 0.71073 \text{ \AA}$, $T = 100(2) \text{ K}$, $F(000) = 632$, crystal size = $0.50 \times 0.25 \times 0.10 \text{ mm}^3$, $\theta(\text{min}) = 2.016^\circ$, $\theta(\text{max}) = 31.561^\circ$, 16796 reflections collected, 5094 reflections unique ($R_{\text{int}} = 0.0251$), $\text{GoF} = 1.041$, $R_1 = 0.0426$ and $wR_2 = 0.1130 [I > 2\sigma(I)]$, $R_1 = 0.0507$ and $wR_2 = 0.1189$ (all indices), min/max residual density = $-0.332/0.386 [e\cdot\text{\AA}^{-3}]$. Completeness to $\theta(31.561^\circ) = 97.8\%$. For further details see CCDC number 1858454.

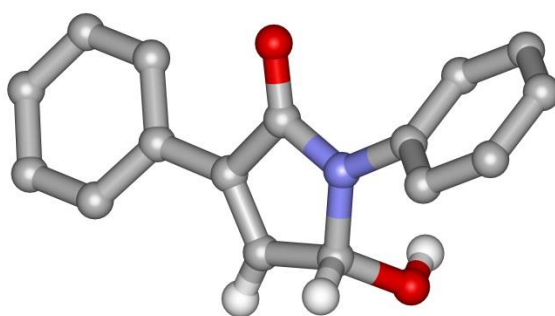
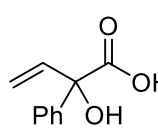


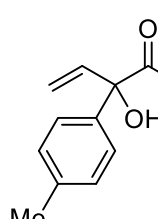
Figure 3.5 X-ray molecular structure of γ -lactam **3.41**.

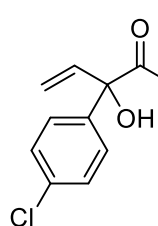
Crystal data for 3.41:

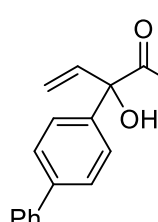
$C_{16}H_{13}NO_2$, $M_r = 251.27$, monoclinic, $P2(1)/c$, $a = 11.2127(4) \text{ \AA}$, $b = 15.6451(6) \text{ \AA}$, $c = 7.0535(3) \text{ \AA}$, $\alpha = 90^\circ$, $\beta = 93.2360(14)^\circ$, $\gamma = 90^\circ$, $V = 1235.38(8) \text{ \AA}^3$, $Z = 4$, $\rho = 1.351 \text{ mg}\cdot\text{M}^{-3}$, $\mu = 0.090 \text{ mm}^{-1}$, $\lambda = 0.71073 \text{ \AA}$, $T = 100(2) \text{ K}$, $F(000) = 528$, crystal size = $0.30 \times 0.10 \times 0.07 \text{ mm}^3$, $\theta(\text{min}) = 2.237^\circ$, $\theta(\text{max}) = 31.556^\circ$, 8716 reflections collected, 3946 reflections unique ($R_{\text{int}} = 0.0200$), $\text{GoF} = 1.041$, $R_1 = 0.0446$ and $wR_2 = 0.1208 [I > 2\sigma(I)]$, $R_1 = 0.0520$ and $wR_2 = 0.1265$ (all indices), min/max residual density = $-0.228/0.452 [e\cdot\text{\AA}^{-3}]$. Completeness to $\theta(31.556^\circ) = 95.5\%$. For further details see CCDC number 1858453.

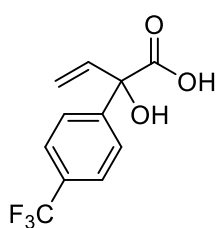
3.4.7 Analytical Data for All Compounds

 **¹H NMR** (400 MHz, CDCl₃) δ 7.60 – 7.53 (m, 2H), 7.42 – 7.30 (m, 3H), 6.44 (dd, *J* = 17.0, 10.6 Hz, 1H), 5.66 (dd, *J* = 17.1, 1.0 Hz, 1H), 5.40 (dd, *J* = 10.5, 1.0 Hz, 1H) ppm. **¹³C NMR** (101 MHz, CDCl₃) δ 178.09, 140.36, 137.40, 128.71, 128.62, 126.21, 116.62, 78.64 ppm. **IR** (neat): ν (cm⁻¹) 3407, 2937, 1712, 1246, 1191, 1152, 720, 698. **HRMS** (ESI⁻, MeOH): *m/z* calcd. 177.0557 (M – H)⁻, found: 177.0549.

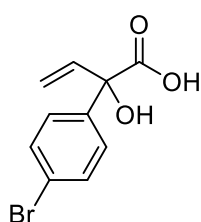
 **¹H NMR** (400 MHz, CDCl₃) δ 7.47 – 7.40 (m, 2H), 7.21 – 7.15 (m, 2H), 6.43 (dd, *J* = 17.0, 10.5 Hz, 1H), 5.64 (dd, *J* = 17.0, 1.0 Hz, 1H), 5.39 (dd, *J* = 10.5, 1.0 Hz, 1H), 2.34 (s, 3H) ppm. **¹³C NMR** (101 MHz, CDCl₃) δ 178.78, 138.43, 137.53, 137.47, 129.36, 126.12, 116.41, 78.49, 21.20 ppm. **IR** (neat): ν (cm⁻¹) 3425, 2923, 1719, 1673, 1180, 1153, 1006, 817, 727. **HRMS** (ESI⁻, MeOH): *m/z* calcd. 191.0714 (M – H)⁻, found: 191.0716.

 **¹H NMR** (400 MHz, CDCl₃) δ 7.54 – 7.47 (m, 2H), 7.37 – 7.31 (m, 2H), 6.38 (dd, *J* = 17.0, 10.5 Hz, 1H), 5.64 (dd, *J* = 17.0, 0.9 Hz, 1H), 5.40 (dd, *J* = 10.5, 0.9 Hz, 1H) ppm. **¹³C NMR** (101 MHz, CDCl₃) δ 178.14, 138.78, 137.09, 134.64, 128.80, 127.76, 117.02, 78.14 ppm. **IR** (neat): ν (cm⁻¹) 3413, 2984, 1729, 1490, 1290, 1149, 1095, 1006, 828, 678. **HRMS** (ESI⁻, MeOH): *m/z* calcd. 211.0167 (M – H)⁻, found: 211.0164.

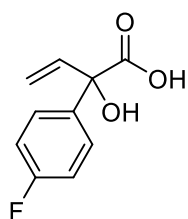
 **¹H NMR** (400 MHz, CDCl₃) δ 7.66 – 7.56 (m, 6H), 7.46 – 7.41 (m, 2H), 7.38 – 7.33 (m, 1H), 6.49 (dd, *J* = 17.0, 10.5 Hz, 1H), 5.70 (dd, *J* = 17.1, 1.0 Hz, 1H), 5.43 (dd, *J* = 10.6, 1.0 Hz, 1H) ppm. **¹³C NMR** (126 MHz, CDCl₃) δ 177.52, 141.57, 140.59, 139.39, 137.41, 128.96, 127.68, 127.45, 127.30, 126.69, 116.68, 78.54 ppm. **IR** (neat): ν (cm⁻¹) 3413, 3384, 3029, 1720, 1486, 1245, 1145, 839, 696. **HRMS** (ESI⁻, MeOH): *m/z* calcd. 209.0966 (M – CO₂ – H)⁻, found: 209.0974.



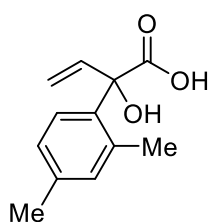
¹H NMR (400 MHz, CDCl₃) δ 7.76 – 7.59 (m, 4H), 6.41 (dd, *J* = 17.0, 10.5 Hz, 1H), 5.66 (dd, *J* = 17.0, 0.8 Hz, 1H), 5.43 (dd, *J* = 10.5, 0.8 Hz, 1H) ppm. **¹³C NMR** (101 MHz, CDCl₃) δ 177.82, 144.04, 136.94, 130.80 (q, *J* = 32.8 Hz), 126.77, 125.60 (q, *J* = 3.7 Hz), 117.31, 78.27 ppm. **¹⁹F NMR** (376 MHz, CDCl₃) δ -62.83 ppm. **IR** (neat): ν (cm⁻¹) 3506, 3032, 2527, 1712, 1619, 1321, 1152, 1113, 1067, 945, 841. **HRMS** (ESI⁻, MeOH): *m/z* calcd. 201.0527 (M – CO₂ – H)⁻, found: 201.0529.



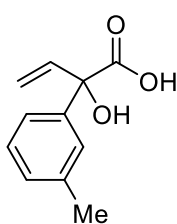
¹H NMR (500 MHz, Methanol-*d*₄) δ 7.52 – 7.44 (m, 4H), 6.48 (dd, *J* = 16.8, 10.4 Hz, 1H), 5.53 (dd, *J* = 17.1, 1.4 Hz, 1H), 5.31 (dd, *J* = 10.6, 1.2 Hz, 1H) ppm. **¹³C NMR** (126 MHz, MeOD) δ 175.86, 142.84, 140.28, 132.19, 129.38, 122.70, 115.53, 79.48 ppm. **IR** (neat): ν (cm⁻¹) 3412, 2952, 1728, 1486, 1153, 1007, 826, 720. **HRMS** (ESI⁻, MeOH): *m/z* calcd. 210.9759 (M – CO₂ – H)⁻, found: 210.9758.



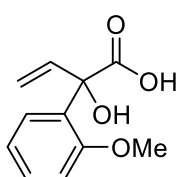
¹H NMR (500 MHz, CDCl₃) δ 7.55 – 7.52 (m, 2H), 7.08 – 7.01 (m, 2H), 6.40 (dd, *J* = 17.0, 10.5 Hz, 1H), 5.64 (d, *J* = 17.0 Hz, 1H), 5.40 (d, *J* = 10.8 Hz, 1H) ppm. **¹³C NMR** (126 MHz, CDCl₃) δ 178.30, 162.84 (d, *J* = 247.8 Hz), 137.30, 136.08 (d, *J* = 3.1 Hz), 128.21 (d, *J* = 8.3 Hz), 116.88, 115.54 (d, *J* = 21.6 Hz), 78.17 ppm. **¹⁹F NMR** (471 MHz, CDCl₃) δ -113.75 ppm. **IR** (neat): ν (cm⁻¹) 3392, 2924, 1716, 1606, 1509, 1346, 1227, 1138, 942, 836, 719. **HRMS** (ESI⁻, MeOH): *m/z* calcd. 195.0463 (M – H)⁻, found: 195.0456.



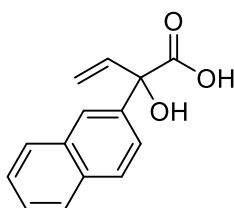
¹H NMR (300 MHz, CDCl₃) δ 7.31 – 7.23 (m, 1H), 7.04 – 6.95 (m, 2H), 6.43 (dd, *J* = 17.1, 10.5 Hz, 1H), 5.73 (dd, *J* = 17.1, 1.0 Hz, 1H), 5.52 (dd, *J* = 10.5, 1.0 Hz, 1H), 2.35 (s, 3H), 2.30 (s, 3H) ppm. **¹³C NMR** (126 MHz, CDCl₃) δ 178.44, 138.85, 138.14, 137.21, 134.98, 133.15, 128.34, 126.51, 117.34, 79.51, 21.05, 20.12 ppm. **IR** (neat): ν (cm⁻¹) 3410, 3372, 2919, 2634, 1716, 1249, 1139, 818, 710. **HRMS** (ESI⁻, MeOH): *m/z* calcd. 205.0870 (M – H)⁻, found: 205.0865.



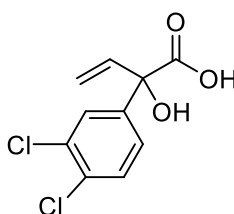
¹H NMR (500 MHz, CDCl₃) δ 7.37 – 7.33 (m, 2H), 7.28 – 7.23 (m, 1H), 7.15 (d, *J* = 7.5 Hz, 1H), 6.44 (dd, *J* = 17.0, 10.5 Hz, 1H), 5.65 (d, *J* = 17.0 Hz, 1H), 5.40 (d, *J* = 10.6 Hz, 1H), 2.36 (s, 3H) ppm. **¹³C NMR** (126 MHz, CDCl₃) δ 178.46, 140.33, 138.48, 137.44, 129.38, 128.61, 126.78, 123.28, 116.48, 78.63, 21.66 ppm. **IR** (neat): ν (cm⁻¹) 3416, 2925, 1718, 1601, 1231, 1163, 939, 721. **HRMS** (ESI⁻, MeOH): *m/z* calcd. 191.0714 (M – H)⁻, found: 191.0712.



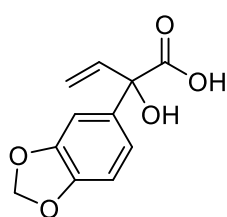
¹H NMR (500 MHz, CDCl₃) δ 7.41 (dd, *J* = 7.7, 1.6 Hz, 1H), 7.36 – 7.33 (m, 1H), 7.00 – 6.97 (m, 1H), 6.94 (d, *J* = 8.2 Hz, 1H), 6.30 (dd, *J* = 17.1, 10.6 Hz, 1H), 5.78 (dd, *J* = 17.1, 1.2 Hz, 1H), 5.53 (dd, *J* = 10.6, 1.2 Hz, 1H), 3.85 (s, 3H) ppm. **¹³C NMR** (126 MHz, CDCl₃) δ 177.34, 156.73, 136.07, 130.41, 129.30, 128.76, 121.30, 117.94, 111.74, 77.73, 55.79 ppm. **IR** (neat): ν (cm⁻¹) 3450, 3003, 2943, 1724, 1587, 1463, 1251, 1219, 1143, 993, 935, 754. **HRMS** (ESI⁻, MeOH): *m/z* calcd. 207.0663 (M – H)⁻, found: 207.0664.



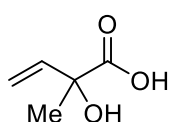
¹H NMR (400 MHz, CDCl₃) δ 8.03 (d, *J* = 1.5 Hz, 1H), 7.88 – 7.79 (m, 3H), 7.64 (dd, *J* = 8.7, 1.9 Hz, 1H), 7.53 – 7.47 (m, 2H), 6.54 (dd, *J* = 17.1, 10.5 Hz, 1H), 5.71 (dd, *J* = 17.1, 0.9 Hz, 1H), 5.46 (dd, *J* = 10.5, 0.9 Hz, 1H) ppm. **¹³C NMR** (101 MHz, CDCl₃) δ 178.21, 137.65, 137.36, 133.21, 133.12, 128.54, 127.69, 126.72, 126.53, 125.43, 124.00, 116.90, 78.81 ppm. **IR** (neat): ν (cm⁻¹) 3419, 3377, 2931, 1722, 1172, 1140, 820, 747. **HRMS** (ESI⁻, MeOH): *m/z* calcd. 227.0714 (M – H)⁻, found: 227.0713.



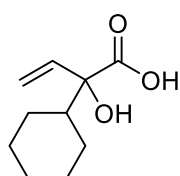
¹H NMR (500 MHz, CDCl₃) δ 7.68 (d, *J* = 1.8 Hz, 1H), 7.46 – 7.37 (m, 2H), 6.34 (dd, *J* = 17.0, 10.5 Hz, 1H), 5.64 (d, *J* = 17.0 Hz, 1H), 5.41 (d, *J* = 10.5 Hz, 1H) ppm. **¹³C NMR** (126 MHz, CDCl₃) δ 178.07, 140.27, 136.63, 132.85, 130.52, 128.51, 125.78, 117.47, 77.78. **IR** (neat): ν (cm⁻¹) 3444, 1714, 1561, 1469, 1380, 1249, 1136, 1030, 938, 806, 720 ppm. **HRMS** (ESI⁻, MeOH): *m/z* calcd. 244.9778 (M – H)⁻, found: 244.9773.



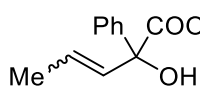
¹H NMR (500 MHz, CDCl₃) δ 7.01 (d, *J* = 9.0 Hz, 2H), 6.77 (d, *J* = 7.9 Hz, 1H), 6.37 (dd, *J* = 17.0, 10.5 Hz, 1H), 5.94 (s, 2H), 5.62 (d, *J* = 17.0 Hz, 1H), 5.37 (d, *J* = 10.5 Hz, 1H) ppm. **¹³C NMR** (126 MHz, CDCl₃) δ 178.14, 147.90, 147.71, 137.41, 134.39, 119.88, 116.50, 108.16, 107.13, 101.38, 78.38 ppm. **IR** (neat): *ν* (cm⁻¹) 3489, 2899, 2780, 1716, 1609, 1486, 1439, 1238, 1036, 930, 811, 731. **HRMS** (ESI⁻, MeOH): *m/z* calcd. 221.0455 (M - H)⁻, found: 221.0456.



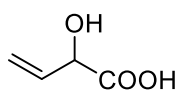
¹H NMR (400 MHz, CDCl₃) δ 6.05 (dd, *J* = 17.1, 10.5 Hz, 1H), 5.50 (dd, *J* = 17.1, 0.9 Hz, 1H), 5.23 (dd, *J* = 10.5, 0.9 Hz, 1H), 1.55 (s, 3H) ppm. **¹³C NMR** (101 MHz, CDCl₃) δ 180.22, 138.99, 115.38, 74.91, 25.84 ppm.¹¹⁶



¹H NMR (400 MHz, CDCl₃) δ 5.95 (dd, *J* = 17.1, 10.5 Hz, 1H), 5.51 (dd, *J* = 17.1, 1.4 Hz, 1H), 5.27 (dd, *J* = 10.5, 1.3 Hz, 1H), 1.86 – 1.60 (m, 5H), 1.49 (d, *J* = 10.4 Hz, 1H), 1.37 – 1.00 (m, 5H) ppm. **¹³C NMR** (101 MHz, CDCl₃) δ 179.82, 137.75, 116.15, 80.49, 44.65, 27.07, 26.40, 26.33, 26.24, 25.61 ppm. **IR** (neat): *ν* (cm⁻¹) 3412, 2921, 2853, 1724, 1224, 1157, 1128, 933. **HRMS** (ESI⁻, MeOH): *m/z* calcd. 183.1027 (M - H)⁻, found: 183.1030.



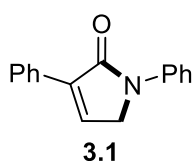
¹H NMR (400 MHz, CDCl₃) δ 7.64 – 7.53 (m, 2H), 7.43 – 7.28 (m, 3H), 6.10 – 5.81 (m, 2H), 1.82 – 1.64 (m, 3H) ppm. **¹³C NMR** (101 MHz, CDCl₃) δ 179.15, 178.71, 141.65, 140.91, 132.31, 130.68, 130.59, 128.57, 128.52, 128.42, 128.27, 128.15, 126.29, 126.17, 78.23, 77.80, 17.83, 14.70 ppm. **IR** (neat): *ν* (cm⁻¹) 3031, 1709, 1448, 1239, 1141, 1057, 964, 696. **HRMS** (ESI⁻, MeOH): *m/z* calcd. 191.0714 (M - H)⁻, found: 191.0722.



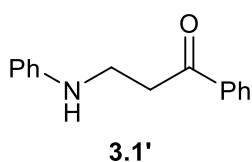
¹H NMR (400 MHz, CDCl₃) δ 5.99 (ddd, *J* = 17.2, 10.5, 5.0 Hz, 1H), 5.56 (ddd, *J* = 17.1, 1.9, 1.0 Hz, 1H), 5.34 (ddd, *J* = 10.4, 1.9, 1.0 Hz, 1H), 4.78 (dt, *J* = 5.0, 1.9 Hz, 1H) ppm. **¹³C NMR** (101 MHz, CDCl₃) δ 177.28, 133.57, 117.99, 71.34 ppm.¹¹⁷

(116) I. Kitahara, A. Horiguchi, K. Mori, *Tetrahedron* **1988**, *44*, 4713.

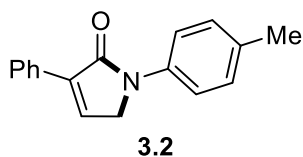
(117) R. Li, V. M. Powers, J. W. Kozarich, G. L. Kenyon, *J. Org. Chem.* **1995**, *60*, 3347.



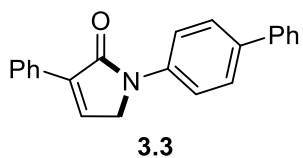
Scale: 0.15 mmol; isolated 32.8 mg (93% yield), white solid, Hexane : EA = 20 : 1, R_f = 0.2. **$^1\text{H NMR}$** (400 MHz, CDCl_3) δ 7.95 – 7.86 (m, 2H), 7.84 – 7.75 (m, 2H), 7.48 – 7.34 (m, 5H), 7.29 (t, J = 2.2 Hz, 1H), 7.21 – 7.13 (m, 1H), 4.47 (d, J = 2.2 Hz, 2H) ppm. **$^{13}\text{C NMR}$** (101 MHz, CDCl_3) δ 168.84, 139.51, 138.27, 135.17, 131.62, 129.26, 128.86, 128.61, 127.33, 124.40, 119.15, 50.76 ppm. **IR** (neat): ν (cm^{-1}) 3282, 2927, 2852, 1597, 1503, 1446, 1338, 995, 748, 692. **HRMS** (ESI+, MeOH): m/z calcd. 258.0889 ($\text{M} + \text{Na}$)⁺, found: 258.0886.



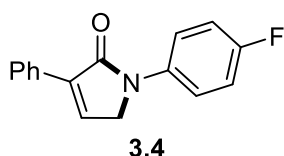
Decarboxylated byproduct: light yellow solid, Hexane : EA = 20 : 1, R_f = 0.2. **$^1\text{H NMR}$** (400 MHz, CDCl_3) δ 7.95 (dd, J = 8.4, 1.3 Hz, 2H), 7.63 – 7.54 (m, 1H), 7.52 – 7.42 (m, 2H), 7.22 – 7.12 (m, 2H), 6.71 (t, J = 7.3 Hz, 1H), 6.65 (dd, J = 8.6, 1.0 Hz, 2H), 3.62 (t, J = 6.1 Hz, 2H), 3.29 (t, J = 6.1 Hz, 2H) ppm. **$^{13}\text{C NMR}$** (101 MHz, CDCl_3) δ 199.46, 147.85, 136.90, 133.49, 129.49, 128.81, 128.18, 117.77, 113.22, 38.89, 37.82 ppm.



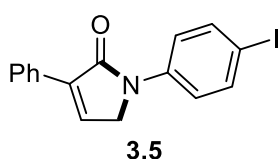
Scale: 0.15 mmol; isolated 34.7 mg (93% yield), white solid, Hexane : EA = 20 : 1, R_f = 0.2. **$^1\text{H NMR}$** (400 MHz, CDCl_3) δ 7.95 – 7.86 (m, 2H), 7.65 (d, J = 8.5 Hz, 2H), 7.45 – 7.33 (m, 3H), 7.26 (t, J = 2.1 Hz, 1H), 7.21 (d, J = 8.5 Hz, 2H), 4.43 (d, J = 2.2 Hz, 2H), 2.35 (s, 3H) ppm. **$^{13}\text{C NMR}$** (101 MHz, CDCl_3) δ 168.73, 138.24, 137.01, 134.98, 134.07, 131.71, 129.76, 128.80, 128.58, 127.32, 119.31, 50.90, 20.96 ppm. **IR** (neat): ν (cm^{-1}) 3099, 2915, 2853, 1672, 1513, 1430, 1379, 1199, 982, 815, 693. **HRMS** (ESI+, MeOH): m/z calcd. 272.1046 ($\text{M} + \text{Na}$)⁺, found: 272.1044.



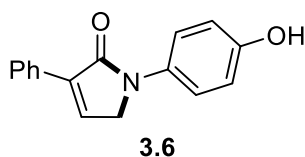
Scale: 0.15 mmol; isolated 42.5 mg (91% yield), white solid (low solubility), Hexane : EA = 10 : 1 to 1 : 1 (gradient), R_f = 0.2. **$^1\text{H NMR}$** (400 MHz, CDCl_3) δ 7.96 – 7.85 (m, 4H), 7.69 – 7.58 (m, 4H), 7.48 – 7.30 (m, 7H), 4.53 (d, J = 2.2 Hz, 2H) ppm. **$^{13}\text{C NMR}$** (101 MHz, CDCl_3) δ 168.90, 140.62, 138.82, 138.44, 137.20, 135.14, 131.60, 128.96, 128.66, 127.88, 127.38, 127.31, 127.02, 119.37, 50.80 ppm. **IR** (neat): ν (cm^{-1}) 2917, 1671, 1520, 1481, 1374, 1188, 826, 693. **HRMS** (ESI+, MeOH): m/z calcd. 334.1202 ($\text{M} + \text{Na}$)⁺, found: 334.1192.



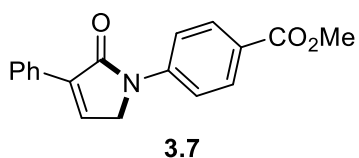
Scale: 0.15 mmol; isolated 34.5 mg (91% yield), white solid, Hexane : EA = 20 : 1, $R_f = 0.2$. $^1\text{H NMR}$ (400 MHz, CDCl_3) δ 7.94 – 7.85 (m, 2H), 7.79 – 7.69 (m, 2H), 7.49 – 7.35 (m, 3H), 7.28 (t, $J = 2.2$ Hz, 1H), 7.15 – 7.03 (m, 2H), 4.44 (d, $J = 2.2$ Hz, 2H) ppm. $^{13}\text{C NMR}$ (101 MHz, CDCl_3) δ 168.76, 159.57 (d, $J = 244.0$ Hz), 138.22, 135.62 (d, $J = 2.9$ Hz), 135.03, 131.52, 128.95, 128.65, 127.32, 121.02 (d, $J = 7.8$ Hz), 115.93 (d, $J = 22.3$ Hz), 51.03 ppm. $^{19}\text{F NMR}$ (376 MHz, CDCl_3) δ -118.22 ppm. **IR** (neat): ν (cm^{-1}) 3366, 2923, 2854, 1665, 1504, 1432, 1377, 1195, 1109, 833, 787. **HRMS** (ESI+, MeOH): m/z calcd. 254.0976 ($\text{M} + \text{H}$) $^+$, found: 254.0971.



Scale: 0.15 mmol; isolated 45.4 mg (84% yield), white solid, Hexane : EA = 20 : 1, $R_f = 0.2$. $^1\text{H NMR}$ (400 MHz, CDCl_3) δ 7.89 – 7.86 (m, 2H), 7.70 (d, $J = 8.9$ Hz, 2H), 7.62 – 7.57 (m, 2H), 7.45 – 7.36 (m, 3H), 7.29 (t, $J = 2.2$ Hz, 1H), 4.43 (d, $J = 2.1$ Hz, 2H) ppm. $^{13}\text{C NMR}$ (101 MHz, CDCl_3) δ 168.86, 139.32, 138.37, 138.18, 135.13, 131.36, 129.03, 128.67, 127.33, 120.71, 87.72, 50.49 ppm. **IR** (neat): ν (cm^{-1}) 2954, 1673, 1585, 1486, 1379, 860, 818. **HRMS** (ESI+, MeOH): m/z calcd. 383.9856 ($\text{M} + \text{Na}$) $^+$, found: 383.9857.



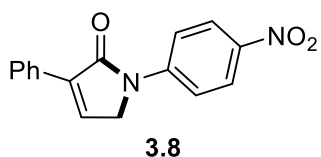
Scale: 0.15 mmol; isolated 30.5 mg (81% yield), light yellow solid, Hexane : EA = 5 : 1, $R_f = 0.1$. $^1\text{H NMR}$ (400 MHz, Acetone- d_6) δ 8.25 (s, 1H), 8.05 – 7.97 (m, 2H), 7.70 – 7.63 (m, 2H), 7.57 (t, $J = 2.2$ Hz, 1H), 7.45 – 7.31 (m, 3H), 6.92 – 6.84 (m, 2H), 4.52 (d, $J = 2.2$ Hz, 2H) ppm. $^{13}\text{C NMR}$ (101 MHz, Acetone) δ 168.85, 154.92, 137.47, 137.19, 133.15, 133.14, 129.17, 129.09, 127.89, 121.84, 116.20, 51.77 ppm. **IR** (neat): ν (cm^{-1}) 3308, 1664, 1512, 1445, 1375, 1247, 1194, 823, 692. **HRMS** (ESI+, MeOH): m/z calcd. 274.0838 ($\text{M} + \text{Na}$) $^+$, found: 274.0835.



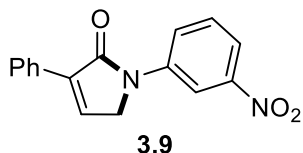
Scale: 0.15 mmol; isolated 39.1 mg (89% yield), white solid, Hexane : EA = 20 : 1, $R_f = 0.15$. $^1\text{H NMR}$ (400 MHz, CDCl_3) δ 8.12 – 8.05 (m, 2H), 7.93 – 7.87 (m, 4H), 7.47 – 7.36 (m, 3H), 7.33 (t, $J = 2.2$ Hz, 1H), 4.51 (d, $J = 2.3$ Hz, 2H), 3.92 (s, 3H) ppm. $^{13}\text{C NMR}$ (101 MHz, CDCl_3) δ 169.12, 166.78, 143.47, 138.42, 135.57, 131.24, 131.04, 129.10, 128.70, 127.35, 125.50, 117.70, 52.17, 50.52 ppm. **IR**

(neat): ν (cm^{-1}) 3092, 2946, 2844, 1714, 1668, 1607, 1435, 1276, 1179, 1099, 790, 739.

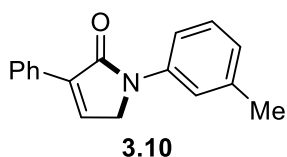
HRMS (ESI+, MeOH): m/z calcd. 316.0944 ($M + \text{Na}$)⁺, found: 316.0956.



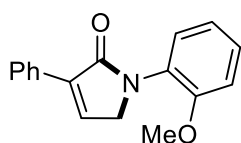
Scale: 0.15 mmol; isolated 27.3 mg (65% yield), yellow solid, Hexane : DCM = 3 : 2, R_f = 0.2. **¹H NMR** (400 MHz, CDCl_3) δ 8.33 – 8.26 (m, 2H), 8.04 – 8.00 (m, 2H), 7.88 – 7.85 (m, 2H), 7.49 – 7.39 (m, 3H), 7.38 (t, J = 2.3 Hz, 1H), 4.54 (d, J = 2.3 Hz, 2H) ppm. **¹³C NMR** (101 MHz, CDCl_3) δ 169.24, 144.97, 143.43, 138.40, 135.94, 130.86, 129.34, 128.79, 127.34, 125.30, 117.76, 50.51 ppm. **IR** (neat): ν (cm^{-1}) 3090, 1671, 1588, 1502, 1446, 1324, 1294, 1112, 841, 740, 686. **HRMS** (ESI+, MeOH): m/z calcd. 303.0740 ($M + \text{Na}$)⁺, found: 303.0742.



Scale: 0.15 mmol; isolated 42.3 mg (96% yield), white solid, Hexane : EA = 20 : 1, R_f = 0.2. **¹H NMR** (500 MHz, CDCl_3) δ 8.56 (t, J = 2.2 Hz, 1H), 8.34 – 8.32 (m, 1H), 7.98 (dd, J = 8.1, 1.5 Hz, 1H), 7.92 – 7.84 (m, 2H), 7.56 (t, J = 8.2 Hz, 1H), 7.46 – 7.37 (m, 3H), 7.35 (t, J = 2.3 Hz, 1H), 4.53 (d, J = 2.3 Hz, 2H) ppm. **¹³C NMR** (101 MHz, CDCl_3) δ 169.12, 148.88, 140.55, 138.16, 135.62, 131.00, 130.14, 129.21, 128.72, 127.29, 124.31, 118.67, 112.98, 50.56 ppm. **IR** (neat): ν (cm^{-1}) 2919, 2851, 1675, 1523, 1447, 1347, 1093, 785, 733. **HRMS** (ESI+, MeOH): m/z calcd. 281.0921 ($M + \text{H}$)⁺, found: 281.0919.

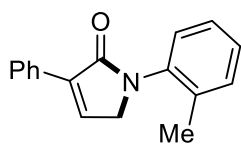


Scale: 0.15 mmol; isolated 32.5 mg (87% yield), white solid, Hexane : EA = 20 : 1, R_f = 0.2. **¹H NMR** (400 MHz, CDCl_3) δ 7.94 – 7.88 (m, 2H), 7.68 (s, 1H), 7.53 (dd, J = 8.2, 1.9 Hz, 1H), 7.45 – 7.35 (m, 3H), 7.31 – 7.26 (m, 2H), 6.99 (d, J = 7.5 Hz, 1H), 4.45 (d, J = 2.2 Hz, 2H), 2.40 (s, 3H) ppm. **¹³C NMR** (101 MHz, CDCl_3) δ 168.84, 139.44, 139.14, 138.24, 135.11, 131.65, 129.05, 128.83, 128.59, 127.33, 125.26, 120.02, 116.24, 50.89, 21.80 ppm. **IR** (neat): ν (cm^{-1}) 3099, 3035, 2912, 1674, 1603, 1446, 1368, 1194, 826, 784, 691. **HRMS** (ESI+, MeOH): m/z calcd. 272.1046 ($M + \text{Na}$)⁺, found: 272.1041.



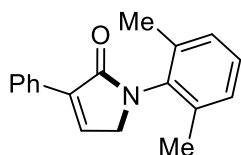
3.11

Scale: 0.15 mmol; isolated 38.5 mg (97% yield), white solid, Hexane : EA = 20 : 1, R_f = 0.15. $^1\text{H NMR}$ (400 MHz, CDCl_3) δ 7.97 – 7.95 (m, 2H), 7.46 – 7.28 (m, 6H), 7.06 – 6.98 (m, 2H), 4.44 (d, J = 2.2 Hz, 2H), 3.83 (s, 3H) ppm. $^{13}\text{C NMR}$ (101 MHz, CDCl_3) δ 169.63, 155.04, 136.96, 136.72, 132.04, 128.98, 128.62, 128.55, 128.51, 127.19, 126.92, 121.01, 112.20, 55.77, 52.39 ppm. **IR** (neat): ν (cm^{-1}) 3083, 2923, 2835, 1687, 1503, 1386, 1237, 1019, 772, 693. **HRMS** (ESI+, MeOH): m/z calcd. 266.1176 ($\text{M} + \text{H}$)⁺, found: 266.1186.



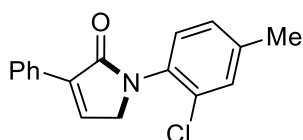
3.12

Scale: 0.15 mmol; isolated 26.9 mg (72% yield), yellow solid, Hexane : EA = 20 : 1, R_f = 0.15. $^1\text{H NMR}$ (400 MHz, CDCl_3) δ 8.04 – 7.89 (m, 2H), 7.48 – 7.17 (m, 8H), 4.36 (d, J = 2.2 Hz, 2H), 2.27 (s, 3H) ppm. $^{13}\text{C NMR}$ (101 MHz, CDCl_3) δ 169.05, 137.19, 137.14, 136.53, 136.15, 131.86, 131.29, 128.76, 128.61, 128.15, 127.57, 127.21, 126.88, 53.07, 18.35 ppm. **IR** (neat): ν (cm^{-1}) 3083, 2922, 2852, 1673, 1490, 1449, 1389, 789, 742, 699. **HRMS** (ESI+, MeOH): m/z calcd. 250.1226 ($\text{M} + \text{H}$)⁺, found: 250.1227.



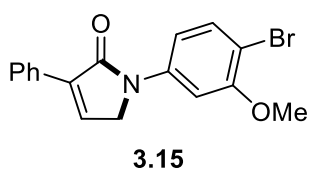
3.13

Scale: 0.15 mmol; isolated 19.7 mg (50% yield), yellow solid, Hexane : EA = 20 : 1, R_f = 0.2. $^1\text{H NMR}$ (500 MHz, CDCl_3) δ 7.98 (d, J = 7.2 Hz, 2H), 7.45 – 7.34 (m, 4H), 7.21 – 7.18 (m, 1H), 7.14 (d, J = 7.5 Hz, 2H), 4.23 (d, J = 2.1 Hz, 2H), 2.20 (s, 6H) ppm. $^{13}\text{C NMR}$ (126 MHz, CDCl_3) δ 169.17, 137.20, 137.10, 136.11, 135.76, 131.86, 128.81, 128.64, 128.62, 128.47, 127.18, 51.34, 18.12 ppm. **IR** (neat): ν (cm^{-1}) 3074, 2922, 1670, 1472, 1446, 1377, 1217, 788, 694. **HRMS** (ESI+, MeOH): m/z calcd. 264.1383 ($\text{M} + \text{H}$)⁺, found: 264.1381.

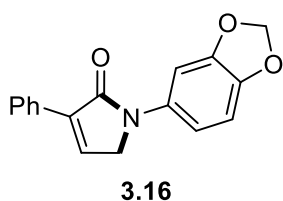


3.14

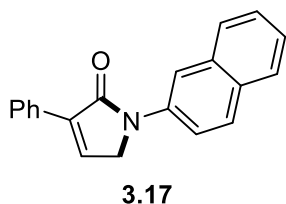
Scale: 0.15 mmol; isolated 33.1 mg (78% yield), white solid, Hexane : EA = 20 : 1, R_f = 0.2. $^1\text{H NMR}$ (400 MHz, CDCl_3) δ 7.96 – 7.93 (m, 2H), 7.45 – 7.34 (m, 4H), 7.34 – 7.30 (m, 1H), 7.28 (d, 1H), 7.16 – 7.13 (m, 1H), 4.40 (d, J = 2.2 Hz, 2H), 2.37 (s, 3H) ppm. $^{13}\text{C NMR}$ (101 MHz, CDCl_3) δ 169.66, 139.77, 136.85, 136.57, 133.24, 132.27, 131.72, 131.00, 129.77, 128.77, 128.61, 128.59, 127.19, 52.40, 21.06 ppm. **IR** (neat): ν (cm^{-1}) 3063, 2915, 2852, 1680, 1502, 1388, 1211, 835, 690. **HRMS** (ESI+, MeOH): m/z calcd. 284.0837 ($\text{M} + \text{H}$)⁺, found: 284.0826.



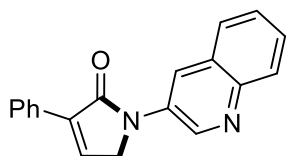
Scale: 0.15 mmol; isolated 38.2 mg (74% yield), light yellow solid, Hexane : EA = 20 : 1, R_f = 0.15. **$^1\text{H NMR}$** (400 MHz, CDCl_3) δ 8.06 (d, J = 2.5 Hz, 1H), 7.91 – 7.81 (m, 2H), 7.50 (d, J = 8.6 Hz, 1H), 7.47 – 7.34 (m, 3H), 7.28 (t, J = 2.2 Hz, 1H), 6.84 (dd, J = 8.6, 2.5 Hz, 1H), 4.44 (d, J = 2.3 Hz, 2H), 3.95 (s, 3H) ppm. **$^{13}\text{C NMR}$** (101 MHz, CDCl_3) δ 169.03, 156.45, 140.14, 138.43, 135.23, 133.13, 131.33, 129.02, 128.68, 127.33, 110.90, 106.28, 103.61, 56.43, 50.82 ppm. **IR** (neat): ν (cm^{-1}) 3085, 2975, 2848, 1675, 1590, 1489, 1449, 1366, 1234, 1053, 692. **HRMS** (ESI+, MeOH): m/z calcd. 366.0100 ($\text{M} + \text{Na}$)⁺, found: 366.0098.



Scale: 0.15 mmol; isolated 35.6 mg (85% yield), yellow solid, Hexane : EA = 20 : 1, R_f = 0.2. **$^1\text{H NMR}$** (400 MHz, CDCl_3) δ 7.95 – 7.89 (m, 2H), 7.50 (d, J = 2.2 Hz, 1H), 7.47 – 7.36 (m, 3H), 7.27 (t, J = 2.2 Hz, 1H), 7.07 – 7.04 (m, 1H), 6.84 (d, J = 8.4 Hz, 1H), 6.00 (s, 2H), 4.42 (d, J = 2.2 Hz, 2H) ppm. **$^{13}\text{C NMR}$** (101 MHz, CDCl_3) δ 168.65, 148.20, 144.53, 138.14, 134.86, 133.90, 131.64, 128.85, 128.60, 127.31, 112.62, 108.26, 102.42, 101.45, 51.52 ppm. **IR** (neat): ν (cm^{-1}) 3101, 3049, 2914, 1671, 1521, 1482, 1443, 1188, 826, 694. **HRMS** (ESI+, MeOH): m/z calcd. 302.0788 ($\text{M} + \text{Na}$)⁺, found: 302.0786.

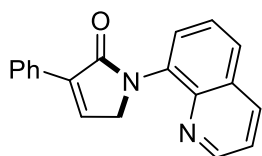


Scale: 0.15 mmol; isolated 37.6 mg (88% yield), white solid, Hexane : EA = 6 : 1, R_f = 0.2. **$^1\text{H NMR}$** (400 MHz, CDCl_3) δ 8.18 (d, J = 2.2 Hz, 1H), 8.07 – 8.04 (m, 1H), 7.96 – 7.86 (m, 3H), 7.83 (t, J = 7.1 Hz, 2H), 7.51 – 7.36 (m, 5H), 7.34 (t, J = 2.2 Hz, 1H), 4.59 (d, J = 2.2 Hz, 2H) ppm. **$^{13}\text{C NMR}$** (101 MHz, CDCl_3) δ 169.06, 138.42, 137.19, 135.25, 133.93, 131.61, 130.72, 129.07, 128.94, 128.66, 127.87, 127.71, 127.39, 126.67, 125.29, 119.05, 116.04, 51.06 ppm. **IR** (neat): ν (cm^{-1}) 1675, 1598, 1432, 1379, 1187, 853, 785, 736, 694. **HRMS** (ESI+, MeOH): m/z calcd. 286.1226 ($\text{M} + \text{H}$)⁺, found: 286.1224.



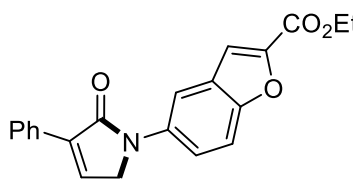
3.18

Scale: 0.15 mmol; isolated 29.0 mg (68% yield), white solid, Hexane : DCM = 1 : 100, $R_f = 0.1$. $^1\text{H NMR}$ (400 MHz, CDCl_3) δ 9.30 (d, $J = 2.6$ Hz, 1H), 8.72 (d, $J = 2.4$ Hz, 1H), 8.08 (d, $J = 8.4$ Hz, 1H), 7.95 – 7.88 (m, 2H), 7.83 (d, $J = 7.1$ Hz, 1H), 7.68 – 7.63 (m, 1H), 7.57 – 7.53 (m, 1H), 7.48 – 7.39 (m, 3H), 7.38 (t, $J = 2.2$ Hz, 1H), 4.63 (d, $J = 2.2$ Hz, 2H) ppm. $^{13}\text{C NMR}$ (101 MHz, CDCl_3) δ 169.32, 145.29, 142.96, 138.15, 135.65, 133.15, 131.19, 129.26, 129.16, 128.73, 128.60, 128.25, 127.86, 127.44, 127.34, 123.34, 50.38 ppm. **IR** (neat): ν (cm^{-1}) 3085, 3055, 2921, 1673, 1600, 1431, 1370, 1245, 1183, 783, 734, 688. **HRMS** (ESI+, MeOH): m/z calcd. 287.1179 ($\text{M} + \text{H}$) $^+$, found: 287.1184.



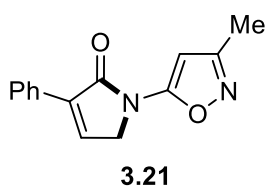
3.19

Scale: 0.15 mmol; isolated 20.2 mg (47% yield), white solid, Hexane : EA = 5 : 1, $R_f = 0.15$. $^1\text{H NMR}$ (400 MHz, CDCl_3) δ 8.92 (dd, $J = 4.2, 1.7$ Hz, 1H), 8.21 (dd, $J = 8.3, 1.7$ Hz, 1H), 8.01 – 7.96 (m, 2H), 7.94 – 7.92 (m, 1H), 7.82 – 7.80 (m, 1H), 7.65 – 7.60 (m, 1H), 7.48 – 7.39 (m, 4H), 7.36 (t, $J = 7.3$ Hz, 1H), 4.96 (d, $J = 2.1$ Hz, 2H) ppm. $^{13}\text{C NMR}$ (101 MHz, CDCl_3) δ 170.29, 150.07, 144.36, 137.59, 136.99, 136.57, 135.64, 132.17, 129.62, 128.55, 128.47, 127.35, 127.34, 126.60, 121.50, 54.14 ppm. **IR** (neat): ν (cm^{-1}) 3055, 2924, 2852, 1682, 1595, 1473, 1396, 866, 787, 693. **HRMS** (ESI+, MeOH): m/z calcd. 287.1179 ($\text{M} + \text{H}$) $^+$, found: 287.1180.

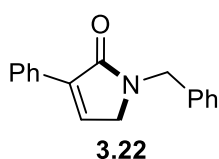


3.20

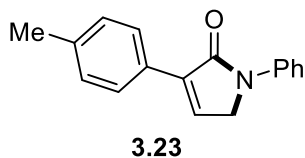
Scale: 0.15 mmol; isolated 38.0 mg (73% yield), white solid, Hexane : EA = 20 : 1, $R_f = 0.15$. $^1\text{H NMR}$ (400 MHz, CDCl_3) δ 8.15 (d, $J = 2.0$ Hz, 1H), 7.91 (dd, $J = 8.2, 1.3$ Hz, 2H), 7.79 (dd, $J = 9.1, 2.2$ Hz, 1H), 7.61 (d, $J = 9.1$ Hz, 1H), 7.52 (s, 1H), 7.47 – 7.35 (m, 3H), 7.32 (t, $J = 2.0$ Hz, 1H), 4.53 (d, $J = 2.2$ Hz, 2H), 4.45 (q, $J = 7.1$ Hz, 2H), 1.44 (t, $J = 7.1$ Hz, 3H) ppm. $^{13}\text{C NMR}$ (101 MHz, CDCl_3) δ 168.93, 159.59, 152.83, 146.81, 138.23, 135.75, 135.13, 131.55, 128.97, 128.67, 127.65, 127.34, 120.33, 114.07, 113.66, 112.83, 61.77, 51.52, 14.48 ppm. **IR** (neat): ν (cm^{-1}) 3112, 3005, 1721, 1670, 1561, 1463, 1306, 1162, 787, 735. **HRMS** (ESI+, MeOH): m/z calcd. 370.1050 ($\text{M} + \text{Na}$) $^+$, found: 370.1055.



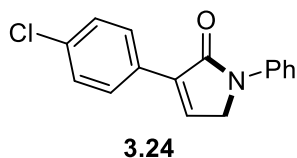
Scale: 0.15 mmol; isolated 20.9 mg (58% yield), white solid, Hexane : EA = 5 : 1, $R_f = 0.15$. $^1\text{H NMR}$ (400 MHz, CDCl_3) δ 7.89 – 7.83 (m, 2H), 7.46 – 7.37 (m, 4H), 6.38 (s, 1H), 4.60 (d, $J = 2.2$ Hz, 2H), 2.31 (s, 3H) ppm. $^{13}\text{C NMR}$ (101 MHz, CDCl_3) δ 166.64, 162.03, 160.29, 137.34, 136.77, 130.57, 129.36, 128.80, 127.16, 87.76, 48.73, 12.04 ppm. **IR** (neat): ν (cm^{-1}) 3158, 3079, 2924, 2854, 1693, 1592, 1491, 1438, 1313, 785, 698. **HRMS** (ESI+, MeOH): m/z calcd. 241.0972 ($\text{M} + \text{H}$)⁺, found: 241.0980.



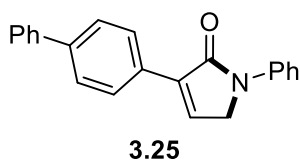
Scale: 0.15 mmol; isolated 9.0 mg (24% yield), white solid, Hexane : DCM = 1 : 3, $R_f = 0.15$. $^1\text{H NMR}$ (500 MHz, CDCl_3) δ 7.97 – 7.88 (m, 2H), 7.43 – 7.38 (m, 2H), 7.37 – 7.31 (m, 3H), 7.29 (d, $J = 7.2$ Hz, 3H), 7.18 (t, $J = 2.1$ Hz, 1H), 4.73 (s, 2H), 3.91 (d, $J = 2.1$ Hz, 2H) ppm. $^{13}\text{C NMR}$ (101 MHz, CDCl_3) δ 170.11, 137.47, 137.23, 135.55, 131.98, 128.92, 128.68, 128.59, 128.25, 127.74, 127.17, 49.94, 46.57 ppm. **IR** (neat): ν (cm^{-1}) 3063, 2922, 1674, 1449, 1233, 789, 695. **HRMS** (ESI+, MeOH): m/z calcd. 272.1046 ($\text{M} + \text{Na}$)⁺, found: 272.1044.



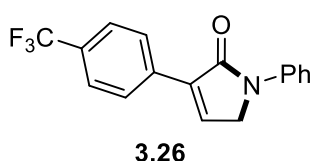
Scale: 0.15 mmol; isolated 34.7 mg (93% yield), white solid, Hexane : EA = 20 : 1, $R_f = 0.15$. $^1\text{H NMR}$ (400 MHz, CDCl_3) δ 7.85 – 7.75 (m, 4H), 7.45 – 7.37 (m, 2H), 7.23 (dd, $J = 5.1$, 2.8 Hz, 3H), 7.16 (t, $J = 7.4$ Hz, 1H), 4.45 (d, $J = 2.3$ Hz, 2H), 2.38 (s, 3H) ppm. $^{13}\text{C NMR}$ (101 MHz, CDCl_3) δ 169.01, 139.59, 138.81, 138.12, 134.24, 129.31, 129.25, 128.80, 127.19, 124.34, 119.14, 50.72, 21.48 ppm. **IR** (neat): ν (cm^{-1}) 3026, 2917, 2853, 1671, 1596, 1497, 1438, 1381, 1293, 1182, 860, 809, 744, 685. **HRMS** (ESI+, MeOH): m/z calcd. 272.1046 ($\text{M} + \text{Na}$)⁺, found: 272.1051.



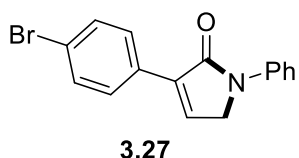
Scale: 0.15 mmol; isolated 38.5 mg (95% yield), white solid, Hexane : EA = 20 : 1, $R_f = 0.15$. $^1\text{H NMR}$ (400 MHz, CDCl_3) δ 7.92 – 7.85 (m, 2H), 7.82 – 7.74 (m, 2H), 7.46 – 7.37 (m, 4H), 7.30 (t, $J = 2.2$ Hz, 1H), 7.17 (t, $J = 7.4$ Hz, 1H), 4.47 (d, $J = 2.2$ Hz, 2H) ppm. $^{13}\text{C NMR}$ (101 MHz, CDCl_3) δ 168.55, 139.35, 137.18, 135.33, 134.88, 130.03, 129.32, 128.86, 128.62, 124.61, 119.25, 50.81 ppm. **IR** (neat): ν (cm^{-1}) 3089, 1667, 1592, 1488, 1379, 1297, 1200, 1091, 817, 751. **HRMS** (ESI+, MeOH): m/z calcd. 292.0500 ($\text{M} + \text{Na}$)⁺, found: 292.0503.



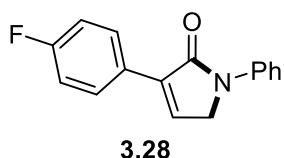
Scale: 0.15 mmol; isolated 42.9 mg (92% yield), white solid, Hexane : EA = 20 : 1, $R_f = 0.15$. **$^1\text{H NMR}$** (400 MHz, CDCl_3) δ 8.03 – 7.97 (m, 2H), 7.84 – 7.78 (m, 2H), 7.68 – 7.62 (m, 4H), 7.49 – 7.33 (m, 6H), 7.17 (t, $J = 7.4$ Hz, 1H), 4.51 (d, $J = 2.3$ Hz, 2H) ppm. **$^{13}\text{C NMR}$** (101 MHz, CDCl_3) δ 168.89, 141.65, 140.80, 139.53, 137.95, 134.95, 130.59, 129.31, 128.97, 127.75, 127.66, 127.34, 127.24, 124.49, 119.23, 50.87 ppm. **IR** (neat): ν (cm^{-1}) 3031, 1666, 1594, 1484, 1183, 815, 748, 687. **HRMS** (ESI+, MeOH): m/z calcd. 334.1202 ($\text{M} + \text{Na}$)⁺, found: 334.1201.



Scale: 0.15 mmol; isolated 23.2 mg (51% yield), white solid, Hexane : EA = 20 : 1, $R_f = 0.15$. **$^1\text{H NMR}$** (400 MHz, CDCl_3) δ 8.04 (d, $J = 8.1$ Hz, 2H), 7.83 – 7.74 (m, 2H), 7.68 (d, $J = 8.2$ Hz, 2H), 7.47 – 7.37 (m, 3H), 7.19 (t, $J = 7.4$ Hz, 1H), 4.52 (d, $J = 2.2$ Hz, 2H) ppm. **$^{13}\text{C NMR}$** (126 MHz, CDCl_3) δ 168.29, 139.23, 137.27, 136.93, 134.98, 130.75 (q, $J = 32.6$ Hz), 129.37, 127.65, 125.58 (q, $J = 3.8$ Hz), 124.77, 119.34, 50.96 ppm. **$^{19}\text{F NMR}$** (376 MHz, CDCl_3) δ -62.83 ppm. **IR** (neat): ν (cm^{-1}) 3103, 2914, 1669, 1596, 1502, 1106, 1068, 820, 742, 691. **HRMS** (ESI+, MeOH): m/z calcd. 326.0763 ($\text{M} + \text{Na}$)⁺, found: 326.0777.

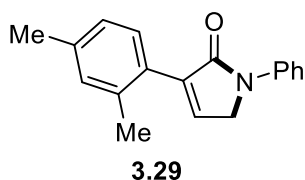


Scale: 0.15 mmol; isolated 44.3 mg (94% yield), white solid, Hexane : EA = 20 : 1, $R_f = 0.15$. **$^1\text{H NMR}$** (400 MHz, CDCl_3) δ 7.85 – 7.74 (m, 4H), 7.58 – 7.51 (m, 2H), 7.44 – 7.38 (m, 2H), 7.32 (t, $J = 2.2$ Hz, 1H), 7.17 (t, $J = 7.4$ Hz, 1H), 4.47 (d, $J = 2.2$ Hz, 2H) ppm. **$^{13}\text{C NMR}$** (101 MHz, CDCl_3) δ 168.49, 139.34, 137.26, 135.40, 131.82, 130.47, 129.33, 128.90, 124.63, 123.20, 119.27, 50.84 ppm. **IR** (neat): ν (cm^{-1}) 3087, 1726, 1664, 1586, 1485, 1294, 979, 818, 748, 690. **HRMS** (ESI+, MeOH): m/z calcd. 335.9994 ($\text{M} + \text{Na}$)⁺, found: 335.9980.

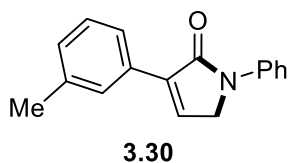


Scale: 0.15 mmol; isolated 32.3 mg (85% yield), white solid, Hexane : EA = 20 : 1, $R_f = 0.15$. **$^1\text{H NMR}$** (400 MHz, CDCl_3) δ 7.96 – 7.88 (m, 2H), 7.82 – 7.74 (m, 2H), 7.45 – 7.37 (m, 2H), 7.24 (t, $J = 2.2$ Hz, 1H), 7.20 – 7.06 (m, 3H), 4.45 (d, $J = 2.2$ Hz, 2H) ppm. **$^{13}\text{C NMR}$** (126 MHz, CDCl_3) δ 168.72, 163.17 (d, $J = 248.6$ Hz), 139.39,

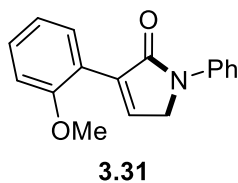
137.19, 134.72 (d, $J = 1.6$ Hz), 129.28, 129.17 (d, $J = 8.1$ Hz), 127.74 (d, $J = 3.3$ Hz), 124.52, 119.19, 115.59 (d, $J = 21.6$ Hz), 50.72 ppm. **^{19}F NMR** (376 MHz, CDCl_3) δ -112.49 ppm. **IR** (neat): ν (cm^{-1}) 3048, 2962, 1667, 1593, 1504, 1427, 1380, 1198, 1095, 980, 814. **HRMS** (ESI+, MeOH): m/z calcd. 276.0795 ($\text{M} + \text{Na}$)⁺, found: 276.0795.



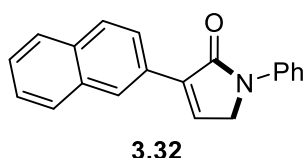
Scale: 0.15 mmol; isolated 38.7 mg (98% yield), white solid, Hexane : EA = 20 : 1, $R_f = 0.15$. **^1H NMR** (400 MHz, CDCl_3) δ 7.81 (d, $J = 7.8$ Hz, 2H), 7.40 (t, $J = 7.2$ Hz, 2H), 7.31 – 7.25 (m, 1H), 7.15 (t, $J = 7.4$ Hz, 1H), 7.11 – 7.02 (m, 3H), 4.50 (d, $J = 2.1$ Hz, 2H), 2.35 (d, 6H) ppm. **^{13}C NMR** (101 MHz, CDCl_3) δ 169.13, 140.47, 139.66, 138.45, 137.62, 136.62, 131.33, 129.79, 129.25, 128.61, 126.52, 124.21, 118.82, 51.12, 21.30, 20.50 ppm. **IR** (neat): ν (cm^{-1}) 3087, 2913, 1680, 1596, 1494, 1371, 1292, 1186, 857, 823, 757. **HRMS** (ESI+, MeOH): m/z calcd. 286.1202 ($\text{M} + \text{Na}$)⁺, found: 286.1189.



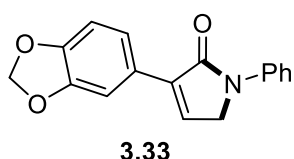
Scale: 0.15 mmol; isolated 32.3 mg (85% yield), white solid, Hexane : EA = 20 : 1, $R_f = 0.15$. **^1H NMR** (400 MHz, CDCl_3) δ 7.83 – 7.74 (m, 3H), 7.68 (d, $J = 7.7$ Hz, 1H), 7.44 – 7.38 (m, 2H), 7.31 (t, $J = 7.7$ Hz, 1H), 7.27 – 7.25 (m, 1H), 7.22 – 7.12 (m, 2H), 4.45 (d, $J = 2.2$ Hz, 2H), 2.41 (s, 3H) ppm. **^{13}C NMR** (101 MHz, CDCl_3) δ 168.91, 139.54, 138.34, 138.20, 135.06, 131.53, 129.63, 129.23, 128.50, 127.97, 124.41, 124.35, 119.10, 50.72, 21.63 ppm. **IR** (neat): ν (cm^{-1}) 3098, 3040, 2915, 1674, 1597, 1499, 1376, 1176, 793. **HRMS** (ESI+, MeOH): m/z calcd. 272.1046 ($\text{M} + \text{Na}$)⁺, found: 272.1046.



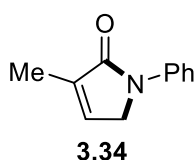
Scale: 0.15 mmol; isolated 34.6 mg (87% yield), white solid, Hexane : EA = 20 : 1, $R_f = 0.15$. **^1H NMR** (400 MHz, CDCl_3) δ 8.12 – 8.09 (m, 1H), 7.85 – 7.75 (m, 2H), 7.56 – 7.54 (m, 1H), 7.44 – 7.37 (m, 2H), 7.36 – 7.31 (m, 1H), 7.15 (t, $J = 7.4$ Hz, 1H), 7.05 (t, $J = 8.1$ Hz, 1H), 6.97 (d, $J = 8.3$ Hz, 1H), 4.47 (d, $J = 2.2$ Hz, 2H), 3.88 (s, 3H) ppm. **^{13}C NMR** (101 MHz, CDCl_3) δ 169.39, 157.74, 139.67, 139.20, 133.81, 130.15, 129.62, 129.17, 124.16, 120.61, 120.49, 119.12, 110.94, 55.60, 51.02 ppm. **IR** (neat): ν (cm^{-1}) 3063, 2934, 2836, 1676, 1596, 1491, 1434, 1375, 1246, 1182, 1107, 1023, 864, 749, 689. **HRMS** (ESI+, MeOH): m/z calcd. 266.1176 ($\text{M} + \text{H}$)⁺, found: 266.1168.



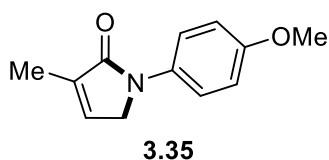
Scale: 0.15 mmol; isolated 35.5 mg (83% yield), white solid, Hexane : EA = 20 : 1, R_f = 0.2. $^1\text{H NMR}$ (400 MHz, CDCl_3) δ 8.69 (s, 1H), 7.96 – 7.90 (m, 1H), 7.89 – 7.80 (m, 5H), 7.50 (dt, J = 6.0, 3.3 Hz, 2H), 7.47 – 7.39 (m, 3H), 7.18 (t, J = 7.4 Hz, 1H), 4.52 (d, J = 2.3 Hz, 2H) ppm. $^{13}\text{C NMR}$ (126 MHz, CDCl_3) δ 168.99, 139.52, 137.90, 135.27, 133.46, 129.31, 128.98, 128.81, 128.22, 127.73, 126.95, 126.67, 126.43, 124.69, 124.51, 119.27, 50.85 ppm. **IR** (neat): ν (cm^{-1}) 3100, 2914, 2846, 1671, 1596, 1498, 1432, 1179, 815, 743. **HRMS** (ESI+, MeOH): m/z calcd. 308.1046 ($\text{M} + \text{Na}$)⁺, found: 308.1044.



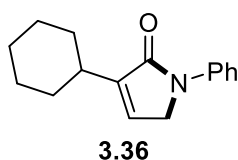
Scale: 0.15 mmol; isolated 33.1 mg (79% yield), white solid, Hexane : EA = 20 : 1, R_f = 0.2. $^1\text{H NMR}$ (400 MHz, CDCl_3) δ 7.81 – 7.74 (m, 2H), 7.49 (dd, J = 8.1, 1.7 Hz, 1H), 7.46 – 7.36 (m, 3H), 7.20 – 7.12 (m, 2H), 6.86 (d, J = 8.1 Hz, 1H), 5.98 (s, 2H), 4.43 (d, J = 2.3 Hz, 2H) ppm. $^{13}\text{C NMR}$ (126 MHz, CDCl_3) δ 168.83, 148.16, 147.89, 139.50, 137.54, 133.65, 129.25, 125.67, 124.41, 121.39, 119.18, 108.49, 107.69, 101.28, 50.59 ppm. **IR** (neat): ν (cm^{-1}) 3098, 2915, 2800, 1672, 1598, 1483, 1453, 1229, 895, 808, 687. **HRMS** (ESI+, MeOH): m/z calcd. 302.0788 ($\text{M} + \text{Na}$)⁺, found: 302.0777.



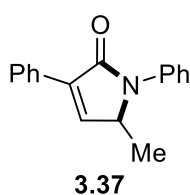
Scale: 0.15 mmol; isolated 14.1 mg (54% yield), white solid, Hexane : EA = 10 : 1, R_f = 0.25. $^1\text{H NMR}$ (400 MHz, CDCl_3) δ 7.80 – 7.70 (m, 2H), 7.42 – 7.33 (m, 2H), 7.11 (t, J = 7.4 Hz, 1H), 6.79 – 6.77 (m, 1H), 4.29 (p, J = 2.1 Hz, 2H), 1.96 (q, J = 1.9 Hz, 3H) ppm. $^{13}\text{C NMR}$ (101 MHz, CDCl_3) δ 170.95, 139.67, 136.92, 134.81, 129.19, 124.02, 118.58, 50.99, 11.43 ppm. **IR** (neat): ν (cm^{-1}) 2915, 1666, 1596, 1489, 1448, 1095, 823, 751, 687. **HRMS** (ESI+, MeOH): m/z calcd. 174.0913 ($\text{M} + \text{H}$)⁺, found: 174.0919.



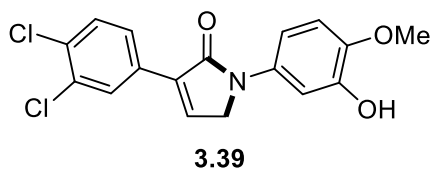
Scale: 0.15 mmol; isolated 20.4 mg (67% yield), light yellow solid, Hexane : EA = 20 : 1, R_f = 0.15. $^1\text{H NMR}$ (400 MHz, CDCl_3) δ 7.65 – 7.59 (m, 2H), 6.95 – 6.88 (m, 2H), 6.75 (q, J = 1.8 Hz, 1H), 4.26 (p, J = 2.0 Hz, 2H), 3.81 (s, 3H), 1.96 (q, J = 1.9 Hz, 3H) ppm. $^{13}\text{C NMR}$ (101 MHz, CDCl_3) δ 170.72, 156.36, 136.86, 134.48, 132.99, 120.70, 114.39, 55.63, 51.48, 11.51 ppm.



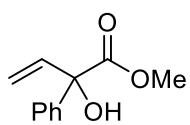
Scale: 0.15 mmol; isolated 23.5 mg (65% yield), white solid, Hexane : EA = 50 : 1, R_f = 0.1. $^1\text{H NMR}$ (400 MHz, CDCl_3) δ 7.80 – 7.70 (m, 2H), 7.40 – 7.32 (m, 2H), 7.11 (t, J = 7.4 Hz, 1H), 6.68 (q, J = 2.0 Hz, 1H), 4.29 (t, J = 1.8 Hz, 2H), 2.46 (t, J = 11.0 Hz, 1H), 1.99 (d, J = 13.5 Hz, 2H), 1.85 – 1.69 (m, 3H), 1.4 – 1.35 (m, 2H), 1.29 – 1.19 (m, 3H) ppm. $^{13}\text{C NMR}$ (101 MHz, CDCl_3) δ 170.26, 146.51, 139.75, 132.41, 129.19, 123.97, 118.62, 51.10, 35.20, 31.92, 26.41, 26.37 ppm. **IR** (neat): ν (cm^{-1}) 2925, 2851, 1671, 1598, 1500, 1446, 1379, 1279, 746, 685. **HRMS** (ESI+, MeOH): m/z calcd. 264.1359 ($\text{M} + \text{Na}$)⁺, found: 264.1360.



Scale: 0.15 mmol; isolated 18.3 mg (49% yield), light yellow solid, Hexane : EA = 20 : 1, R_f = 0.2. $^1\text{H NMR}$ (500 MHz, CDCl_3) δ 8.00 – 7.88 (m, 2H), 7.55 (dd, J = 8.6, 1.1 Hz, 2H), 7.47 – 7.34 (m, 5H), 7.28 (d, J = 2.1 Hz, 1H), 7.21 (t, J = 7.4 Hz, 1H), 4.81 (qd, J = 6.9, 2.1 Hz, 1H), 1.35 (d, J = 6.9 Hz, 3H) ppm. $^{13}\text{C NMR}$ (126 MHz, CDCl_3) δ 168.34, 141.80, 137.20, 136.22, 131.61, 129.18, 128.83, 128.60, 127.43, 125.20, 122.78, 56.27, 17.48 ppm. **IR** (neat): ν (cm^{-1}) 3061, 2976, 2930, 1682, 1596, 1496, 1371, 1274, 1128, 788, 751, 691. **HRMS** (ESI⁺, MeOH): m/z calcd. 272.1046 ($\text{M} + \text{Na}$)⁺, found: 272.1047.

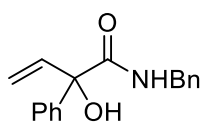


Scale: 0.15 mmol; isolated 25.5 mg (56% yield), light yellow solid, Hexane : DCM = 3 : 1, R_f = 0.12. $^1\text{H NMR}$ (400 MHz, CDCl_3) δ 8.12 – 8.01 (m, 1H), 7.78 (dd, J = 8.4, 2.1 Hz, 1H), 7.48 (d, J = 8.4 Hz, 1H), 7.35 – 7.29 (m, 2H), 7.24 (d, J = 2.6 Hz, 1H), 6.87 (d, J = 8.8 Hz, 1H), 5.69 (s, 1H), 4.42 (d, J = 2.2 Hz, 2H), 3.90 (s, 3H) ppm. $^{13}\text{C NMR}$ (101 MHz, CDCl_3) δ 167.93, 146.11, 143.94, 136.05, 135.95, 133.11, 132.92, 132.86, 131.55, 130.58, 129.14, 126.53, 111.67, 111.15, 106.95, 56.36, 51.30 ppm. **IR** (neat): ν (cm^{-1}) 3503, 3076, 2925, 1673, 1510, 1467, 1247, 1216, 1011, 824, 795. **HRMS** (ESI+, MeOH): m/z calcd. 372.0165 ($\text{M} + \text{Na}$)⁺, found: 372.0164.

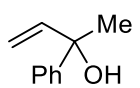


$^1\text{H NMR}$ (400 MHz, CDCl_3) δ 7.55 – 7.49 (m, 2H), 7.40 – 7.28 (m, 3H), 6.42 (dd, J = 17.0, 10.5 Hz, 1H), 5.63 (dd, J = 17.0, 1.2 Hz, 1H), 5.35 (dd, J = 10.5, 1.2 Hz, 1H), 3.88 – 3.84 (m, 1H), 3.81 (s, 3H) ppm. ^{13}C

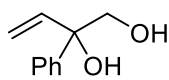
NMR (101 MHz, CDCl₃) δ 174.72, 141.19, 137.89, 128.55, 128.23, 126.18, 115.96, 78.67, 53.61 ppm. **IR** (neat): ν (cm⁻¹) 3505, 2955, 1727, 1436, 1250, 1152, 932, 733, 699. **HRMS** (ESI+, MeOH): m/z calcd. 215.0679 (M + Na)⁺, found: 215.0677.



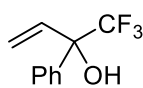
¹H NMR (400 MHz, CDCl₃) δ 7.52 – 7.50 (m, 2H), 7.37 – 7.27 (m, 6H), 7.23 – 7.17 (m, 2H), 6.71 (s, 1H), 6.51 (dd, J = 17.2, 10.6 Hz, 1H), 5.52 (dd, J = 17.2, 1.0 Hz, 1H), 5.41 (dd, J = 10.6, 1.0 Hz, 1H), 4.54 – 4.41 (m, 2H), 3.40 (s, 1H) ppm. **¹³C NMR** (101 MHz, CDCl₃) δ 172.80, 141.86, 139.41, 137.92, 128.89, 128.81, 128.49, 127.76, 126.56, 116.23, 79.56, 43.91 ppm. **IR** (neat): ν (cm⁻¹) 3391, 3030, 2921, 2851, 1653, 1519, 1449, 1155, 926, 695. **HRMS** (ESI-, MeOH): m/z calcd. 266.1187 (M – H)⁻, found: 266.1186.



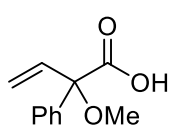
¹H NMR (400 MHz, CDCl₃) δ 7.55 – 7.44 (m, 2H), 7.38 – 7.33 (m, 2H), 7.30 – 7.24 (m, 1H), 6.19 (dd, J = 17.3, 10.6 Hz, 1H), 5.31 (dd, J = 17.3, 1.1 Hz, 1H), 5.16 (dd, J = 10.6, 1.1 Hz, 1H), 2.04 (d, J = 1.3 Hz, 1H), 1.67 (s, 3H) ppm. **¹³C NMR** (126 MHz, CDCl₃) δ 146.54, 144.96, 128.34, 127.10, 125.28, 112.45, 74.87, 29.42 ppm.



¹H NMR (400 MHz, CDCl₃) δ 7.47 – 7.45 (m, 2H), 7.41 – 7.33 (m, 2H), 7.32 – 7.26 (m, 1H), 6.16 (dd, J = 17.4, 10.8 Hz, 1H), 5.39 (dd, J = 17.3, 1.1 Hz, 1H), 5.30 (dd, J = 10.8, 1.1 Hz, 1H), 3.79 (d, J = 2.8 Hz, 2H), 2.98 (s, 1H), 2.13 (s, 1H) ppm. **¹³C NMR** (101 MHz, CDCl₃) δ 142.51, 140.70, 128.57, 127.60, 125.76, 115.67, 77.50, 69.53 ppm.

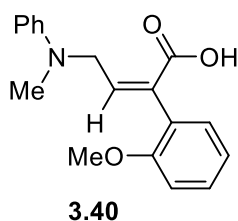


¹H NMR (400 MHz, CDCl₃) δ 7.71 – 7.55 (m, 2H), 7.45 – 7.38 (m, 3H), 6.47 (dd, J = 17.3, 10.9 Hz, 1H), 5.65 (d, J = 17.2 Hz, 1H), 5.54 (d, J = 10.9 Hz, 1H), 2.64 (s, 1H) ppm. **¹³C NMR** (101 MHz, CDCl₃) δ 137.13, 135.78, 128.90, 128.47, 126.81, 126.80, 126.78, 126.77, 126.41, 123.57, 118.56 ppm. **¹⁹F NMR** (376 MHz, CDCl₃) δ -78.82 ppm.

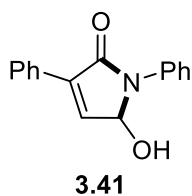


¹H NMR (400 MHz, CDCl₃) δ 7.48 – 7.45 (m, 2H), 7.42 – 7.32 (m, 3H), 6.31 (dd, J = 17.6, 10.7 Hz, 1H), 5.62 – 5.53 (m, 2H), 3.25 (s, 3H) ppm. **¹³C NMR** (101 MHz, CDCl₃) δ 174.59, 137.68, 134.55, 128.85, 128.67, 127.59, 119.48, 84.72, 53.11 ppm. **IR** (neat): ν (cm⁻¹) 3062, 2945, 2843, 1753, 1448, 1366,

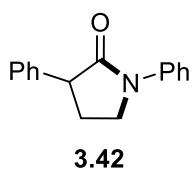
1194, 1131, 951, 776, 700, 682. **HRMS** (ESI⁻, MeOH): m/z calcd. 191.0714 (M - H)⁻, found: 191.0706.



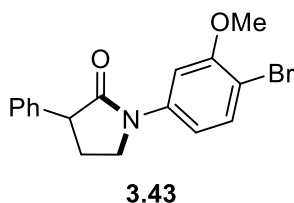
Scale: 0.15 mmol; isolated 31.6 mg (71% yield), light yellow solid, Hexane : EA = 5 : 1, R_f = 0.1. **¹H NMR** (400 MHz, CDCl₃) δ 7.33 – 7.23 (m, 3H), 7.15 (dd, J = 7.5, 1.6 Hz, 1H), 6.95 – 6.86 (m, 2H), 6.78 (dd, J = 16.1, 8.0 Hz, 3H), 6.29 (t, J = 5.7 Hz, 1H), 4.49 (d, J = 5.7 Hz, 2H), 3.82 (s, 3H), 3.02 (s, 3H) ppm. **¹³C NMR** (101 MHz, CDCl₃) δ 172.12, 156.95, 149.15, 144.69, 133.10, 130.40, 129.88, 129.42, 127.83, 120.98, 117.54, 113.51, 111.02, 55.79, 52.43, 39.02 ppm. **IR** (neat): ν (cm⁻¹) 3057, 2931, 2836, 1683, 1596, 1490, 1246, 1179, 1116, 1029, 753. **HRMS** (ESI⁻, MeOH): m/z calcd. 296.1292 (M - H)⁻, found: 296.1290.



Scale: 0.15 mmol; isolated 19.9 mg (53% yield), light yellow solid, Hexane : EA = 10 : 1, R_f = 0.15. **¹H NMR** (400 MHz, CDCl₃) δ 7.90 – 7.87 (m, 2H), 7.78 – 7.65 (m, 2H), 7.44 – 7.40 (m, 5H), 7.22 (t, J = 7.4 Hz, 1H), 7.13 (d, J = 2.0 Hz, 1H), 6.02 (dd, J = 10.7, 2.1 Hz, 1H), 2.48 (d, J = 10.7 Hz, 1H) ppm. **¹³C NMR** (101 MHz, CDCl₃) δ 167.39, 138.41, 137.03, 136.79, 130.44, 129.65, 129.31, 128.75, 127.83, 125.34, 121.55, 81.63 ppm. **IR** (neat): ν (cm⁻¹) 3267, 3060, 2922, 2853, 1685, 1594, 1490, 1402, 1243, 1070, 874, 731, 689. **HRMS** (ESI⁺, MeOH): m/z calcd. 274.0838 (M + Na)⁺, found: 274.0836.

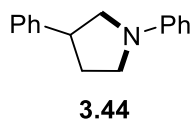


Scale: 0.15 mmol; isolated 32.7 mg (92% yield), white solid, Hexane : EA = 10 : 1, R_f = 0.2. **¹H NMR** (400 MHz, CDCl₃) δ 7.77 – 7.64 (m, 2H), 7.46 – 7.27 (m, 7H), 7.17 (t, J = 7.4 Hz, 1H), 3.96 – 3.85 (m, 3H), 2.65 (ddt, J = 12.8, 8.9, 5.6 Hz, 1H), 2.37 – 2.23 (m, 1H) ppm. **¹³C NMR** (126 MHz, CDCl₃) δ 174.13, 139.67, 139.37, 128.96, 128.88, 128.11, 127.29, 124.69, 119.93, 49.75, 46.84, 27.71 ppm.

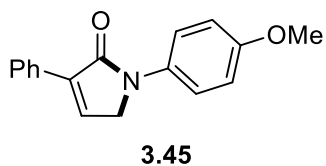


Scale: 0.1 mmol; isolated 32.9 mg (95% yield), white solid, Hexane : EA = 10 : 1, R_f = 0.2. **¹H NMR** (400 MHz, CDCl₃) δ 7.91 (d, J = 2.4 Hz, 1H), 7.50 (d, J = 8.6 Hz, 1H), 7.42 – 7.35 (m, 2H), 7.35 – 7.27 (m, 3H), 6.79 (dd, J = 8.6, 2.5 Hz, 1H), 3.97 – 3.85 (m, 6H), 2.69 – 2.59 (m, 1H), 2.33 (dq, J = 12.8, 8.4 Hz, 1H) ppm. **¹³C NMR**

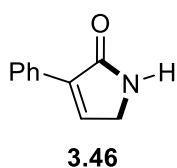
(101 MHz, CDCl₃) δ 174.49, 156.12, 140.21, 138.83, 132.86, 128.96, 128.10, 127.49, 111.69, 106.70, 104.51, 56.38, 49.98, 46.82, 27.24 ppm. **IR** (neat): ν (cm⁻¹) 2943, 2876, 1690, 1578, 1482, 1449, 1388, 1321, 1216, 1046, 1020, 726, 696. **HRMS** (ESI⁺, MeOH): m/z calcd. 368.0257 (M + Na)⁺, found: 368.0257.



Scale: 0.15 mmol; isolated 25.1 mg (75% yield), yellow oil, Hexane : EA = 50 : 1, R_f = 0.5. **¹H NMR** (400 MHz, CDCl₃) δ 7.38 – 7.22 (m, 7H), 6.70 (t, J = 7.3 Hz, 1H), 6.61 (d, J = 7.8 Hz, 2H), 3.74 (dd, J = 8.8, 7.8 Hz, 1H), 3.59 – 3.34 (m, 4H), 2.47– 2.39 (m, 1H), 2.20 – 2.10 (m, 1H) ppm. **¹³C NMR** (101 MHz, CDCl₃) δ 147.77, 142.84, 129.36, 128.74, 127.29, 126.79, 115.83, 111.71, 54.61, 47.74, 44.27, 33.40 ppm. **IR** (neat): ν (cm⁻¹) 3059, 3026, 2835, 1596, 1505, 1480, 1365, 1156, 997, 743, 690. **HRMS** (ESI⁺, MeOH): m/z calcd. 224.1434 (M + H)⁺, found: 224.1429.



Scale: 0.15 mmol; isolated 33.4 mg (84% yield), light yellow solid, Hexane : EA = 20 : 1, R_f = 0.15. **¹H NMR** (400 MHz, CDCl₃) δ 7.95 – 7.86 (m, 2H), 7.69 – 7.63 (m, 2H), 7.47 – 7.32 (m, 3H), 7.28 – 7.24 (m, 1H), 6.97 – 6.91 (m, 2H), 4.43 (d, J = 2.2 Hz, 2H), 3.82 (s, 3H) ppm. **¹³C NMR** (101 MHz, CDCl₃) δ 168.65, 156.66, 138.21, 134.83, 132.75, 131.76, 128.81, 128.60, 127.33, 121.30, 114.46, 55.65, 51.26 ppm. **IR** (neat): ν (cm⁻¹) 3042, 3013, 2953, 2836, 1669, 1511, 1436, 1251, 1180, 825, 786, 694. **HRMS** (ESI⁺, MeOH): m/z calcd. 288.0995 (M + Na)⁺, found: 288.0993.



Scale: 0.15 mmol; isolated 23.9 mg (99% yield), white solid, Hexane : EA = 1 : 1, R_f = 0.2. **¹H NMR** (400 MHz, CDCl₃) δ 7.89 – 7.80 (m, 2H), 7.43 – 7.27 (m, 4H), 4.09 (s, 2H) ppm. **¹³C NMR** (101 MHz, CDCl₃) δ 173.69, 138.65, 137.26, 131.70, 128.67, 128.62, 127.22, 46.18 ppm. **IR** (neat): ν (cm⁻¹) 3198, 3058, 2922, 2852, 1712, 1663, 1626, 1438, 789, 695. **HRMS** (ESI⁺, MeOH): m/z calcd. 182.0576 (M + Na)⁺, found: 182.0571.

Chapter 4.

Pd-Catalyzed Stereodivergent Allylic Amination of α -Tertiary Allylic Alcohols towards α,β -Unsaturated γ -Amino Acids

This chapter has been published in:

J. Xie, C. Qiao, M. Martínez Belmonte, E. C. Escudero-Adán, A. W. Kleij,
ChemSusChem **2019**, *12*, 3152-3158.

4.1 Introduction

4.1.1 α,β -Unsaturated γ -Amino Acids

α,β -Unsaturated γ -amino acids (and their corresponding esters) are of considerable significance due to their functional character allowing for their transformation into γ -amino amides, γ -amino alcohols and γ -lactams.¹¹⁸ These compounds have also value as key structural building blocks in peptide-based natural products and related congeners, which can have interesting pharmaceutical activities¹¹⁹ as exemplified by syringolin A,¹²⁰ Hemiasterlin,¹²¹ and Symplostatin 4.¹²² Thus, the development of new, general methodologies for the syntheses of α,β -unsaturated γ -amino acids, particularly stereoselective protocols, are of general interest but remain elusive.

4.1.2 Stereoselective Olefin Synthesis

Olefins play an essential role in the area of chemical synthesis, because they are among the most commonly occurring and important class of organic compounds widely used in the chemical and pharmaceutical industry and materials science.¹²³ Traditional methods for olefin construction include elimination reactions, the reduction of alkynes, and the Wittig- or Julia-Kocienski olefination. Additionally, efficient catalytic methods using TMs have been developed, such as the Heck reaction, olefin metathesis, and cross-coupling reactions that involve alkenyl metal reagents or alkenyl halides, providing convenient access to a variety of olefin products.

Particularly, stereoselective construction of carbon-carbon double bonds with well-defined configurations has been an overarching goal in synthetic chemistry.¹²⁴ The stereochemistry of olefins (namely either *E* or *Z*) not only determines the properties of

-
- (118) a) F. Palacios, D. Aparicio, J. García, E. Rodríguez, A. Fernández-Acebes, *Tetrahedron* **2001**, *57*, 3131; b) A. K. Ghosh, M. Brindisi, J. Tang, *J. Neurochem.* **2012**, *120*, 71; c) S. Chandrasekhar, M. V. Reddy, *Tetrahedron* **2000**, *56*, 1111; d) M. T. Reetz, *Angew. Chem. Int. Ed.* **1991**, *30*, 1531.
- (119) a) N. Schaschke, *Bioorg. Med. Chem. Lett.*, **2004**, *14*, 855; b) Y. Nakao, M. Fujita, K. Warabi, S. Matsunaga, N. Fusetani, *J. Am. Chem. Soc.* **2000**, *122*, 10462; c) T. Conroy, J. T. Guo, R. G. Linnington, N. H. Hunt, R. J. Payne, *Chem. Eur. J.* **2011**, *17*, 13544; d) J. A. Nieman, J. E. Coleman, D. J. Wallace, E. Piers, L. Y. Lim, M. Roberge, R. J. Andersen, *J. Nat. Prod.* **2003**, *66*, 183.
- (120) C. S. Coleman, J. P. Rocetes, D. J. Park, C. J. Wallick, B. J. Warn-Cramer, K. Michel, R. Dudler, A. S. Bachmann, *Cell Prolif.* **2006**, *39*, 599.
- (121) R. Talpir, Y. Benayahu, Y. Kashman, L. Pannell, M. Schleyer, *Tetrahedron Lett.* **1994**, *35*, 4453.
- (122) K. Taori, Y. Liu, V. J. Paul, H. Luesch, *ChemBioChem* **2009**, *10*, 1634.
- (123) a) M. Fuchs, A. Fürstner, *Angew. Chem., Int. Ed.* **2015**, *54*, 3978; b) C. Oger, L. Balas, T. Durand, J.-M. Galano, *Chem. Rev.* **2013**, *113*, 1313; c) A. Cirila, J. Mann, *Nat. Prod. Rep.* **2003**, *20*, 558.
- (124) E. Negishi, Z. Huang, G. Wang, S. Mohan, C. Wang, H. Hattori, *Acc. Chem. Res.* **2008**, *41*, 1474.

the molecules but also in most cases alters the stereochemical outcome of the reactions utilizing these compounds as starting materials. In general, methods for highly selective access to *Z*-olefins are less established than those for the *E*-configured ones. One of the reasons is that thermodynamically *E*-olefins are favored, at least in the case of disubstituted double bonds.

Switchable catalysis can provide straightforward access to both *E* and *Z* isomeric olefins through a stereodivergent conversion of a common precursor by carefully tuning the catalytic conditions. Although challenging, TM-catalyzed stereodivergent synthesis of olefins has witnessed progress. For instance, Liu *et al.* disclosed a cobalt-catalyzed stereodivergent transfer hydrogenation of alkynes enabling the synthesis of both *Z*- and *E*-olefins selectively promoted by different ligands.¹²⁵ Lalic *et al.* reported a *Z*- and *E*-selective hydroarylation of terminal alkynes, and these transformations were promoted by a combination of palladium and copper catalysts operating in tandem.¹²⁶ Very recently, photoredox/nickel dual catalysis was disclosed by Chu and coworkers describing a stereodivergent cross-electrophile coupling reaction between allylic carbonates and vinyl triflates selectively providing different stereoisomers of 1,4-dienes by adjusting/variation of the structure of the photocatalyst.^{127,128}

TM-catalyzed allylic substitution reactions may provide an alternative and powerful route for stereodivergent olefin synthesis by nucleophilic attack onto the least hindered carbon terminus (γ -position) of an *in situ* formed metal allyl species. The product isomer that will form depends on the stereochemistry of the η^3 -allyl complex (*syn* or *anti*). Thus, the nucleophilic addition to the unsubstituted *syn* complex will give an *E*-olefin, and addition to an *anti* complex will produce a *Z*-olefin (Scheme 4.1). In this context, *anti-syn* isomerization of η^3 -allyl metal complexes occurs via π - σ - π interconversion, which has been shown to be controlled by a proper choice of a (bis)phosphine ligand.¹²⁹

(125) S. Fu, N.-Y. Chen, X. Liu, Z. Shao, S.-P. Luo, Q. Liu, *J. Am. Chem. Soc.* **2016**, *138*, 8588.

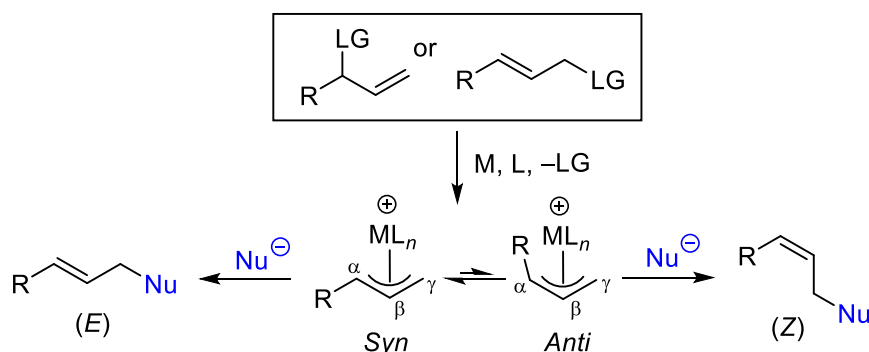
(126) M. K. Armstrong, M. B. Goodstein, G. Lalic, *J. Am. Chem. Soc.* **2018**, *140*, 10233.

(127) F. Song, F. Wang, L. Guo, X. Feng, Y. Zhang, L. Chu, *Angew. Chem. Int. Ed.* **2020**, *59*, 177.

(128) For other examples: a) K. Murugesan, C. B. Bheeter, P. R. Linnebank, A. Spannenberg, J. N. H. Reek, R. V. Jagadeesh, M. Beller, *ChemSusChem* **2019**, *12*, 3363; b) C.-Q. Zhao, Y.-G. Chen, H. Qiu, L. Wei, P. Fang, T.-S. Mei, *Org. Lett.* **2019**, *21*, 1412; c) R. J. Armstrong, C. García-Ruiz, E. L. Myers, V. K. Aggarwal, *Angew. Chem. Int. Ed.* **2017**, *56*, 786.

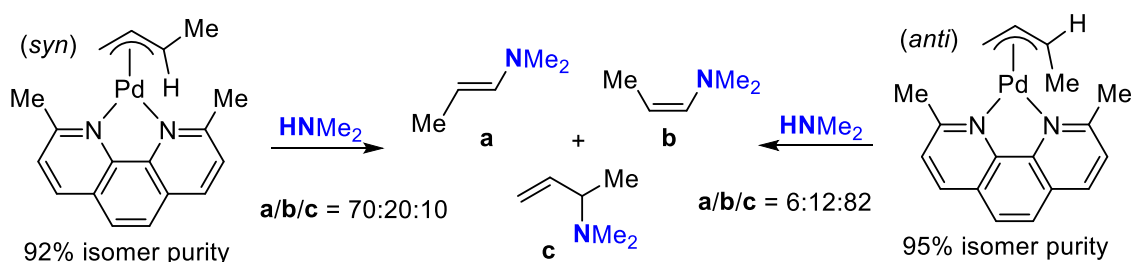
(129) a) M. Ogasawara, K. Takizawa, T. Hayashi, *Organometallics* **2002**, *21*, 4853; b) M. Kranenburg, P. C. J. Kamer, P. W. N. M. van Leeuwen, *Eur. J. Inorg. Chem.* **1998**, *25*; c) R. J. van Haaren, G. P. F. van Strijdonck, H. Oevering, J. N. H. Reek, P. C. J. Kamer, P. W. N. M. van Leeuwen, *Eur. J. Inorg. Chem.* **2001**, 837.

Therefore, it is reasonable to assume that both *Z*- or *E*-olefins can be obtained from a common allylic precursor, in which the configurations of π -allyl metal intermediate is controlled by suitable conditions and the nature of the supporting ligand.



Scheme 4.1 Stereodivergent allylic substitution affording disubstituted olefins controlled through a π -allyl metal intermediate.

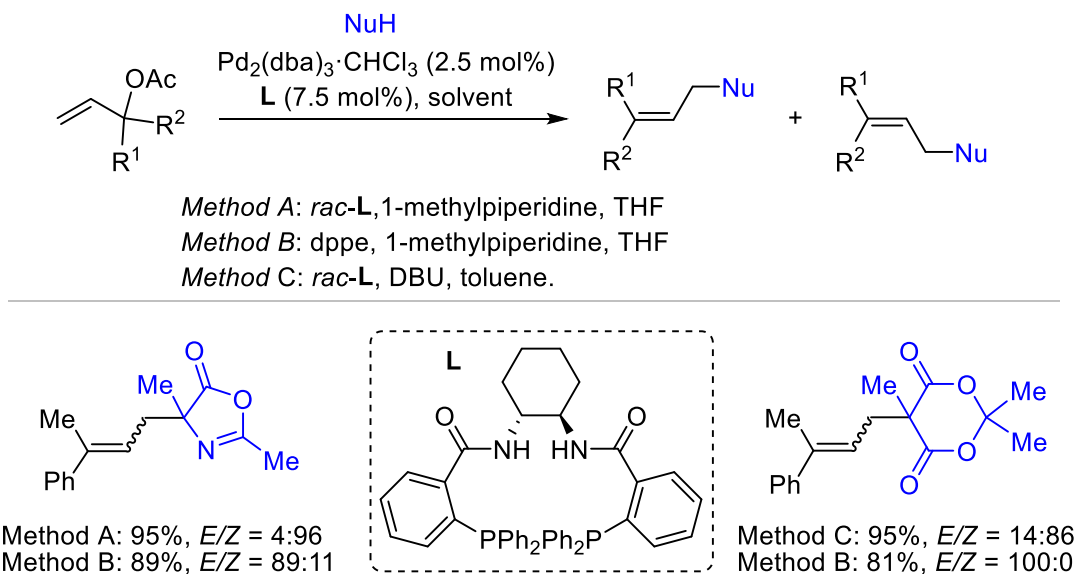
Although efficient methodologies have been developed for the construction of the (typically) thermodynamically more stable *E*-configured, γ -mono-substituted allylic scaffolds,¹³⁰ reports pertaining to stereodivergent allylic substitution affording either a *Z*- or *E*-configured product from a single substrate are scarce. A pioneering example using dimethylamine as nucleophile was reported by Vitagliano *et al.* using differently configured complexes prepared from η^3 -allyl-chloride precursors in the presence of AgBF_4 and 2,9-dimethyl-1,10-phenanthroline (Scheme 4.2).¹³¹ Although the observed *Z/E* ratios were not ideal, retention of stereochemistry was noted to a fair extent, and these reactions favored the nucleophilic attack to occur at the secondary position in the case of the *anti* isomer.



Scheme 4.2 A previously reported stereodivergent allylic amination.

- (130) a) N. A. Butt, W. Zhang, *Chem. Soc. Rev.* **2015**, *44*, 7929; b) J. S. Arnold, Q. Zhang, H. M. Nguyen, *Eur. J. Org. Chem.* **2014**, *2014*, 4925; c) A. Leitner, C. Shu, J. F. Hartwig, *Org. Lett.* **2005**, *7*, 1093; d) S. Shekhar, B. Trantow, A. Leitner, J. F. Hartwig, *J. Am. Chem. Soc.* **2006**, *128*, 11770; e) B. Plietker, *Angew. Chem. Int. Ed.* **2006**, *45*, 6053.
- (131) B. Aakermark, S. Hansson, A. Vitagliano, *J. Am. Chem. Soc.* **1990**, *112*, 4587.

In 1999, the Trost group disclosed a method to control the alkene geometry in Pd-catalyzed allylic alkylation reactions that were based on chiral recognition (Scheme 4.3).¹³² By changing the achiral ligand to a chiral (though racemic) one, a switch in the geometry of the trisubstituted alkene product from *E* to the thermodynamically less stable *Z* could be achieved, with the chiral, enantiomerically pure ligand not able to provide geometrical selectivity. By using an appropriate ligand, either alkene geometry of the product could be generated from the same starting material.



Scheme 4.3 Pd-catalyzed stereodivergent allylic alkylation controlled by chiral recognition.

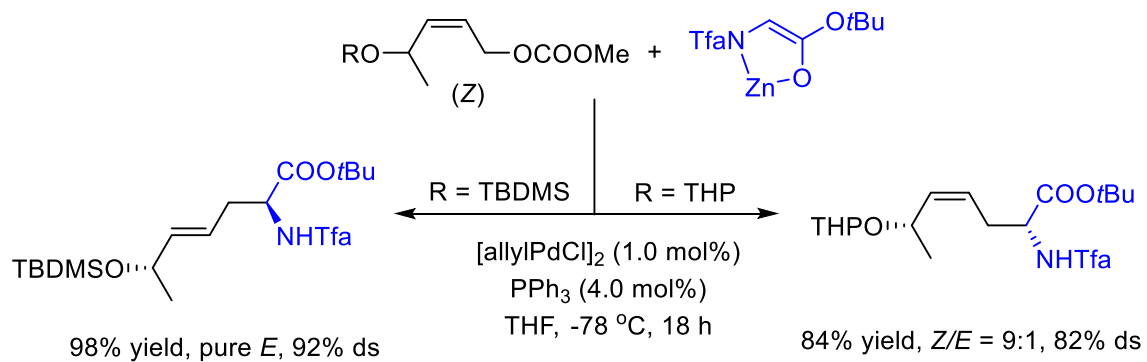
If the allylic substitution is fast enough using a highly reactive nucleophile, the intermediate *anti* configured η^3 -allyl complex can be intercepted before it isomerizes to the more stable *syn* isomer. Additionally, π - σ - π isomerization of these terminal π -allyl Pd(II) complexes is much faster compared to the 1,3-disubstituted analogues.¹³³ In this regard, Kazmaier *et al.* found that a zinc amino acid ester enolate acts as an efficient nucleophile and terminal η -allyl palladium complexes react without significant isomerization (Scheme 4.4).¹³⁴ However, if the nucleophilic attack becomes slower, for example by introduction of steric bulk in the η^3 -allyl complex, *anti*-to-*syn* isomerization

(132) B. M. Trost, C. Heinemann, X. Ariza and S. Weigand, *J. Am. Chem. Soc.* **1999**, *121*, 8667.

(133) a) P. Corradini, G. Maglio, A. Musco, G. Paiaro, *J. Chem. Soc., Chem. Commun.* **1966**, 618; b) T. Cavigny, M. Julia, C. Rolando, *J. Organomet. Chem.* **1985**, 285, 395.

(134) K. Krämer, U. Kazmaier, *J. Org. Chem.* **2006**, *71*, 8950.

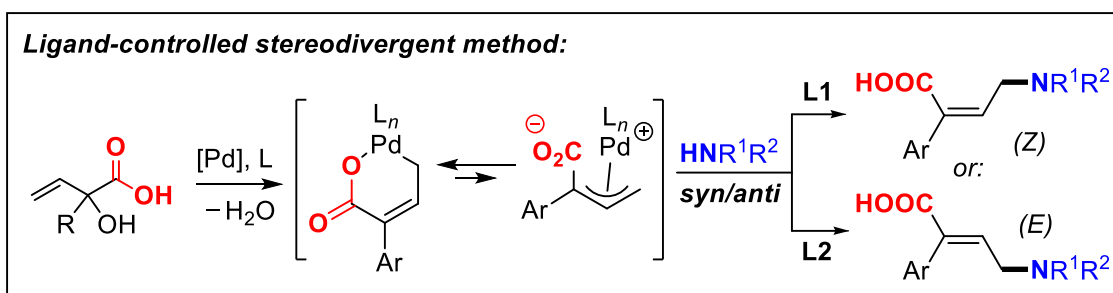
becomes competitive and influences the stereochemical course of the allylic substitution reaction.



Scheme 4.4 Pd-catalyzed stereoselective allylic alkylations of *Z*-configured substrate. THP = tetrahydropyranyl; TBDMS = *tert*-butyldimethylsilyl; ds stands for diastereospecificity.

4.1.3 Aim of the Work presented in this Chapter

In our previous work (see chapter 3) focusing on the synthesis of α,β -unsaturated γ -lactams via Pd-mediated stereoselective amination of α -tertiary allylic alcohols, the carboxyl group present in the substrate plays a crucial role that allows to activate the allylic alcohol and to direct the stereochemical course of the reaction through chelation. We wondered whether this Pd–O coordination could be controlled via the use of an appropriate ligand and reaction conditions (i.e., solvent polarity, additives) as to increase its dynamic character allowing thus for well-established π - σ - π interconversion and switching between *syn* and *anti* Pd(allyl) species (Scheme 4.5). Such ligand-controlled reactivity would facilitate stereodivergent allylic amination producing either a *Z*- or *E*-configured γ -amino acid as product, which represents a step forward in the area of allylic amination combining improved stereocontrol, facile operation, and attractive eco-friendly features.



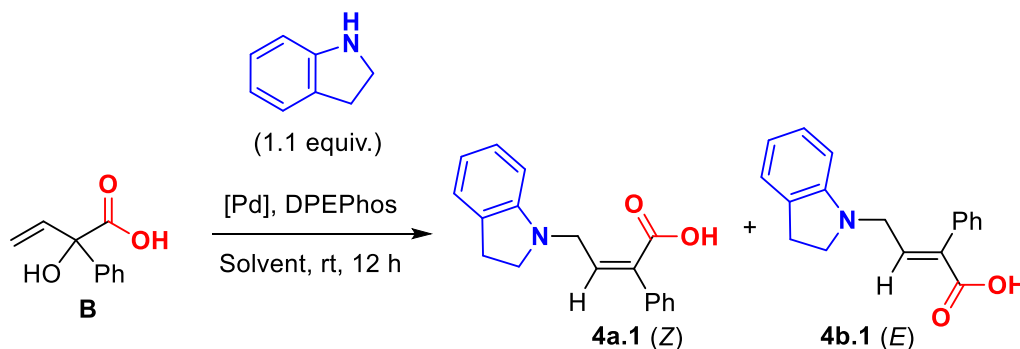
Scheme 4.5 Pd-catalyzed stereodivergent allylic amination towards α,β -unsaturated γ -amino acids.

In this chapter we describe a stereodivergent allylic amination route that establishes the preparation of both stereoisomers (*E* and *Z*) of α,β -unsaturated γ -amino acids from carboxyl-functionalized allylic alcohols by a judicious choice of a supporting (di)phosphine ligand.

4.2 Results and Discussion

4.2.1 Screening Studies

Table 4.1: Optimization of the reaction conditions of allylic amination of substrate **B**^a



Entry	[Pd]	Solvent	Conv. [%] ^b	Yield of 4a.1 + 4b.1 [%] ^b	Z/E ^c
1	[allylPdCl] ₂	DMF	18	10	70:30
2	Pd ₂ (dba) ₃ ·CHCl ₃	DMF	52	19	94:6
3	Pd(dba) ₂	DMF	34	17	97:3
4	Pd(PPh ₃) ₄	DMF	42	22	74:26
5	Pd/bis-sulf.	DMF	35	14	64:36
6	Pd(OAc) ₂	DMF	28	14	49:51
7	Pd(TFA) ₂	DMF	41	25	42:58
8	Pd(acac) ₂	DMF	24	13	50:50
9	Pd(TFA) ₂	CH ₃ CN	38	10	58:42
10	Pd(TFA) ₂	DCM	35	9	62:38
11	Pd(TFA) ₂	MeOH	36	16	61:39
12	Pd(TFA) ₂	HFIP	97	79	99:1
13	Pd(TFA) ₂	DMSO	75	60	45:55

^aReaction conditions: **B** (0.15 mmol), indoline (0.165 mmol, 1.1 equiv.), solvent (0.15 mL; 1.0 M), [Pd] (4.0 mol%), DPEPhos **L1** (4.0 mol%), 12 h, rt. ^bDetermined by ¹H NMR analysis in CDCl₃ using CH₂Br₂ as an internal standard. ^cDetermined from the crude ¹H NMR by signal integration. Pd/bis-sulf stands for the White catalyst precursor, which is a bis-sulfoxide ligated Pd(OAc)₂.

To test our working hypothesis illustrated in Scheme 4.5, we chose substrates **B** and indoline (Table 4.1) for the screening phase that should ideally selectively allow to access either *Z*- or *E*-configured γ -amino acid products **4a.1** and **4b.1**, respectively. As an initial ligand, DPEPhos (**L1**) was selected as we recently observed that it was an effective ligand system for Pd-catalyzed allylic amination.^{36a}

Various Pd(0) and Pd(II) precursors were scrutinized (entries 1–8) showing, however, only modest variation in the conversion levels. Since the use of Pd(TFA)₂ provided a slightly higher selectivity towards products **4a.1**+**4b.1** (*cf.*, entries 4 and 7), we decided to further use this precursor and to vary the solvent (entries 9–13). Interestingly, while most other solvents did not improve the reactivity, the presence of HFIP (hexafluoroisopropanol) afforded the γ -amino acid products in (a combined) 79% yield and with a high *Z/E* ratio of 99:1 (entry 12). Despite that the use of HFIP and DMSO provide overall higher yield of the targeted products, we further focused on the use of DMF for optimization as it gave the highest amount of *E*-isomer. Additionally, in a second optimization phase the use of DMF allowed for a direct comparison of ligand effects under otherwise identical reaction conditions (*vide infra*, Table 4.2).

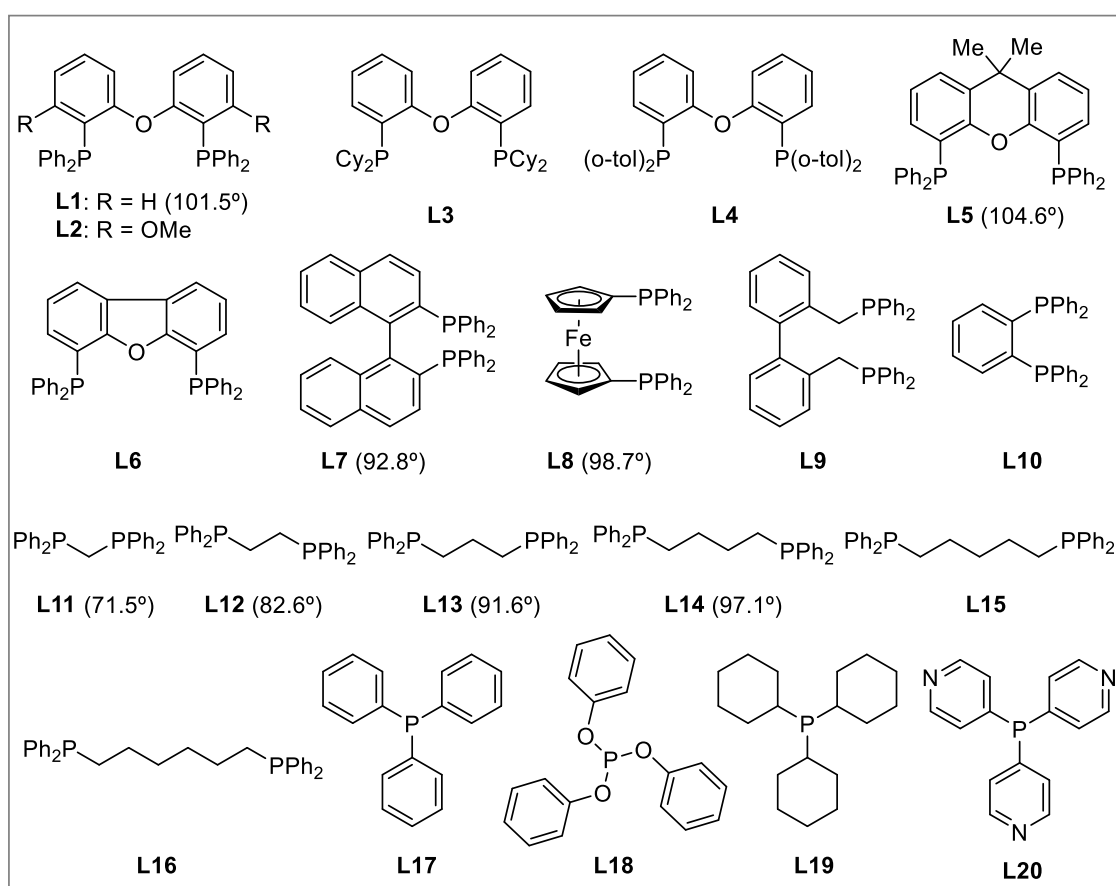
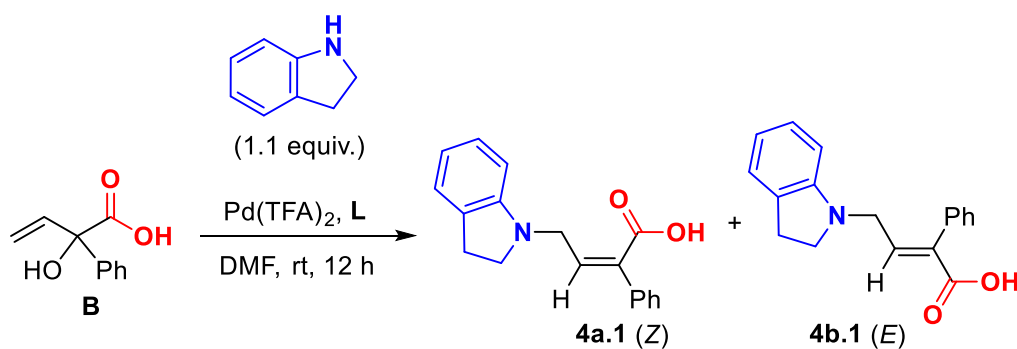


Figure 4.1 Phosphine ligands **1–17** and **19–20**, and phosphite **18** used in the optimization process towards either **4a.1** or **4b.1** and related to Table 4.2. In brackets, some of the diphosphine *bite angles* are also provided.

Table 4.2: Effect of the ligand in the stereoselective allylic amination of substrate **B**^a



Entry	Ligand	Conv. [%] ^b	Yield of 4a.1 + 4b.1 [%] ^b	Z/E ^c
1	L2	60	42	21:79
2 ^d	L2	100	83	16:84
3 ^{d,e}	L2	100	82	14:86
4	L3	38	16	80:20
5	L4	16	4	>99:1
6	L5	37	9	80:20
7	L6	56	38	>99:1
8	L7	88	51	92:8
9	L8	100	74	62:38
10	L9	63	42	99:1
11	L10	26	10	95:5
12	L11	42	20	>99:1
13	L12	17	10	>99:1
14	L13	100	94	>99:1
15	L14	100	90	98:2
16	L15	67	38	73:27
17	L16	84	65	69:31
18	L17	83	56	95:5
19	L18	80	54	90:10
20	L19	28	14	99:1
21	L20	16	4	>99:1

^aReaction conditions: **B** (0.15 mmol), indoline (0.165 mmol, 1.1 equiv.), DMF (0.15 mL; 1.0 M), Pd(TFA)₂ (4.0 mol%) and **L** (4.0 mol%), 12 h, rt. ^bConversion of **B** determined by ¹H NMR analysis in CDCl₃ using CH₂Br₂ as an internal standard. ^cDetermined from the crude ¹H NMR by signal integration. ^dPd(TFA)₂ (10.0 mol%) and **L** (10.0 mol%). ^eDMF (0.30 mL; 0.5 M).

In order to improve the overall reactivity, chemo-selectivity and stereoselectivity bias for the process, an additional set of 19 phosphorus ligands were evaluated (see Figure 4.1). Introduction of *ortho*-methoxy substituents in the DPEPhos ligand structure (*cf.*, **L2**)

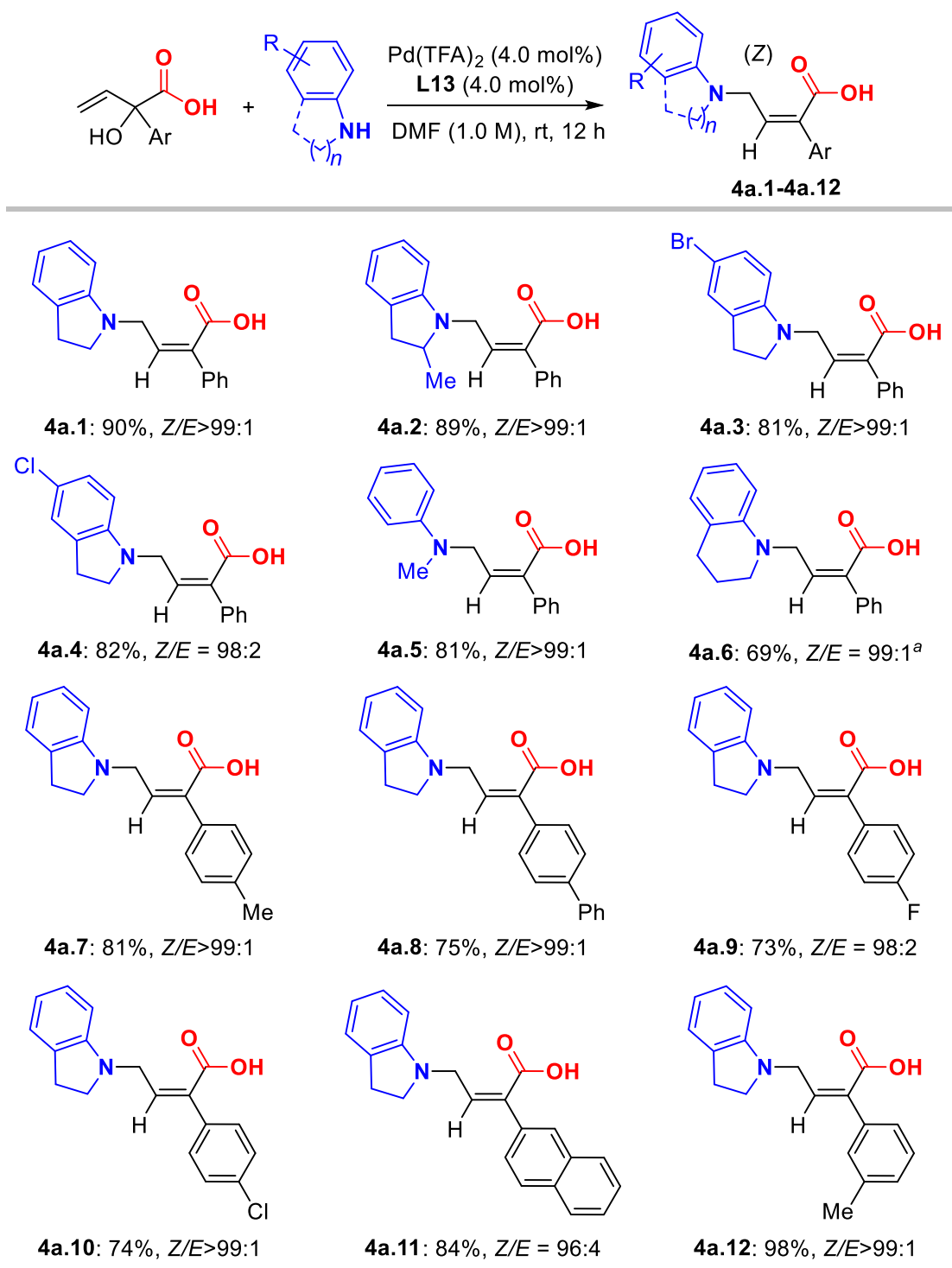
provided a catalyst system that gave, after increasing both the Pd precursor and ligand amount to 10.0 mol% and using a 0.5 M dilution (Table 4.2, entries 1–3), the highest *E/Z* ratio of around 6:1 providing the amino acid product **4b.1** in a combined 82% yield.

While the selectivity towards the *E*-product could not be further improved, further experiments then focused on achieving an optimal yield and stereocontrol towards the *Z*-configured product **4a.1** (entries 4–21). Various ligands, including **L8** (dppf),¹³⁵ **L14** (dppb) and **L16** (dpph) proved to be efficient catalyst systems for the conversion of **B**, though **L13** (dppp) was outstanding in terms of substrate conversion (quantitative), product yield (94%) and stereocontrol towards **4a.1** (>99:1). These conditions differ markedly from those previously found optimal for the formation of α,β -unsaturated γ -lactams from **B** (dppf **L8**, Pd₂(dba)₃·CHCl₃, CH₃CN, rt; see chapter 3).

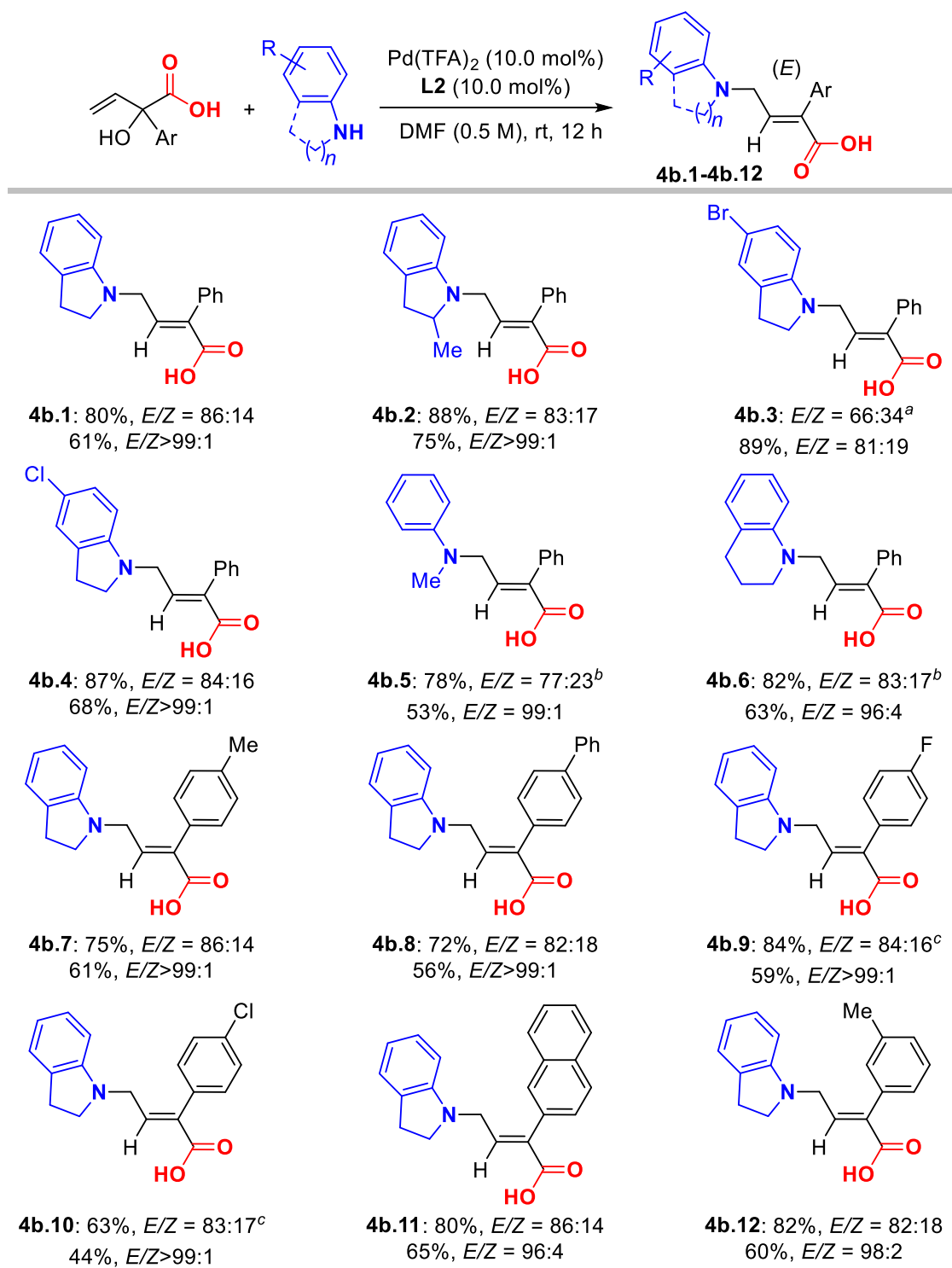
4.2.2 Scope of Substrates

With these optimized conditions in hand for both the *Z*-**4a.1** as well as the *E*-stereoisomer **4b.1**, the scope of this stereodivergent allylic amination process was examined focusing first on the synthesis of the *Z*-stereoisomers using the conditions reported in entry 14 of Table 4.2 (Scheme 4.6). The indoline based amino acid **4a.1** was isolated in high yield (90%) under excellent stereocontrol (*Z/E*>99:1). Other substituted indolines proved to be productive substrates when combined with **B** (Ar = Ph) giving smooth access to *Z*-amino acids **4a.2–4a.4** in good yields and with high *Z/E* values. Apart from indolines, the use of secondary amines such as *N*-methylaniline and 1,2,3,4-tetrahydroquinoline gave easy access to the targeted amino acids **4a.5** (81%) and **4a.6** (69%) preserving a high stereoselectivity. Next, we examined the use of other tertiary allylic alcohol derivatives by variation of the Ar group (*cf.*, formation of **4a.7–4a.12**). Good to excellent yields of the amino acids were obtained and all products were isolated with high *Z/E* ratios of at least 96:4. Electron-withdrawing and -donating groups did not significantly influence the outcome of the allylic amination protocol, and a larger aromatic group (naphthyl; *cf.*, preparation of **4a.11**) in the substrate was also tolerated.

(135) J. Xie, S. Xue, E. C. Escudero-Adán, A. W. Kleij, *Angew. Chem. Int. Ed.* **2018**, *57*, 16727.



Scheme 4.6 Reaction conditions for *Z*-isomers unless stated otherwise: all reactions were performed under the optimized conditions (Table 4.2, entry 14). ^aUsing Pd(TFA)₂ (8.0 mol%) and **L13** (8.0 mol%), 24 h. Reported yields are of the isolated product after column purification.



Scheme 4.7 Reaction conditions for *E*-isomers unless stated otherwise: all reactions were performed under the optimized conditions (Table 4.2, entry 3); both the combined isolated yield of the *E/Z* mixture and the column-purified *E* compounds were determined, alongside their respective *E/Z* ratios determined by ¹H NMR. ^aThe *E*- and *Z*-isomers could not be (fully) separated by column chromatography; the product was isolated with an *E/Z* ratio of 81:19. ^bUsing DPEPhos **L1** (10.0 mol%) as ligand. ^cReaction time was 24 h.

The synthesis of the *E*-configured analogues of **4b.1–4b.12** (Scheme 4.7) was then also probed using the optimal conditions found for the preparation of **4b.1** (Table 4.2, entry 3). All substrate substitutions and variations scrutinized in the scope presented for the *Z*-amino acids (Scheme 4.7) were kept the same for the sake of comparison and to allow for investigation of the generality of the stereodivergent protocol. In general, the products **4b.1–4b.12** were obtained in good isolated yields of up to 89% (**4b.3**) with *E/Z* ratios up to 6:1. Fortunately, all *E*-isomers (except in the case of **4b.3**) could be separated from these isomer mixtures by column chromatography to afford the virtually pure stereoisomers in typical yields in the range 60–70%. Neither the substitution pattern in the secondary amine reagent nor in the tertiary allylic alcohol affected the overall yield or stereoinduction.

These results (Scheme 4.6) combined with those reported in Scheme 4.7 demonstrate that both stereoisomers can be readily obtained from the same allylic alcohol precursor by simply switching from **L2** (giving the *E*-isomer as the major product) to **L13** (favouring the *Z*-isomer) at ambient temperature under rather comparable reaction conditions. Suitable crystals of **4a.1** and **4b.1** were obtained and the molecular structures of these stereoisomers were determined by X-ray crystallography (Figure 4.2). These data

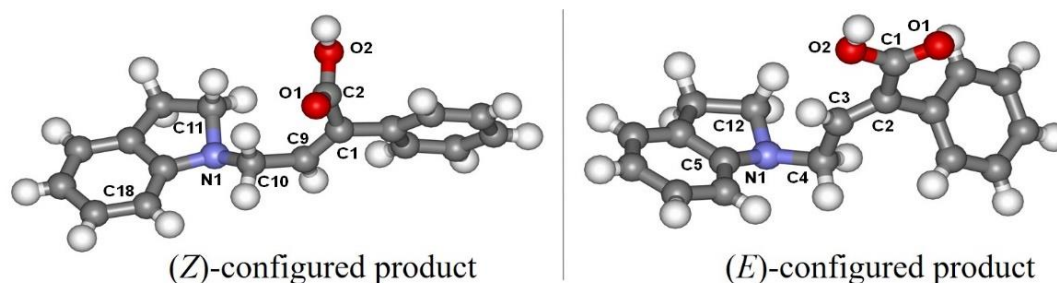
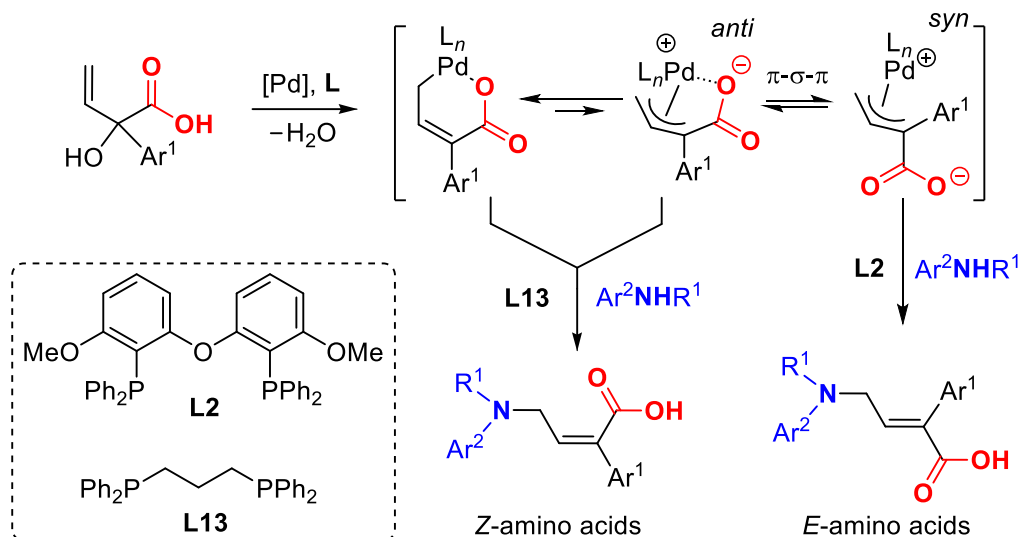


Figure 4.2 X-ray molecular structures determined for **4a.1** (*Z*; left structure) and **4b.1** (*E*; right structure). Selected bond lengths/angles (\AA°) for **4a.1** with esd's in parentheses: N(1)–C(10) = 1.4753(14), N(1)–C(11) = 1.4926(15), N(1)–C(18) = 1.4343(14), C(1)–C(9) = 1.3362(15), C(1)–C(2) = 1.5023(16), C(2)–O(1) = 1.2159(13); C(11)–N(1)–C(18) = 105.22(9), O(1)–C(2)–O(2) = 124.16(11), C(2)–C(1)–C(9) = 119.79(10). Selected bond lengths/angles (\AA°) for **4b.1** with esd's in parentheses: N(1)–C(4) = 1.475(3), N(1)–C(5) = 1.441(3), N(1)–C(12) = 1.491(3), C(2)–C(3) = 1.342(3), C(1)–C(2) = 1.498(3), C(1)–O(1) = 1.217(3); C(5)–N(1)–C(12) = 105.43(18), O(1)–C(1)–O(2) = 123.1(2), C(1)–C(2)–C(3) = 119.3(2).

therefore provide unambiguous proof of the proposed connectivity present in the *Z*- as well as *E*-isomer obtained from the reaction between substrate **B** and indoline. Their NMR features provided a useful reference to determine the stereochemistry of the other products (*i.e.*, **4a.2–4a.12** and **4b.2–4b.12**).

4.2.3 Proposed Stereocontrolled Manifold

To rationalize the experimental observations, we first performed a closer inspection of the nature of the diphosphine ligand needed to favour the formation of the *E*-isomer. This revealed that a slightly more bulky ligand such as **L2** (a bis-*ortho*-substituted DPEPhos analogue, see Figure 4.1) is required. This is reasonable, as coordination of such a bulky ligand may disfavour the stability of the *in situ* formed palladacycle (Scheme 4.8; after initial loss of H₂O) and allow for isomerization of the allyl Pd(II) species through π - σ - π interconversion. From this point on, an electrostatic interaction of the carboxyl group and the Pd centre in the *anti*-isomer may increase the overall 1,3-allylic strain, allowing for some degree of *anti*/*syn* interconversion and increased steric shielding of the allyl carbon terminus. The *syn*-isomer is likely to be thermodynamically less stable, but it is believed to be kinetically more competent (*i.e.*, following a Curtin-Hammett principle). As a consequence, the *E*-isomer is preferentially formed when a more rigid, wide bite angle diphosphine ligand such as **L2** is present.



Scheme 4.8 Proposed mechanistic rationale for the stereodivergent Pd-catalyzed synthesis of *E*- and *Z*-amino acids from tertiary allylic alcohols and amines. L_n refers here to a diphosphine ligand.

Alternatively, when a more flexible, smaller bite angle ligand such as **L13** (dppp) is used, the stereoselectivity is fully reversed towards the formation of the *Z*-product. The diphosphine ligands that result in the highest conversion rates (Table 4.2, **L7**: BINAP; **L8**: dppf; **L13**: dppp; **L14**: dppb and **L16**: dppe) demonstrate that the diphosphine bite angle plays indeed an important role, with **L13** (dppp, bite angle around 91.6°, Figure 4.1)¹³⁶ resulting in both quantitative conversion of the tertiary allylic alcohol and the highest selectivity towards the *Z*-configured product (*Z/E*>99:1). Therefore, diphosphines comprising of a semi-flexible alkyl spacer (propyl/butyl, **L13** and **L14**) between the two P-donors provide optimal steric/electronic control towards the formation of the *Z*-configured amino acid with the amine reagent proposed to attack either the palladacyclic intermediate or the *anti* Pd(π -allyl) intermediate.

(136) a) P. Dierkes, P. W. N. M. van Leeuwen, *J. Chem. Soc., Dalton Trans.* **1999**, 1519; b) P. W. N. M. van Leeuwen, P. C. J. Kamer, J. N. H. Reek, P. Dierkes, *Chem. Rev.* **2000**, *100*, 2741.

4.3 Conclusions

The efficient and stereoselective synthesis of (functional) olefins is an important goal in organic synthesis. Particularly, stereodivergent catalytic protocols that allow the construction of both *Z*- and *E*-isomers from the same substrates, is an attractive yet challenging strategy in the synthesis of olefin products. In this context, allylic substitution reactions provide a versatile platform for the construction of new olefin compounds.

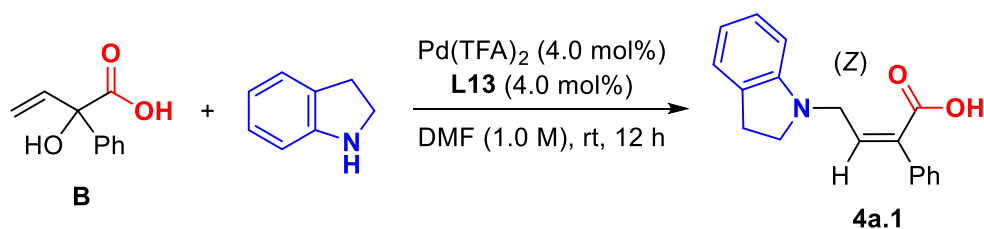
In this chapter, a new stereodivergent protocol is described for the Pd-mediated formation of either *Z*- or *E*-configured α,β -unsaturated γ -amino acids from easily accessed tertiary allylic alcohols and secondary amines. Key to the observed stereocontrol is the presence of a suitable diphosphine ligand that triggers, most likely through steric control, the attack of the amine onto either a *syn* or *anti* Pd(allyl) intermediate. The scope of this protocol demonstrates a reasonable generality, with the *Z*-isomers being isolated in good to excellent yield under excellent stereocontrol, and the corresponding *E*-isomers being produced with *E/Z* ratios of up to 6:1 and in good yields. This work provides a useful step forward in stereodivergent allylic amination chemistry.

4.4 Experimental Section

4.4.1 General Considerations

The vinyl aryl glycolic acids were prepared following a previously reported procedure.¹³⁷ Commercially available amines and solvents were purchased from Aldrich or TCI, and used without further purification. The palladium precursors and ligands were purchased from Aldrich or TCI. The ligand bis(2-diphenylphosphino(3-methoxy)phenyl)ether (**L2**) was prepared according to a reported procedure.¹³⁸ ¹H NMR, ¹³C NMR and ¹⁹F NMR spectra were recorded at room temperature on a Bruker AV-400 or AV-500 spectrometer and referenced to the residual deuterated solvent signals. All reported NMR values are given in parts per million (ppm). FT-IR measurements were carried out on a Bruker Optics FTIR Alpha spectrometer. Mass spectrometric analyses and X-ray diffraction studies were performed by the Research Support Group at ICIQ and the Universidad de Santiago de Compostela (Spain). In the screening phase, the internal standard CH₂Br₂ (1.0 equiv.) was added to the crude product, and then an aliquot of the mixture was taken for NMR analysis.

4.4.2 Typical Procedure for the Z-Selective Allylic Aminations



Representative case:

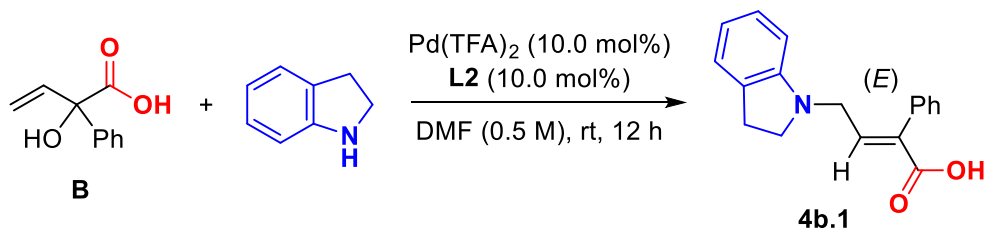
In a screw-capped vial, vinyl glycolic acid **B** (0.0267 g, 0.15 mmol, 1.0 equiv.) was combined with Pd(TFA)₂ (0.0020 g, 4.0 mol%), dppp (0.0025 g, 4.0 mol%) and indoline (0.165 mmol, 1.1 equiv.) in DMF (0.15 mL). The reaction mixture was stirred at room temperature for 12 h, after which 15 mL DCM was added, and the organic phase washed with water (2 × 30 mL), dried (MgSO₄), filtered and the solvent removed *in vacuo*. The pure product (**4a.1**) was isolated by flash chromatography (37.7 mg, 90%, Hexane/EtOAc

(137) J. Xie, S. Xue, E. C. Escudero-Adán, A. W. Kleij, *Angew. Chem. Int. Ed.* **2018**, *57*, 16727.

(138) C. F. Czauderna, A. G. Jarvis, F. J. L. Heutz, D. B. Cordes, A. M. Z. Slawin, J. I. van der Vlugt, P. C. J. Kamer, *Organometallics* **2015**, *34*, 1608.

= 3:1, $R_f = 0.1$). All purified *Z*-configured products were fully characterized by NMR (^1H , $^{13}\text{C}\{^1\text{H}\}$, $^{19}\text{F}\{^1\text{H}\}$), IR and HRMS.

4.4.3 Typical Procedure for the *E*-Selective Allylic Aminations



Representative case:

$\text{Pd}(\text{TFA})_2$ (0.0050 g, 10.0 mol%) and the methoxy-substituted DPEPhos **L2** (0.0090 g, 10.0 mol%) were added to a screw-capped vial equipped with a magnetic stirring bar. The vial was then charged with DMF (0.30 mL) and stirred at rt for 1 h. Vinyl glycolic acid **B** (0.0267 g, 0.15 mmol, 1.0 equiv.) and indoline (0.165 mmol, 1.1 equiv.) were added, and then the reaction mixture was stirred at rt for 12 h. Hereafter, 15 mL DCM was added and the organic phase washed with water (2×30 mL), dried (MgSO_4), filtered and the solvent removed *in vacuo*. The pure product (**4b.1**) was isolated by flash chromatography (25.5 mg, 61%, Hexane/EtOAc = 3:1, $R_f = 0.18$). All purified *E*-configured products were fully characterized by NMR (^1H , $^{13}\text{C}\{^1\text{H}\}$, $^{19}\text{F}\{^1\text{H}\}$), IR and HRMS.

4.4.4 X-ray Crystallographic Studies

The experimental procedure for the X-ray analyses of compounds **4a.1** and **4b.1** was the same as detailed in chapter 2. The structures themselves are provided on page 121.

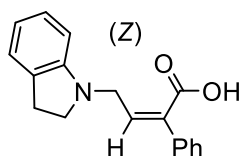
Crystal data for 4a.1:

$\text{C}_{18}\text{H}_{17}\text{NO}_2$, $M_r = 279.32$, monoclinic, $P2_1/n$, $a = 5.6162(3)$ Å, $b = 27.9447(13)$ Å, $c = 9.4836(4)$ Å, $\alpha = 90^\circ$, $\beta = 91.4146(14)^\circ$, $\gamma = 90^\circ$, $V = 1487.93(3)$ Å³, $Z = 4$, $\rho = 1.247$ mg·M⁻³, $\mu = 0.08$ ethyl acetate m⁻¹, $\lambda = 0.71073$ Å, $T = 100(2)$ K, $F(000) = 592$, crystal size = $0.20 \times 0.10 \times 0.01$ mm³, $\theta(\text{min}) = 2.268^\circ$, $\theta(\text{max}) = 31.693^\circ$, 12702 reflections collected, 4604 reflections unique ($R_{\text{int}} = 0.0285$), GoF = 1.025, $R_1 = 0.0474$ and $wR_2 = 0.1167$ [$I > 2\sigma(I)$], $R_1 = 0.0628$ and $wR_2 = 0.1261$ (all indices), min/max residual density = $-0.235/0.472$ [$\text{e} \cdot \text{Å}^{-3}$]. Completeness to $\theta(31.693^\circ) = 91.4\%$. For further details see CCDC number 1895598.

Crystal data for 4b.1:

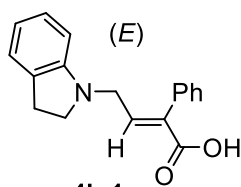
$C_{9.5}H_{9.5}N_{0.5}OCl$, $M_r = 182.13$, triclinic, $P-1$, $a = 7.4617(13) \text{ \AA}$, $b = 11.272(2) \text{ \AA}$, $c = 11.3361(18) \text{ \AA}$, $\alpha = 72.069(5)^\circ$, $\beta = 77.994(5)^\circ$, $\gamma = 78.711(5)^\circ$, $V = 878.4(3) \text{ \AA}^3$, $Z = 4$, $\rho = 1.377 \text{ mg} \cdot \text{M}^{-3}$, $\mu = 0.380 \text{ mm}^{-1}$, $\lambda = 0.71073 \text{ \AA}$, $T = 100(2) \text{ K}$, $F(000) = 380$, crystal size = $0.10 \times 0.05 \times 0.03 \text{ mm}^3$, $\theta(\text{min}) = 1.912^\circ$, $\theta(\text{max}) = 32.411^\circ$, 8818 reflections collected, 5094 reflections unique ($R_{\text{int}} = 0.0353$), $\text{GoF} = 1.066$, $R_1 = 0.0616$ and $wR_2 = 0.1641 [I > 2\sigma(I)]$, $R_1 = 0.0964$ and $wR_2 = 0.1829$ (all indices), min/max residual density = $-0.449/0.427 [e \cdot \text{\AA}^{-3}]$. Completeness to $\theta(32.411^\circ) = 80.8\%$. For further details see CCDC number 1895597.

4.4.5 Analytical Data for All Compounds



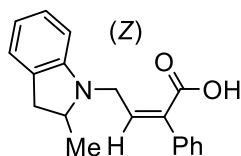
4a.1

Scale: 0.15 mmol; isolated 37.7 mg (90% yield), light yellow solid, Hexane : EA = 3 : 1, R_f = 0.1; $Z/E > 99:1$. $^1\text{H NMR}$ (400 MHz, CDCl_3) δ 7.40 – 7.30 (m, 5H), 7.14 – 7.06 (m, 2H), 6.73 (td, J = 7.5, 0.8 Hz, 1H), 6.59 (d, J = 7.8 Hz, 1H), 6.50 (t, J = 6.0 Hz, 1H), 4.26 (d, J = 6.0 Hz, 2H), 3.46 (t, J = 8.2 Hz, 2H), 3.00 (t, J = 8.2 Hz, 2H) ppm. $^{13}\text{C NMR}$ (101 MHz, CDCl_3) δ 171.99, 151.39, 141.98, 137.40, 136.00, 130.66, 128.42, 128.26, 128.17, 127.56, 124.81, 118.93, 108.14, 53.86, 49.18, 28.77 ppm. **IR** (neat): ν (cm^{-1}) 2923, 2846, 1702, 1605, 1486, 1459, 1205, 745, 695. **HRMS** (ESI $^-$, MeOH): m/z calcd. 278.1187 ($\text{M} - \text{H}$) $^-$, found: 278.1185.



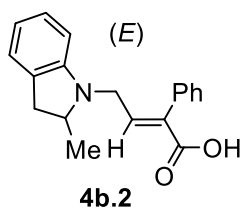
4b.1

Scale: 0.15 mmol; isolated 25.5 mg (61% yield isolated *E* product, 80% of total mixture), light yellow solid, Hexane : EA = 3 : 1, R_f = 0.18; $E/Z > 99:1$ (crude $^1\text{H NMR}$: E/Z = 86:14). $^1\text{H NMR}$ (400 MHz, CDCl_3) δ 7.43 – 7.33 (m, 3H), 7.29 (d, J = 6.6 Hz, 1H), 7.25 – 7.19 (m, 2H), 7.10 – 6.99 (m, 2H), 6.73 – 6.62 (m, 1H), 6.36 (d, J = 7.8 Hz, 1H), 3.78 (d, J = 6.7 Hz, 2H), 3.31 (t, J = 8.2 Hz, 2H), 2.94 (t, J = 8.2 Hz, 2H) ppm. $^{13}\text{C NMR}$ (101 MHz, CDCl_3) δ 171.29, 151.48, 142.91, 135.45, 134.08, 130.30, 129.68, 128.39, 128.30, 127.46, 124.73, 118.56, 107.60, 53.61, 48.10, 28.72 ppm. **IR** (neat): ν (cm^{-1}) 2843, 1685, 1605, 1486, 1241, 743, 700. **HRMS** (ESI $^-$, MeOH): m/z calcd. 278.1187 ($\text{M} - \text{H}$) $^-$, found: 278.1188.

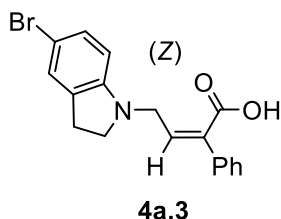


4a.2

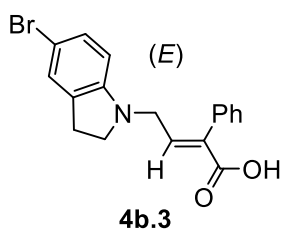
Scale: 0.15 mmol; isolated 39.1 mg (89% yield), light yellow solid, Hexane : EA = 3 : 1, R_f = 0.1; $Z/E > 99:1$. $^1\text{H NMR}$ (400 MHz, CDCl_3) δ 7.38–7.32 (m, 5H), 7.13 – 7.03 (m, 2H), 6.71 (td, J = 7.4, 1.0 Hz, 1H), 6.55 – 6.46 (m, 2H), 4.36 (dd, J = 5.7, 2.3 Hz, 2H), 3.84 – 3.71 (m, 1H), 3.17 (dd, J = 15.5, 8.4 Hz, 1H), 2.68 (dd, J = 15.4, 9.9 Hz, 1H), 1.38 (d, J = 6.1 Hz, 3H) ppm. $^{13}\text{C NMR}$ (101 MHz, CDCl_3) δ 172.75, 151.71, 145.17, 137.49, 134.99, 129.34, 128.35, 128.30, 128.14, 127.58, 124.48, 118.30, 107.31, 60.54, 46.41, 37.47, 19.48 ppm. **IR** (neat): ν (cm^{-1}) 3027, 2963, 1687, 1605, 1482, 1350, 1230, 907, 730, 696. **HRMS** (ESI $^-$, MeOH): m/z calcd. 292.1343 ($\text{M} - \text{H}$) $^-$, found: 292.1339.



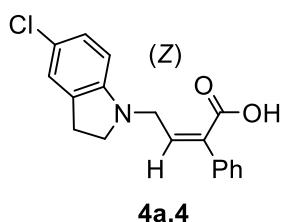
Scale: 0.15 mmol; isolated 33.0 mg (75% yield isolated *E* product, 88% of total mixture), light yellow solid, Hexane : EA = 3 : 1, R_f = 0.16; *E/Z* > 99:1 (crude $^1\text{H NMR}$: *E/Z* = 83:17). $^1\text{H NMR}$ (500 MHz, CDCl_3) δ 7.44 – 7.35 (m, 3H), 7.26 – 7.18 (m, 3H), 7.02 (dt, J = 7.2, 4.1 Hz, 2H), 6.66 (t, J = 7.3 Hz, 1H), 6.29 (d, J = 8.1 Hz, 1H), 3.89 – 3.72 (m, 2H), 3.67 – 3.57 (m, 1H), 3.09 (dd, J = 15.4, 8.4 Hz, 1H), 2.58 (dd, J = 15.3, 9.9 Hz, 1H), 1.16 (d, J = 6.1 Hz, 3H) ppm. $^{13}\text{C NMR}$ (126 MHz, CDCl_3) δ 171.65, 151.48, 143.76, 135.09, 134.10, 129.70, 129.11, 128.38, 128.31, 127.52, 124.43, 118.27, 107.14, 60.19, 45.15, 37.39, 19.28 ppm. **IR** (neat): ν (cm^{-1}) 3049, 2926, 2862, 1694, 1477, 1440, 1224, 1185, 1047, 784, 750, 699, 574. **HRMS** (ESI $^-$, MeOH): m/z calcd. 292.1343 ($\text{M} - \text{H}$) $^-$, found: 292.1344.



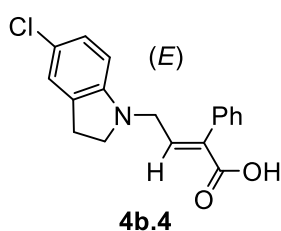
Scale: 0.15 mmol; isolated 43.5 mg (81% yield), light yellow solid, Hexane : EA = 3 : 1, R_f = 0.1; *Z/E* > 99:1. $^1\text{H NMR}$ (500 MHz, CDCl_3) δ 7.38 – 7.31 (m, 5H), 7.17 (dd, J = 10.9, 2.7 Hz, 2H), 6.44 (t, J = 5.9 Hz, 1H), 6.40 (d, J = 8.2 Hz, 1H), 4.25 (d, J = 5.9 Hz, 2H), 3.46 (t, J = 8.3 Hz, 2H), 2.98 (t, J = 8.3 Hz, 2H) ppm. $^{13}\text{C NMR}$ (126 MHz, CDCl_3) δ 172.56, 150.77, 142.16, 137.18, 135.78, 132.84, 130.12, 128.46, 128.35, 128.13, 127.74, 110.10, 108.83, 53.79, 48.82, 28.50 ppm. **IR** (neat): ν (cm^{-1}) 3027, 2923, 2844, 1687, 1597, 1485, 1467, 1233, 752, 696. **HRMS** (ESI $^-$, MeOH): m/z calcd. 356.0292 ($\text{M} - \text{H}$) $^-$, found: 356.0278.



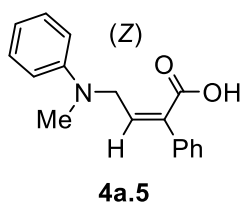
Scale: 0.15 mmol; isolated 47.8 mg (89% of total isolated mixture), light yellow solid, Hexane : EA = 3 : 1, R_f = 0.1-0.12; *E/Z* = 81:19 (crude $^1\text{H NMR}$: *E/Z* = 66:34). $^1\text{H NMR}$ (400 MHz, CDCl_3) δ 7.44 – 7.36 (m, 3H), 7.35 – 7.31 (m, 1H), 7.23 (t, J = 6.7 Hz, 3H), 7.18 – 7.08 (m, 2H), 6.18 (d, J = 8.3 Hz, 1H), 3.75 (d, J = 6.6 Hz, 2H), 3.33 (t, J = 8.3 Hz, 2H), 2.92 (t, J = 8.2 Hz, 2H) ppm. $^{13}\text{C NMR}$ (101 MHz, CDCl_3) δ 171.73, 150.64, 142.30, 135.77, 133.88, 132.57, 130.01, 129.63, 128.42, 128.05, 127.68, 109.98, 108.57, 53.53, 47.70, 28.45 ppm. **IR** (neat): ν (cm^{-1}) 2852, 1686, 1597, 1481, 1467, 1260, 907, 799, 700. **HRMS** (ESI $^-$, MeOH): m/z calcd. 356.0292 ($\text{M} - \text{H}$) $^-$, found: 356.0280.



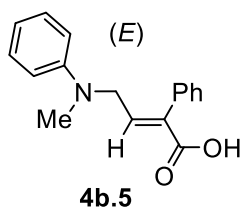
Scale: 0.15 mmol; isolated 38.7 mg (82% yield), light yellow solid, Hexane : EA = 3 : 1, R_f = 0.1; Z/E = 98:2. **$^1\text{H NMR}$** (400 MHz, CDCl_3) δ 7.39 – 7.30 (m, 5H), 7.02 (m, 2H), 6.47 – 6.40 (m, 2H), 4.22 (d, J = 5.9 Hz, 2H), 3.46 (t, J = 8.3 Hz, 2H), 2.96 (t, J = 8.2 Hz, 2H) ppm. **$^{13}\text{C NMR}$** (101 MHz, CDCl_3) δ 171.62, 150.33, 141.65, 137.24, 135.92, 132.39, 128.48, 128.36, 128.11, 127.22, 125.00, 123.19, 108.33, 53.92, 48.94, 28.58 ppm. **IR** (neat): ν (cm^{-1}) 3059, 2923, 2850, 1756, 1690, 1486, 1247, 1118, 866, 797, 693, 648. **HRMS** (ESI⁻, MeOH): m/z calcd. 312.0797 ($\text{M} - \text{H}$)⁻, found: 312.0772.



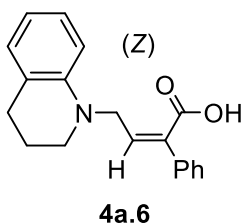
Scale: 0.15 mmol; isolated 32.1 mg (68% yield isolated *E* product, 87% of total mixture), light yellow solid, Hexane : EA = 3 : 1, R_f = 0.16; E/Z > 99:1 (crude $^1\text{H NMR}$: E/Z = 84:16). **$^1\text{H NMR}$** (400 MHz, CDCl_3) δ 7.43 – 7.33 (m, 3H), 7.23 – 7.19 (m, 3H), 7.01 – 6.94 (m, 2H), 6.21 (d, J = 8.3 Hz, 1H), 3.74 (d, J = 6.6 Hz, 2H), 3.32 (t, J = 8.3 Hz, 2H), 2.91 (t, J = 8.3 Hz, 2H) ppm. **$^{13}\text{C NMR}$** (126 MHz, CDCl_3) δ 171.44, 150.23, 142.32, 135.74, 133.94, 132.11, 130.33, 129.64, 128.61, 128.44, 128.40, 127.11, 124.94, 122.99, 107.99, 53.65, 47.86, 28.51 ppm. **IR** (neat): ν (cm^{-1}) 2923, 2848, 1686, 1602, 1487, 1261, 798, 702. **HRMS** (ESI⁻, MeOH): m/z calcd. 312.0797 ($\text{M} - \text{H}$)⁻, found: 312.0790.



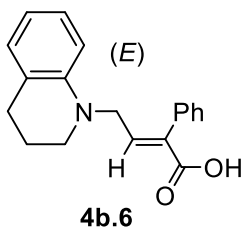
Scale: 0.15 mmol; isolated 31.6 mg (79% yield), yellow liquid, Hexane : EA = 3 : 1, R_f = 0.1; Z/E > 99:1. **$^1\text{H NMR}$** (400 MHz, CDCl_3) δ 7.33 (m, 5H), 7.27 (m, 2H), 6.84 – 6.77 (m, 3H), 6.39 (t, J = 5.5 Hz, 1H), 4.47 (d, J = 5.6 Hz, 2H), 3.02 (s, 3H) ppm. **$^{13}\text{C NMR}$** (101 MHz, CDCl_3) δ 172.17, 148.97, 144.44, 137.53, 135.71, 129.50, 128.35, 128.31, 128.17, 117.98, 113.74, 53.09, 39.23 ppm. **IR** (neat): ν (cm^{-1}) 3058, 2890, 1701, 1597, 1495, 1344, 1202, 1118, 747, 690, 509. **HRMS** (ESI⁻, MeOH): m/z calcd. 266.1187 ($\text{M} - \text{H}$)⁻, found: 266.1185.



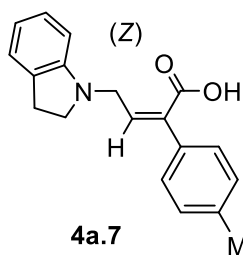
Scale: 0.15 mmol; isolated 21.2 mg (53% yield isolated *E* product, 78% of total mixture), yellow solid, Hexane : EA = 3 : 1, R_f = 0.15; E/Z = 99:1 (crude $^1\text{H NMR}$: E/Z = 77:23). $^1\text{H NMR}$ (400 MHz, CDCl_3) δ 7.44 – 7.34 (m, 3H), 7.25 – 7.09 (m, 5H), 6.74 (t, J = 7.2 Hz, 1H), 6.62 (d, J = 8.0 Hz, 2H), 3.97 (d, J = 6.4 Hz, 2H), 2.88 (s, 3H) ppm. $^{13}\text{C NMR}$ (101 MHz, CDCl_3) δ 171.55, 148.87, 143.51, 135.17, 134.01, 129.69, 129.36, 128.38, 128.35, 117.53, 113.23, 51.77, 38.68 ppm. **IR** (neat): ν (cm^{-1}) 3026, 1685, 1598, 1504, 1270, 748, 701. **HRMS** (ESI $^-$, MeOH): m/z calcd. 266.1187 ($\text{M} - \text{H}$) $^-$, found: 266.1187.



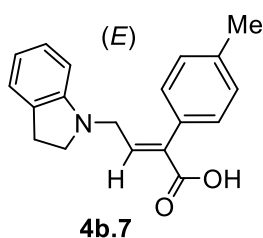
Scale: 0.15 mmol; isolated 30.4 mg (69% yield), yellow liquid, Hexane : EA = 3 : 1, R_f = 0.1; Z/E = 99:1. $^1\text{H NMR}$ (400 MHz, CDCl_3) δ 7.38 – 7.30 (m, 5H), 7.09 – 7.04 (m, 1H), 7.01 – 6.96 (m, 1H), 6.66 – 6.58 (m, 2H), 6.45 (t, J = 5.5 Hz, 1H), 4.45 (d, J = 5.5 Hz, 2H), 3.41 – 3.32 (m, 2H), 2.79 (t, J = 6.4 Hz, 2H), 2.04 – 1.97 (m, 2H) ppm. $^{13}\text{C NMR}$ (101 MHz, CDCl_3) δ 172.36, 146.49, 144.99, 137.55, 135.11, 129.45, 128.36, 128.33, 128.13, 127.31, 123.37, 116.83, 111.41, 51.70, 49.88, 28.02, 22.47 ppm. **IR** (neat): ν (cm^{-1}) 2931, 2850, 1679, 1595, 1497, 1417, 1337, 1235, 1169, 1064, 792, 746, 695. **HRMS** (ESI $^-$, MeOH): m/z calcd. 292.1343 ($\text{M} - \text{H}$) $^-$, found: 292.1339.



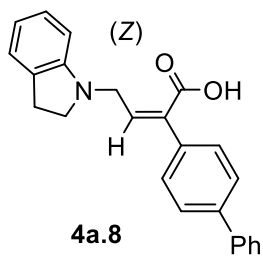
Scale: 0.15 mmol; isolated 27.7 mg (63% yield isolated *E* product, 82% of total mixture), yellow solid, Hexane : EA = 3 : 1, R_f = 0.15; E/Z = 96:4 (crude $^1\text{H NMR}$: E/Z = 83:17). $^1\text{H NMR}$ (400 MHz, CDCl_3) δ 7.45 – 7.36 (m, 3H), 7.27 – 7.23 (m, 2H), 7.21 (t, J = 6.3 Hz, 1H), 7.01 (td, J = 8.2, 1.6 Hz, 1H), 6.98 – 6.92 (m, 1H), 6.64 – 6.59 (m, 1H), 6.37 (d, J = 8.2 Hz, 1H), 3.93 (d, J = 6.4 Hz, 2H), 3.24 – 3.18 (m, 2H), 2.75 (t, J = 6.4 Hz, 2H), 1.98 – 1.90 (m, 2H) ppm. $^{13}\text{C NMR}$ (101 MHz, CDCl_3) δ 171.84, 144.72, 143.92, 135.21, 134.08, 129.69, 129.38, 128.35, 128.29, 127.18, 123.20, 116.83, 111.31, 50.35, 49.78, 49.61, 27.94, 22.35 ppm. **IR** (neat): ν (cm^{-1}) 2927, 1683, 1600, 1495, 1271, 1192, 907, 700. **HRMS** (ESI $^-$, MeOH): m/z calcd. 292.1343 ($\text{M} - \text{H}$) $^-$, found: 292.1343.



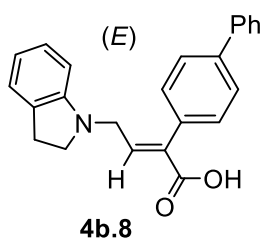
Scale: 0.15 mmol; isolated 35.6 mg (81% yield), yellow solid, Hexane : EA = 3 : 1, R_f = 0.1; $Z/E > 99:1$. **$^1\text{H NMR}$** (500 MHz, CDCl_3) δ 7.28 (d, J = 8.1 Hz, 2H), 7.19 – 7.08 (m, 4H), 6.78 – 6.68 (m, 1H), 6.59 (d, J = 7.8 Hz, 1H), 6.49 (t, J = 6.0 Hz, 1H), 4.27 (d, J = 6.0 Hz, 2H), 3.46 (t, J = 8.2 Hz, 2H), 3.01 (t, J = 8.2 Hz, 2H), 2.37 (s, 3H) ppm. **$^{13}\text{C NMR}$** (126 MHz, CDCl_3) δ 172.50, 151.56, 141.30, 138.15, 135.75, 134.52, 130.61, 129.12, 128.02, 127.54, 124.76, 118.74, 108.02, 53.83, 49.11, 28.77, 21.29 ppm. **IR** (neat): ν (cm^{-1}) 3027, 2921, 2853, 1747, 1699, 1605, 1485, 1459, 1236, 1116, 821, 731. **HRMS** (ESI $^-$, MeOH): m/z calcd. 292.1343 ($\text{M} - \text{H}$) $^-$, found: 292.1342.



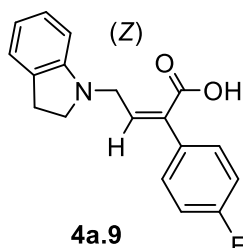
Scale: 0.15 mmol; isolated 26.8 mg (61% yield isolated *E* product, 75% of total mixture), yellow solid, Hexane : EA = 3 : 1, R_f = 0.18; $E/Z > 99:1$ (crude $^1\text{H NMR}$: E/Z = 86:14). **$^1\text{H NMR}$** (500 MHz, CDCl_3) δ 7.24 (t, J = 6.7 Hz, 1H), 7.22 – 7.18 (m, 2H), 7.14 – 7.09 (m, 2H), 7.08 – 7.00 (m, 2H), 6.67 (t, J = 7.3 Hz, 1H), 6.36 (d, J = 7.8 Hz, 1H), 3.78 (d, J = 6.6 Hz, 2H), 3.31 (t, J = 8.2 Hz, 2H), 2.94 (t, J = 8.2 Hz, 2H), 2.37 (s, 3H) ppm. **$^{13}\text{C NMR}$** (126 MHz, CDCl_3) δ 171.49, 151.71, 142.70, 138.11, 135.34, 131.15, 130.23, 129.60, 129.12, 127.43, 124.69, 118.36, 107.46, 53.61, 48.07, 28.74, 21.40 ppm. **IR** (neat): ν (cm^{-1}) 2959, 2918, 2855, 1691, 1603, 1480, 1246, 1221, 1178, 907, 734, 565. **HRMS** (ESI $^-$, MeOH): m/z calcd. 292.1343 ($\text{M} - \text{H}$) $^-$, found: 292.1350.



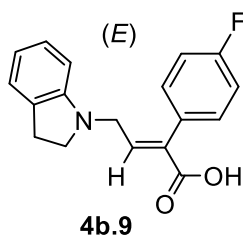
Scale: 0.15 mmol; isolated 39.9 mg (75% yield), yellow solid, Hexane : EA = 3 : 1, R_f = 0.1; $Z/E > 99:1$. **$^1\text{H NMR}$** (400 MHz, CDCl_3) δ 7.62 – 7.56 (m, 4H), 7.49 – 7.42 (m, 4H), 7.39 – 7.34 (m, 1H), 7.16 – 7.07 (m, 2H), 6.75 (td, J = 7.4, 1.0 Hz, 1H), 6.63 – 6.56 (m, 2H), 4.29 (d, J = 5.9 Hz, 2H), 3.48 (t, J = 8.2 Hz, 2H), 3.02 (t, J = 8.2 Hz, 2H) ppm. **$^{13}\text{C NMR}$** (101 MHz, CDCl_3) δ 172.14, 151.49, 141.99, 141.18, 140.66, 136.31, 135.59, 130.64, 128.94, 128.58, 127.62, 127.58, 127.23, 127.18, 124.82, 118.89, 108.09, 53.91, 49.22, 28.80 ppm. **IR** (neat): ν (cm^{-1}) 2921, 2853, 1709, 1605, 1485, 1231, 837, 749, 694. **HRMS** (ESI $^-$, MeOH): m/z calcd. 354.1500 ($\text{M} - \text{H}$) $^-$, found: 354.1494.



Scale: 0.15 mmol; isolated 29.8 mg (56% yield isolated *E* product, 72% of total mixture), light yellow solid, Hexane : EA = 3 : 1, R_f = 0.18; $E/Z > 99:1$ (crude $^1\text{H NMR}$: $E/Z = 82:18$). $^1\text{H NMR}$ (400 MHz, CDCl_3) δ 7.65 – 7.58 (m, 4H), 7.48 – 7.42 (m, 2H), 7.39 – 7.29 (m, 4H), 7.08–7.02 (m, 2H), 6.68 (t, $J = 7.3$ Hz, 1H), 6.39 (d, $J = 7.8$ Hz, 1H), 3.85 (d, $J = 6.6$ Hz, 2H), 3.34 (t, $J = 8.2$ Hz, 2H), 2.95 (t, $J = 8.2$ Hz, 2H) ppm. $^{13}\text{C NMR}$ (101 MHz, CDCl_3) δ 171.23, 143.23, 141.22, 140.73, 135.02, 132.97, 130.29, 130.18, 128.96, 127.65, 127.47, 127.31, 127.14, 124.75, 118.54, 107.57, 53.66, 48.18, 28.74 ppm. **IR** (neat): ν (cm^{-1}) 3027, 2919, 2847, 1681, 1602, 1481, 1423, 1287, 1230, 1097, 731, 693. **HRMS** (ESI $^-$, MeOH): m/z calcd. 354.1500 ($\text{M} - \text{H}$) $^-$, found: 354.1492.

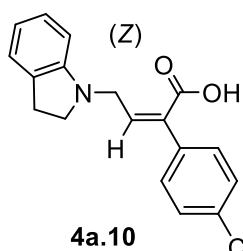


Scale: 0.15 mmol; isolated 32.5 mg (73% yield), yellow liquid, Hexane : EA = 3 : 1, R_f = 0.1; $Z/E = 98:2$. $^1\text{H NMR}$ (400 MHz, CDCl_3) δ 7.33 (m, 2H), 7.14 – 7.06 (m, 2H), 7.05 – 7.00 (m, 2H), 6.74 (td, $J = 7.5, 0.8$ Hz, 1H), 6.57 (d, $J = 7.8$ Hz, 1H), 6.48 (t, $J = 5.9$ Hz, 1H), 4.25 (d, $J = 5.9$ Hz, 2H), 3.44 (t, $J = 8.2$ Hz, 2H), 3.00 (t, $J = 8.2$ Hz, 2H) ppm. $^{13}\text{C NMR}$ (126 MHz, CDCl_3) δ 171.64, 162.80 (d, $J = 247.9$ Hz), 151.40, 142.47, 134.95, 133.55 (d, $J = 3.5$ Hz), 130.02 (d, $J = 8.3$ Hz), 127.58, 124.85, 118.99, 115.35 (d, $J = 21.7$ Hz), 108.06, 53.91, 49.19, 28.79 ppm. $^{19}\text{F NMR}$ (376 MHz, CDCl_3) δ -113.90 ppm. **IR** (neat): ν (cm^{-1}) 3049, 2847, 1697, 1600, 1508, 1485, 1345, 1222, 1159, 832, 731, 554, 506. **HRMS** (ESI $^-$, MeOH): m/z calcd. 296.1092 ($\text{M} - \text{H}$) $^-$, found: 296.1087.

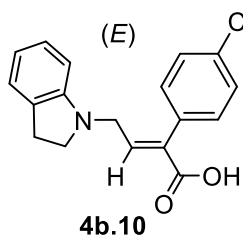


Scale: 0.15 mmol; isolated 26.3 mg (59% yield isolated *E* product, 84% of total mixture), light yellow solid, Hexane : EA = 3 : 1, R_f = 0.15; $E/Z > 99:1$ (crude $^1\text{H NMR}$: $E/Z = 84:16$). $^1\text{H NMR}$ (400 MHz, CDCl_3) δ 7.30 – 7.27 (m, 1H), 7.21 (m, 2H), 7.13 – 7.06 (m, 3H), 7.06 – 7.01 (m, 1H), 6.73 – 6.65 (m, 1H), 6.34 (d, $J = 7.8$ Hz, 1H), 3.77 (d, $J = 6.6$ Hz, 2H), 3.31 (t, $J = 8.2$ Hz, 2H), 2.95 (t, $J = 8.2$ Hz, 2H) ppm. $^{13}\text{C NMR}$ (101 MHz, CDCl_3) δ 170.77, 162.67 (d, $J = 248.0$ Hz), 151.45, 143.43, 134.34, 131.52 (d, $J = 8.1$ Hz), 130.25, 129.93 (d, $J = 3.5$ Hz), 127.47, 124.79, 118.61, 115.49 (d, $J = 21.5$ Hz), 107.47, 53.65, 48.08, 28.73 ppm. $^{19}\text{F NMR}$ (376 MHz, CDCl_3) δ -113.47 ppm. **IR** (neat): ν (cm^{-1}) 3053, 2915, 2853, 1690, 1602, 1510, 1482, 1249, 1221, 1162, 907,

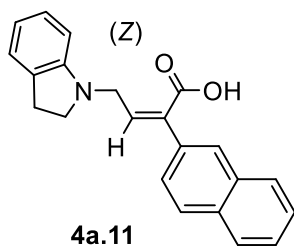
840, 734, 690, 565. **HRMS** (ESI⁻, MeOH): m/z calcd. 296.1092 (M - H)⁻, found: 296.1094.



Scale: 0.15 mmol; isolated 35.0 mg (74% yield), yellow solid, Hexane : EA = 3 : 1, R_f = 0.1; $Z/E > 99:1$. **¹H NMR** (400 MHz, CDCl₃) δ 7.33 – 7.27 (m, 4H), 7.14 – 7.07 (m, 2H), 6.74 (td, J = 7.3, 0.7 Hz, 1H), 6.57 (d, J = 7.8 Hz, 1H), 6.51 (t, J = 5.9 Hz, 1H), 4.26 (d, J = 5.9 Hz, 2H), 3.45 (t, J = 8.2 Hz, 2H), 3.00 (t, J = 8.2 Hz, 2H) ppm. **¹³C NMR** (126 MHz, CDCl₃) δ 171.82, 151.36, 143.20, 135.87, 134.77, 134.32, 130.61, 129.58, 128.60, 127.58, 124.86, 119.01, 108.04, 53.92, 49.27, 28.78 ppm. **IR** (neat): ν (cm⁻¹) 3030, 2845, 1693, 1605, 1485, 1345, 1218, 1093, 1012, 823, 752, 718, 491. **HRMS** (ESI⁻, MeOH): m/z calcd. 312.0797 (M - H)⁻, found: 312.0791.

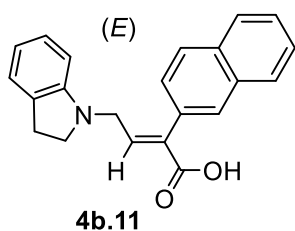


Scale: 0.15 mmol; isolated 20.8 mg (44% yield isolated *E* product, 63% of total mixture), light yellow solid, Hexane : EA = 3 : 1, R_f = 0.18; $E/Z > 99:1$ (crude ¹H NMR: E/Z = 83:17). **¹H NMR** (400 MHz, CDCl₃) δ 7.40 – 7.36 (m, 2H), 7.29 (t, J = 6.6 Hz, 1H), 7.20 – 7.15 (m, 2H), 7.09 – 6.99 (m, 2H), 6.68 (td, J = 7.5, 0.8 Hz, 1H), 6.34 (d, J = 7.8 Hz, 1H), 3.76 (d, J = 6.6 Hz, 2H), 3.30 (t, J = 8.2 Hz, 2H), 2.94 (t, J = 8.2 Hz, 2H) ppm. **¹³C NMR** (101 MHz, CDCl₃) δ 170.71, 151.48, 143.71, 134.45, 134.23, 132.47, 131.12, 130.22, 128.69, 127.47, 124.79, 118.58, 107.41, 53.66, 48.04, 28.73 ppm. **IR** (neat): ν (cm⁻¹) 2919, 1687, 1605, 1486, 1245, 1090, 1015, 744, 719. **HRMS** (ESI⁻, MeOH): m/z calcd. 312.0797 (M - H)⁻, found: 312.0781.

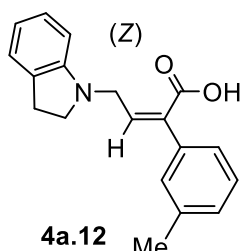


Scale: 0.15 mmol; isolated 41.5 mg (84% yield), yellow solid, Hexane : EA = 3 : 1, R_f = 0.1; Z/E = 96:4. **¹H NMR** (400 MHz, CDCl₃) δ 7.85 – 7.79 (m, 4H), 7.53 – 7.46 (m, 3H), 7.15 – 7.08 (m, 2H), 6.74 (td, J = 7.5, 0.8 Hz, 1H), 6.66 – 6.60 (m, 2H), 4.31 (d, J = 5.9 Hz, 2H), 3.49 (t, J = 8.2 Hz, 2H), 3.02 (t, J = 8.2 Hz, 2H) ppm. **¹³C NMR** (101 MHz, CDCl₃) δ 172.25, 151.53, 142.18, 135.98, 134.79, 133.27, 133.05, 130.63, 128.32, 127.98, 127.73, 127.58, 127.23, 126.49, 126.48, 125.96, 124.81, 118.87, 108.07, 53.93, 49.29, 28.79 ppm. **IR** (neat): ν (cm⁻¹) 3053, 2922, 2848, 1695,

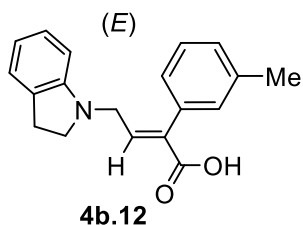
1605, 1486, 1212, 1182, 817, 745, 478. **HRMS** (ESI⁻, MeOH): m/z calcd. 328.1343 (M - H)⁻, found: 328.1343.



Scale: 0.15 mmol; isolated 32.1 mg (65% yield isolated *E* product, 80% of total mixture), light yellow solid, Hexane : EA = 3 : 1, R_f = 0.17; *E/Z* = 96:4 (crude ¹H NMR: *E/Z* = 86:14). **¹H NMR** (400 MHz, CDCl₃) δ 7.90 – 7.82 (m, 3H), 7.69 (s, 1H), 7.53 – 7.48 (m, 2H), 7.40 – 7.31 (m, 2H), 7.09 – 6.95 (m, 2H), 6.67 (t, J = 7.3 Hz, 1H), 6.37 (d, J = 7.8 Hz, 1H), 3.84 (d, J = 6.6 Hz, 2H), 3.33 (t, J = 8.2 Hz, 2H), 2.94 (t, J = 8.2 Hz, 2H) ppm. **¹³C NMR** (101 MHz, CDCl₃) δ 171.09, 151.55, 143.38, 135.31, 133.09, 133.03, 131.60, 130.22, 129.00, 128.21, 128.07, 127.88, 127.44, 127.35, 126.63, 126.50, 124.71, 118.42, 107.47, 53.62, 48.09, 28.72 ppm. **IR** (neat): ν (cm⁻¹) 3050, 2924, 1694, 1596, 1484, 1220, 1166, 818, 738, 476. **HRMS** (ESI⁻, MeOH): m/z calcd. 328.1343 (M - H)⁻, found: 328.1337.



Scale: 0.15 mmol; isolated 43.1 mg (98% yield), yellow liquid, Hexane : EA = 3 : 1, R_f = 0.1; *Z/E* > 99:1. **¹H NMR** (400 MHz, CDCl₃) δ 7.28 – 7.21 (m, 1H), 7.20 – 7.07 (m, 5H), 6.73 (t, J = 7.3 Hz, 1H), 6.59 (d, J = 7.8 Hz, 1H), 6.48 (t, J = 6.0 Hz, 1H), 4.26 (d, J = 6.0 Hz, 2H), 3.46 (t, J = 8.2 Hz, 2H), 3.00 (t, J = 8.2 Hz, 2H), 2.37 (s, 3H) ppm. **¹³C NMR** (101 MHz, CDCl₃) δ 172.44, 151.57, 141.68, 138.07, 137.32, 136.01, 130.59, 129.02, 128.79, 128.32, 127.54, 125.24, 124.76, 118.72, 107.97, 53.83, 49.08, 28.77, 21.54 ppm. **IR** (neat): ν (cm⁻¹) 2921, 2847, 1691, 1604, 1485, 1232, 1174, 907, 732. **HRMS** (ESI⁻, MeOH): m/z calcd. 292.1343 (M - H)⁻, found: 292.1339.



Scale: 0.15 mmol; isolated 26.4 mg (60% yield isolated *E* product, 82% of total mixture), yellow solid, Hexane : EA = 3 : 1, R_f = 0.18; *E/Z* = 98:2 (crude ¹H NMR: *E/Z* = 82:18). **¹H NMR** (400 MHz, CDCl₃) δ 7.32 – 7.24 (m, 2H), 7.17 (d, J = 7.6 Hz, 1H), 7.10 – 7.01 (m, 4H), 6.68 (td, J = 7.5, 0.9 Hz, 1H), 6.38 (d, J = 7.8 Hz, 1H), 3.79 (d, J = 6.6 Hz, 2H), 3.32 (t, J = 8.2 Hz, 2H), 2.95 (t, J = 8.2 Hz, 2H), 2.38 (s, 3H) ppm. **¹³C NMR** (101 MHz, CDCl₃) δ 171.87, 151.63, 142.85, 138.00, 135.56, 134.01, 130.27, 130.25, 129.05, 128.26, 127.41, 126.70, 124.69, 118.40, 107.51,

53.60, 48.05, 28.72, 21.58 ppm. **IR** (neat): ν (cm^{-1}) 3025, 2920, 2849, 1755, 1687, 1605, 1485, 1459, 1259, 1115, 743, 709. **HRMS** (ESI⁻, MeOH): m/z calcd. 292.1343 (M - H)⁻, found: 292.1343.

Chapter 5.

Pd-Catalyzed Stereoselective Tandem Ring-opening Amination/cyclization of Vinyl γ -Lactones: Access to Caprolactam Diversity

This chapter has been published in:

J. Xie, X. Li, A. W. Kleij, *Chem. Sci.* **2020**, *11*, 8839-8845.

5.1 Introduction

5.1.1 Caprolactam

Caprolactams represent a class of important seven-membered nitrogen heterocycles and are key structural motifs in numerous natural products and biologically active compounds¹³⁹ such as Benzepiril, Cephalofortunone and Bengamides (Figure 5.1). Additionally, caprolactams often serve as versatile synthetic intermediates for bicyclic amino compounds and azepane ring systems.¹⁴⁰ The simplest non-substituted caprolactam, also known as azepan-2-one, was first described in the late 1800s and prepared by the cyclization of ϵ -aminocaproic acid. Furthermore, poly(caprolactam) has been proved to be a high-performance, semi-crystalline thermoplastic with large potential for industrial, biological and medical applications.¹⁴¹ Currently, caprolactam is manufactured on a massive scale around 4.6 billion tons annually.¹⁴²

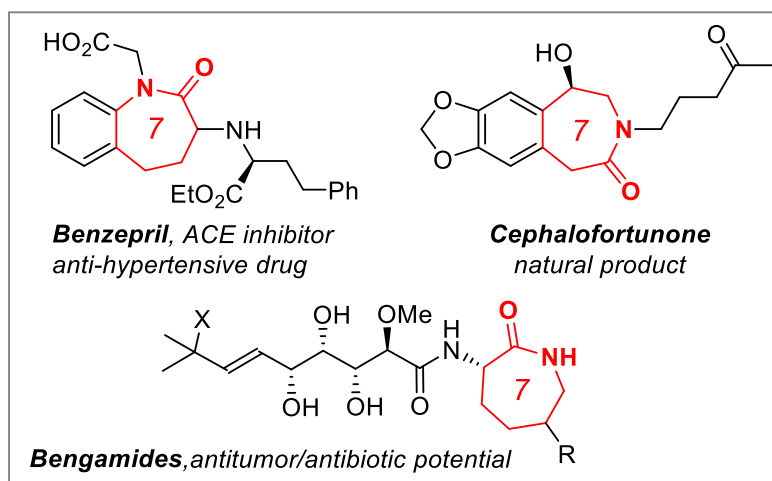
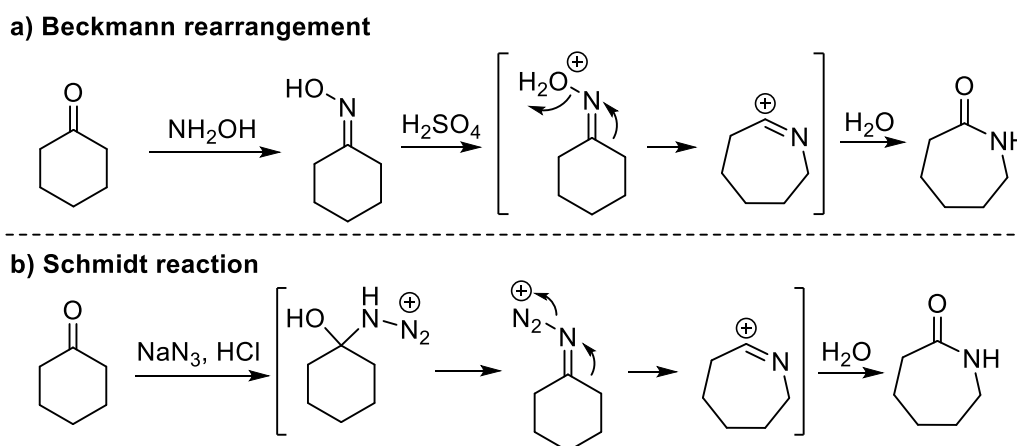


Figure 5.1 Selected examples of bioactive compounds with a caprolactam core.

- (139) For examples: a) H. Hotoda, M. Furukawa, M. Daigo, K. Murayama, M. Kaneko, Y. Muramatsu, M. M. Ishii, S.-I. Miyakoshi, T. Takatsu, M. Inukai, M. Kakuta, T. Abe, T. Harasaki, T. Fukuoka, Y. Utsui, S. Ohya, *Bioorg. Med. Chem. Lett.* **2003**, *13*, 2829; b) X. Liu, Y. Jin, W. Cai, K. D. Green, A. Goswami, S. Garneau-Tsodikova, K. Nonaka, S. Baba, M. Funabashi, Z. Yang, S. G. van Lanen, *Org. Biomol. Chem.* **2016**, *14*, 3956. Caprolactam can be used to prepare meptazinol: c) B. Holmes, A. Ward, *Drugs* **1985**, *30*, 285; d) L. Edvinsson, M. Linde, *Lancet* **2010**, *376*, 645; e) G. Liu, Y.-M. Ma, W.-Y. Tai, C.-M. Xie, Y.-L. Li, J. Li, F.-J. Nan, *ChemMedChem* **2008**, *3*, 74.
- (140) a) *Amide Linkage: Selected Structural Aspects in Chemistry, Biochemistry, and Materials Science*, Eds. A. Greenberg, C. M. Breneman, J. F. Liebman, Wiley, New York **2000**; b) S. J. Lee, P. Beak, *J. Am. Chem. Soc.* **2006**, *128*, 2178; c) J. T. Bagdanoff, D. C. Behenna, J. L. Stockdill, B. M. Stoltz, *Eur. J. Org. Chem.* **2016**, 2101.
- (141) a) W. H. Carothers, G. J. Berchet, *J. Am. Chem. Soc.* **1930**, *52*, 5289; b) K. Marchildon, *Macromol. React. Eng.* **2011**, *5*, 22; c) M. Winnacker, *Biomater. Sci.* **2017**, *5*, 1230.
- (142) Caprolactam (CPL): 2017 World Market Outlook and Forecast up to 2021, Market publisher, report database (**2017**).

An estimated 90% of all caprolactam is synthesized from cyclohexanone, which is first converted to its oxime. Treatment of this oxime with strong acid induces a Beckmann rearrangement to provide non-*N*-alkylated caprolactam, which was discovered by Prussian chemist and Nobel Prize winner Otto Wallach back in 1900 (Scheme 5.1 a). However, the typically used harsh reaction conditions for performing a Beckmann rearrangement being incompatible with the presence of various functional groups. The large amounts of co-generated ammonium sulfate in the industrial process for caprolactam prompted chemists to pay more attention toward minimizing the amount of waste salt and improving the overall sustainability. Thus, numerous contributions have been devoted to improve this process motivated by its high commercial value. Another route leading to (bicyclic) caprolactams from ketones is based on the Schmidt reaction, which was first reported in 1924 by K. F. Schmidt¹⁴³ employing hydrazoic acid as the azide component (Scheme 5.1, b).



Scheme 5.1 Classical method to prepare caprolactam from cyclohexanone.

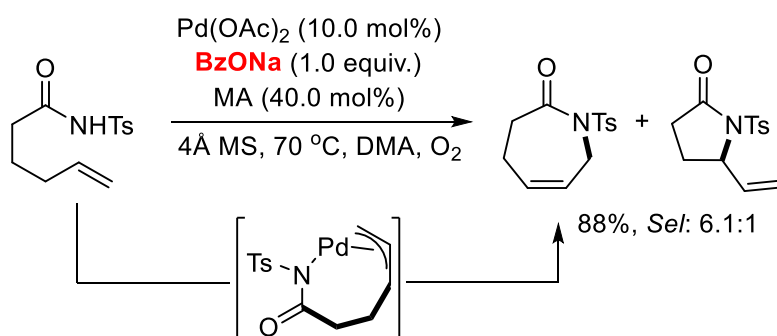
Apart from the easy access to stoichiometric methodologies, the catalytic formation of lactams has materialized as a more sustainable alternative within the synthetic community fueled by the need for a higher atom and resource economy. However, despite the recent progress noted for the catalytic synthesis of the more common five- and six-membered lactams,¹⁴⁴ the scope of functional and modular seven-membered analogues remains surprisingly limited. Therefore, designing new synthetic procedures that can streamline

(143) K. F. Schmidt, *Ber. Dtsch. Chem. Ges.* **1924**, 57, 704.

(144) a) K.-I. Fujita, Y. Takahashi, M. Owaki, K. Yamamoto, R. Yamaguchi, *Org. Lett.* **2004**, 6, 2785; b) K. Kim, S. H. Hong, *J. Org. Chem.* **2015**, 80, 4152; c) B. El Ali, K. Okuro, G. Vasapollo, H. Alper, *J. Am. Chem. Soc.* **1996**, 118, 4264; d) J. Qi, C. Sun, Y. Tian, X. Wang, G. Li, Q. Xiao, D. Yin, *Org. Lett.* **2014**, 16, 190. Using ring-closing metathesis; e) H. M. A. Hassan, *Chem. Commun.* **2010**, 46, 9100; f) A. Deiters, S. F. Martin, *Chem. Rev.* **2004**, 104, 2199, and references cited therein.

the preparation of such functional caprolactam building blocks can create new incentives for their use as synthons in drug-development programs and the creation of new polyamide monomers.

The formation of thermodynamically favored five- and six-membered heterocycles have dominated palladium-catalyzed oxidative intramolecular aminations of alkenes, and only in a rare example producing a seven-membered lactam with good regioselectivity was reported by Liu *et al.* through an allylic C–H amination approach (Scheme 5.2).¹⁴⁵ The use of sodium benzoate was found to be crucial in promoting the *endo*-cyclization, which competes with an *exo*-cyclization path leading to a five-membered lactam product.



Scheme 5.2 Regioselective allylic C–H amination towards the formation of a seven-membered lactam.

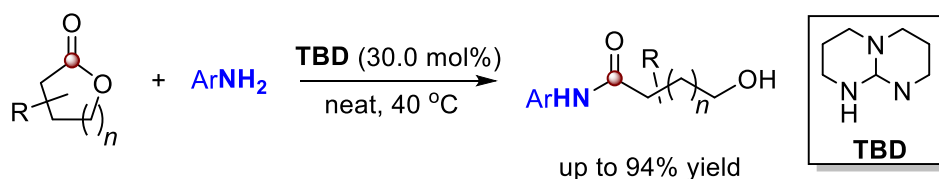
5.1.2 Catalytic Ring-opening of γ -Lactones

γ -Lactone, also named γ -butyrolactone, is important as an intermediate in the manufacturing of pyrrolidone derivatives and as a solvent for polymers and agrochemicals. However, γ -lactones are thermodynamically highly stable and in the presence of dilute acids at room temperature, γ -hydroxy acids (that are produced after hydrolysis of lactone precursor) will undergo spontaneous esterification/cyclization reforming the lactone. As a consequence, γ -butyrolactone has been long regarded as a “non-polymerizable” cyclic ester in polymer chemistry.¹⁴⁶ Ring-opening of γ -lactones generally happens via nucleophilic acyl substitution in the presence of bases, hydrogen halides and alcohols (in the presence of acids) yielding derivatives of γ -hydroxybutyric acid. In this context, ring-opening aminolysis (ROA) of non-strained γ -lactones using aryl

(145) L. Wu, S. Qiu, G. Liu, *Org. Lett.* **2009**, *11*, 2707.

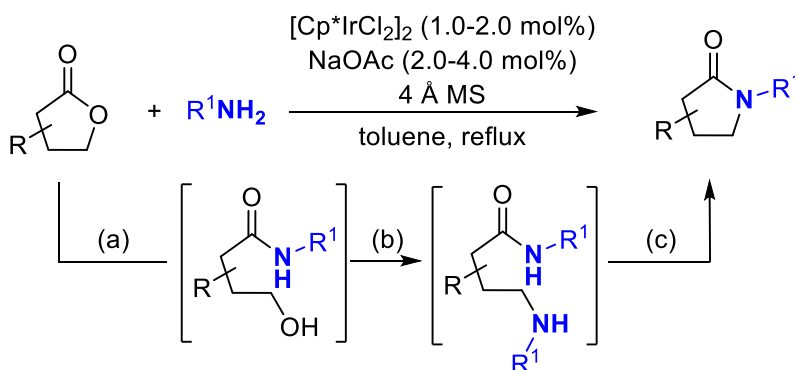
(146) a) D. Myers, A. Cyriac, C. K. Williams, *Nat. Chem.* **2016**, *8*, 3; b) M. Hong, E. Y.-X. Chen, *Nat. Chem.* **2016**, *8*, 42.

amines is an attractive approach to arrive at aryl-substituted *N*-aryl amides, though conventional methods normally require pre-activation of the aromatic amine with butyl lithium or other types of (over)stoichiometric amounts of sensitive reagents under harsh conditions. Recently, our group disclosed the formation of *N*-aryl amides from aryl amines and non-strained lactones under mild conditions in the presence of TBD (1,5,7-triazabicyclo[4.4.0]dec-5-ene) as organocatalyst,¹⁴⁷ and most of the reactions could be performed under solvent-free conditions providing good yields of the targeted compounds (Scheme 5.3).



Scheme 5.3 Organocatalytic ring-opening aminolysis of γ -lactones.

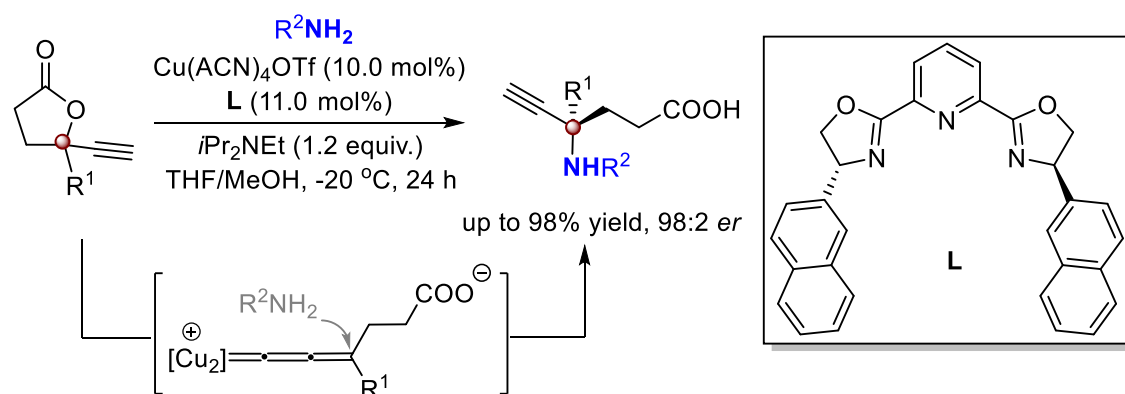
Compared with aryl amines, the more nucleophilic primary alkyl amines can be converted to the respective *N*-alkyl amide products in the absence of catalyst under mild conditions. Based on this established reactivity, Hong and coworkers reported a sequential transformation comprising of (a) an aminolysis of the lactone, (b) an Ir-catalyzed amination of the pendent alcohol of this hydroxyamide intermediate via “hydrogen autotransfer”, and (c) an intramolecular transamidation of the amino amide (Scheme 5.4).^{6b} Moreover, they provided evidence that Ir catalysis is only necessary for the *N*-alkylation step, and as such this protocol gave access to a variety of *N*-substituted lactams in moderate to excellent yields.



Scheme 5.4 Lactam synthesis from γ -lactones and amines.

(147) W. Guo, J. E. Gómez, L. Martínez-Rodríguez, N. A. G. Bandeira, C. Bo, A. W. Kleij, *ChemSusChem* **2017**, *10*, 1969.

On the other hand, γ -lactones are precursors to their free carboxyl acid derivatives after ring-opening at the γ -position. Ring-opening reactions can be performed using nucleophilic reagents such as sodium sulfide or phenols. In this context, our group reported the asymmetric synthesis of γ,γ -disubstituted γ -amino acids based on a copper mediated ring-opening of non-strained ethynyl-substituted γ -lactones with amines, and the overall manifold is believed to proceed via a copper-allenylidene complex acting as a key intermediate (Scheme 5.5).¹⁴⁸



Scheme 5.5 Cu-catalyzed formation of γ -amino acids from γ -lactones.

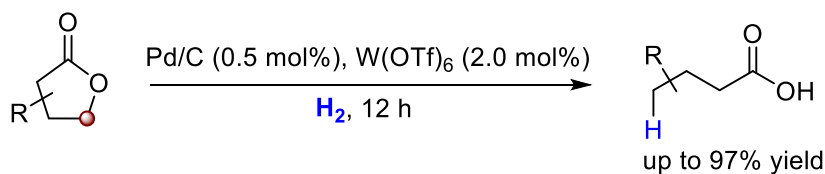
Apart from catalytic ring-opening of γ -lactones promoted by initial nucleophilic attack, a direct method for the hydrogenolysis of lactones affording a series of carboxylic acids was developed by the Fu group: in this protocol, $W(OTf)_6$ plays an essential role as co-catalyst for the transformation.¹⁴⁹ Very recently, Li and coworkers reported a redox strategy for quinone functionalization with diverse lactones through a key C–C bond-forming Friedel-Crafts alkylation (Scheme 5.6).¹⁵⁰

(148) J. E. Gómez, W. Guo, S. Gaspa, A. W. Kleij, *Angew. Chem. Int. Ed.* **2017**, *56*, 15035.

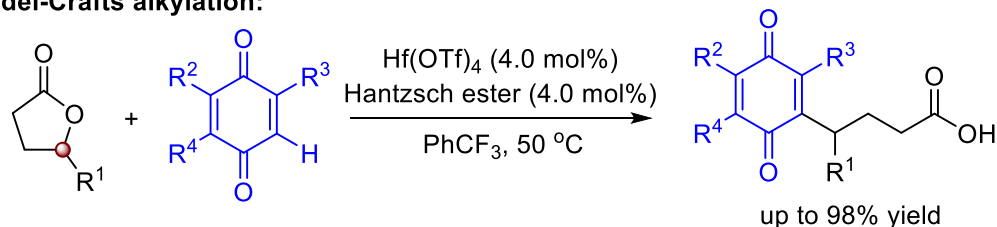
(149) R. Zhu, J.-L. Jiang, X.-L. Li, J. Deng, Y. Fu, *ACS Catal.* **2017**, *7*, 7520.

(150) X.-L. Xu, Z. Li, *Org. Lett.* **2019**, *21*, 5078.

Hydrogenolysis:



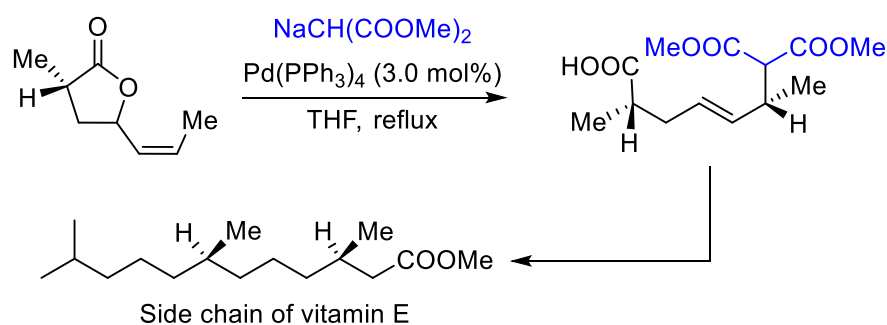
Friedel-Crafts alkylation:



Scheme 5.6 Ring-opening of γ -lactones by hydrogenolysis and Friedel-Crafts alkylation.

5.1.3 Ring-opening of γ -Lactones in Allylic Substitution Reactions

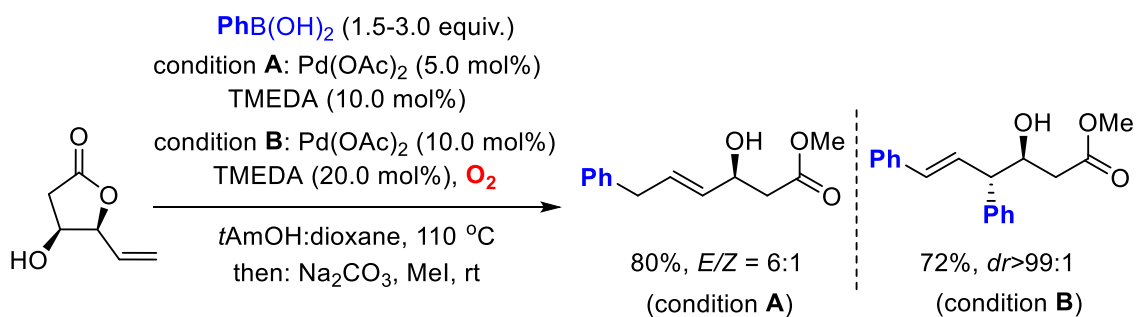
Despite the recent examples demonstrating catalytic ring-opening of non-strained γ -lactones, unfortunately, ring-opening methodology based on TM-catalyzed allylic substitution remains underdeveloped. Vinyl γ -lactones can be considered as pro-electrophiles being similar to allylic acetates, and have been shown to be prone π -allyl Pd(II) complex formation in the presence of Pd(0) enabling the interception by nucleophiles. In 1979, the Trost group reported a stereocontrolled Pd-catalyzed allylic alkylation of vinyl γ -lactones using methyl sodium malonates as carbon-based nucleophiles (Scheme 5.7).¹⁵¹ The observed selectivity was explained by (1) selective formation of a conformationally preferred Pd(allyl) species, and (2) with alkylation of the Pd(allyl) intermediate being faster than manifolds giving loss of stereochemical information. Additionally, this method was shown to be useful towards the side chain of vitamin E.



Scheme 5.7 Stereoselective allylic alkylation using vinyl γ -lactones and Na-malonate.

(151) B. M. Trost, T. P. Klun, *J. Am. Chem. Soc.* **1979**, *101*, 6756.

Recently, Fernandes and coworkers reported an example of ring-opening and arylation of a vinyl γ -lactone by aryl boronic acids giving mostly a mono-arylated products under a relatively high temperature (110 °C), whereas a bis-arylation products were generated as a single enantiomer by using excess aryl boronic acid and requiring O₂-mediated oxidation of the Pd(0) to Pd(II) (Scheme 5.8). No targeted ring-opening product could be detected at room temperature even for 72 hours, and the resultant epimerized lactone product was attributed to the thermodynamically stable nature of the γ -lactone while undergoing an intramolecular ring-opening/closing process.¹⁵²

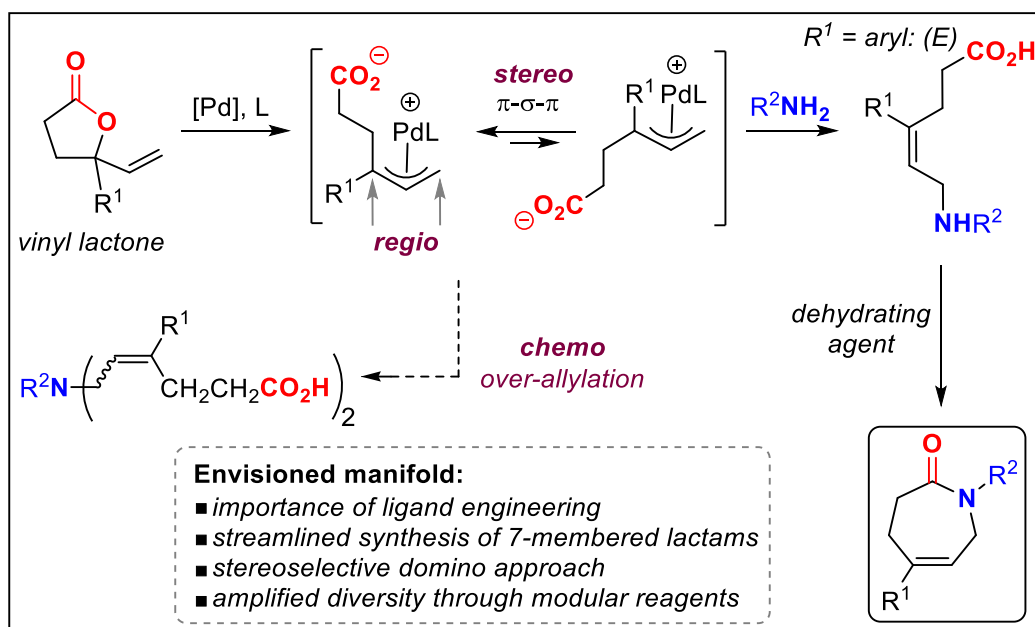


Scheme 5.8 An example of allylic alkylation using a vinyl γ -lactone and aryl boronic acids.

(152) J. L. Nallasivam, R. A. Fernandes, *J. Am. Chem. Soc.* **2016**, *138*, 13238.

5.1.4 Aim of the Work presented in this Chapter

Despite the progress in Pd-catalyzed allylic substitution reactions involving ring-opening of non-strained vinyl γ -lactone substrates,¹⁵³ high reaction temperatures and strong carbon-based nucleophiles are needed to overcome the competitive intramolecular reaction of the carboxylate species reforming the lactone precursor. However, a similar allylic substitution of γ -lactones can offer a rationale way to prepare ε -amino acid intermediates through allylic amination under Pd catalysis in the presence of suitable amine reagents. In the overall envisioned manifold, proper ligand engineering¹⁵⁴ would be of crucial importance to control and optimize simultaneously the chemo-, regio- and stereo-selectivity in order to generate the required *E*-configured ε -amino acid intermediate in high yield (Scheme 5.9) *en route* to the caprolactam target.



Scheme 5.9 Regioselective allylic amination approach towards seven-membered lactams.

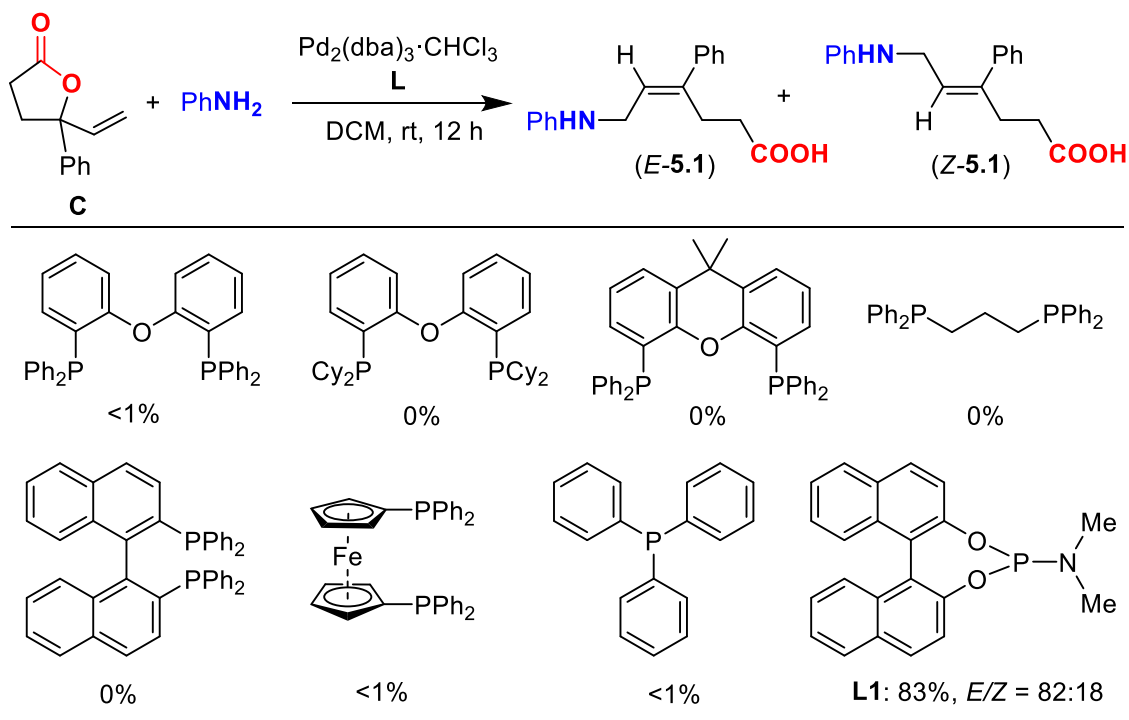
In this chapter, we present a general approach for the preparation of a series of functional caprolactam building blocks through a formal tandem ring-opening/allylic amination/cyclization process facilitated by the use of a newly developed, readily accessible phosphoramidite-based Pd catalyst.

- (153) For examples using strained bicyclic five- and six-membered lactones, see: a) V. K. Aggarwal, N. Monteiro, G. J. Tarver, S. D. Lindell, *J. Org. Chem.* **1996**, *61*, 1192; b) B. M. Trost, T. Zhang, *Angew. Chem. Int. Ed.* **2008**, *47*, 3759; c) B. M. Trost, T. Zhang, *Chem. Eur. J.* **2011**, *17*, 3630.
 (154) a) L. Hu, A. Cai, Z. Wu, A. W. Kleij, G. Huang, *Angew. Chem. Int. Ed.* **2019**, *58*, 14694; b) A. Cai, A. W. Kleij, *Angew. Chem. Int. Ed.* **2019**, *58*, 14944.

5.2 Results and Discussion

5.2.1 Screening Studies

Table 5.1: Preliminary evaluation of ligands^a



^aReaction conditions: lactone **C** (0.20 mmol), aniline (0.30 mmol, 1.5 equiv.), DCM (0.20 mL), $\text{Pd}_2(\text{dba})_3 \cdot \text{CHCl}_3$ (2.0 mol%), monodentate ligand (8.0 mol%) or bidentate ligand (4.0 mol%), rt, 12 h; the yields and *E/Z* ratios were determined by ^1H NMR analysis of the crude reaction mixture, using CH_2Br_2 (1.0 equiv.) as internal standard.

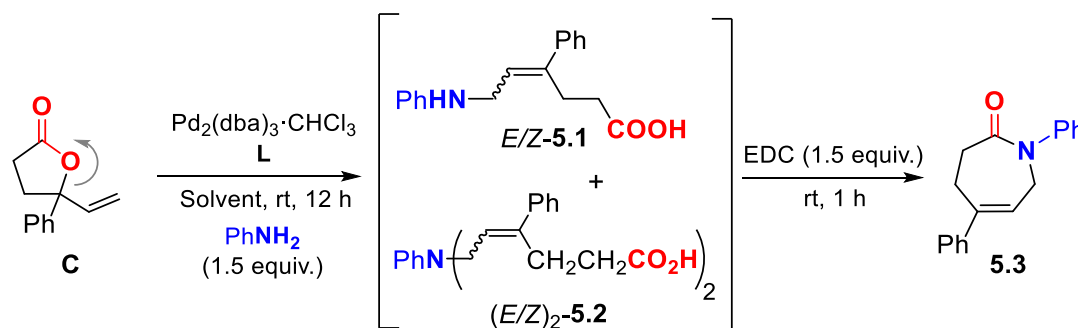
To test our working hypothesis illustrated in Scheme 5.9, we chose substrates **C** and aniline (Table 5.1) for the screening phase that should allow to access ϵ -amino acid products **E-5.1** or **Z-5.1**, respectively. At the onset of the screening studies, we considered to use previously shown successful phosphorus ligands to examine their efficacy to generate Pd-catalysts derived from $\text{Pd}_2(\text{dba})_3 \cdot \text{CHCl}_3$. We were pleased to find that the presence of phosphoramidite ligand **L1** proved to be highly beneficial for the ring-opening allylic amination step under ambient conditions.

Furthermore, the *in situ* rapid cyclization of the intermediate *E*- ϵ -amino acid towards the lactam target using the well-known reagent EDC¹⁵⁵ was combined in a one-pot two

(155) EDC, 1-ethyl-3-(3-dimethylaminopropyl)carbodiimide, was selected as it represents a practical and standard dehydrative reagent/carboxylic acid activator. See for instance: J. Sheehan, P. Cruickshank, G. Boshart, *J. Org. Chem.* **1961**, 26, 2525.

step sequence. The screening phase then focused on producing the intermediate ϵ -amino acids **5.1** in the most efficient way from lactone **C** using phosphoramidite **L1** (Table 5.2, entries 1–6) as to favour the formation of the desired lactam **5.3**. The solvent appears to have a significant effect, as the use of both DCM and MeOH gave access to moderate yields of **5.3** while minimizing the formation of the double allylated byproduct **5.2**. The presence of highly polar solvents such as DMSO and DMF or THF resulted in unproductive processes, whereas the utilization of CH₃CN lowered the chemo-selectivity of the process. It is important to note that in the absence of **L1** (entry 7), there was no formation of any product pointing at the crucial role of the ligand.

Table 5.2: Effect of solvent towards the caprolactam product **5.3**^a



Entry	Ligand	Solvent	Yield of 5.1 [%] ^b	E/Z- 5.1 ^c	5.1/5.2 ^c	Yield of 5.3 [%] ^b
1	L1	DCM	83	82:18	16:1	66
2	L1	THF	0	–	–	–
3	L1	CH ₃ CN	67	89:11	5:1	59
4	L1	MeOH	78	82:18	17:1	64
5	L1	DMF	0	–	–	–
6	L1	DMSO	0	–	–	–
7	–	DCM	0	–	–	–

^aReaction conditions: lactone **C** (0.20 mmol), PhNH₂ (0.30 mmol, 1.5 equiv.), solvent (0.20 mL), Pd₂(dba)₃·CHCl₃ (2.0 mol%), **L1** (8.0 mol%), rt, 12 h; then EDC (0.30 mmol), 1 h. ^bDetermined by ¹H NMR analysis in CDCl₃ using CH₂Br₂ as an internal standard. ^cDetermined by ¹H NMR analysis.

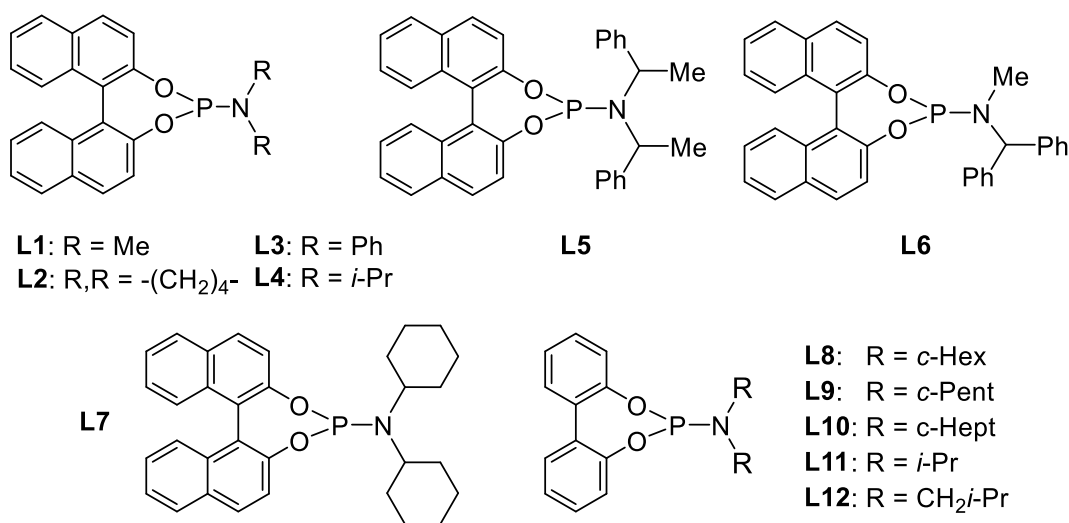
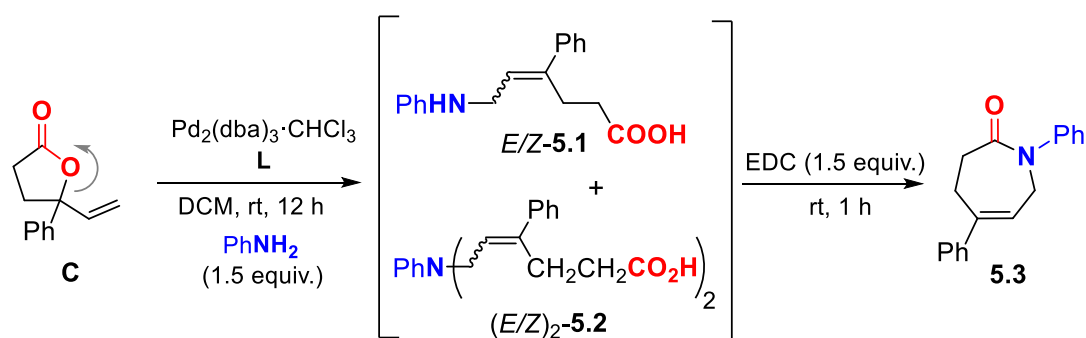
A variety of phosphoramidite ligands **L2–L12** (Table 5.3, entries 1–11) were then scrutinized under the conditions of entry 1 (Table 5.2), illustrating the critical influence of the *N*-substitution and nature of the biaryl backbone on the chemo-, regio- and stereo-selectivity of this catalytic process. For instance, too bulky *N*-substituents (**L4–L6**, entries 3–5) did not permit the formation of **5.3**, whereas ligands equipped with piperidine and phenyl (**L2** and **L3**) provided good yields of intermediate **5.1** with high chemo-selectivity

and moderate *E/Z* ratios (entries 1–2). To our delight, the introduction of cyclohexyl groups (**L7**, entry 6) further increased the *E*-stereoselective formation of **5.1** and the yield of **5.3** while retaining good chemo-selectivity.

Interestingly, a binaphthyl ligand backbone was not essential to achieve high selectivity, which became clear from studying the biphenyl based ligands **L8–L12** and the steric effect of their *N*-substituents (entries 7–11). Cyclopentyl and *i*-Bu substituted ligands **L9** and **L12** provided productive and rather selective catalysts for the formation of **5.3** though with slightly lower yields and stereoselectivity as compared to **L8**. The reaction did not proceed with ligands comprising of cycloheptyl or *i*-Pr groups (**L10** and **L11**). These results indicate that steric modulation of the *N*-substituent of the ligand is key to the success of the formation of caprolactam **5.3**.

From all ligands studied, the novel ligand **L8** (entry 7) provided the best combination of yield (for **5.1** and **5.3**) and selectivity features. A further increase in the yield of **5.3** in the presence of **L8** was finally obtained by increasing the amount of catalyst, aniline and solvent (entries 12–13) providing the caprolactam product in 84% yield and with high stereo- (*E/Z* = 98:2) and chemo-selectivity (**5.1:5.2** > 20:1). This process could be scaled up to 5.5 mmol (1.034 g, substrate **C**) without influencing the process outcome (*i.e.*, 80% product yield and a 97:3 *E/Z* ratio were observed for the intermediate ϵ -amino acid).

Table 5.3: Effect of the ligand towards the formation of caprolactam **5.3**^a



Entry	Ligand	Yield of 5.1 [%] ^b	E/Z - 5.1 ^c	5.1/5.2 ^c	Yield of 5.3 [%] ^b
1	L2	85	77:23	16:1	65
2	L3	82	61:39	>20:1	53
3	L4	<1	–	–	–
4	L5	0	–	–	–
5	L6	0	–	–	–
6	L7	79	96:4	10:1	76
7	L8	80	97:3	10:1	77
8	L9	79	94:6	13:1	74
9	L10	<1	–	–	–
10	L11	0	–	–	–
11	L12	82	91:9	15:1	75
12 ^{d-e}	L8	88	93:7	>20:1	82
13 ^{d-f}	L8	86	98:2	>20:1	84

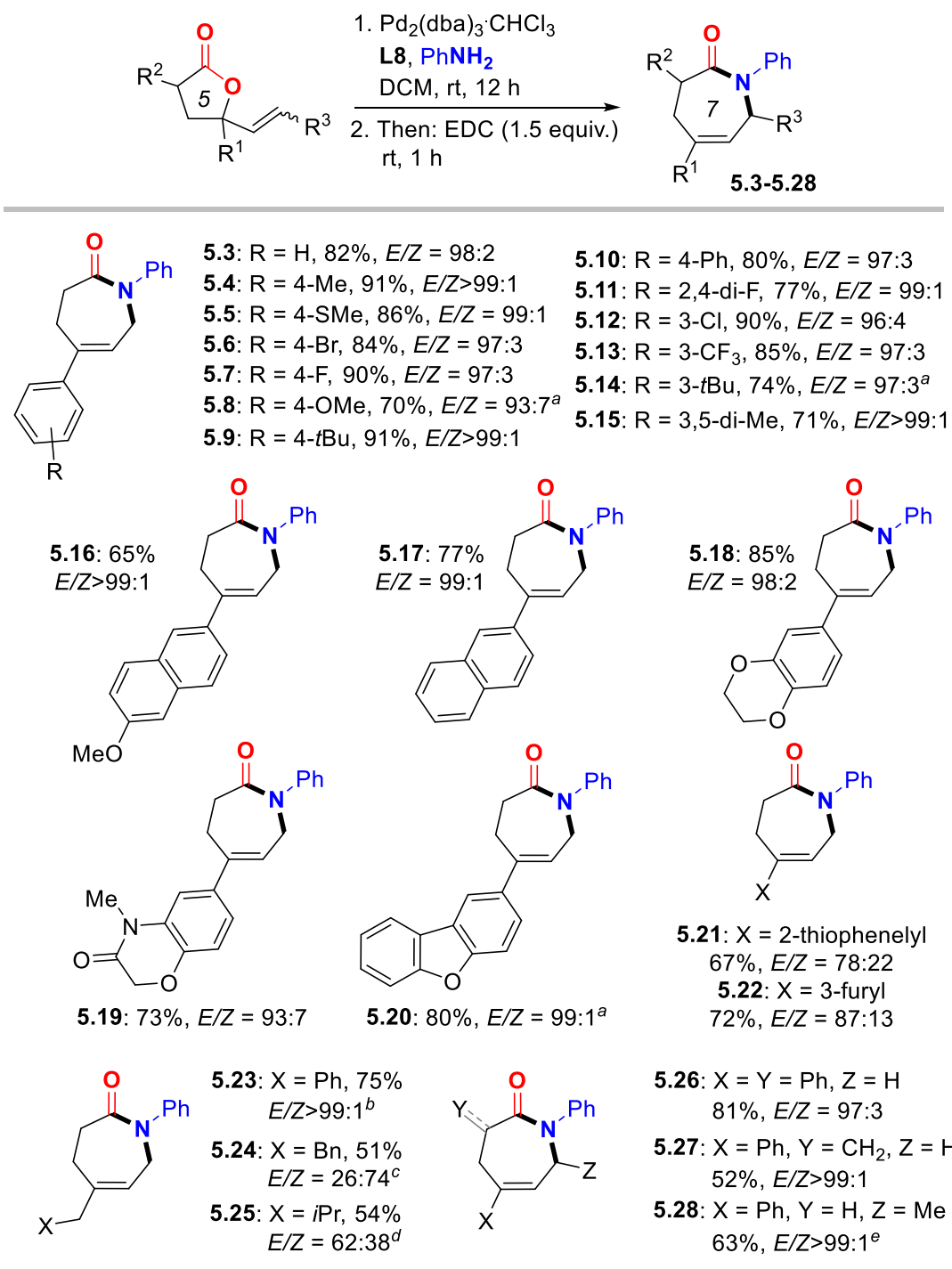
^aReaction conditions: refer to Table 5.2, entry 1. ^bDetermined by ¹H NMR analysis in CDCl₃ using CH₂Br₂ as an internal standard. ^cDetermined by ¹H NMR analysis. ^dPhNH₂ (2.0 equiv.). ^ePd₂(dba)₃·CHCl₃ (3.0 mol%), **L1** (12.0 mol%). ^fSolvent (0.30 mL).

5.2.2 Scope of Substrates

With the optimized conditions of entry 13 in Table 5.3, we then set out to examine the scope of this new transformation (Scheme 5.10, compounds **5.3–5.28**) focusing first on variation of the vinyl lactone reagent. Lactones with *para*-substituted aryl substituents were productive substrates giving the caprolactam derivatives **5.3–5.10** in high isolated yields (>80% in most cases) and with excellent stereo- (typically with *E/Z* ratios >95:5), regio- and chemo-selectivity control. The molecular structure of compound **5.3** was confirmed by X-ray analysis (see section 5.4.7, Figure 5.2). The presence of *meta*-, *ortho*-, *para*-di- or 3,5-di-substituted aryl groups (**5.11–5.15**; 71-90%, *E/Z* ≥96:4) did not have any significant effect on the outcome of the tandem process, and the desired products could be easily formed and isolated. Larger aromatic surfaces such as those present in lactam products **5.16** and **5.17** are also tolerated, while this new protocol furthermore allows the introduction of heteroaromatic fragments (**5.18–5.22**) in the final products.

In the case of **5.21** and **5.22** bearing a 2-thienyl and 3-furyl group, respectively, the observed stereoselectivity was significantly lower which may be ascribed to the potential of these groups to interact with the Pd-catalyst while affecting the π - σ - π equilibrium as depicted in Scheme 5.9. Finally, introducing other γ -substituents in the lactam product such as different alkyl groups (**5.23–5.25**; 51-75%),¹⁵⁶ and the introduction of additional α -positioned groups (**5.26**, 81%; **5.27**, 52%) was also feasible preserving excellent stereoselectivity. The methylenedioxy substituted product **5.27** could act as a potential Michael acceptor for late-stage modification towards the formation of biologically active compounds. The preparation of **5.28** (63%) additionally demonstrates that also lactones with substituted vinyl groups are productive substrates.

(156) Martin *et al.* reported previously a Pd-catalyzed allylic alkylation process involving an γ -alkyl- γ -vinyl substituted lactone and a carbon based nucleophile affording the allylic alkylation product with a 1:1 *E/Z* ratio, see: B. L. Ashfeld, S. F. Martin, *Org. Lett.* **2005**, *7*, 4535. We recently reported that also for related vinyl substituted cyclic carbonates a decrease in stereo-induction is noted when “aryl” groups are replaced by “alkyl” ones. We ascribed this to hyper-conjugation effects (in the case of aryl substituents) stabilizing the allyl-Pd intermediate towards undesirably fast π - σ - π isomerization that would favor the formation of a mixture of *E/Z* stereoisomers. See: W. Guo, L. Martínez-Rodríguez, E. Martín, E. C. Escudero-Adán, A. W. Kleij, *Angew. Chem. Int. Ed.* **2016**, *55*, 11037.

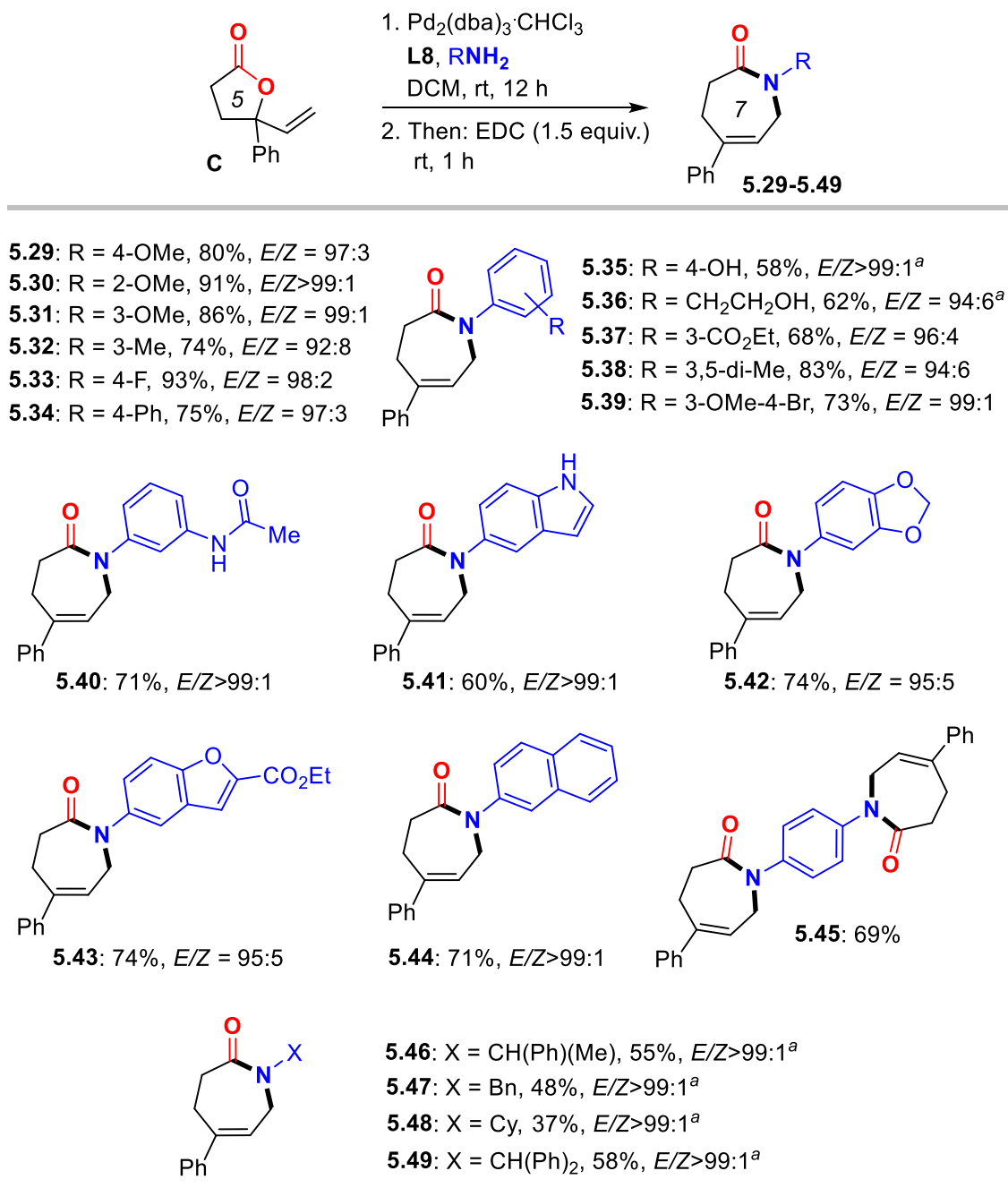


Scheme 5.10 Variation of the vinyl-substituted γ -lactones. Reaction conditions unless stated otherwise: all reactions were performed under the optimized conditions (Table 5.3, entry 13). Isolated yields are reported, and the *E/Z* ratios for the intermediate ϵ -amino acids were determined by ¹H NMR; ^aUsing DCM/EtOH (1:1 v/v) as solvent. ^b**L1** (12.0 mol%), MeOH (0.30 mL), 24 h. ^cUsing **L1** (12.0 mol%), MeOH, 24 h, 30 °C. ^dUsing P(OPh)₃ (12.0 mol%), MeOH, 24 h. ^e**L1** (12.0 mol%), MeOH, 60 °C.

Our attention then shifted towards widening the scope of the caprolactam products by combining vinyl lactone **C** and various amine reaction partners (Scheme 5.11, compounds **5.29–5.49**). A range of anilines with different substituents at the *meta*-, *ortho*-, or *para*-position could be coupled to ring-opened lactone **C** under the optimized conditions providing overall good to excellent yields of caprolactams **5.29–5.40** under high stereocontrol. The use of larger (hetero)aromatic amines (**5.41–5.44**) gave access to lactam products with *N*-indole, *N*-1,3-benzodioxole, *N*-benzofuran and *N*-naphthyl groups. The di-lactam derivative **5.45** could be prepared in appreciable yield (69%) despite the more challenging nature of this formal tandem *bis* allylic amination/cyclization process.

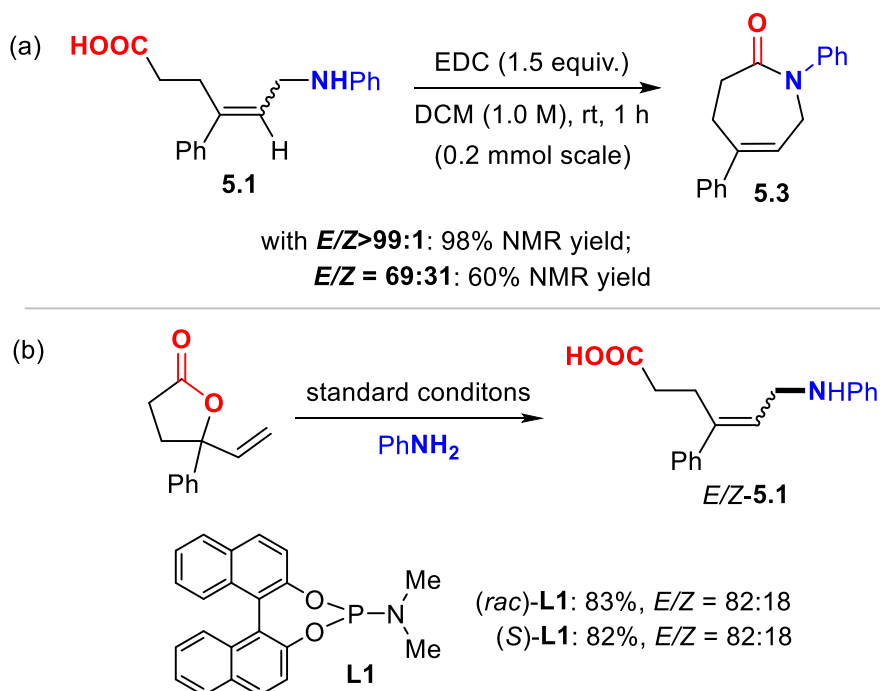
Lastly, we tested several, more nucleophilic aliphatic amines to challenge the chemoselectivity of our developed protocol. As may be expected, substantially lower yields for **5.46–5.49** were obtained (37–58%) though under excellent stereocontrol (*E/Z*>99:1) in a mixed solvent system consisting of DCM and EtOH. The ¹H NMR analysis of the crude products indeed indicated that larger amounts of bis-allylated amines of type **5.2** had been formed.¹⁵⁷

(157) Bis-allylation of primary aliphatic amines has been observed before, see: a) A. Trowbridge, S. M. Walton, M. J. Gaunt, *Chem. Rev.* **2020**, *120*, 2613. For original examples: b) M. Kimura, M. Futamata, K. Shibata, Y. Tamaru, *Chem. Commun.* **2003**, 234; c) F. Ozawa, H. Okamoto, S. Kawagishi, S. Yamamoto, T. Minami, M. Yoshifuji, *J. Am. Chem. Soc.* **2002**, *124*, 10968.



Scheme 5.11 Variation of the amine reagents. Reaction conditions unless stated otherwise: all reactions were performed under the optimized conditions (Table 5.3, entry 13). Isolated yields are reported, and the *E/Z* ratios for the intermediate ϵ -amino acids were determined by ¹H NMR, though for **5.45**, the *E/Z* selectivity could not be determined accurately. ^aUsing DCM/EtOH (1:1 v/v) as solvent.

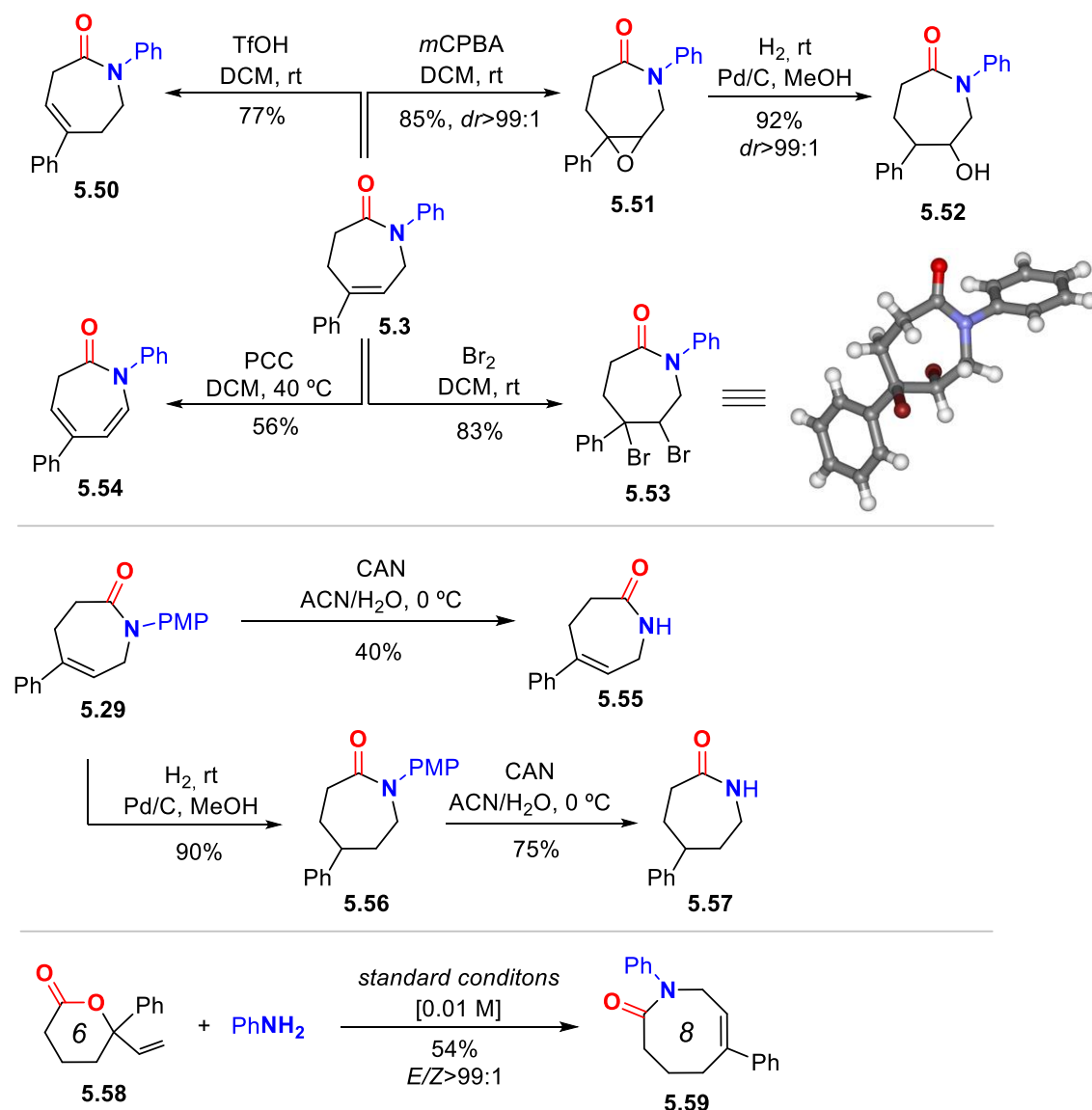
5.2.3 Mechanistic Control Reactions



Scheme 5.12 Assessment of the stereo-purity of **5.1** and the ligand on the product yield.

In order to test whether the stereoselectivity indeed plays an important role prior to the cyclization step (Scheme 5.9), we compared the yield of lactam **5.3** attained from a configurationally pure sample of **5.1** ($E/Z > 99:1$) and one being a 69:31 E/Z mixture (Scheme 5.12a). From the results, it may be concluded that the maximum yield unquestionably depends on the amount of E -**5.1** that is initially formed, and also molecular models strongly suggest that the Z -isomer of **5.1** is unable to cyclize towards a lactam product. These results reinforce the assumption that stereocontrol in the first step is vital to the success of the overall manifold. The use of a simple ligand structure (*cf.*, **L8**) shows that the presence of a chiral ligand is not a requisite. This is demonstrated by the fact that both (*rac*)- and enantiopure (*S*)-**L1** give virtually the same stereocontrol (in the preparation of **5.1**) and lead to a similar yield of **5.3** (Scheme 5.12b), thus being consistent with the results described in Tables 5.2 and 5.3.

5.2.4 Synthetic Transformations



Scheme 5.13 Synthetic transformations using lactam precursors **5.3**, **5.29** and **5.58**.

Product diversification studies using **5.3** and **5.29** were carried out (Scheme 5.13). Triflic acid mediated double bond isomerization in **5.3** was feasible to produce **5.50** in good yield, whereas epoxidation afforded **5.51** with excellent diastereoselectivity. The latter compound could be reduced by using Pd-catalyzed hydrogenation leading to **5.52** in high yield. Dibromination of **5.3** gives **5.53** (83%, with its molecular structure confirmed by X-ray analysis, Figure 5.3 *vide infra*), whereas pyridinium chlorochromate (PCC) assisted oxidation of **5.3** furnished the conjugated, bis-unsaturated caprolactam derivative **5.54**. In order to provide free lactams potentially useful as a new type of monomer for polyamide synthesis or pharmaceutical precursors, compound **5.29** was treated with

cerium ammonium nitrate (CAN) to afford **5.55** in 40% yield. Alternatively, standard hydrogenation of **5.29** (**5.56**; 90%) followed by deprotection gave easy access to free lactam **5.57** in 75% yield. Finally, six-membered vinyl lactone **5.58** could be transformed into eight-membered lactam **5.59** (54%) with high stereocontrol, and this implies that the developed cascade process may be suitable for the preparation of an even wider range of larger-ring lactams.

5.3 Conclusions

In the past decades, continuous synthetic efforts have been devoted toward the development of lactams, however, the scope of functional and modular seven-membered analogues remained limited. Therefore, designing new synthetic routes to access functional caprolactam diversity with various substitution patterns will be of high interest for the synthetic community to reinforce their implementation as synthons in drug and monomer for polyamide synthesis.

In this chapter, we report a new, efficient and practical approach for valuable caprolactam synthons that involves (after ring-opening of vinyl γ -lactones) a Pd-mediated stereo- and regioselective allylic amination followed by a cyclization step affording the lactam target. This formal tandem process relies on the use of a new, easily prepared phosphoramidite ligand (**L8**) that allows to control the stereo-induction and as such the yield of the final product under ambient conditions. The scale-up and diversification studies show that more functional scaffolds may be created that can be of great value to build up molecular complexity from readily accessible lactam precursors.

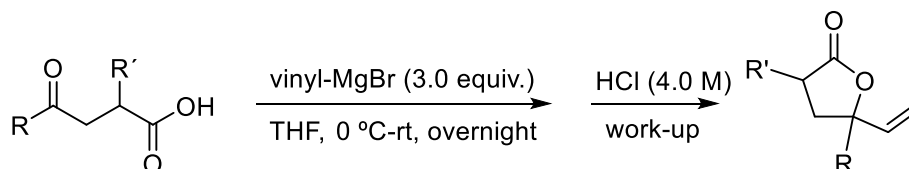
5.4 Experimental Section

5.4.1 General Considerations

The amine reagents and solvents were purchased from Aldrich or TCI, and used without further purification. Phosphoramidite ligands **L1**,^{158a} **L2**,^{158b} **L3**,^{158c} **L4–L5**,^{158d} **L6**,^{158c} and **L7–L12**^{158d} were prepared according to previously reported protocols. Other ligands and palladium precursors were purchased from Aldrich or TCI. The γ -oxobutanoic acids were synthesized following reported procedures if not commercially available.¹⁵⁹ ¹H NMR, ¹³C{¹H} NMR, ³¹P{¹H} NMR and ¹⁹F{¹H} NMR spectra were recorded at room temperature on a Bruker AV-400 or AV-500 spectrometer and referenced to the residual deuterated solvent signals. All reported NMR values are given in parts per million (ppm). FT-IR measurements were carried out on a Bruker Optics FTIR Alpha spectrometer. Mass spectrometric analyses and X-ray diffraction studies were performed by the Research Support Group at ICIQ.

5.4.2 Procedure for the Preparation of Vinyl γ -Lactones

General Procedure A:

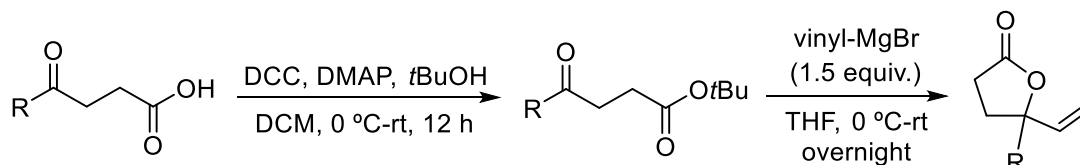


Under a N₂ atmosphere, to a separate flame-dried round-bottom flask equipped with a stirring bar was added the respective γ -oxobutanoic acid (10.0 mmol) and anhydrous THF (30 mL). The solution was cooled down to 0 °C (ice/water), followed by dropwise addition of vinyl magnesium bromide in THF (1.0 M, 30.0 mL, 30.0 mmol). The reaction mixture was allowed to warm to room temperature and stirred for 16 h. The reaction

- (158) a) A. Z. González, F. D. Toste, *Org. Lett.* **2010**, *12*, 200; b) N. Mršić, A. J. Minnaard, B. L. Feringa, J. G. de Vries, *J. Am. Chem. Soc.* **2009**, *131*, 8358; c) B. Zhao, H. Du, R. Fu, Y. Shi, *Org. Synth.* **2010**, *87*, 263; d) A. Mercier, W. C. Yeo, J. Chou, P. D. Chaudhuri, G. Bernardinelli, E. P. Kündig, *Chem. Commun.* **2009**, 5227.
- (159) a) N. Sakai, T. Kobayashi, Y. Ogiwara, *Chem. Lett.* **2015**, *44*, 1503; b) P. Saravanan, P. Anbarasan, *Adv. Synth. Catal.* **2018**, *360*, 2894; c) P. B. Cranwell, A. T. Russell, C. D. Smith, *Synlett* **2016**, 27, 131; d) C. Chen, Z. Zhang, S. Jin, X. Fan, M. Geng, Y. Zhou, S. Wen, X. Wang, L. W. Chung, X.-Q. Dong, X. Zhang, *Angew. Chem. Int. Ed.* **2017**, *56*, 6808; e) S. Cuadros, L. Dell'Amico, P. Melchiorre, *Angew. Chem. Int. Ed.* **2017**, *56*, 11875; f) T. Song, S. Arseniyadis, J. Cossy, *Org. Lett.* **2019**, *21*, 603; g) J. Koyanagi, K. Yamamoto, K. Nakayama, A. Tanaka, *J. Nat. Prod.* **1995**, *58*, 1955; h) S. Li, J. Zhang, H. Li, L. Feng, P. Jiao, *J. Org. Chem.* **2019**, *84*, 9460; i) S. Lee, H. Y. Bae, B. List, *Angew. Chem. Int. Ed.* **2018**, *57*, 12162.

mixture was quenched with saturated aqueous NH_4Cl , then treated with HCl (4.0 M) until the pH was 3. The organic components were extracted with EtOAc (3×20 mL). Hereafter, the combined organic layers were washed with brine, dried over anhydrous Na_2SO_4 , filtered, and then concentrated under reduced pressure. The residue was purified by flash chromatography to afford the corresponding lactone.

General Procedure B:



According to a previously reported procedure,¹⁶⁰ to a solution of γ -oxobutanoic acid (10.0 mmol, 1.0 equiv.) and *tert*-butyl alcohol (20.0 mmol, 2.0 equiv.) in DCM (20 mL), DMAP (3.0 mmol, 0.3 equiv.) was added. The resultant solution was cooled down to $0\text{ }^\circ\text{C}$ and *N,N'*-dicyclohexylcarbodiimide (DCC, 12.0 mmol, 1.2 equiv.) was added. The reaction mixture was stirred at room temperature for 12 h. The urea byproduct was filtered off and the organic layer was concentrated under vacuum. The crude residue was purified by a rapid flash chromatographic purification to give the corresponding ester product.

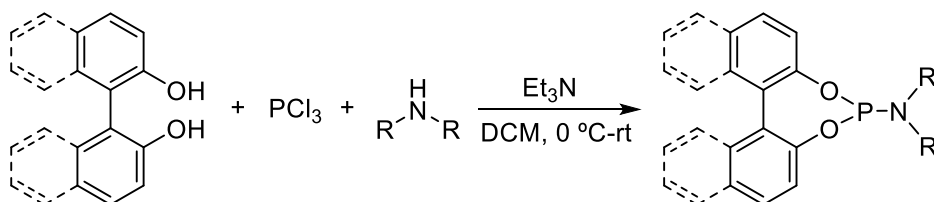
Under a N_2 atmosphere, to a separate flame-dried round-bottom flask equipped with a stirring bar was added the respective γ -oxobutanoic ester (5.0 mmol) and anhydrous THF (15 mL). The solution was cooled down to $0\text{ }^\circ\text{C}$ (ice/water), followed by dropwise addition of vinyl magnesium bromide in THF (1.0 M, 7.5 mL, 7.5 mmol). The reaction mixture was allowed to warm to room temperature and stirred for 16 h. The reaction mixture was quenched with saturated aqueous NH_4Cl . The organic components were extracted with EtOAc (3×20 mL), and the combined organic layers were washed with brine, dried over anhydrous Na_2SO_4 , filtered, and then concentrated under reduced pressure. The residue was purified by flash chromatography to afford the corresponding lactone.

The desired starting materials could be prepared by methods **A** or **B** in 30-70% isolated yields without further optimization.

(160) J. E. Gómez, W. Guo, S. Gaspa, A. W. Kleij, *Angew. Chem. Int. Ed.* **2017**, *56*, 15035.

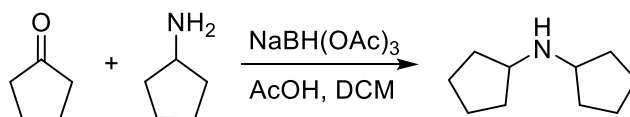
5.4.3 Procedure for the Preparation of Phosphoramidite Ligands

The non-reported ligands **L8–L12** were prepared according to a reported procedure with slight modifications.^{158d}



To an oven-dried round bottom flask, distilled PCl_3 (180.0 μL , 2.06 mmol) was added to a solution of anhydrous Et_3N (1.68 mL, 12.06 mmol) in DCM (15 mL) at 0 °C and the mixture stirred for 0.5 h at this temperature. Then, the respective amine (2.0 mmol) was added dropwise at 0 °C, and the reaction mixture stirred for 4 h at room temperature. The resultant solution was cooled to 0 °C, and then [1,1-biphenyl]-2,2-diol (372.4 mg, 2.0 mmol) or (\pm)-1,1'-binaphthalene-2,2'-diol (572.7 mg, 2.0 mmol) was added. The mixture was stirred for 16 h at room temperature, diluted with water and extracted with DCM (3 \times 20 mL). The combined organic layers were dried over anhydrous Na_2SO_4 , filtered, and then concentrated under reduced pressure. The residue was purified by flash chromatography to afford the respective phosphoramidite ligand. All purified ligands were fully characterized by NMR (^1H , ^{13}C , ^{31}P), IR and HRMS. [Note that, in some cases, it proved to be crucial to isolate the pure ligand by chromatography under a N_2 atmosphere]

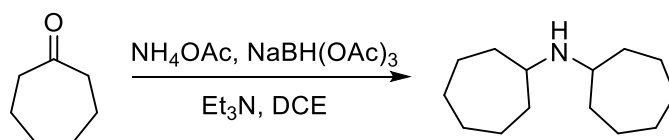
Dicyclopentylamine and dicycloheptylamine, being the starting materials of **L9–L10**, were prepared following reported procedures.¹⁶¹



To a stirred solution of the cyclopentanone (420.6 mg, 5.0 mmol) and cyclopentylamine (425.8 mg, 5.0 mmol) in DCM (15 mL) were added sodium triacetoxyborohydride (1.4836 g, 7.0 mmol) and acetic acid (300.0 mg, 5.0 mmol). The reaction

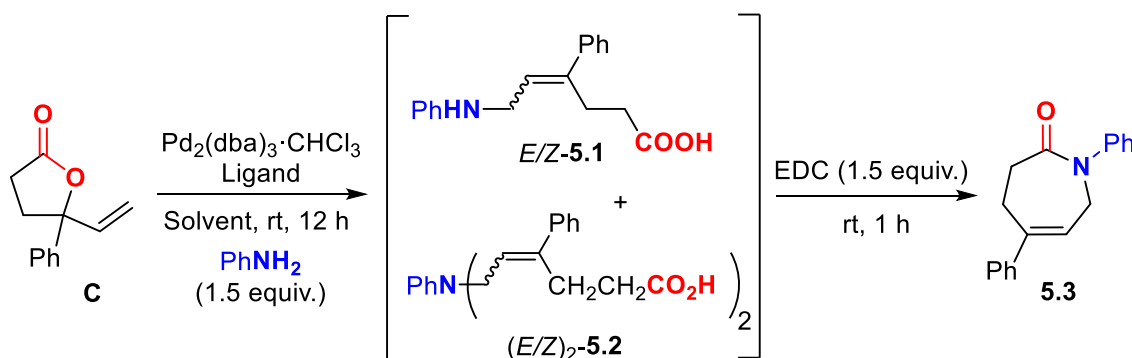
(161) a) Y. Odabachian, Q. Wang, J. Zhu, *Chem. Eur. J.* **2013**, *19*, 12229; b) L. F. R. Gomes, L. F. Veiros, N. Maulide, C. A. M. Afonso, *Chem. Eur. J.* **2015**, *21*, 1449.

mixture was stirred for 12 h at room temperature, and hereafter, 1 N aqueous NaOH was added. The resultant mixture was extracted with ester (3 × 20 mL). The combined organic layers were dried over anhydrous Na₂SO₄, filtered, and then concentrated under reduced pressure. The crude product could be directly used without further purification.



To a stirred solution of cycloheptanone (1.0 g, 8.9 mmol) and NH₄OAc (6.63 g, 86.0 mmol) in DCE (30 mL) were added sodium triacetoxy borohydride (2.65 g, 12.5 mmol) and Et₃N (2.5 mL, 17.9 mmol). The reaction mixture was stirred for 48 h at room temperature, followed by addition of saturated aqueous NaHCO₃. The resultant mixture was extracted with EtOAc (3 × 20 mL). The combined organic layers were washed with brine, dried over anhydrous Na₂SO₄, filtered, and then concentrated under reduced pressure. The residue was purified by flash chromatography to afford the desired amine as a yellow liquid.

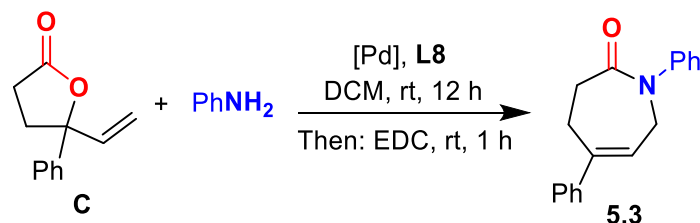
5.4.4 Procedure for the Screening Phase in the Preparation of Caprolactam



Vinyl γ -lactone **C** (37.6 mg, 0.20 mmol, 1.0 equiv.) was combined with Pd₂(dba)₃·CHCl₃, the ligand, aniline and the solvent at room temperature under air. The internal standard CH₂Br₂ (1.0 equiv.) was added after the reaction mixture had been stirred at room temperature for 12 h, and then an aliquot of the mixture was taken for analysis allowing to determine the NMR yield of the amino acid intermediate, the *Z/E* ratio and the ratio of **5.1/5.2** using signal integration. Hereafter, EDC (57.5 mg, 0.30 mmol, 1.5 equiv.) was

added and the reaction mixture stirred for another 1 h, after which the yield of the targeted product **5.3** was determined by ^1H NMR spectroscopy.

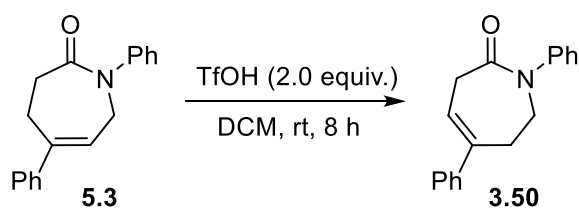
5.4.5 Typical Procedure for the Preparation of Caprolactams



Representative case:

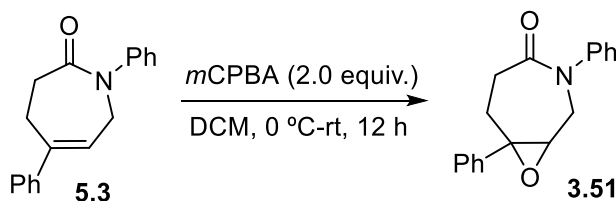
Vinyl γ -lactone **C** (37.6 mg, 0.20 mmol, 1.0 equiv.) was combined with $\text{Pd}_2(\text{dba})_3 \cdot \text{CHCl}_3$ (6.0 mg, 3.0 mol%), **L8** (9.6 mg, 12.0 mol%) and aniline (38.0 mg, 0.40 mmol) in DCM (0.30 mL) at room temperature under air. The reaction mixture was stirred at room temperature for 12 h, then an aliquot of the mixture was taken for NMR analysis, which provided the unsaturated amino acid intermediate with an *E/Z* ratio of 98:2. Then, EDC (57.5 mg, 0.30 mmol) was added and the reaction mixture stirred for another 1 h. The desired product was isolated by flash chromatography (43.2 mg, 82%, Hexane/EtOAc = 2:1, $R_f = 0.25$). Note that all purified caprolactam products were fully characterized by NMR (^1H , ^{13}C ; ^{19}F where appropriate), IR and HRMS.

5.4.6 Post-synthetic Potential of the Caprolactam Scaffolds

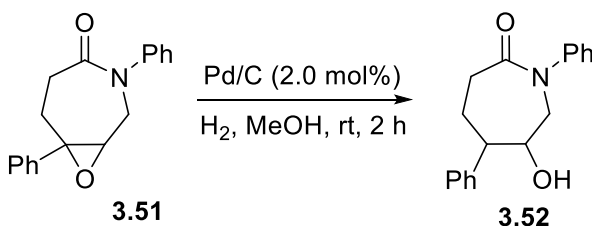


In a vial equipped with a magnetic stirring bar, caprolactam **5.3** (52.7 mg, 0.20 mmol, 1.0 equiv.) was dissolved into DCM (0.20 mL), and then trifluoromethanesulfonic acid (0.035 mL, 0.40 mmol, 2.0 equiv.) was added with a syringe. The resultant solution was stirred for 8 h at room temperature. Hereafter, saturated aqueous NaHCO_3 was slowly added and the organic components were extracted with DCM (3×10 mL). Then, the combined organic layers were dried over Na_2SO_4 , filtered, and concentrated under

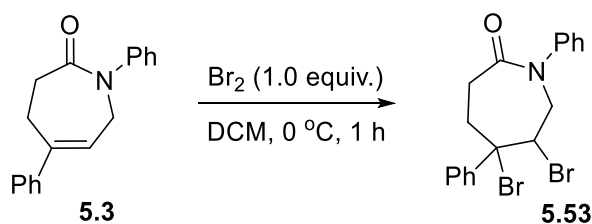
vacuum. The crude product was purified by flash chromatography to afford the isomerized product **3.50** (40.6 mg, 77%) as a light yellow solid.



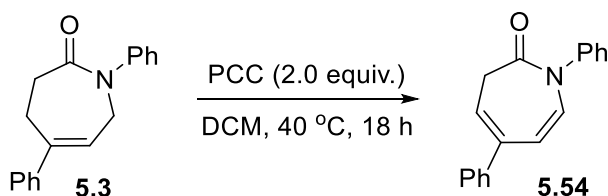
To a solution of caprolactam **5.3** (52.7 mg, 0.20 mmol, 1.0 equiv.) in DCM (0.40 mL) was added *m*CPBA (0.40 mmol, 69.0 mg, 2.0 equiv.) at 0 °C under air. Then the reaction mixture was allowed to warm to room temperature, and stirred for 12 h. The reaction mixture was filtered through Celite. The solvent in the filtrate was evaporated under reduced pressure, and the crude product was purified by flash chromatography to afford the pure epoxide product **5.51** (47.5 mg, 85%, >99:1 *dr*) as a yellow solid.



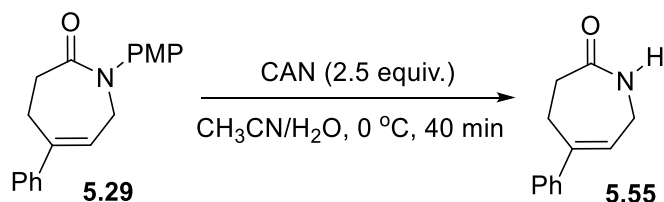
A Schlenk tube charged with **5.51** (83.8 mg, 0.30 mmol, 1.0 equiv.) and Pd/C catalyst (6.4 mg, 10.0 wt % palladium on carbon) was evacuated and filled with H₂ (balloon) for three times. After that, MeOH (1.0 mL) was added and the reaction mixture was stirred under a H₂ atmosphere (balloon) for 2 h at room temperature and monitored by NMR. The reaction mixture was filtered through Celite. The solvent in the filtrate was evaporated under reduced pressure. The residue was purified by flash chromatography to afford the pure product **3.52** (77.7 mg, 92%, >99:1 *dr*) as a white solid.



To an oven-dried Schlenk tube was added caprolactam **5.3** (52.7 mg, 0.20 mmol, 1.0 equiv.) and anhydrous DCM (0.40 mL), and the solution was cooled to $0\text{ }^\circ\text{C}$. A solution of Br_2 (10.2 μL , 0.40 mmol 1.0 equiv.) in DCM (0.20 mL) was added dropwise under N_2 and the reaction mixture stirred at $0\text{ }^\circ\text{C}$. After completion (about 1 h, followed by TLC), the reaction mixture was diluted with DCM and washed with 5% NaHCO_3 solution. The organic layer was then dried over MgSO_4 , filtered, and then concentrated. The residue was purified by flash chromatography to afford the dibrominated product **5.53** (70.2 mg, 83%, $>99:1$ *dr*) as a colorless solid. The X-ray molecular structure was also determined (Figure 5.3).

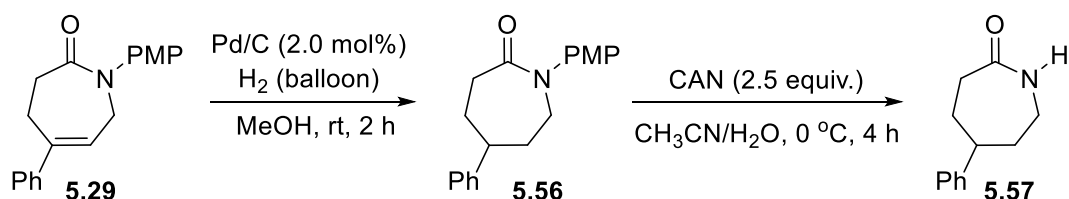


Under N_2 , to a magnetically stirred solution of caprolactam **5.3** (52.7 mg, 0.20 mmol, 1.0 equiv.) in DCM (1.0 mL) was added pyridinium chlorochromate (PCC, 86.2 mg, 0.40 mmol, 2.0 equiv.). The mixture was stirred at $40\text{ }^\circ\text{C}$ for 18 h, then cooled, diluted with water (10 mL), and extracted with EtOAc (3×10 mL). The combined organic layers were washed with 5% aqueous NaHCO_3 (10 mL), and dried with sodium sulfate, filtered, and then concentrated. Purification of the residue by flash chromatography to afford the desired product **5.54** (29.3 mg, 56%) as a colorless oil.



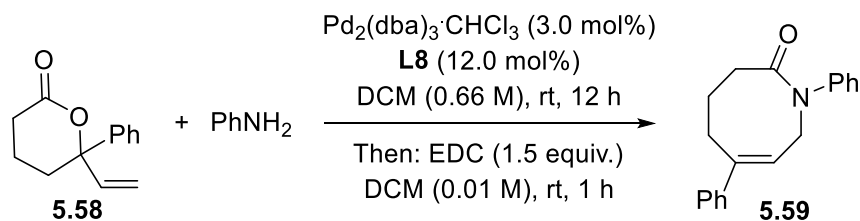
In a vial equipped with a magnetic stirring bar, caprolactam **5.29** (44.0 mg, 0.15 mmol, 1.0 equiv.) was dissolved into CH_3CN (0.9 mL) and stirred at $0\text{ }^\circ\text{C}$. A solution of CAN

(205.6 mg, 0.375 mmol, 2.5 equiv.) in H₂O (1.3 mL) was added dropwise. The resultant solution was stirred at 0 °C until no starting materials could be detected by TLC (about 40 min). Hereafter, saturated aqueous NaHCO₃ was added and the organic components were extracted with DCM (3 × 10 mL). The combined organic layers were then dried over MgSO₄, filtered, and then concentrated, the crude product was purified by flash chromatography to afford the deprotected lactam **5.55** (11.2 mg, 40%) as a light yellow solid.

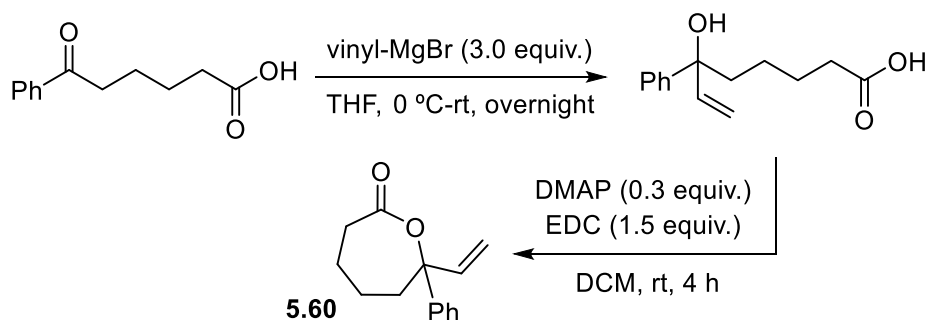


A Schlenk tube was charged with **5.29** (176.0 mg, 0.6 mmol, 1.0 equiv.) and Pd/C as catalyst (12.8 mg, 10.0 wt % palladium on carbon), and then the reactor was evacuated/filled with H₂ (balloon) for three times. After that, MeOH (2.0 mL) was added and the reaction mixture was stirred under H₂ atmosphere (balloon) for 2 h at room temperature, and monitored by NMR. The reaction mixture was filtered through Celite. The solvent in the filtrate was evaporated under reduced pressure. The residue was purified by flash chromatography to afford the pure saturated lactam **5.56** (159.5 mg, 90%) as a yellow solid.

In a vial equipped with a magnetic stirring bar, caprolactam **5.56** (44.3 mg, 0.15 mmol, 1.0 equiv.) was dissolved into CH₃CN (0.9 mL) and stirred at 0 °C. A solution of CAN (205.6 mg, 0.375 mmol, 2.5 equiv.) in H₂O (1.3 mL) was added dropwise. The resultant solution was stirred at 0 °C for 4 h. Hereafter, saturated aqueous NaHCO₃ was added and the organic components were extracted with DCM (3 × 10 mL). The combined organic layers were then dried over MgSO₄, filtered, and then concentrated, the crude product was purified by flash chromatography to afford the deprotected lactam **5.57** (21.3 mg, 75%) as a light brown solid.



Six-membered vinyl lactone **5.58** (40.5 mg, 0.20 mmol, 1.0 equiv.) was combined with $\text{Pd}_2(\text{dba})_3 \cdot \text{CHCl}_3$ (6.0 mg, 3.0 mol%), **L8** (9.6 mg, 12.0 mol%) and aniline (38.0 mg, 0.40 mmol) in DCM (0.30 mL) at room temperature in air. The reaction mixture was stirred at room temperature for 12 h, then an aliquot of the mixture was taken for NMR analysis, which showed the unsaturated amino acid intermediate to have an *E/Z* ratio of >99:1. Hereafter, the mixture was diluted to 0.01 M and EDC (57.5 mg, 0.30 mmol) was added and the reaction mixture stirred for another 1 h. The desired eight-membered lactam **5.59** (30.0 mg, 54%) was isolated by flash chromatography (Hexane/EtOAc = 2:1).



Under a N_2 atmosphere, to a separate flame-dried round-bottom flask equipped with a stirring bar was added the respective 5-benzoylpentanoic acid (1.0300 g, 5.0 mmol) and anhydrous THF (15 mL). The solution was cooled down to 0 °C (ice/water), followed by dropwise addition of vinyl magnesium bromide in THF (1.0 M, 15.0 mL, 15.0 mmol). The reaction mixture was allowed to warm to room temperature and stirred for 12 h. The reaction mixture was quenched with saturated aqueous NH_4Cl , then treated with HCl (4.0 M) until the pH was 3. The organic components were extracted with EtOAc (3×20 mL). Hereafter, the combined organic layers were washed with brine, dried over anhydrous Na_2SO_4 , filtered, and then concentrated under reduced pressure. The residue could be used directly for next step. To a solution of the 5-hydroxyl acid (1.0 equiv.) in DCM (15 mL) was added DMAP (0.1833 g, 0.3 equiv.) and EDC (1.4375 g, 1.5 equiv.). The reaction was stirred at room temperature for 4 h. The reaction mixture was then

concentrated under reduced pressure. The residue was purified by flash chromatography on silica to afford the vinyl ϵ -lactone substrate.

5.4.7 X-ray Crystallographic Studies

For the experimental procedure involved in the X-ray analyses of compounds **5.3** and **5.53** see chapter 2.

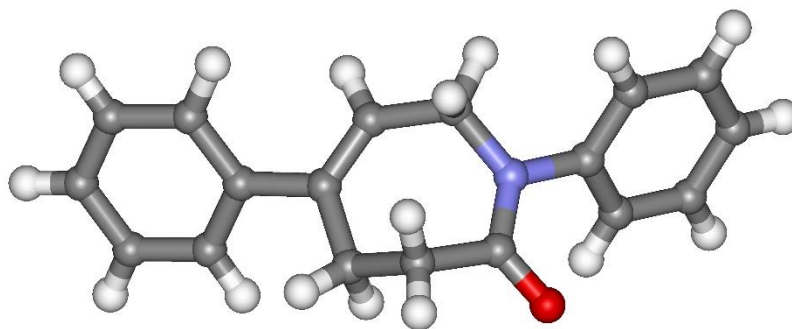


Figure 5.2 X-ray molecular structure determined for **5.3**.

Crystallographic data for 5.3:

$C_{18}H_{17}NO$, $M_r = 263.32$, monoclinic, $P21/c$, $a = 6.2396(2) \text{ \AA}$, $b = 23.7102(7) \text{ \AA}$, $c = 9.2667(3) \text{ \AA}$, $\alpha = 90^\circ$, $\beta = 96.543(3)^\circ$, $\gamma = 90^\circ$, $V = 1362.00(7) \text{ \AA}^3$, $Z = 4$, $\rho = 1.284 \text{ mg}\cdot\text{M}^{-3}$, $\mu = 0.079 \text{ mm}^{-1}$, $\lambda = 0.71073 \text{ \AA}$, $T = 100(2) \text{ K}$, $F(000) = 560$, crystal size = $0.30 \times 0.30 \times 0.20 \text{ mm}^3$, $\theta(\text{min}) = 2.373^\circ$, $\theta(\text{max}) = 29.432^\circ$, 12489 reflections collected, 3456 reflections unique ($R_{\text{int}} = 0.0208$), $\text{GoF} = 1.074$, $R_1 = 0.0389$ and $wR_2 = 0.1064 [I > 2\sigma(I)]$, $R_1 = 0.0429$ and $wR_2 = 0.1088$ (all indices), min/max residual density = $-0.182/0.348 \text{ [e}\cdot\text{\AA}^{-3}]$. Completeness to $\theta(29.432^\circ) = 91.5\%$. For further details see CCDC number 1998235.

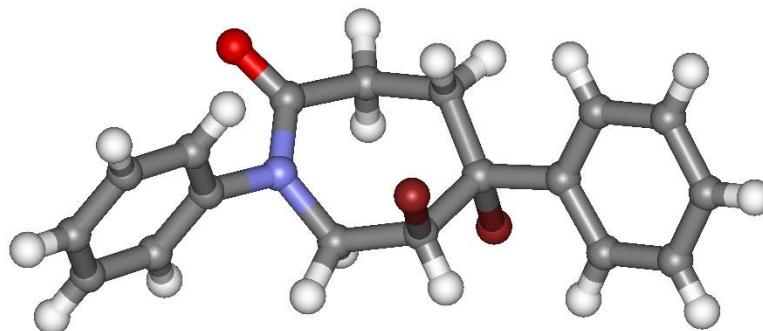
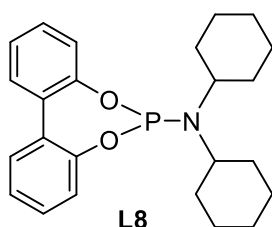


Figure 5.3 X-ray molecular structure determined for **5.53**.

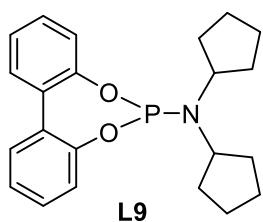
Crystallographic data for 5.53:

$C_{18}H_{17}Br_2NO$, $M_r = 423.14$, monoclinic, $P21/n$, $a = 13.0644(10) \text{ \AA}$, $b = 7.0550(6) \text{ \AA}$, $c = 17.3068(15) \text{ \AA}$, $\alpha = 90^\circ$, $\beta = 94.551(2)^\circ$, $\gamma = 90^\circ$, $V = 1590.1(2) \text{ \AA}^3$, $Z = 4$, $\rho = 1.768 \text{ mg} \cdot \text{M}^{-3}$, $\mu = 5.099 \text{ mm}^{-1}$, $\lambda = 0.71073 \text{ \AA}$, $T = 100(2) \text{ K}$, $F(000) = 840$, crystal size = $0.55 \times 0.35 \times 0.22 \text{ mm}^3$, $\theta(\text{min}) = 1.883^\circ$, $\theta(\text{max}) = 30.038^\circ$, 13440 reflections collected, 4162 reflections unique ($R_{\text{int}} = 0.0604$), $\text{GoF} = 1.050$, $R_1 = 0.0400$ and $wR_2 = 0.0923 [I > 2\sigma(I)]$, $R_1 = 0.0545$ and $wR_2 = 0.0979$ (all indices), min/max residual density = $-1.273/1.290 [e \cdot \text{\AA}^{-3}]$. Completeness to $\theta(30.038^\circ) = 89.5\%$. For further details see CCDC number 2001102.

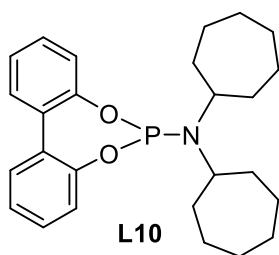
5.4.8 Analytical Data for All Compounds



White solid; Column conditions: Hexane : EA = 50 : 1, $R_f = 0.30$. $^1\text{H NMR}$ (400 MHz, CDCl_3) δ 7.45 (dd, $J = 7.6, 1.7 \text{ Hz}$, 2H), 7.32 (td, $J = 7.7, 1.7 \text{ Hz}$, 2H), 7.24 – 7.13 (m, 4H), 3.01 – 2.90 (m, 2H), 1.81 (d, $J = 12.4 \text{ Hz}$, 4H), 1.73 – 1.65 (m, 4H), 1.62 – 1.49 (m, 6H), 1.07 – 0.96 (m, 6H) ppm. $^{13}\text{C NMR}$ (101 MHz, CDCl_3) δ 152.09, 152.04, 131.13, 131.10, 129.79, 129.78, 129.00, 128.99, 124.20, 124.20, 122.09, 122.08, 54.08, 53.97, 35.40, 26.62, 25.63 ppm. $^{31}\text{P NMR}$ (162 MHz, CDCl_3) δ 155.25 ppm. **IR** (neat): ν (cm^{-1}) 2920, 2852, 1498, 1475, 1434, 1246, 1193, 1109, 1059, 879, 845, 763, 730, 674. **HRMS** (ESI+, MeOH): m/z calcd. 396.2087 ($\text{M} + \text{H}$)⁺, found: 396.2090.



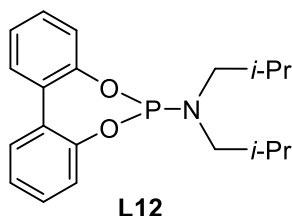
White solid; Column conditions: Hexane : EA = 50 : 1, $R_f = 0.30$. $^1\text{H NMR}$ (400 MHz, CDCl_3) δ 7.50 – 7.42 (m, 2H), 7.35 – 7.30 (m, 2H), 7.26 – 7.14 (m, 4H), 3.66 – 3.48 (m, 2H), 1.85 – 1.61 (m, 12H), 1.48 – 1.34 (m, 4H) ppm. $^{13}\text{C NMR}$ (101 MHz, CDCl_3) δ 151.79, 151.74, 131.14, 131.11, 129.82, 129.81, 128.98, 124.32, 122.32, 55.88, 55.76, 33.75, 33.67, 24.22 ppm. $^{31}\text{P NMR}$ (162 MHz, CDCl_3) δ 154.97 ppm. **IR** (neat): ν (cm^{-1}) 2951, 2868, 1496, 1474, 1434, 1247, 1191, 1096, 1065, 880, 844, 763, 731, 671. **HRMS** (ESI+, MeOH): m/z calcd. 368.1774 ($\text{M} + \text{H}$)⁺, found: 368.1778.



White solid; Column conditions: Hexane : EA = 50 : 1, R_f = 0.30.

$^1\text{H NMR}$ (400 MHz, CDCl_3) δ 7.45 (dd, J = 7.6, 1.8 Hz, 2H), 7.32 (td, J = 7.6, 1.7 Hz, 2H), 7.25 – 7.10 (m, 4H), 3.15 (qt, J = 11.1, 3.9 Hz, 2H), 1.98 – 1.87 (m, 4H), 1.83 – 1.68 (m, 4H), 1.65 – 1.55 (m, 4H), 1.50 – 1.37 (m, 8H), 1.27 – 1.08 (m, 4H) ppm.

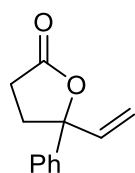
$^{13}\text{C NMR}$ (101 MHz, CDCl_3) δ 152.04, 151.99, 131.17, 131.15, 129.80, 129.79, 129.07, 129.06, 124.18, 124.17, 122.15, 122.14, 56.75, 56.65, 27.42, 25.39 ppm. **$^{31}\text{P NMR}$** (162 MHz, CDCl_3) δ 154.50 ppm. **IR** (neat): ν (cm^{-1}) 2921, 2853, 1497, 1474, 1434, 1247, 1193, 1093, 1066, 880, 844, 760, 730, 672. **HRMS** (ESI+, MeOH): m/z calcd. 424.2400 ($\text{M} + \text{H}$)⁺, found: 424.2421.



White solid; Column conditions: Hexane : EA = 50 : 1, R_f = 0.33.

$^1\text{H NMR}$ (400 MHz, CDCl_3) δ 7.46 (dd, J = 7.6, 1.7 Hz, 2H), 7.33 (td, J = 7.7, 1.7 Hz, 2H), 7.25 – 7.11 (m, 4H), 2.78 (dd, J = 10.5, 7.3 Hz, 4H), 1.86 (dp, J = 13.6, 6.8 Hz, 2H), 0.87 (d, J = 6.6 Hz, 12H) ppm. **$^{13}\text{C NMR}$** (101 MHz, CDCl_3) δ 151.93,

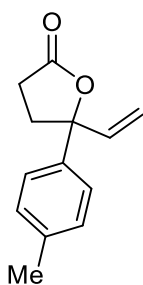
151.87, 131.13, 131.09, 129.76, 129.75, 129.16, 129.16, 124.33, 124.32, 122.20, 122.19, 52.45, 52.25, 25.52, 25.50, 20.31 ppm. **$^{31}\text{P NMR}$** (162 MHz, CDCl_3) δ 151.88 ppm. **IR** (neat): ν (cm^{-1}) 2960, 2924, 2855, 1498, 1474, 1464, 1433, 1371, 1245, 1186, 1095, 1019, 874, 865, 759, 730, 675, 514. **HRMS** (ESI+, MeOH): m/z calcd. 344.1774 ($\text{M} + \text{H}$)⁺, found: 344.1776.



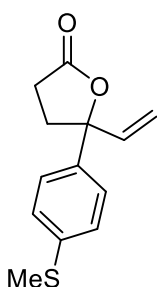
General procedure A: Colorless oil; Column conditions: Hexane : EA = 20 :

1, R_f = 0.18. **$^1\text{H NMR}$** (400 MHz, CDCl_3) δ 7.40 – 7.35 (m, 4H), 7.33 – 7.29 (m, 1H), 6.09 (dd, J = 17.2, 10.7 Hz, 1H), 5.32 (dd, J = 17.1, 0.7 Hz, 1H), 5.23 (dd, J = 10.7, 0.7 Hz, 1H), 2.68 – 2.47 (m, 4H) ppm. **$^{13}\text{C NMR}$** (101

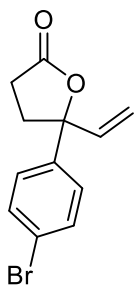
MHz, CDCl_3) δ 176.31, 141.72, 139.69, 128.75, 128.06, 125.02, 114.71, 88.32, 34.43, 28.65 ppm.¹⁵⁰



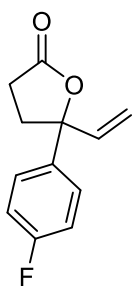
General procedure A: Colorless solid; Column conditions: Hexane : EA = 20 : 1, R_f = 0.18. **$^1\text{H NMR}$** (500 MHz, CDCl_3) δ 7.29 – 7.25 (m, 2H), 7.18 (d, J = 7.8 Hz, 2H), 6.07 (dd, J = 17.1, 10.7 Hz, 1H), 5.30 (dd, J = 17.1, 0.8 Hz, 1H), 5.20 (dd, J = 10.7, 0.8 Hz, 1H), 2.67 – 2.47 (m, 4H), 2.34 (s, 3H) ppm. **$^{13}\text{C NMR}$** (126 MHz, CDCl_3) δ 176.38, 139.83, 138.69, 137.83, 129.36, 124.98, 114.49, 88.34, 34.36, 28.67, 21.12 ppm. **IR** (neat): ν (cm^{-1}) 2947, 1772, 1510, 1414, 1197, 1159, 1066, 944, 805, 505. **HRMS** (ESI+, MeOH): m/z calcd. 203.1067 ($\text{M} + \text{H}$)⁺, found: 203.1068.



General procedure A: Yellow oil; Column conditions: Hexane : EA = 20 : 1, R_f = 0.15. **$^1\text{H NMR}$** (400 MHz, CDCl_3) δ 7.32 – 7.28 (m, 2H), 7.27 – 7.23 (m, 3H), 6.06 (dd, J = 17.1, 10.7 Hz, 1H), 5.31 (dd, J = 17.2, 0.7 Hz, 1H), 5.22 (dd, J = 10.7, 0.7 Hz, 1H), 2.66 – 2.45 (m, 7H) ppm. **$^{13}\text{C NMR}$** (101 MHz, CDCl_3) δ 176.23, 139.58, 138.73, 138.40, 126.67, 125.64, 114.87, 88.12, 34.36, 28.68, 15.81 ppm. **IR** (neat): ν (cm^{-1}) 2922, 1771, 1598, 1493, 1195, 1162, 1095, 967, 922, 819. **HRMS** (ESI+, MeOH): m/z calcd. 235.0787 ($\text{M} + \text{H}$)⁺, found: 235.0790.

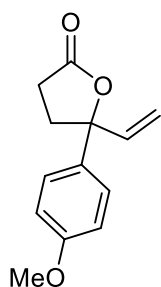


General procedure A: Yellow oil; Column conditions: Hexane : EA = 20 : 1, R_f = 0.15. **$^1\text{H NMR}$** (300 MHz, CDCl_3) δ 7.54 – 7.45 (m, 2H), 7.30 – 7.23 (m, 2H), 6.04 (dd, J = 17.1, 10.7 Hz, 1H), 5.31 (d, J = 17.1 Hz, 1H), 5.24 (d, J = 10.7 Hz, 1H), 2.69 – 2.41 (m, 4H) ppm. **$^{13}\text{C NMR}$** (101 MHz, CDCl_3) δ 175.87, 140.77, 139.09, 131.79, 126.79, 122.07, 115.10, 87.70, 34.22, 28.48 ppm. **IR** (neat): ν (cm^{-1}) 2949, 1773, 1590, 1487, 1396, 1195, 1160, 1008, 979, 922, 721. **HRMS** (ESI+, MeOH): m/z calcd. 288.9835 ($\text{M} + \text{Na}$)⁺, found: 288.9835.

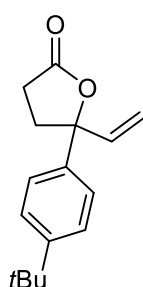


General procedure A: Yellow oil; Column conditions: Hexane : EA = 20 : 1, R_f = 0.18. **$^1\text{H NMR}$** (400 MHz, CDCl_3) δ 7.39 – 7.32 (m, 2H), 7.08 – 7.00 (m, 2H), 6.04 (dd, J = 17.1, 10.7 Hz, 1H), 5.29 (dd, J = 17.2, 0.6 Hz, 1H), 5.22 (dd, J = 10.7, 0.6 Hz, 1H), 2.67 – 2.43 (m, 4H) ppm. **$^{13}\text{C NMR}$** (101 MHz, CDCl_3) δ 176.03, 162.38 (d, J = 247.0 Hz), 139.48, 137.51 (d, J = 3.3 Hz), 126.95 (d, J = 8.4 Hz), 115.58 (d, J = 21.6 Hz), 114.89, 87.83, 34.35, 28.59 ppm. **$^{19}\text{F NMR}$** (376 MHz, CDCl_3) δ -114.34 ppm. **IR** (neat): ν (cm^{-1}) 2991, 1773,

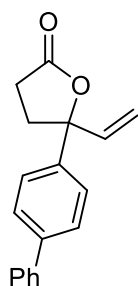
1602, 1508, 1415, 1227, 1195, 1158, 923, 835, 812, 642, 539. **HRMS** (ESI+, MeOH): m/z calcd. 207.0816 (M + H)⁺, found: 207.0818.



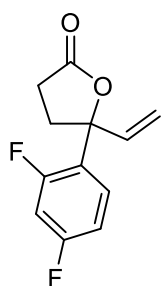
General procedure **A**: Yellow oil; Column conditions: Hexane : DCM = 1 : 1, R_f = 0.20. **¹H NMR** (500 MHz, CDCl₃) δ 7.33 – 7.26 (m, 2H), 6.91 – 6.86 (m, 2H), 6.06 (dd, J = 17.2, 10.7 Hz, 1H), 5.28 (dd, J = 17.2, 0.8 Hz, 1H), 5.20 (dd, J = 10.7, 0.7 Hz, 1H), 3.79 (s, 3H), 2.65 – 2.47 (m, 4H) ppm. **¹³C NMR** (126 MHz, CDCl₃) δ 176.39, 159.35, 139.88, 133.54, 126.68, 126.46, 114.47, 114.02, 113.81, 88.25, 55.40, 34.26, 28.73 ppm.¹⁵⁰



General procedure **A**: Slight yellow oil; Column conditions: Hexane : EA = 20 : 1, R_f = 0.20. **¹H NMR** (400 MHz, CDCl₃) δ 7.42 – 7.36 (m, 2H), 7.35 – 7.27 (m, 2H), 6.09 (dd, J = 17.2, 10.7 Hz, 1H), 5.33 (dd, J = 17.2, 0.7 Hz, 1H), 5.21 (dd, J = 10.7, 0.7 Hz, 1H), 2.66 – 2.49 (m, 4H), 1.32 (s, 9H) ppm. **¹³C NMR** (101 MHz, CDCl₃) δ 176.46, 151.11, 139.85, 138.65, 125.67, 124.80, 114.42, 88.38, 34.67, 34.36, 31.42, 28.72 ppm. **IR** (neat): ν (cm⁻¹) 2960, 2870, 1771, 1514, 1408, 1236, 1193, 1166, 976, 905, 835, 579. **HRMS** (ESI+, MeOH): m/z calcd. 267.1356 (M + Na)⁺, found: 267.1359.

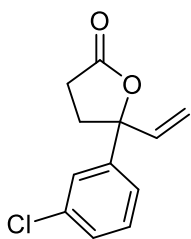


General procedure **A**: White solid; Column conditions: Hexane : EA = 20 : 1, R_f = 0.10. **¹H NMR** (400 MHz, CDCl₃) δ 7.63 – 7.56 (m, 4H), 7.49 – 7.42 (m, 4H), 7.39 – 7.33 (m, 1H), 6.13 (dd, J = 17.2, 10.7 Hz, 1H), 5.37 (dd, J = 17.2, 0.7 Hz, 1H), 5.26 (dd, J = 10.7, 0.7 Hz, 1H), 2.71 – 2.51 (m, 4H) ppm. **¹³C NMR** (101 MHz, CDCl₃) δ 176.29, 141.07, 140.69, 140.51, 139.62, 128.98, 127.69, 127.49, 127.24, 125.53, 114.84, 88.25, 34.46, 28.69 ppm. **IR** (neat): ν (cm⁻¹) 3033, 1768, 1487, 1410, 1230, 1182, 982, 919, 762, 730, 690. **HRMS** (ESI+, MeOH): m/z calcd. 265.1223 (M + H)⁺, found: 265.1226.

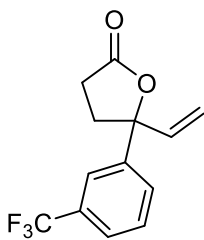


General procedure **A**: Yellow oil; Column conditions: Hexane : DCM = 1 : 1, R_f = 0.15. **¹H NMR** (400 MHz, CDCl₃) δ 7.51 (td, J = 8.9, 6.4 Hz, 1H), 6.92 – 6.81 (m, 2H), 6.15 (ddd, J = 17.1, 10.7, 1.6 Hz, 1H), 5.35 (ddd, J = 17.1, 1.5, 0.6 Hz, 1H), 5.22 (d, J = 10.7 Hz, 1H), 2.76 – 2.48 (m, 4H) ppm. **¹³C NMR** (101 MHz, CDCl₃) δ 175.80, 162.86 (dd, J = 249.8, 12.1 Hz), 159.11 (dd, J = 249.1, 11.7 Hz), 137.61 (d, J = 2.6 Hz), 127.52 (dd, J = 9.5,

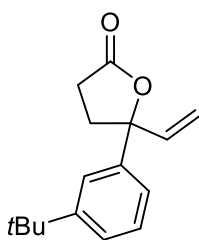
5.5 Hz), 125.53 (dd, $J = 12.5, 4.0$ Hz), 115.08, 111.59 (dd, $J = 20.9, 3.7$ Hz), 104.78 (t, $J = 25.7$ Hz), 85.85 (d, $J = 3.7$ Hz), 33.93 (d, $J = 5.1$ Hz), 28.04 (d, $J = 1.8$ Hz) ppm. **^{19}F NMR** (376 MHz, CDCl_3) δ -109.75 (d, $J = 8.0$ Hz), -110.45 (d, $J = 8.0$ Hz) ppm. **IR** (neat): ν (cm^{-1}) 3083, 2956, 1780, 1616, 1600, 1422, 1272, 1142, 1109, 965, 849, 613, 576. **HRMS** (ESI+, MeOH): m/z calcd. 247.0541 ($\text{M} + \text{Na}$)⁺, found: 247.0544.



General procedure A: Yellow oil; Column conditions: Hexane : DCM = 1 : 1, $R_f = 0.18$. **^1H NMR** (400 MHz, CDCl_3) δ 7.40 – 7.36 (m, 1H), 7.36 – 7.29 (m, 2H), 7.29 – 7.25 (m, 1H), 6.05 (dd, $J = 17.1, 10.7$ Hz, 1H), 5.34 (dd, $J = 17.1, 0.5$ Hz, 1H), 5.26 (dd, $J = 10.7, 0.5$ Hz, 1H), 2.69 – 2.44 (m, 4H) ppm. **^{13}C NMR** (101 MHz, CDCl_3) δ 175.85, 143.89, 139.07, 134.85, 130.13, 128.30, 125.42, 123.21, 115.30, 87.60, 34.40, 28.53 ppm. **IR** (neat): ν (cm^{-1}) 3071, 1774, 1573, 1415, 1231, 1195, 1162, 984, 904, 786, 695. **HRMS** (ESI+, MeOH): m/z calcd. 245.0340 ($\text{M} + \text{Na}$)⁺, found: 245.0344.

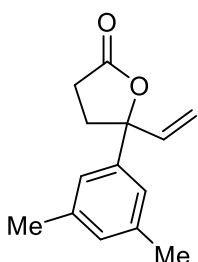


General procedure A: Yellow oil; Column conditions: Hexane : EA = 20 : 1, $R_f = 0.15$. **^1H NMR** (400 MHz, CDCl_3) δ 7.64 (s, 1H), 7.61 – 7.55 (m, 2H), 7.53 – 7.41 (m, 1H), 6.07 (dd, $J = 17.2, 10.7$ Hz, 1H), 5.36 (d, $J = 17.1$ Hz, 1H), 5.28 (d, $J = 10.7$ Hz, 1H), 2.72 – 2.61 (m, 2H), 2.59 – 2.45 (m, 2H) ppm. **^{13}C NMR** (101 MHz, CDCl_3) δ 175.75, 142.99, 138.95, 131.27 (q, $J = 32.5$ Hz), 129.40, 128.47, 128.46, 125.02 (q, $J = 3.8$ Hz), 124.02 (q, $J = 272.4$ Hz), 121.90 (q, $J = 3.9$ Hz), 115.50, 87.62, 77.48, 77.16, 76.84, 34.37, 28.51 ppm. **^{19}F NMR** (376 MHz, CDCl_3) δ -62.34 ppm. **IR** (neat): ν (cm^{-1}) 2956, 1779, 1416, 1332, 1230, 1164, 1119, 1073, 986, 906, 803, 700. **HRMS** (ESI+, MeOH): m/z calcd. 279.0603 ($\text{M} + \text{Na}$)⁺, found: 279.0609.

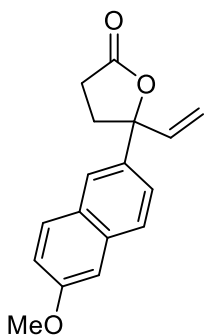


General procedure A: Colorless oil; Column conditions: Hexane : EA = 20 : 1, $R_f = 0.20$. **^1H NMR** (400 MHz, CDCl_3) δ 7.42 – 7.38 (m, 1H), 7.36 – 7.28 (m, 2H), 7.21 – 7.13 (m, 1H), 6.09 (dd, $J = 17.1, 10.7$ Hz, 1H), 5.33 (dd, $J = 17.2, 0.7$ Hz, 1H), 5.22 (dd, $J = 10.7, 0.7$ Hz, 1H), 2.68 – 2.48 (m, 4H), 1.32 (s, 9H) ppm. **^{13}C NMR** (101 MHz, CDCl_3) δ 176.46, 151.83, 141.41, 139.92, 128.41, 125.08, 122.13, 121.86, 114.43, 88.61, 35.01, 34.45, 31.48, 28.70 ppm. **IR** (neat): ν (cm^{-1}) 2982, 2870, 1776, 1487, 1419, 1365, 1230,

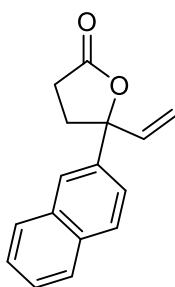
1195, 1164, 908, 796, 706. **HRMS** (ESI+, MeOH): m/z calcd. 267.1356 (M + Na)⁺, found: 267.1357.



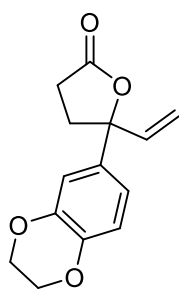
General procedure A: Colorless oil; Column conditions: Hexane : EA = 20 : 1, R_f = 0.20. **¹H NMR** (400 MHz, CDCl₃) δ 6.99 (s, 2H), 6.94 (s, 1H), 6.08 (dd, J = 17.2, 10.7 Hz, 1H), 5.32 (dd, J = 17.2, 0.8 Hz, 1H), 5.21 (dd, J = 10.7, 0.7 Hz, 1H), 2.66 – 2.46 (m, 4H), 2.32 (s, 6H) ppm. **¹³C NMR** (101 MHz, CDCl₃) δ 176.48, 141.72, 139.84, 138.41, 129.65, 122.72, 114.39, 88.41, 34.45, 28.69, 21.53 ppm. **IR** (neat): ν (cm⁻¹) 2916, 1774, 1606, 1457, 1412, 1237, 1186, 1158, 910, 849, 704. **HRMS** (ESI+, MeOH): m/z calcd. 239.1043 (M + Na)⁺, found: 239.1032.



General procedure A: White solid; Column conditions: Hexane : EA = 10 : 1, R_f = 0.11. **¹H NMR** (400 MHz, CDCl₃) δ 7.80 – 7.72 (m, 3H), 7.42 (dd, J = 8.6, 1.9 Hz, 1H), 7.19 – 7.12 (m, 2H), 6.17 (dd, J = 17.2, 10.7 Hz, 1H), 5.36 (dd, J = 17.2, 0.7 Hz, 1H), 5.26 (dd, J = 10.7, 0.7 Hz, 1H), 3.92 (s, 3H), 2.71 – 2.52 (m, 4H) ppm. **¹³C NMR** (101 MHz, CDCl₃) δ 176.45, 158.28, 139.73, 136.55, 134.13, 129.83, 128.53, 127.52, 123.81, 123.66, 119.53, 114.98, 105.72, 88.53, 55.48, 34.35, 28.75 ppm. **IR** (neat): ν (cm⁻¹) 2995, 2954, 1773, 1602, 1484, 1390, 1266, 1199, 1163, 914, 852, 819, 479. **HRMS** (ESI+, MeOH): m/z calcd. 291.0992 (M + Na)⁺, found: 291.0989.

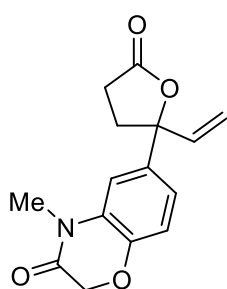


General procedure A: White solid; Column conditions: Hexane : EA = 10 : 1, R_f = 0.13. **¹H NMR** (400 MHz, CDCl₃) δ 7.90 – 7.82 (m, 4H), 7.54 – 7.43 (m, 3H), 6.18 (dd, J = 17.1, 10.7 Hz, 1H), 5.38 (dd, J = 17.2, 0.7 Hz, 1H), 5.28 (dd, J = 10.7, 0.7 Hz, 1H), 2.72 – 2.52 (m, 4H) ppm. **¹³C NMR** (101 MHz, CDCl₃) δ 176.34, 139.57, 138.90, 133.11, 132.90, 128.72, 128.37, 127.74, 126.72, 126.62, 123.74, 123.23, 115.18, 88.46, 34.38, 28.69 ppm. **IR** (neat): ν (cm⁻¹) 3059, 2960, 1764, 1600, 1505, 1422, 1248, 1226, 1149, 1027, 926, 818, 750, 475. **HRMS** (ESI+, MeOH): m/z calcd. 239.1067 (M + H)⁺, found: 239.1059.



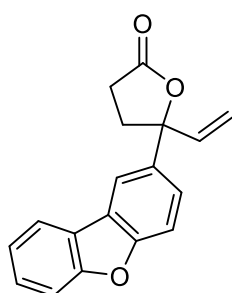
General procedure A: Colorless oil; Column conditions: Hexane : EA = 20 : 1, R_f = 0.15. $^1\text{H NMR}$ (400 MHz, CDCl_3) δ 6.91 – 6.87 (m, 1H), 6.86 – 6.81 (m, 2H), 6.04 (dd, J = 17.2, 10.7 Hz, 1H), 5.30 (dd, J = 17.2, 0.6 Hz, 1H), 5.20 (dd, J = 10.7, 0.6 Hz, 1H), 4.25 (s, 4H), 2.66 – 2.45 (m, 4H) ppm. $^{13}\text{C NMR}$ (101 MHz, CDCl_3) δ 176.31, 143.60, 143.40, 139.71, 134.89, 118.21, 117.49, 114.53, 114.49, 88.02, 64.51, 34.32, 28.75 ppm.

IR (neat): ν (cm^{-1}) 2991, 2938, 2881, 1776, 1589, 1504, 1425, 1309, 1282, 1181, 1097, 1064, 891, 809, 647. **HRMS** (ESI+, MeOH): m/z calcd. 247.0965 ($\text{M} + \text{H}$)⁺, found: 247.0955.



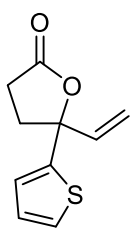
General procedure A: Colorless solid; Column conditions: Hexane : EA = 5 : 1, R_f = 0.10. $^1\text{H NMR}$ (400 MHz, CDCl_3) δ 7.02 (dd, J = 1.7, 0.8 Hz, 1H), 6.99 – 6.93 (m, 2H), 6.05 (dd, J = 17.2, 10.7 Hz, 1H), 5.32 (dd, J = 17.1, 0.6 Hz, 1H), 5.24 (dd, J = 10.7, 0.7 Hz, 1H), 4.61 (s, 2H), 3.36 (s, 3H), 2.70 – 2.46 (m, 4H) ppm. $^{13}\text{C NMR}$ (101 MHz, CDCl_3) δ 176.08, 164.53, 144.81, 139.48, 136.47, 129.83,

120.38, 116.93, 114.90, 111.91, 87.93, 67.63, 34.31, 28.66, 28.28 ppm. **IR** (neat): ν (cm^{-1}) 2929, 1773, 1679, 1477, 1421, 1281, 1198, 1169, 917, 802, 637. **HRMS** (ESI+, MeOH): m/z calcd. 274.1074 ($\text{M} + \text{H}$)⁺, found: 274.1075.

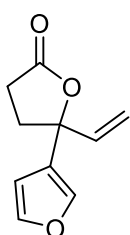


General procedure A: White solid; Column conditions: Hexane : EA = 10 : 1, R_f = 0.10. $^1\text{H NMR}$ (400 MHz, CDCl_3) δ 8.03 – 8.00 (m, 1H), 7.98 – 7.92 (m, 1H), 7.58 – 7.52 (m, 2H), 7.49 – 7.42 (m, 2H), 7.37 – 7.32 (m, 1H), 6.16 (dd, J = 17.2, 10.7 Hz, 1H), 5.36 (dd, J = 17.2, 0.7 Hz, 1H), 5.26 (dd, J = 10.7, 0.7 Hz, 1H), 2.74 – 2.52 (m, 4H) ppm. $^{13}\text{C NMR}$ (101 MHz, CDCl_3) δ 176.26, 156.74, 155.65,

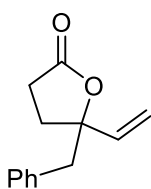
139.92, 136.36, 127.62, 124.49, 124.27, 123.95, 123.03, 120.86, 117.38, 114.75, 111.84, 111.79, 88.46, 34.66, 28.73 ppm. **IR** (neat): ν (cm^{-1}) 2947, 1771, 1447, 1402, 1232, 1197, 1071, 906, 810, 750, 646. **HRMS** (ESI+, MeOH): m/z calcd. 301.0835 ($\text{M} + \text{Na}$)⁺, found: 301.0841.



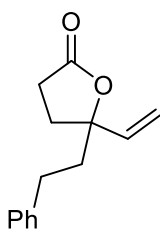
General procedure **B**: Yellow oil; Column conditions: Hexane : EA = 20 : 1, $R_f = 0.15$. $^1\text{H NMR}$ (400 MHz, CDCl_3) δ 7.32 (dd, $J = 5.1, 1.3$ Hz, 1H), 7.08 – 7.02 (m, 1H), 7.00 (dd, $J = 5.0, 3.6$ Hz, 1H), 6.15 (dd, $J = 17.1, 10.7$ Hz, 1H), 5.41 (dd, $J = 17.1, 0.6$ Hz, 1H), 5.30 (dd, $J = 10.6, 0.6$ Hz, 1H), 2.70 – 2.52 (m, 4H) ppm. $^{13}\text{C NMR}$ (101 MHz, CDCl_3) δ 175.82, 144.80, 138.94, 127.14, 126.21, 125.31, 115.46, 86.16, 35.49, 28.86 ppm. **IR** (neat): ν (cm^{-1}) 3098, 1771, 1412, 1238, 1180, 1149, 952, 909, 844, 703. **HRMS** (ESI+, MeOH): m/z calcd. 195.0474 ($\text{M} + \text{H}$) $^+$, found: 195.0471.



General procedure **B**: Colorless oil; Column conditions: Hexane : DCM = 1 : 1, $R_f = 0.13$. $^1\text{H NMR}$ (400 MHz, CDCl_3) δ 7.48 – 7.37 (m, 2H), 6.37 (dd, $J = 1.9, 1.0$ Hz, 1H), 6.06 (dd, $J = 17.2, 10.7$ Hz, 1H), 5.35 (dd, $J = 17.1, 0.7$ Hz, 1H), 5.27 (dd, $J = 10.7, 0.7$ Hz, 1H), 2.68 – 2.53 (m, 2H), 2.50 – 2.38 (m, 2H) ppm. $^{13}\text{C NMR}$ (101 MHz, CDCl_3) δ 176.24, 144.11, 139.55, 138.63, 127.06, 115.62, 108.83, 84.22, 34.10, 28.66 ppm. **IR** (neat): ν (cm^{-1}) 3147, 2926, 1769, 1504, 1414, 1198, 1162, 1018, 911, 868, 795, 600. **HRMS** (ESI+, MeOH): m/z calcd. 179.0703 ($\text{M} + \text{H}$) $^+$, found: 179.0700.

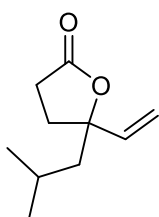


General procedure **B**: Yellow oil; Column conditions: Hexane : EA = 20 : 1, $R_f = 0.18$. $^1\text{H NMR}$ (400 MHz, CDCl_3) δ 7.34 – 7.20 (m, 5H), 5.90 (dd, $J = 17.2, 10.9$ Hz, 1H), 5.28 (dd, $J = 17.2, 0.9$ Hz, 1H), 5.17 (dd, $J = 10.9, 0.9$ Hz, 1H), 3.10 (d, $J = 14.0$ Hz, 1H), 2.96 (d, $J = 14.0$ Hz, 1H), 2.46 – 2.35 (m, 1H), 2.24 – 2.04 (m, 3H) ppm. $^{13}\text{C NMR}$ (101 MHz, CDCl_3) δ 176.71, 139.38, 135.06, 130.72, 128.48, 127.19, 114.56, 87.35, 45.82, 31.00, 28.52 ppm. **IR** (neat): ν (cm^{-1}) 3063, 3030, 2937, 1769, 1497, 1455, 1415, 1175, 1000, 924, 702. **HRMS** (ESI+, MeOH): m/z calcd. 225.0886 ($\text{M} + \text{Na}$) $^+$, found: 225.0887.

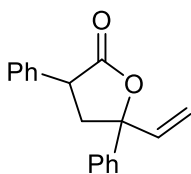


General procedure **B**: Light yellow oil; Column conditions: Hexane : EA = 20 : 1, $R_f = 0.15$. $^1\text{H NMR}$ (400 MHz, CDCl_3) δ 7.35 – 7.28 (m, 2H), 7.26 – 7.16 (m, 3H), 5.90 (dd, $J = 17.3, 10.9$ Hz, 1H), 5.39 (dd, $J = 17.2, 0.9$ Hz, 1H), 5.29 (dd, $J = 10.9, 0.9$ Hz, 1H), 2.81 – 2.50 (m, 4H), 2.25 – 2.01 (m, 4H) ppm. $^{13}\text{C NMR}$ (101 MHz, CDCl_3) δ 176.76, 141.39, 138.63, 128.60, 128.37, 126.16, 115.02, 87.58, 42.00, 32.70, 30.20, 28.33 ppm. **IR** (neat): ν (cm^{-1})

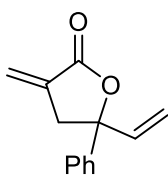
¹) 3026, 2944, 1769, 1497, 1455, 1414, 1185, 997, 939, 752, 699. **HRMS** (ESI+, MeOH): *m/z* calcd. 239.1043 (M + Na)⁺, found: 239.1052.



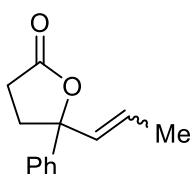
General procedure **A**: Light yellow oil; Column conditions: Hexane : EA = 20 : 1, *R_f* = 0.15. **¹H NMR** (400 MHz, CDCl₃) δ 5.81 (dd, *J* = 17.2, 10.9 Hz, 1H), 5.29 (dd, *J* = 17.2, 0.9 Hz, 1H), 5.19 (dd, *J* = 10.9, 0.9 Hz, 1H), 2.56 – 2.40 (m, 2H), 2.17 – 2.00 (m, 2H), 1.84 – 1.74 (m, 1H), 1.72 – 1.60 (m, 2H), 0.93 (dd, *J* = 9.6, 6.6 Hz, 6H) ppm. **¹³C NMR** (101 MHz, CDCl₃) δ 177.10, 139.02, 114.31, 88.32, 48.92, 33.82, 28.11, 24.64, 24.33, 23.70 ppm. **IR** (neat): *ν* (cm⁻¹) 2955, 2872, 1770, 1467, 1414, 1186, 1131, 965, 918. **HRMS** (ESI+, MeOH): *m/z* calcd. 191.1043 (M + Na)⁺, found: 191.1036.



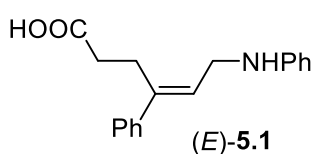
General procedure **B**: Slight yellow oil (39:61 *dr*); Column conditions: Hexane : DCM = 1 : 1, *R_f* = 0.20. **¹H NMR** (400 MHz, CDCl₃) δ 7.50 – 7.25 (m, 10H), 6.29 – 6.07 (m, 1H), 5.51 (d, *J* = 17.1 Hz, 0.39H), 5.34 – 5.23 (m, 2H), 4.03 (dd, *J* = 12.6, 8.3 Hz, 0.39H), 3.74 (dd, *J* = 12.5, 8.3 Hz, 0.61H), 3.17 – 3.08 (m, 1H), 2.78 – 2.62 (m, 1H) ppm. **¹³C NMR** (126 MHz, CDCl₃) δ 176.19, 176.14, 142.07, 140.76, 140.31, 139.25, 136.14, 136.13, 129.00, 128.97, 128.86, 128.85, 128.36, 128.30, 128.26, 128.15, 127.85, 127.83, 125.46, 124.80, 115.69, 114.52, 86.19, 85.70, 46.22, 46.02, 43.90, 43.08 ppm. **IR** (neat): *ν* (cm⁻¹) 3030, 1770, 1496, 1448, 1176, 987, 931, 755, 695. **HRMS** (ESI+, MeOH): *m/z* calcd. 287.1043 (M + Na)⁺, found: 287.1044.



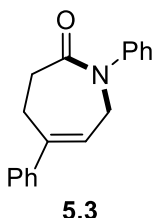
General procedure **A**: Yellow oil; Column conditions: Hexane : EA = 20 : 1, *R_f* = 0.15. **¹H NMR** (400 MHz, CDCl₃) δ 7.46 – 7.25 (m, 5H), 6.25 (t, *J* = 2.7 Hz, 1H), 6.10 (dd, *J* = 17.1, 10.7 Hz, 1H), 5.64 (t, *J* = 2.4 Hz, 1H), 5.33 – 5.17 (m, 2H), 3.38 – 3.18 (m, 2H) ppm. **¹³C NMR** (101 MHz, CDCl₃) δ 169.46, 141.90, 140.08, 134.33, 128.68, 128.03, 125.06, 122.70, 114.82, 85.17, 40.93 ppm. **IR** (neat): *ν* (cm⁻¹) 3063, 1761, 1448, 1408, 1273, 1172, 983, 931, 763, 699. **HRMS** (ESI+, MeOH): *m/z* calcd. 223.0730 (M + Na)⁺, found: 223.0731.



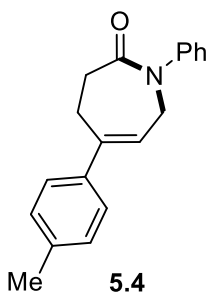
General procedure **B** (from 1-propenylmagnesium bromide): Yellow oil; Column conditions: Hexane : EA = 20 : 1, R_f = 0.13. $^1\text{H NMR}$ (400 MHz, CDCl_3) δ 7.44 – 7.33 (m, 4H), 7.33 – 7.26 (m, 1H), 5.85 – 5.64 (m, 2H), 2.70 – 2.44 (m, 4H), 1.72 – 1.60 (m, 3H) ppm. The lactone is a mixture of two stereoisomers with a ratio of E/Z = 54:46. $^{13}\text{C NMR}$ (101 MHz, CDCl_3) δ 176.66, 176.53, 143.54, 142.45, 133.09, 132.22, 130.69, 128.69, 128.64, 127.87, 127.78, 126.74, 125.11, 124.93, 88.39, 88.27, 38.00, 34.96, 28.92, 28.90, 17.79, 14.60 ppm. **IR** (neat): ν (cm^{-1}) 3029, 2918, 2851, 1771, 1448, 1228, 1190, 1161, 908, 759, 699. **HRMS** (ESI+, MeOH): m/z calcd. 225.0886 ($\text{M} + \text{Na}$) $^+$, found: 225.0877.



$^1\text{H NMR}$ (400 MHz, CDCl_3) δ 7.35 – 7.27 (m, 5H), 7.23 – 7.17 (m, 3H), 6.76 (tt, J = 7.4, 1.1 Hz, 1H), 6.72 – 6.66 (m, 2H), 5.86 (t, J = 6.6 Hz, 1H), 3.96 (d, J = 6.7 Hz, 2H), 2.93 (t, J = 7.7 Hz, 2H), 2.44 – 2.38 (m, 2H) ppm. $^{13}\text{C NMR}$ (101 MHz, CDCl_3) δ 178.89, 147.99, 141.16, 129.43, 128.64, 127.65, 127.14, 126.61, 118.12, 113.52, 42.50, 32.89, 25.16 ppm. **IR** (neat): ν (cm^{-1}) 3372, 3055, 3026, 2921, 1703, 1600, 1560, 1492, 1411, 1316, 1278, 1195, 906, 746, 691. **HRMS** (ESI+, MeOH): m/z calcd. 280.1343 ($\text{M} - \text{H}$) $^-$, found: 280.1349.

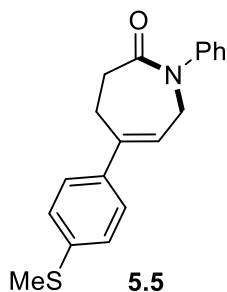


Scale: 0.20 mmol; E/Z = 98:2, isolated 43.2 mg (82% yield), slight yellow solid, Hexane : EA = 2 : 1, R_f = 0.25. $^1\text{H NMR}$ (500 MHz, CDCl_3) δ 7.37 – 7.29 (m, 6H), 7.28 – 7.17 (m, 4H), 6.13 (tt, J = 6.1, 1.9 Hz, 1H), 4.41 (dt, J = 6.1, 2.2 Hz, 2H), 3.07 – 3.01 (m, 2H), 2.91– 2.85 (m, 2H) ppm. $^{13}\text{C NMR}$ (126 MHz, CDCl_3) δ 173.78, 143.78, 142.90, 142.51, 129.17, 128.60, 127.90, 126.67, 125.95, 125.90, 122.19, 49.49, 34.17, 28.36 ppm. **IR** (neat): ν (cm^{-1}) 2929, 1656, 1594, 1492, 1445, 1412, 1214, 1164, 735, 693. **HRMS** (ESI+, MeOH): m/z calcd. 264.1383 ($\text{M} + \text{H}$) $^+$, found: 264.1379.

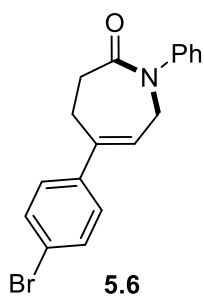


Scale: 0.20 mmol; E/Z = 96:4, isolated 44.9 mg (81% yield), yellow solid, Hexane : EA = 2 : 1, R_f = 0.25. $^1\text{H NMR}$ (400 MHz, CDCl_3) δ 7.40 – 7.34 (m, 2H), 7.32 – 7.19 (m, 8H), 6.17 (tt, J = 6.1, 1.9 Hz, 1H), 4.44 (dt, J = 6.1, 2.1 Hz, 2H), 3.12 – 3.01 (m, 2H), 2.94 – 2.86 (m, 2H), 2.49 (s, 3H) ppm. $^{13}\text{C NMR}$ (101 MHz, CDCl_3) δ (101 MHz, CDCl_3) δ 173.74, 143.75, 142.12, 139.18, 138.28, 129.18, 126.68, 126.65,

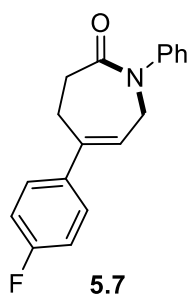
126.26, 125.94, 121.74, 49.48, 34.12, 28.19, 15.95 ppm. **IR** (neat): ν (cm^{-1}) 3307, 3027, 2920, 1659, 1595, 1494, 1444, 1218, 1163, 909, 813, 731, 694. **HRMS** (ESI+, MeOH): m/z calcd. 300.1359 ($\text{M} + \text{Na}$)⁺, found: 300.1360.



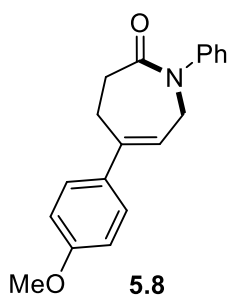
Scale: 0.20 mmol $E/Z = 90:10$, isolated 50.7 mg (82% yield), yellow solid, Hexane : EA = 2 : 1, $R_f = 0.25$. **¹H NMR** (400 MHz, CDCl_3) δ 7.40 – 7.34 (m, 2H), 7.32 – 7.19 (m, 8H), 6.17 (tt, $J = 6.1, 1.9$ Hz, 1H), 4.44 (dt, $J = 6.1, 2.1$ Hz, 2H), 3.12 – 3.01 (m, 2H), 2.94 – 2.86 (m, 2H), 2.49 (s, 3H) ppm. **¹³C NMR** (101 MHz, CDCl_3) δ 173.74, 143.75, 142.12, 139.18, 138.28, 129.18, 126.68, 126.65, 126.26, 125.94, 121.74, 49.48, 34.12, 28.19, 15.95 ppm. **IR** (neat): ν (cm^{-1}) 3307, 3042, 2919, 1659, 1593, 1493, 1442, 1414, 1215, 1094, 757, 694. **HRMS** (ESI+, MeOH): m/z calcd. 310.1260 ($\text{M} + \text{H}$)⁺, found: 310.1267.



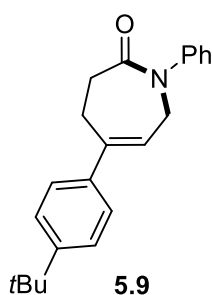
Scale: 0.20 mmol; $E/Z = 97:3$, isolated 57.5 mg (84% yield), yellow solid, Hexane : EA = 2 : 1, $R_f = 0.25$. **¹H NMR** (400 MHz, CDCl_3) δ 7.50 – 7.44 (m, 2H), 7.40 – 7.34 (m, 2H), 7.28 – 7.19 (m, 5H), 6.17 (tt, $J = 6.1, 1.9$ Hz, 1H), 4.44 (dt, $J = 6.1, 2.2$ Hz, 2H), 3.08 – 3.04 (m, 2H), 2.90 – 2.86 (m, 2H) ppm. **¹³C NMR** (101 MHz, CDCl_3) δ 173.58, 143.62, 141.78, 141.28, 131.66, 129.16, 127.51, 126.71, 125.88, 122.74, 121.82, 49.36, 34.01, 28.15 ppm. **IR** (neat): ν (cm^{-1}) 3307, 3059, 2917, 1657, 1594, 1490, 1444, 1398, 1213, 1007, 818, 733, 693. **HRMS** (ESI+, MeOH): m/z calcd. 342.0488 ($\text{M} + \text{H}$)⁺, found: 342.0499.



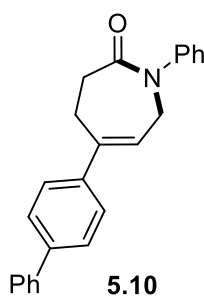
Scale: 0.20 mmol; $E/Z = 97:3$, isolated 50.6 mg (90% yield), yellow solid, Hexane : EA = 2 : 1, $R_f = 0.25$. **¹H NMR** (400 MHz, CDCl_3) δ 7.41 – 7.30 (m, 4H), 7.30 – 7.20 (m, 3H), 7.09 – 6.97 (m, 2H), 6.13 (tt, $J = 6.1, 1.8$ Hz, 1H), 4.44 (dt, $J = 6.1, 2.1$ Hz, 2H), 3.11 – 3.02 (m, 2H), 2.92 – 2.83 (m, 2H) ppm. **¹³C NMR** (101 MHz, CDCl_3) δ 173.62, 162.51 (d, $J = 246.6$ Hz), 143.68, 141.87, 138.51 (d, $J = 3.3$ Hz), 129.15, 127.49 (d, $J = 8.1$ Hz), 126.67, 125.88, 122.23 (d, $J = 1.5$ Hz), 115.39 (d, $J = 21.6$ Hz), 49.37, 34.07, 28.45 ppm. **¹⁹F NMR** (376 MHz, CDCl_3) δ -114.64 ppm. **IR** (neat): ν (cm^{-1}) 3040, 2905, 1651, 1593, 1496, 1446, 1221, 1157, 828, 810, 756, 694. **HRMS** (ESI+, MeOH): m/z calcd. 304.1108 ($\text{M} + \text{Na}$)⁺, found: 304.1105.



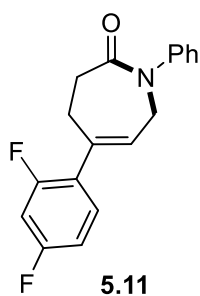
Scale: 0.20 mmol; *E/Z* = 93:7, isolated 41.1 mg (70% yield), yellow solid, Hexane : EA = 2 : 1, R_f = 0.25. **$^1\text{H NMR}$** (400 MHz, CDCl_3) δ 7.41 – 7.20 (m, 7H), 6.93 – 6.84 (m, 2H), 6.12 (tt, J = 6.1, 1.8 Hz, 1H), 4.43 (dt, J = 6.1, 2.1 Hz, 2H), 3.82 (s, 3H), 3.08 – 3.04 (m, 2H), 2.95 – 2.87 (m, 2H) ppm. **$^{13}\text{C NMR}$** (101 MHz, CDCl_3) δ 173.78, 159.39, 143.74, 142.05, 134.87, 129.10, 126.89, 126.57, 125.88, 120.70, 113.87, 55.41, 49.45, 34.12, 28.29. **IR** (neat): ν (cm^{-1}) 2921, 2841, 1649, 1509, 1443, 1413, 1241, 1216, 1165, 1025, 820, 695. **HRMS** (ESI+, MeOH): m/z calcd. 294.1489 ($\text{M} + \text{H}$)⁺, found: 294.1502.



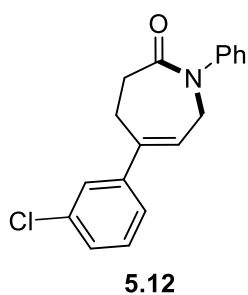
Scale: 0.20 mmol; *E/Z* > 99:1, isolated 58.1 mg (91% yield), white solid, Hexane : EA = 2 : 1, R_f = 0.25. **$^1\text{H NMR}$** (400 MHz, CDCl_3) δ 7.40 – 7.31 (m, 6H), 7.29 – 7.21 (m, 3H), 6.19 (tt, J = 6.1, 1.8 Hz, 1H), 4.45 (dt, J = 6.1, 2.1 Hz, 2H), 3.10 – 3.03 (m, 2H), 2.96 – 2.90 (m, 2H), 1.34 (s, 9H) ppm. **$^{13}\text{C NMR}$** (101 MHz, CDCl_3) δ 173.83, 150.98, 143.78, 142.47, 139.44, 129.14, 126.62, 125.94, 125.48, 121.47, 49.49, 34.65, 34.15, 31.42, 28.21 ppm. **IR** (neat): ν (cm^{-1}) 3027, 2955, 2902, 2866, 1645, 1594, 1492, 1412, 1216, 829, 754, 693. **HRMS** (ESI+, MeOH): m/z calcd. 320.2009 ($\text{M} + \text{H}$)⁺, found: 320.2008.



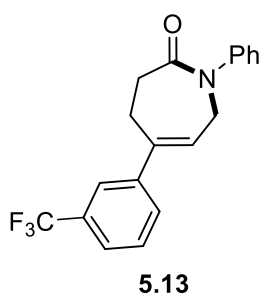
Scale: 0.20 mmol; *E/Z* = 97:3, isolated 54.3 mg (80% yield), white solid, Hexane : EA = 2 : 1, R_f = 0.20. **$^1\text{H NMR}$** (400 MHz, CDCl_3) δ 7.66 – 7.60 (m, 4H), 7.51 – 7.46 (m, 4H), 7.44 – 7.36 (m, 3H), 7.34 – 7.25 (m, 3H), 6.28 (tt, J = 6.1, 1.8 Hz, 1H), 4.50 (dt, J = 6.1, 2.1 Hz, 2H), 3.18 – 3.09 (m, 2H), 3.03 – 2.95 (m, 2H) ppm. **$^{13}\text{C NMR}$** (101 MHz, CDCl_3) δ 173.77, 143.76, 142.32, 141.29, 140.76, 140.64, 129.18, 128.95, 127.56, 127.26, 127.12, 126.68, 126.25, 125.95, 122.15, 49.50, 34.15, 28.24 ppm. **IR** (neat): ν (cm^{-1}) 3056, 2919, 2886, 1652, 1594, 1486, 1439, 1228, 829, 734, 693. **HRMS** (ESI+, MeOH): m/z calcd. 340.1696 ($\text{M} + \text{H}$)⁺, found: 340.1696.



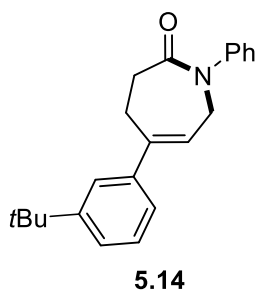
Scale: 0.20 mmol; *E/Z* = 99:1, isolated 46.1 mg (77% yield), yellow solid, Hexane : EA = 2 : 1, R_f = 0.25. $^1\text{H NMR}$ (400 MHz, CDCl_3) δ 7.44 – 7.38 (m, 2H), 7.32 – 7.18 (m, 4H), 6.95 – 6.78 (m, 2H), 6.01 (tt, J = 5.9, 2.2 Hz, 1H), 4.46 (dt, J = 5.9, 2.2 Hz, 2H), 3.11 – 3.04 (m, 2H), 2.89 – 2.81 (m, 2H) ppm. $^{13}\text{C NMR}$ (126 MHz, CDCl_3) δ 173.77, 162.41 (dd, J = 248.1, 10.9 Hz), 159.84 (dd, J = 249.2, 11.6 Hz), 143.79, 138.43, 130.45 (dd, J = 9.7, 5.5 Hz), 129.24, 127.04 (dd, J = 14.8, 3.7 Hz), 126.79, 126.01, 125.74 (d, J = 2.3 Hz), 111.41 (dd, J = 21.3, 3.7 Hz), 104.38 (dd, J = 26.7, 25.1 Hz), 49.36, 34.18, 29.20 (d, J = 3.2 Hz) ppm. $^{19}\text{F NMR}$ (376 MHz, CDCl_3) δ -111.12 (d, J = 7.5 Hz), -111.50 (d, J = 7.5 Hz) ppm. **IR** (neat): ν (cm^{-1}) 3281, 3063, 2925, 1647, 1593, 1498, 1422, 1265, 1231, 1389, 1097, 971, 850, 693. **HRMS** (ESI+, MeOH): m/z calcd. 322.1013 ($\text{M} + \text{Na}$)⁺, found: 322.1014.



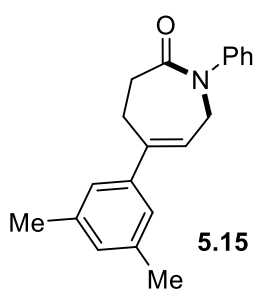
Scale: 0.20 mmol; *E/Z* = 96:4, isolated 53.6 mg (90% yield), yellow solid, Hexane : EA = 2 : 1, R_f = 0.25. $^1\text{H NMR}$ (400 MHz, CDCl_3) δ 7.41 – 7.35 (m, 3H), 7.30 – 7.22 (m, 6H), 6.18 (tt, J = 6.0, 1.9 Hz, 1H), 4.45 (dt, J = 6.1, 2.2 Hz, 2H), 3.11 – 3.04 (m, 2H), 2.93 – 2.85 (m, 2H) ppm. $^{13}\text{C NMR}$ ((101 MHz, CDCl_3) δ 173.54, 144.25, 143.64, 141.73, 134.52, 129.83, 129.20, 127.90, 126.74, 126.21, 125.91, 124.05, 123.30, 49.36, 34.03, 28.22 ppm. **IR** (neat): ν (cm^{-1}) 3308, 3064, 2923, 2853, 1654, 1593, 1493, 1444, 1412, 1212, 1167, 731, 692. **HRMS** (ESI+, MeOH): m/z calcd. 298.0993 ($\text{M} + \text{H}$)⁺, found: 298.0993.



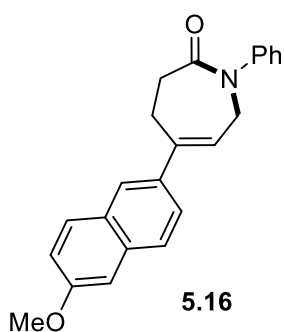
Scale: 0.20 mmol; *E/Z* = 97:3, isolated 56.3 mg (85% yield), yellow solid, Hexane : EA = 2 : 1, R_f = 0.15. $^1\text{H NMR}$ (400 MHz, CDCl_3) δ 7.62 (s, 1H), 7.58 – 7.53 (m, 2H), 7.49 – 7.44 (m, 1H), 7.41 – 7.35 (m, 2H), 7.30 – 7.21 (m, 3H), 6.23 (tt, J = 6.0, 1.8 Hz, 1H), 4.48 (dt, J = 6.1, 2.1 Hz, 2H), 3.15 – 3.04 (m, 2H), 2.97 – 2.87 (m, 2H) ppm. $^{13}\text{C NMR}$ (126 MHz, CDCl_3) δ 173.45, 143.57, 143.13, 141.64, 130.91 (q, J = 32.3 Hz), 129.14, 129.06, 126.69, 125.85, 124.49 (q, J = 3.8 Hz), 124.15 (q, J = 272.4 Hz), 123.77, 122.68 (q, J = 3.9 Hz), 49.27, 33.95, 28.18 ppm. $^{19}\text{F NMR}$ (376 MHz, CDCl_3) δ -62.74 ppm. **IR** (neat): ν (cm^{-1}) 3064, 2925, 1658, 1595, 1445, 1327, 1163, 1119, 1073, 757, 694. **HRMS** (ESI+, MeOH): m/z calcd. 332.1257 ($\text{M} + \text{H}$)⁺, found: 332.1259.



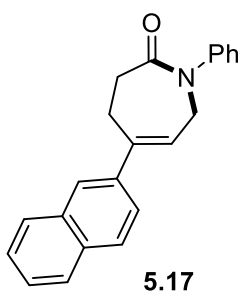
Scale: 0.20 mmol; *E/Z* = 97:3, isolated 47.3 mg (74% yield), white solid, Hexane : EA = 2 : 1, R_f = 0.25. $^1\text{H NMR}$ (400 MHz, CDCl_3) δ 7.41 – 7.33 (m, 4H), 7.32 – 7.21 (m, 4H), 7.20 – 7.16 (m, 1H), 6.16 (tt, J = 6.1, 1.9 Hz, 1H), 4.46 (dt, J = 6.1, 2.1 Hz, 2H), 3.18 – 3.03 (m, 2H), 2.97 – 2.87 (m, 2H), 1.35 (s, 9H) ppm. $^{13}\text{C NMR}$ ((126 MHz, CDCl_3) δ 173.85, 151.44, 143.80, 143.44, 142.31, 129.14, 128.27, 126.62, 125.94, 124.96, 123.11, 122.83, 121.94, 49.48, 34.91, 34.21, 31.50, 28.53 ppm. **IR** (neat): ν (cm^{-1}) 2961, 2868, 1656, 1596, 1492, 1445, 1413, 1214, 1166, 756, 694. **HRMS** (ESI+, MeOH): m/z calcd. 320.2009 ($\text{M} + \text{H}$)⁺, found: 320.2013.



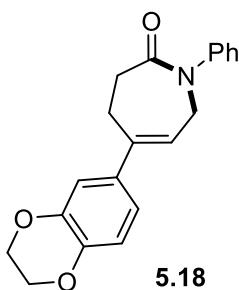
Scale: 0.20 mmol; *E/Z* > 99:1, isolated 41.4 mg (71% yield), yellow solid, Hexane : EA = 2 : 1, R_f = 0.25. $^1\text{H NMR}$ (400 MHz, CDCl_3) δ 7.41 – 7.36 (m, 2H), 7.30 – 7.22 (m, 3H), 7.00 – 6.95 (m, 3H), 6.14 (tt, J = 6.1, 1.9 Hz, 1H), 4.44 (dt, J = 6.1, 2.1 Hz, 2H), 3.11 – 3.02 (m, 2H), 2.95 – 2.87 (m, 2H), 2.34 (s, 6H) ppm. $^{13}\text{C NMR}$ (101 MHz, CDCl_3) δ 173.82, 143.81, 143.11, 142.60, 138.06, 129.50, 129.14, 126.61, 125.94, 123.83, 121.76, 49.50, 34.19, 28.44, 21.48 ppm. **IR** (neat): ν (cm^{-1}) 3307, 3038, 2915, 1661, 1596, 1443, 1412, 1220, 843, 733, 693. **HRMS** (ESI+, MeOH): m/z calcd. 292.1698 ($\text{M} + \text{H}$)⁺, found: 292.1696.



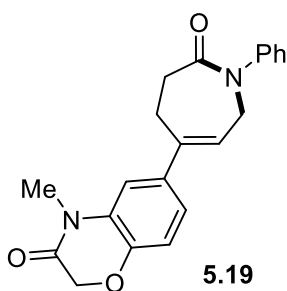
Scale: 0.20 mmol; *E/Z* > 99:1, isolated 44.6 mg (65% yield), white solid, Hexane : EA = 2 : 1, R_f = 0.15. $^1\text{H NMR}$ (400 MHz, CDCl_3) δ 7.76 – 7.69 (m, 3H), 7.50 (dd, J = 8.6, 2.0 Hz, 1H), 7.41 – 7.36 (m, 2H), 7.32 – 7.27 (m, 2H), 7.27 – 7.22 (m, 1H), 7.18 – 7.12 (m, 2H), 6.30 (tt, J = 6.1, 1.8 Hz, 1H), 4.49 (dt, J = 6.1, 2.0 Hz, 2H), 3.93 (s, 3H), 3.13 – 3.09 (m, 2H), 3.07 – 3.00 (m, 2H) ppm. $^{13}\text{C NMR}$ (101 MHz, CDCl_3) δ 173.81, 158.01, 143.78, 142.56, 137.45, 134.18, 129.79, 129.15, 128.84, 126.98, 126.63, 125.95, 124.65, 124.40, 121.93, 119.31, 105.72, 55.45, 49.57, 34.20, 28.31 ppm. **IR** (neat): ν (cm^{-1}) 2945, 2849, 1651, 1595, 1450, 1218, 1165, 849, 695. **HRMS** (ESI+, MeOH): m/z calcd. 344.1645 ($\text{M} + \text{H}$)⁺, found: 344.1646.



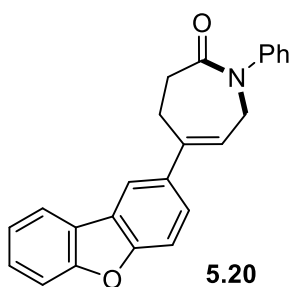
Scale: 0.2 mmol; *E/Z* = 99:1, isolated 48.3 mg (77% yield), white solid, Hexane : EA = 2 : 1, R_f = 0.18. **$^1\text{H NMR}$** (500 MHz, CDCl_3) δ 7.89 – 7.79 (m, 4H), 7.55 – 7.46 (m, 3H), 7.42 – 7.35 (m, 2H), 7.31 (d, J = 7.3 Hz, 2H), 7.27 – 7.22 (m, 1H), 6.33 (tt, J = 6.1, 1.7 Hz, 1H), 4.50 (dt, J = 6.1, 2.1 Hz, 2H), 3.14 – 3.10 (m, 2H), 3.08 – 3.03 (m, 2H) ppm. **$^{13}\text{C NMR}$** (126 MHz, CDCl_3) δ 173.77, 143.76, 142.61, 139.63, 133.42, 132.99, 129.17, 128.27, 128.15, 127.67, 126.66, 126.49, 126.20, 125.94, 124.58, 124.19, 122.69, 49.54, 34.18, 28.32 ppm. **IR** (neat): ν (cm^{-1}) 3056, 2919, 2846, 1651, 1593, 1418, 1230, 820, 744, 693. **HRMS** (ESI+, MeOH): m/z calcd. 314.1539 ($\text{M} + \text{H}$)⁺, found: 314.1545.



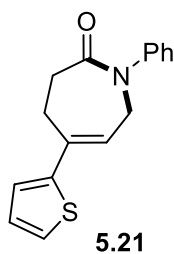
Scale: 0.2 mmol; *E/Z* = 98:2, isolated 54.6 mg (85% yield), white solid, Hexane : EA = 2 : 1, R_f = 0.18. **$^1\text{H NMR}$** (400 MHz, CDCl_3) δ 7.39 – 7.34 (m, 2H), 7.27 – 7.26 (m, 1H), 7.26 – 7.19 (m, 2H), 6.90 – 6.81 (m, 3H), 6.11 (tt, J = 6.1, 1.9 Hz, 1H), 4.42 (dt, J = 6.1, 2.1 Hz, 2H), 4.26 (s, 4H), 3.08 – 3.00 (m, 2H), 2.90 – 2.82 (m, 2H) ppm. **$^{13}\text{C NMR}$** (126 MHz, CDCl_3) δ 173.77, 143.77, 143.46, 143.41, 141.95, 135.99, 129.14, 126.62, 125.93, 121.06, 118.94, 117.24, 114.80, 64.58, 64.53, 49.45, 34.13, 28.27 ppm. **IR** (neat): ν (cm^{-1}) 3058, 2931, 2875, 1655, 1581, 1498, 1284, 1244, 1129, 1065, 890, 732, 694. **HRMS** (ESI+, MeOH): m/z calcd. 322.1438 ($\text{M} + \text{H}$)⁺, found: 322.1443.



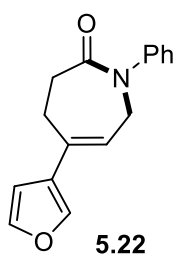
Scale: 0.20 mmol; *E/Z* = 93:7, isolated 50.9 mg (73% yield), white solid, Hexane : EA = 1 : 1, R_f = 0.10. **$^1\text{H NMR}$** (400 MHz, CDCl_3) δ 7.41 – 7.34 (m, 2H), 7.28 (s, 1H), 7.26 – 7.21 (m, 2H), 7.04 – 6.99 (m, 1H), 6.98 – 6.92 (m, 2H), 6.16 – 6.09 (m, 1H), 4.62 (s, 2H), 4.46 (d, J = 6.1 Hz, 2H), 3.39 (s, 3H), 3.11 – 3.04 (m, 2H), 2.92 – 2.87 (m, 2H) ppm. **$^{13}\text{C NMR}$** (126 MHz, CDCl_3) δ 173.63, 164.61, 144.87, 143.67, 142.16, 137.53, 129.57, 129.20, 126.74, 125.90, 122.16, 121.43, 116.80, 112.44, 67.74, 49.38, 34.10, 28.57, 28.18 ppm. **IR** (neat): ν (cm^{-1}) 3315, 2922, 2851, 1678, 1655, 1594, 1477, 1423, 1224, 1036, 722, 695. **HRMS** (ESI+, MeOH): m/z calcd. 349.1547 ($\text{M} + \text{H}$)⁺, found: 349.1549.



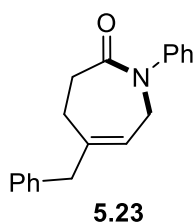
Scale: 0.20 mmol; *E/Z* = 99:1, isolated 56.5 mg (80% yield), yellow solid, Hexane : EA = 2 : 1, R_f = 0.15. $^1\text{H NMR}$ (400 MHz, CDCl_3) δ 7.99 – 7.93 (m, 2H), 7.60 – 7.52 (m, 2H), 7.50 – 7.44 (m, 2H), 7.43 – 7.35 (m, 3H), 7.35 – 7.30 (m, 2H), 7.28 – 7.23 (m, 1H), 6.23 (tt, J = 6.1, 1.9 Hz, 1H), 4.50 (dt, J = 6.1, 2.2 Hz, 2H), 3.16 – 3.09 (m, 2H), 3.06 – 2.98 (m, 2H) ppm. $^{13}\text{C NMR}$ (101 MHz, CDCl_3) δ 173.74, 156.78, 155.91, 143.78, 142.93, 137.70, 129.18, 127.52, 126.67, 125.94, 125.34, 124.45, 124.21, 122.97, 122.29, 120.76, 118.01, 111.91, 111.57, 49.53, 34.24, 28.95 ppm. **IR** (neat): ν (cm^{-1}) 3053, 2935, 1645, 1594, 1475, 1448, 1197, 806, 749, 690. **HRMS** (ESI+, MeOH): m/z calcd. 376.1308 ($\text{M} + \text{Na}$)⁺, found: 376.1305.



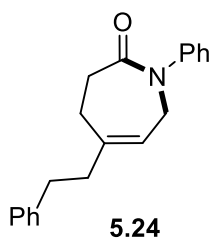
Scale: 0.20 mmol; *E/Z* = 78:22, isolated 36.1 mg (67% yield), yellow solid, Hexane : EA = 3 : 1, R_f = 0.25. $^1\text{H NMR}$ (400 MHz, CDCl_3) δ 7.40 – 7.33 (m, 2H), 7.27 – 7.21 (m, 3H), 7.20 – 7.15 (m, 1H), 7.07 – 7.04 (m, 1H), 7.03 – 6.96 (m, 1H), 6.37 (tt, J = 6.1, 1.8 Hz, 1H), 4.44 (dt, J = 6.1, 2.1 Hz, 2H), 3.10 – 3.03 (m, 2H), 3.01 – 2.92 (m, 2H) ppm. $^{13}\text{C NMR}$ (126 MHz, CDCl_3) δ 173.53, 145.67, 143.62, 136.04, 129.19, 127.61, 126.73, 125.96, 124.29, 123.19, 120.52, 49.33, 33.95, 28.03 ppm. **IR** (neat): ν (cm^{-1}) 3118, 2920, 1652, 1446, 1415, 1226, 1166, 698. **HRMS** (ESI+, MeOH): m/z calcd. 270.0947 ($\text{M} + \text{H}$)⁺, found: 270.0943.



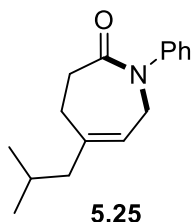
Scale: 0.20 mmol; ; *E/Z* = 87:13, isolated 36.5 mg (72% yield), yellow oil, Hexane : EA = 4 : 1, R_f = 0.15. $^1\text{H NMR}$ (500 MHz, CDCl_3) δ 7.46 (s, 1H), 7.40 – 7.34 (m, 3H), 7.26 – 7.20 (m, 3H), 6.53 – 6.48 (m, 1H), 6.18 (tt, J = 6.1, 1.8 Hz, 1H), 4.42 (dt, J = 6.1, 2.0 Hz, 2H), 3.06 – 3.00 (m, 2H), 2.83 – 2.77 (m, 2H) ppm. $^{13}\text{C NMR}$ (126 MHz, CDCl_3) δ 173.72, 143.69, 143.57, 138.68, 133.66, 129.13, 127.60, 126.65, 125.93, 119.56, 107.42, 49.23, 33.89, 27.16 ppm. **IR** (neat): ν (cm^{-1}) 3146, 3120, 2824 1653, 1594, 1448, 1235, 1162, 1026, 851, 730, 692. **HRMS** (ESI+, MeOH): m/z calcd. 276.0995 ($\text{M} + \text{Na}$)⁺, found: 276.0996.



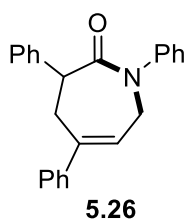
Scale: 0.20 mmol; *E/Z* > 99:1, isolated 41.6 mg (75% yield), slight yellow solid, Hexane : EA = 2 : 1, R_f = 0.2. **¹H NMR** (500 MHz, CDCl₃) δ 7.32 – 7.27 (m, 2H), 7.25 – 7.21 (m, 2H), 7.18 – 7.08 (m, 6H), 5.65 (t, J = 6.1 Hz, 1H), 4.21 (d, J = 5.9 Hz, 2H), 3.25 (s, 2H), 2.85 – 2.76 (m, 2H), 2.36 – 2.29 (m, 2H) ppm. **¹³C NMR** (126 MHz, CDCl₃) δ 173.91, 143.91, 143.08, 139.03, 129.12, 128.99, 128.64, 126.60, 126.54, 125.91, 121.09, 49.22, 45.49, 34.00, 28.40 ppm. **IR** (neat): ν (cm⁻¹) 3026, 2917, 2849, 1639, 1594, 1493, 1447, 1027, 694. **HRMS** (ESI+, MeOH): m/z calcd. 278.1539 (M + H)⁺, found: 278.1542.



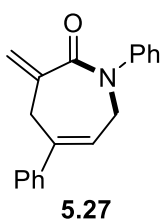
Scale: 0.20 mmol; *E/Z* = 26:74, isolated 29.7 mg (51% yield), yellow oil, Hexane : EA = 2 : 1, R_f = 0.20. **¹H NMR** (400 MHz, CDCl₃) δ 7.37 – 7.27 (m, 4H), 7.24 – 7.20 (m, 2H), 7.19 – 7.14 (m, 4H), 5.62 (tt, J = 6.0, 1.5 Hz, 1H), 4.21 (d, J = 5.9 Hz, 2H), 2.96 – 2.89 (m, 2H), 2.80 – 2.74 (m, 2H), 2.54 – 2.47 (m, 2H), 2.37 – 2.31 (m, 2H) ppm. **¹³C NMR** (101 MHz, CDCl₃) δ 173.96, 143.84, 142.53, 141.51, 129.04, 128.53, 128.51, 126.52, 126.07, 125.90, 119.96, 49.19, 40.66, 34.37, 34.01, 28.69 ppm. **IR** (neat): ν (cm⁻¹) 3025, 2921, 2857, 1657, 1595, 1444, 1225, 755, 695. **HRMS** (ESI+, MeOH): m/z calcd. 292.1696 (M + H)⁺, found: 292.1693.



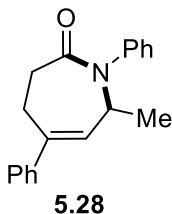
Scale: 0.20 mmol; *E/Z* = 62:38, isolated 26.3 mg (54% yield), yellow oil, Hexane : EA = 2 : 1, R_f = 0.25. **¹H NMR** (500 MHz, CDCl₃) δ 7.38 – 7.33 (m, 2H), 7.24 – 7.18 (m, 3H), 5.62 (tt, J = 6.0, 1.0 Hz, 1H), 4.24 (d, J = 5.9 Hz, 2H), 2.93 – 2.89 (m, 2H), 2.44 – 2.40 (m, 2H), 1.88 (d, J = 7.4 Hz, 2H), 1.82 – 1.74 (m, 1H), 0.88 (d, J = 6.5 Hz, 6H) ppm. **¹³C NMR** (126 MHz, CDCl₃) δ 174.06, 143.94, 142.61, 129.08, 126.50, 125.89, 120.33, 49.31, 48.85, 34.06, 28.57, 26.18, 22.46 ppm. **IR** (neat): ν (cm⁻¹) 2953, 2922, 2867, 1661, 1595, 1495, 1444, 1220, 758, 693. **HRMS** (ESI+, MeOH): m/z calcd. 266.1515 (M + Na)⁺, found: 266.1519.



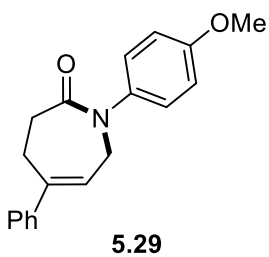
Scale: 0.20 mmol; *E/Z* = 97:3, isolated 55.0 mg (81% yield), yellow oil, Hexane : EA = 6 : 1, R_f = 0.15. $^1\text{H NMR}$ (500 MHz, CDCl_3) δ 7.48 – 7.44 (m, 2H), 7.43 – 7.35 (m, 8H), 7.34 – 7.28 (m, 4H), 7.24 (t, J = 7.3 Hz, 1H), 6.25 (ddt, J = 7.8, 4.1, 1.9 Hz, 1H), 4.98 – 4.88 (m, 1H), 4.70 (dd, J = 11.7, 3.6 Hz, 1H), 4.08 (dd, J = 18.0, 7.5 Hz, 1H), 3.35 – 3.27 (m, 1H), 3.10 – 3.04 (m, 1H) ppm. $^{13}\text{C NMR}$ (126 MHz, CDCl_3) δ 173.40, 144.08, 142.55, 142.44, 139.44, 128.97, 128.67, 128.61, 128.42, 127.95, 127.36, 126.58, 126.00, 122.54, 49.15, 47.60, 35.79 ppm. **IR** (neat): ν (cm^{-1}) 3025, 2910, 1656, 1595, 1492, 1421, 1217, 756, 692. **HRMS** (ESI+, MeOH): m/z calcd. 340.1696 ($\text{M} + \text{H}$)⁺, found: 340.1699.



Scale: 0.20 mmol; *E/Z* > 99:1, isolated 28.6 mg (52% yield), yellow oil, Hexane : EA = 5 : 1, R_f = 0.15. $^1\text{H NMR}$ (400 MHz, CDCl_3) δ 7.43 – 7.31 (m, 9H), 7.27 – 7.22 (m, 1H), 6.28 (tt, J = 6.5, 1.8 Hz, 1H), 5.63 (d, J = 1.2 Hz, 1H), 5.44 (d, J = 1.3 Hz, 1H), 4.39 (d, J = 6.5 Hz, 2H), 3.64 (d, J = 1.5 Hz, 2H) ppm. $^{13}\text{C NMR}$ (101 MHz, CDCl_3) δ 171.28, 143.97, 142.99, 142.35, 141.37, 129.21, 128.68, 128.12, 126.70, 125.85, 125.67, 122.60, 118.90, 48.75, 38.02 ppm. **IR** (neat): ν (cm^{-1}) 3059, 2924, 2853, 1655, 1594, 1492, 1427, 1214, 1073, 754, 692. **HRMS** (ESI+, MeOH): m/z calcd. 276.1383 ($\text{M} + \text{H}$)⁺, found: 276.1380.

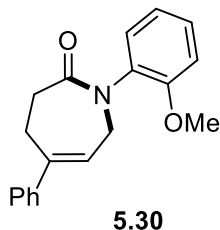


Scale: 0.20 mmol; *E/Z* > 99:1, isolated 34.9 mg (63% yield), colorless oil, Hexane : EA = 1 : 1, R_f = 0.25. $^1\text{H NMR}$ (400 MHz, CDCl_3) δ 7.43 – 7.28 (m, 8H), 7.21 – 7.14 (m, 2H), 5.95 (dt, J = 6.0, 1.7 Hz, 1H), 4.88 – 4.77 (m, 1H), 3.21 (td, J = 12.4, 11.8, 5.2 Hz, 1H), 3.01 – 2.83 (m, 3H), 1.36 (d, J = 7.2 Hz, 3H) ppm. $^{13}\text{C NMR}$ (101 MHz, CDCl_3) δ 174.11, 142.86, 141.96, 141.30, 129.25, 129.23, 128.56, 128.30, 127.74, 127.46, 125.96, 54.31, 34.95, 28.15, 21.37 ppm. **IR** (neat): ν (cm^{-1}) 3057, 2973, 1655, 1493, 1457, 1229, 963, 756, 698. **HRMS** (ESI+, MeOH): m/z calcd. 278.1539 ($\text{M} + \text{H}$)⁺, found: 278.1542.

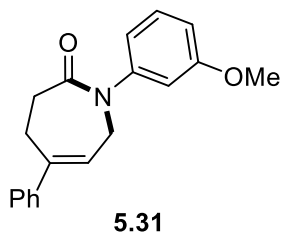


Scale: 0.20 mmol; *E/Z* = 97:3, isolated 46.9 mg (80% yield), slight yellow solid, Hexane : EA = 2 : 1, R_f = 0.25. $^1\text{H NMR}$ (400 MHz, CDCl_3) δ 7.39 – 7.27 (m, 5H), 7.20 – 7.15 (m, 2H), 6.92 – 6.86 (m, 2H), 6.16 (tt, J = 6.1, 1.9 Hz, 1H), 4.41 (dt, J = 6.1, 2.2 Hz, 2H), 3.80 (s, 3H), 3.08 – 3.02 (m, 2H), 2.95 – 2.89 (m, 2H) ppm. $^{13}\text{C NMR}$ (101 MHz, CDCl_3) δ 174.07, 158.14, 142.77, 142.55, 136.90, 128.59, 127.87,

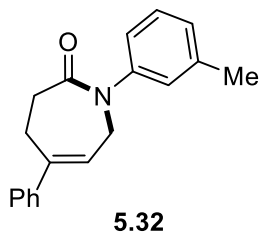
127.17, 125.88, 122.23, 114.47, 55.61, 49.82, 34.04, 28.30 ppm. **IR** (neat): ν (cm^{-1}) 2932, 2835, 1656, 1606, 1508, 1445, 1243, 1029, 828, 732, 696. **HRMS** (ESI+, MeOH): m/z calcd. 294.1489 ($\text{M} + \text{H}$)⁺, found: 294.1489.



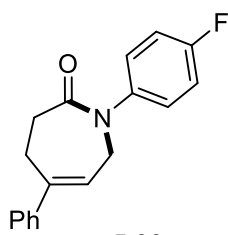
Scale: 0.20 mmol; $E/Z > 99:1$, isolated 53.4 mg (91% yield), slight yellow solid, Hexane : EA = 2 : 1, $R_f = 0.25$. **¹H NMR** (400 MHz, CDCl_3) δ 7.40 – 7.32 (m, 4H), 7.31 – 7.28 (m, 1H), 7.27 – 7.23 (m, 1H), 7.23 – 7.18 (m, 1H), 6.99 – 6.92 (m, 2H), 6.09 (tt, $J = 5.9, 1.8$ Hz, 1H), 4.29 (s, 2H), 3.82 (s, 3H), 2.94 (s, 2H), 2.96 – 2.87 (m, 2H) ppm. **¹³C NMR** (126 MHz, CDCl_3) δ 174.35, 154.51, 142.94, 142.01, 132.60, 128.98, 128.69, 128.55, 127.67, 125.95, 122.69, 120.99, 112.40, 55.93, 49.43, 33.98, 28.32 ppm. **IR** (neat): ν (cm^{-1}) 3056, 2922, 2838, 1661, 1595, 1499, 1459, 1249, 1024, 749, 697. **HRMS** (ESI+, MeOH): m/z calcd. 294.1489 ($\text{M} + \text{H}$)⁺, found: 294.1490.



Scale: 0.20 mmol; $E/Z = 99:1$, isolated 50.5 mg (86% yield), yellow solid, Hexane : EA = 2 : 1, $R_f = 0.25$. **¹H NMR** (400 MHz, CDCl_3) δ 7.39 – 7.27 (m, 6H), 6.88 – 6.77 (m, 3H), 6.17 (tt, $J = 6.1, 1.8$ Hz, 1H), 4.44 (dt, $J = 6.1, 2.1$ Hz, 2H), 3.80 (s, 3H), 3.10 – 3.04 (m, 2H), 2.96 – 2.89 (m, 2H) ppm. **¹³C NMR** (101 MHz, CDCl_3) δ 173.78, 160.19, 144.90, 142.85, 142.49, 129.86, 128.60, 127.90, 125.90, 122.15, 118.23, 112.43, 112.07, 55.52, 49.52, 34.20, 28.33 ppm. **IR** (neat): ν (cm^{-1}) 3281, 2934, 2835, 1647, 1598, 1487, 1448, 1202, 1159, 1043, 730, 691. **HRMS** (ESI+, MeOH): m/z calcd. 294.1489 ($\text{M} + \text{H}$)⁺, found: 294.1489.

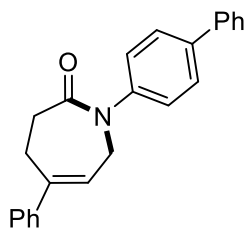


Scale: 0.20 mmol; $E/Z = 92:8$, isolated 41.1 mg (74% yield), yellow solid, Hexane : EA = 2 : 1, $R_f = 0.25$. **¹H NMR** (500 MHz, CDCl_3) δ 7.39 – 7.33 (m, 4H), 7.32 – 7.28 (m, 1H), 7.28 – 7.24 (m, 1H), 7.09 – 7.04 (m, 3H), 6.17 (tt, $J = 6.1, 1.8$ Hz, 1H), 4.43 (dt, $J = 6.1, 2.1$ Hz, 2H), 3.09 – 3.03 (m, 2H), 2.95 – 2.89 (m, 2H), 2.35 (s, 3H) ppm. **¹³C NMR** (126 MHz, CDCl_3) δ 173.81, 143.73, 142.74, 142.51, 139.09, 129.00, 128.57, 127.85, 127.56, 126.68, 125.86, 122.97, 122.21, 49.53, 34.13, 28.29, 21.48 ppm. **IR** (neat): ν (cm^{-1}) 3028, 2917, 1661, 1587, 1490, 1445, 1184, 731, 695. **HRMS** (ESI+, MeOH): m/z calcd. 278.1539 ($\text{M} + \text{H}$)⁺, found: 278.1546.



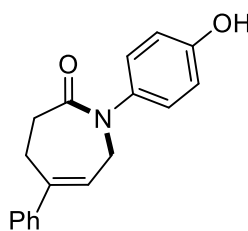
5.33

Scale: 0.20 mmol; *E/Z* = 98:2, isolated 52.3 mg (93% yield), yellow solid, Hexane : EA = 2 : 1, R_f = 0.25. **$^1\text{H NMR}$** (400 MHz, CDCl_3) δ 7.39 – 7.28 (m, 5H), 7.26 – 7.20 (m, 2H), 7.09 – 7.02 (m, 2H), 6.17 (tt, J = 6.0, 1.8 Hz, 1H), 4.42 (dt, J = 6.1, 2.1 Hz, 2H), 3.09 – 3.03 (m, 2H), 2.95 – 2.89 (m, 2H) ppm. **$^{13}\text{C NMR}$** (101 MHz, CDCl_3) δ 173.99, 161.03 (d, J = 245.9 Hz), 143.02, 142.38, 139.74 (d, J = 3.3 Hz), 128.62, 127.97, 127.69 (d, J = 8.4 Hz), 125.87, 121.91, 115.98 (d, J = 22.7 Hz), 49.61, 34.01, 28.29 ppm. **$^{19}\text{F NMR}$** (376 MHz, CDCl_3) δ -115.48 ppm. **IR** (neat): ν (cm^{-1}) 3059, 2889, 1649, 1599, 1508, 1441, 1210, 1160, 852, 736, 693. **HRMS** (ESI+, MeOH): m/z calcd. 282.1289 ($\text{M} + \text{H}$)⁺, found: 282.1295.



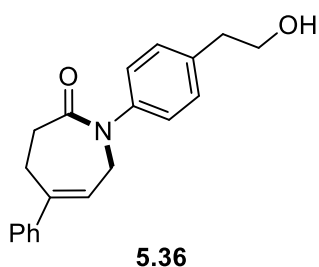
5.34

Scale: 0.20 mmol; *E/Z* = 97:3, isolated 50.9 mg (75% yield), white solid, Hexane : EA = 2 : 1, R_f = 0.15. **$^1\text{H NMR}$** (400 MHz, CDCl_3) δ 7.62 – 7.56 (m, 4H), 7.47 – 7.42 (m, 2H), 7.41 – 7.32 (m, 8H), 6.21 (tt, J = 6.1, 1.8 Hz, 1H), 4.50 (dt, J = 6.1, 2.1 Hz, 2H), 3.13 – 3.07 (m, 2H), 2.98 – 2.91 (m, 2H) ppm. **$^{13}\text{C NMR}$** (126 MHz, CDCl_3) δ 173.91, 142.94, 142.88, 142.45, 140.68, 139.62, 128.91, 128.60, 127.92, 127.89, 127.47, 127.24, 126.15, 125.89, 122.09, 49.47, 34.16, 28.34 ppm. **IR** (neat): ν (cm^{-1}) 3055, 1644, 1601, 1484, 1448, 1214, 762, 733, 692. **HRMS** (ESI+, MeOH): m/z calcd. 340.1696 ($\text{M} + \text{H}$)⁺, found: 340.1705.

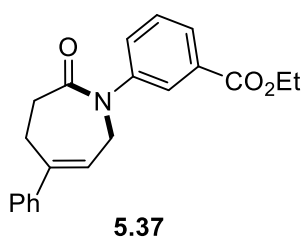


5.35

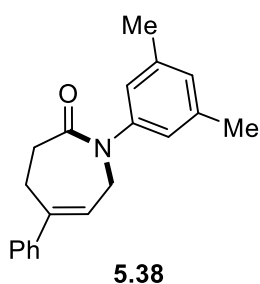
Scale: 0.20 mmol; *E/Z* > 99:1, isolated 32.4 mg (58% yield), white solid, DCM : MeOH = 50 : 1, R_f = 0.13. **$^1\text{H NMR}$** (400 MHz, CDCl_3) δ 7.73 (s, 1H), 7.39 – 7.27 (m, 5H), 6.98 – 6.88 (m, 2H), 6.63 – 6.57 (m, 2H), 6.12 (tt, J = 6.0, 1.8 Hz, 1H), 4.37 (dt, J = 6.1, 2.2 Hz, 2H), 3.12 – 3.00 (m, 2H), 2.96 – 2.86 (m, 2H) ppm. **$^{13}\text{C NMR}$** (126 MHz, CDCl_3) δ 175.27, 155.84, 142.52, 142.35, 135.46, 128.58, 127.90, 126.98, 125.87, 121.92, 116.75, 50.22, 33.90, 27.99 ppm. **IR** (neat): ν (cm^{-1}) 3252, 3028, 2917, 1631, 1591, 1510, 1445, 1213, 1165, 908, 729, 695. **HRMS** (ESI+, MeOH): m/z calcd. 280.1332 ($\text{M} + \text{H}$)⁺, found: 280.1330.



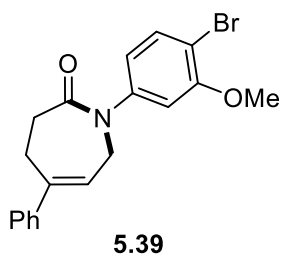
Scale: 0.20 mmol; *E/Z* = 94:6, isolated 38.1 mg (62% yield), yellow solid, Hexane : EA = 1 : 3, R_f = 0.2. **¹H NMR** (400 MHz, CDCl₃) δ 7.39 – 7.27 (m, 5H), 7.24 – 7.18 (m, 4H), 6.16 (tt, *J* = 6.1, 1.8 Hz, 1H), 4.43 (dt, *J* = 6.1, 2.2 Hz, 2H), 3.79 (t, *J* = 6.7 Hz, 2H), 3.10 – 3.02 (m, 2H), 2.95 – 2.88 (m, 2H), 2.83 (t, *J* = 6.6 Hz, 2H) ppm. **¹³C NMR** (101 MHz, CDCl₃) δ 173.94, 142.85, 142.47, 142.13, 137.14, 129.81, 128.59, 127.90, 126.06, 125.88, 122.12, 63.62, 49.51, 38.87, 34.10, 28.30 ppm. **IR** (neat): ν (cm⁻¹) 3332, 2895, 2852, 1632, 1605, 1456, 1226, 1070, 812, 686. **HRMS** (ESI+, MeOH): *m/z* calcd. 308.1645 (M + H)⁺, found: 308.1652.



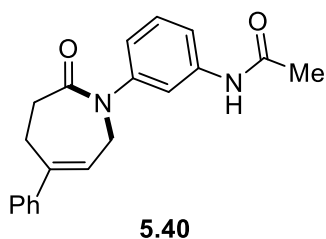
Scale: 0.20 mmol; *E/Z* = 96:4, isolated 45.6 mg (68% yield), yellow solid, Hexane : EA = 1 : 1, R_f = 0.15. **¹H NMR** (400 MHz, CDCl₃) δ 7.94 – 7.90 (m, 2H), 7.52 – 7.46 (m, 1H), 7.47 – 7.40 (m, 1H), 7.40 – 7.30 (m, 5H), 6.18 (tt, *J* = 6.1, 1.8 Hz, 1H), 4.47 (dt, *J* = 6.1, 2.1 Hz, 2H), 4.37 (q, *J* = 7.1 Hz, 2H), 3.14 – 3.03 (m, 2H), 2.97 – 2.89 (m, 2H), 1.38 (t, *J* = 7.2 Hz, 3H) ppm. **¹³C NMR** (101 MHz, CDCl₃) δ 173.90, 166.14, 143.80, 143.08, 142.37, 131.71, 130.70, 129.09, 128.62, 127.98, 127.77, 126.79, 125.91, 121.85, 61.31, 49.35, 34.11, 28.30, 14.46 ppm. **IR** (neat): ν (cm⁻¹) 2980, 1714, 1665, 1585, 1445, 1285, 1254, 1102, 740, 690. **HRMS** (ESI+, MeOH): *m/z* calcd. 336.1594 (M + H)⁺, found: 336.1595.



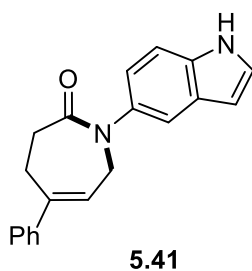
Scale: 0.20 mmol; *E/Z* = 94:6, isolated 48.4 mg (83% yield), yellow solid, Hexane : EA = 2 : 1, R_f = 0.25. **¹H NMR** (500 MHz, CDCl₃) δ 7.40 – 7.28 (m, 5H), 6.92 – 6.82 (m, 3H), 6.16 (tt, *J* = 6.1, 1.8 Hz, 1H), 4.41 (dt, *J* = 6.1, 2.1 Hz, 2H), 3.08 – 3.04 (m, 2H), 2.95 – 2.90 (m, 2H), 2.31 (s, 6H) ppm. **¹³C NMR** (126 MHz, CDCl₃) δ 173.87, 143.72, 142.64, 142.56, 138.91, 128.61, 128.58, 127.84, 125.87, 123.76, 122.28, 49.61, 34.13, 28.28, 21.39 ppm. **IR** (neat): ν (cm⁻¹) 3031, 2917, 2858, 1646, 1595, 1446, 1190, 1164, 844, 730, 695. **HRMS** (ESI+, MeOH): *m/z* calcd. 292.1696 (M + H)⁺, found: 292.1704.



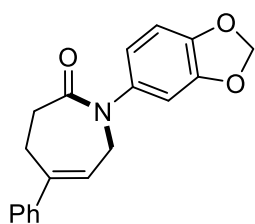
Scale: 0.20 mmol; *E/Z* = 99:1, isolated 54.4 mg (73% yield), yellow solid, Hexane : EA = 2 : 1, R_f = 0.18. **$^1\text{H NMR}$** (400 MHz, CDCl_3) δ 7.51 (d, J = 8.4 Hz, 1H), 7.38 – 7.28 (m, 5H), 6.88 (d, J = 2.3 Hz, 1H), 6.72 (dd, J = 8.4, 2.3 Hz, 1H), 6.17 (tt, J = 6.0, 1.8 Hz, 1H), 4.44 (dt, J = 6.1, 2.1 Hz, 2H), 3.88 (s, 3H), 3.12 – 3.03 (m, 2H), 2.97 – 2.89 (m, 2H) ppm. **$^{13}\text{C NMR}$** (101 MHz, CDCl_3) δ 173.84, 156.18, 144.06, 143.04, 142.29, 133.46, 128.65, 128.03, 125.85, 121.77, 118.85, 110.68, 109.66, 56.48, 49.47, 34.15, 28.26 ppm. **IR** (neat): ν (cm^{-1}) 2918, 2851, 1662, 1585, 1481, 1446, 1400, 1202, 1049, 1024, 729, 693. **HRMS** (ESI+, MeOH): m/z calcd. 372.0594 ($\text{M} + \text{H}$)⁺, found: 372.0599.



Scale: 0.20 mmol; *E/Z* > 99:1, isolated 45.5 mg (71% yield), yellow solid, Hexane : EA = 1 : 1, R_f = 0.15. **$^1\text{H NMR}$** (500 MHz, CDCl_3) δ 7.99 (s, 1H), 7.40 (t, J = 2.1 Hz, 1H), 7.39 – 7.33 (m, 4H), 7.32 – 7.27 (m, 2H), 7.24 (t, J = 7.9 Hz, 1H), 6.91 (dt, J = 7.6, 1.6 Hz, 1H), 6.16 (tt, J = 6.1, 2.0 Hz, 1H), 4.46 – 4.40 (m, 2H), 3.09 – 3.01 (m, 2H), 2.94 – 2.86 (m, 2H), 2.02 (s, 3H) ppm. **$^{13}\text{C NMR}$** (126 MHz, CDCl_3) δ 174.54, 168.79, 143.74, 142.63, 142.34, 139.39, 129.61, 128.63, 127.99, 125.93, 122.08, 120.87, 118.82, 118.22, 49.61, 34.06, 28.15, 24.44 ppm. **IR** (neat): ν (cm^{-1}) 3253, 3070, 2962, 1686, 1644, 1595, 1439, 1260, 1088, 1014, 788, 734, 696. **HRMS** (ESI+, MeOH): m/z calcd. 321.1598 ($\text{M} + \text{H}$)⁺, found: 321.1604.

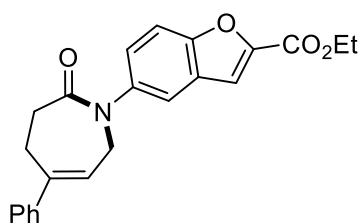


Scale: 0.20 mmol; *E/Z* > 99:1, isolated 36.3 mg (60% yield), yellow solid, Hexane : EA = 1 : 2, R_f = 0.15. **$^1\text{H NMR}$** (400 MHz, CDCl_3) δ 8.58 (s, 1H), 7.47 (d, J = 2.1 Hz, 1H), 7.42 – 7.34 (m, 4H), 7.33 – 7.28 (m, 1H), 7.24 – 7.19 (m, 1H), 7.13 (t, J = 2.8 Hz, 1H), 7.02 – 6.96 (m, 1H), 6.47 (t, J = 2.8 Hz, 1H), 6.19 (tt, J = 6.0, 1.9 Hz, 1H), 4.48 (dt, J = 6.1, 2.1 Hz, 2H), 3.14 – 3.07 (m, 2H), 3.00 – 2.92 (m, 2H) ppm. **$^{13}\text{C NMR}$** (101 MHz, CDCl_3) δ 174.51, 142.66, 142.45, 136.52, 134.70, 128.57, 128.27, 127.79, 125.91, 125.55, 122.55, 120.46, 117.84, 111.75, 102.75, 50.50, 34.11, 28.29 ppm. **IR** (neat): ν (cm^{-1}) 3243, 2916, 1630, 1615, 1482, 1451, 1342, 1175, 808, 701, 645. **HRMS** (ESI+, MeOH): m/z calcd. 303.1492 ($\text{M} + \text{H}$)⁺, found: 303.1494.



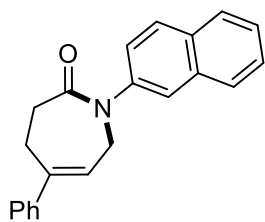
5.42

Scale: 0.20 mmol; *E/Z* = 95:5, isolated 45.5 mg (74% yield), yellow solid, Hexane : EA = 1 : 1, R_f = 0.15. **$^1\text{H NMR}$** (400 MHz, CDCl_3) δ 7.30 – 7.20 (m, 5H), 6.73 – 6.66 (m, 2H), 6.63 – 6.60 (m, 1H), 6.07 (tt, J = 6.0, 1.8 Hz, 1H), 5.88 (s, 2H), 4.30 (dt, J = 6.1, 2.1 Hz, 2H), 2.99 – 2.92 (m, 2H), 2.86 – 2.78 (m, 2H) ppm. **$^{13}\text{C NMR}$** (101 MHz, CDCl_3) δ 174.11, 147.95, 146.32, 142.78, 142.44, 137.90, 128.58, 127.89, 125.86, 122.05, 119.20, 108.38, 107.80, 101.60, 49.91, 33.97, 28.25 ppm. **IR** (neat): ν (cm^{-1}) 3055, 2895, 1656, 1502, 1481, 1443, 1240, 1196, 1033, 805, 731, 696. **HRMS** (ESI+, MeOH): m/z calcd. 308.1281 ($\text{M} + \text{H}$)⁺, found: 308.1273.



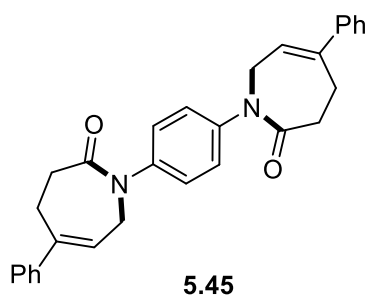
5.43

Scale: 0.20 mmol; *E/Z* = 95:5, isolated 60.8 mg (81% yield), yellow solid, Hexane : EA = 1 : 1, R_f = 0.15. **$^1\text{H NMR}$** (400 MHz, CDCl_3) δ 7.59 – 7.54 (m, 2H), 7.48 (d, J = 0.9 Hz, 1H), 7.40 – 7.28 (m, 6H), 6.19 (tt, J = 6.1, 1.8 Hz, 1H), 4.53 – 4.47 (m, 2H), 4.44 (q, J = 7.1 Hz, 2H), 3.16 – 3.02 (m, 2H), 3.00 – 2.88 (m, 2H), 1.43 (t, J = 7.1 Hz, 3H) ppm. **$^{13}\text{C NMR}$** (101 MHz, CDCl_3) δ 174.21, 159.51, 154.06, 146.80, 143.00, 142.36, 139.92, 128.62, 127.97, 127.56, 126.22, 125.86, 121.94, 120.21, 113.88, 112.99, 61.76, 49.95, 34.00, 28.28, 14.42 ppm. **IR** (neat): ν (cm^{-1}) 3058, 2979, 2908, 1719, 1662, 1563, 1445, 1295, 1205, 1161, 1093, 733, 697. **HRMS** (ESI+, MeOH): m/z calcd. 398.1363 ($\text{M} + \text{Na}$)⁺, found: 398.1363.

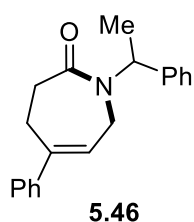


5.44

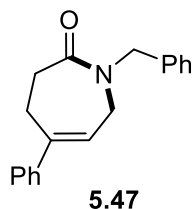
Scale: 0.20 mmol; *E/Z* > 99:1, isolated 44.5 mg (71% yield), yellow solid, Hexane : EA = 2 : 1, R_f = 0.20. **$^1\text{H NMR}$** (500 MHz, CDCl_3) δ 7.78 – 7.70 (m, 3H), 7.63 (d, J = 2.4 Hz, 1H), 7.42 – 7.37 (m, 2H), 7.36 – 7.31 (m, 3H), 7.30 – 7.27 (m, 2H), 7.26 – 7.22 (m, 1H), 6.16 (tt, J = 6.1, 1.8 Hz, 1H), 4.47 (dt, J = 6.1, 2.1 Hz, 2H), 3.07 – 3.02 (m, 2H), 2.93 – 2.86 (m, 2H) ppm. **$^{13}\text{C NMR}$** (126 MHz, CDCl_3) δ 174.02, 142.95, 142.50, 141.37, 133.75, 132.07, 128.92, 128.64, 127.96, 127.77, 126.45, 126.10, 125.92, 124.92, 123.67, 122.18, 49.74, 34.22, 28.38 ppm. **IR** (neat): ν (cm^{-1}) 3055, 2921, 2851, 1661, 1594, 1445, 1415, 1212, 1154, 828, 752, 695. **HRMS** (ESI+, MeOH): m/z calcd. 314.1539 ($\text{M} + \text{H}$)⁺, found: 314.1531.



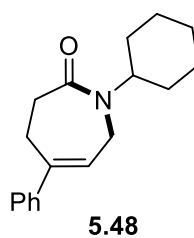
Scale: 0.1 mmol *p*-phenylenediamine, 0.2 mmol vinyl lactone **C**; isolated 31.0 mg (69% yield), yellow solid, DCM : MeOH = 50 : 1, R_f = 0.10. $^1\text{H NMR}$ (400 MHz, CDCl_3) δ 7.39 – 7.27 (m, 14H), 6.15 (tt, J = 6.1, 1.8 Hz, 2H), 4.45 (dt, J = 6.1, 2.1 Hz, 4H), 3.13 – 3.00 (m, 4H), 2.97 – 2.84 (m, 4H) ppm. $^{13}\text{C NMR}$ ((101 MHz, CDCl_3) δ 173.95, 142.88, 142.40, 141.71, 128.61, 127.93, 126.61, 125.90, 122.05, 49.35, 34.09, 28.30 ppm. **IR** (neat): ν (cm^{-1}) 3053, 2930, 2851, 1650, 1507, 1445, 1309, 1214, 855, 740, 691. **HRMS** (ESI+, MeOH): m/z calcd. 449.2224 ($\text{M} + \text{H}$) $^+$, found: 449.2225.



Scale: 0.20 mmol; $E/Z > 99:1$, isolated 32.1 mg (55% yield), yellow solid, Hexane : EA = 2 : 1, R_f = 0.25. $^1\text{H NMR}$ (400 MHz, CDCl_3) δ 7.39 – 7.23 (m, 10H), 6.08 (q, J = 7.0 Hz, 1H), 5.80 (tt, J = 6.0, 1.8 Hz, 1H), 3.74 (dt, J = 6.0, 2.2 Hz, 2H), 3.06 – 2.76 (m, 4H), 1.53 (d, J = 7.0 Hz, 3H) ppm. $^{13}\text{C NMR}$ (101 MHz, CDCl_3) δ 174.09, 142.72, 142.15, 140.86, 128.52, 128.48, 127.66, 127.43, 127.40, 125.87, 123.00, 50.86, 40.43, 33.82, 28.21, 16.59 ppm. **IR** (neat): ν (cm^{-1}) 3028, 2969, 2913, 2878, 1625, 1493, 1453, 1181, 738, 689. **HRMS** (ESI+, MeOH): m/z calcd. 292.1696 ($\text{M} + \text{H}$) $^+$, found: 292.1700.

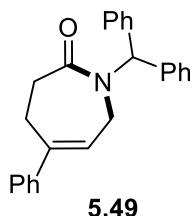


Scale: 0.20 mmol; $E/Z > 99:1$, isolated 26.6 mg (48% yield), yellow solid, Hexane : EA = 2 : 1, R_f = 0.25. $^1\text{H NMR}$ (400 MHz, CDCl_3) δ 7.38 – 7.23 (m, 10H), 5.89 (tt, J = 5.9, 1.8 Hz, 1H), 4.71 (s, 2H), 3.98 (dt, J = 5.9, 2.2 Hz, 2H), 3.04 – 2.94 (m, 2H), 2.89 – 2.81 (m, 2H) ppm. $^{13}\text{C NMR}$ (101 MHz, CDCl_3) δ 174.44, 142.69, 142.35, 137.62, 128.67, 128.47, 127.99, 127.68, 127.48, 125.89, 122.30, 51.09, 45.57, 33.64, 28.20 ppm. **IR** (neat): ν (cm^{-1}) 3050, 2937, 2900, 1634, 1493, 1424, 1257, 1151, 738, 693, 591. **HRMS** (ESI+, MeOH): m/z calcd. 278.1539 ($\text{M} + \text{H}$) $^+$, found: 278.1544.

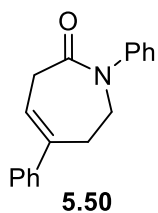


Scale: 0.20 mmol; $E/Z > 99:1$, isolated 19.9 mg (37% yield), yellow solid, Hexane : EA = 2 : 1, R_f = 0.25. $^1\text{H NMR}$ (500 MHz, CDCl_3) δ 7.32 – 7.23 (m, 5H), 6.02 (tt, J = 6.1, 1.9 Hz, 1H), 4.47 (tt, J = 11.8, 3.8 Hz, 1H), 3.91 (dt, J = 6.1, 2.1 Hz, 2H), 2.89 – 2.85 (m, 2H), 2.78 – 2.73 (m, 2H), 1.79 – 1.73 (m, 2H), 1.68 – 1.64 (m, 3H), 1.43 – 1.34 (m, 2H), 1.33 – 1.25 (m, 2H), 1.10 – 1.01 (m, 1H) ppm. $^{13}\text{C NMR}$ (126 MHz, CDCl_3) δ 173.69, 142.75,

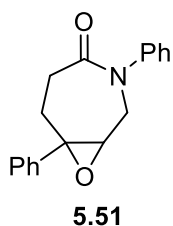
142.48, 128.50, 127.68, 125.81, 123.12, 52.39, 39.67, 33.89, 30.87, 28.25, 25.75, 25.71 ppm. **IR** (neat): ν (cm⁻¹) 2927, 2854, 1625, 1448, 1251, 1184, 1139, 748, 696. **HRMS** (ESI+, MeOH): m/z calcd. 270.1852 (M + H)⁺, found: 270.1855.



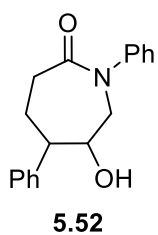
Scale: 0.20 mmol; *E/Z* >99:1, isolated 41.0 mg (58% yield), yellow solid, Hexane : EA = 2 : 1, R_f = 0.15. **¹H NMR** (500 MHz, CDCl₃) δ 7.33 – 7.20 (m, 13H), 7.17 (s, 1H), 7.14 – 7.10 (m, 2H), 5.59 (tt, J = 6.0, 1.8 Hz, 1H), 3.92 (dt, J = 6.0, 2.2 Hz, 2H), 2.99 – 2.92 (m, 2H), 2.83 – 2.75 (m, 2H) ppm. **¹³C NMR** (101 MHz, CDCl₃) δ (126 MHz, CDCl₃) δ 174.62, 142.73, 142.31, 139.70, 128.79, 128.60, 128.46, 127.68, 127.55, 125.97, 122.94, 61.08, 42.76, 33.94, 28.21 ppm. **IR** (neat): ν (cm⁻¹) 3032, 2924, 2850, 1639, 1471, 1445, 1206, 1156, 856, 735, 697. **HRMS** (ESI+, MeOH): m/z calcd. 376.1672 (M + Na)⁺, found: 376.1669.



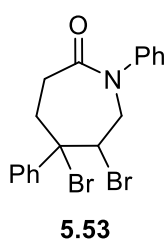
Scale: 0.20 mmol; isolated 40.6 mg (77% yield), light yellow solid, Hexane : EA = 2 : 1, R_f = 0.25. **¹H NMR** (400 MHz, CDCl₃) δ 7.43 – 7.28 (m, 9H), 7.27 – 7.24 (m, 1H), 6.04 (tt, J = 6.2, 1.8 Hz, 1H), 4.16 – 4.10 (m, 2H), 3.59 (dt, J = 6.2, 2.3 Hz, 2H), 2.83 (ddq, J = 8.1, 4.2, 2.2 Hz, 2H) ppm. **¹³C NMR** (126 MHz, CDCl₃) δ 172.40, 142.99, 142.76, 139.56, 129.40, 128.56, 127.63, 126.91, 126.56, 125.93, 118.91, 49.48, 36.83, 32.05 ppm. **IR** (neat): ν (cm⁻¹) 3058, 2947, 2908, 1655, 1593, 1406, 1175, 904, 757, 693. **HRMS** (ESI+, MeOH): m/z calcd. 264.1383 (M + H)⁺, found: 264.1386.



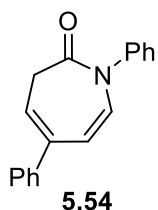
Scale: 0.20 mmol; isolated 47.5 mg (85% yield, >99:1 *dr*), yellow solid, Hexane : EA = 1 : 1, R_f = 0.15. **¹H NMR** (400 MHz, CDCl₃) δ 7.48 – 7.37 (m, 6H), 7.36 – 7.31 (m, 1H), 7.31 – 7.25 (m, 3H), 4.26 (qd, J = 16.4, 5.3 Hz, 2H), 3.33 (td, J = 5.3, 0.8 Hz, 1H), 2.85 – 2.52 (m, 4H) ppm. **¹³C NMR** (101 MHz, CDCl₃) δ 173.62, 143.55, 141.43, 129.38, 128.73, 128.06, 126.99, 126.30, 125.54, 62.87, 61.80, 51.80, 31.93, 28.41 ppm. **IR** (neat): ν (cm⁻¹) 3072, 2956, 2917, 1649, 1595, 1495, 1447, 1408, 1233, 1179, 978, 750, 693. **HRMS** (ESI+, MeOH): m/z calcd. 280.1332 (M + H)⁺, found: 280.1328.



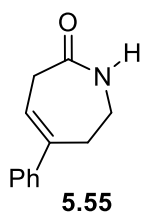
Scale: 0.3 mmol; isolated 77.7 mg (92% yield, >99:1 *dr*), white solid, Hexane : EA = 1 : 2, R_f = 0.15. $^1\text{H NMR}$ (400 MHz, DMSO) δ 7.37 – 7.32 (m, 4H), 7.32 – 7.26 (m, 4H), 7.22 – 7.15 (m, 2H), 4.85 (d, J = 6.8 Hz, 1H), 4.19 (d, J = 15.1 Hz, 1H), 3.90 (t, J = 7.3 Hz, 1H), 3.65 (dd, J = 15.2, 6.7 Hz, 1H), 2.97 – 2.91 (m, 1H), 2.88 – 2.80 (m, 1H), 2.57 – 2.52 (m, 1H), 2.33 – 2.21 (m, 1H), 1.73 – 1.66 (m, 1H) ppm. $^{13}\text{C NMR}$ (101 MHz, DMSO) δ 173.56, 145.70, 144.53, 128.26, 128.11, 127.85, 127.09, 126.00, 125.50, 68.67, 56.63, 51.54, 36.94, 22.16 ppm. **IR** (neat): ν (cm^{-1}) 3208, 2932, 1621, 1591, 1490, 1445, 1416, 1196, 1079, 746, 694. **HRMS** (ESI+, MeOH): m/z calcd. 282.1489 ($\text{M} + \text{H}$)⁺, found: 282.1495.



Scale: 0.20 mmol; isolated 70.2 mg (83% yield, >99:1 *dr*), colorless solid, Hexane : EA = 5 : 1, R_f = 0.10. $^1\text{H NMR}$ (400 MHz, CDCl_3) δ 7.60 – 7.54 (m, 2H), 7.46 – 7.35 (m, 7H), 7.29 – 7.24 (m, 1H), 5.25 (d, J = 15.9 Hz, 1H), 5.10 (dd, J = 5.8, 2.1 Hz, 1H), 4.00 (dd, J = 15.9, 6.1 Hz, 1H), 3.55 – 3.46 (m, 1H), 3.09 – 2.86 (m, 2H), 2.81 – 2.68 (m, 1H) ppm. $^{13}\text{C NMR}$ (101 MHz, CDCl_3) δ 173.69, 144.44, 144.04, 129.10, 128.86, 128.70, 127.17, 126.88, 126.50, 74.58, 58.90, 53.30, 35.03, 30.40 ppm. **IR** (neat): ν (cm^{-1}) 3061, 2922, 1655, 1489, 1430, 1245, 965, 754, 699. **HRMS** (ESI+, MeOH): m/z calcd. 421.9750 ($\text{M} + \text{H}$)⁺, found: 421.9755.



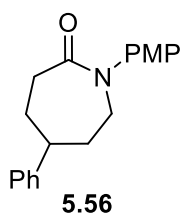
Scale: 0.20 mmol; isolated 29.3 mg (56% yield), colorless oil, Hexane : EA = 10 : 1, R_f = 0.15. $^1\text{H NMR}$ (400 MHz, CDCl_3) δ 7.48 – 7.27 (m, 10H), 6.54 (d, J = 9.0 Hz, 1H), 6.23 (d, J = 9.1 Hz, 1H), 6.06 (t, J = 7.2 Hz, 1H), 3.29 (d, J = 7.2 Hz, 2H) ppm. $^{13}\text{C NMR}$ (101 MHz, CDCl_3) δ 166.60, 141.20, 139.53, 138.90, 132.21, 129.25, 128.70, 128.05, 127.62, 127.02, 126.96, 119.15, 116.36, 38.50 ppm. **IR** (neat): ν (cm^{-1}) 3040, 2925, 1680, 1585, 1492, 1346, 1265, 1166, 760, 729, 692. **HRMS** (ESI+, MeOH): m/z calcd. 262.1226 ($\text{M} + \text{H}$)⁺, found: 262.1225.



Scale: 0.15 mmol; isolated 11.2 mg (40% yield), light yellow solid, DCM : MeOH = 30 : 1, R_f = 0.15. $^1\text{H NMR}$ (400 MHz, CDCl_3) δ 7.35 – 7.25 (m, 5H), 6.46 (s, 1H), 5.97 (tt, J = 5.6, 1.6 Hz, 1H), 3.96 – 3.90 (q, J = 5.5, 3.9 Hz, 2H), 2.86 – 2.76 (m, 4H) ppm. $^{13}\text{C NMR}$ (101 MHz, CDCl_3) δ 176.98, 143.00, 142.30, 128.55, 127.69, 125.97, 122.73, 40.01, 33.17, 27.63 ppm.

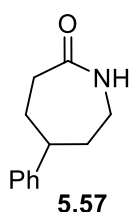
IR (neat): ν (cm⁻¹) 3183, 3042, 2885, 1659, 1491, 1448, 1358, 1164, 817, 743, 698.

HRMS (ESI+, MeOH): m/z calcd. 210.0889 (M + Na)⁺, found: 210.0884.

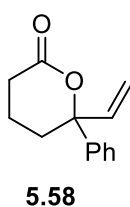


Scale: 0.6 mmol; isolated 159.5 mg (90% yield), yellow solid, Hexane : EA = 3 : 1, R_f = 0.18. **¹H NMR** (400 MHz, CDCl₃) δ 7.36 – 7.30 (m, 2H), 7.26 – 7.20 (m, 3H), 7.20 – 7.13 (m, 2H), 6.96 – 6.88 (m, 2H), 4.02 (dd, J = 15.2, 10.7 Hz, 1H), 3.81 (s, 3H), 3.67 (ddd, J = 15.4, 6.4, 1.7 Hz, 1H), 2.92 – 2.75 (m, 3H), 2.17 – 2.05 (m, 2H), 2.00 – 1.88 (m, 2H) ppm. **¹³C**

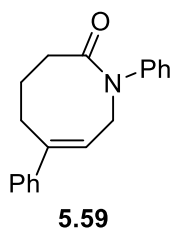
NMR (101 MHz, CDCl₃) δ 175.32, 158.16, 146.14, 137.49, 128.83, 127.43, 126.87, 126.77, 114.63, 55.63, 52.64, 48.37, 37.09, 36.74, 31.05 ppm. **IR** (neat): ν (cm⁻¹) 2931, 2836, 1639, 1603, 1506, 1409, 1242, 1177, 1029, 962, 835, 701. **HRMS** (ESI+, MeOH): m/z calcd. 296.1645 (M + H)⁺, found: 296.1640.



Scale: 0.15 mmol; isolated 21.3 mg (75% yield), yellow solid, DCM : MeOH = 30 : 1, R_f = 0.14. **¹H NMR** (500 MHz, CDCl₃) δ 7.33 – 7.28 (m, 2H), 7.24 – 7.15 (m, 3H), 6.66 (s, 1H), 3.47 – 3.21 (m, 2H), 2.76 (tt, J = 12.1, 3.4 Hz, 1H), 2.67 – 2.53 (m, 2H), 2.05 – 1.96 (m, 2H), 1.85 – 1.69 (m, 2H) ppm. **¹³C** **NMR** (101 MHz, CDCl₃) δ 178.64, 146.46, 128.76, 126.76, 126.65, 48.96, 42.24, 37.48, 35.99, 30.65 ppm.¹⁶²



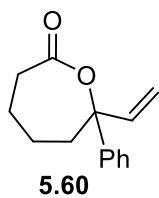
¹H NMR (400 MHz, CDCl₃) δ 7.44 – 7.34 (m, 4H), 7.32 – 7.27 (m, 1H), 6.05 (dd, J = 17.2, 10.7 Hz, 1H), 5.32 (dd, J = 17.2, 0.8 Hz, 1H), 5.24 (dd, J = 10.8, 0.8 Hz, 1H), 2.62 – 2.53 (m, 1H), 2.51 – 2.42 (m, 1H), 2.31 – 2.15 (m, 2H), 1.96 – 1.85 (m, 1H), 1.80 – 1.69 (m, 1H) ppm. **¹³C** **NMR** (126 MHz, CDCl₃) δ 171.12, 142.52, 141.09, 128.73, 127.79, 125.22, 114.90, 86.58, 32.70, 29.45, 16.54 ppm.¹⁵⁰



Scale: 0.20 mmol; isolated 30.0 mg (54% yield), slight yellow solid, Hexane : EA = 2 : 1, R_f = 0.25. **¹H NMR** (400 MHz, CDCl₃) δ 7.42 – 7.33 (m, 6H), 7.31 – 7.23 (m, 4H), 5.98 (t, J = 6.2 Hz, 1H), 4.45 (d, J = 6.2 Hz, 2H), 2.89 – 2.83 (m, 4H), 2.14 – 2.07 (m, 2H) ppm. **¹³C** **NMR** (101 MHz, CDCl₃) δ 174.62, 144.35, 144.13, 143.54, 129.27, 128.55, 127.47, 126.87,

(162) D. Kong, M. Li, G. Zi, G. Hou, *Org. Biomol. Chem.* **2016**, *14*, 4046.

126.62, 126.12, 125.43, 52.38, 36.07, 30.68, 26.37 ppm. **IR** (neat): ν (cm^{-1}) 2924, 2856, 1648, 1594, 1491, 1445, 1402, 1199, 1153, 911, 756, 694. **HRMS** (ESI+, MeOH): m/z calcd. 300.1359 ($M + \text{Na}$)⁺, found: 300.1347.

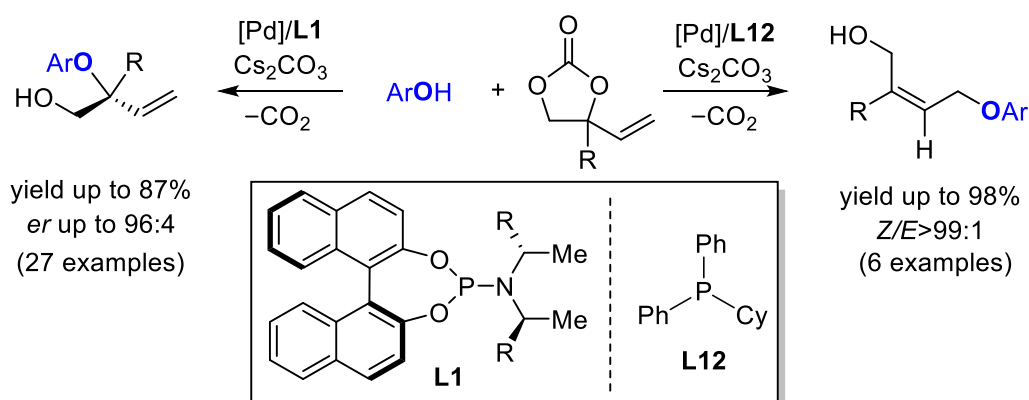


¹H NMR (400 MHz, CDCl_3) δ 7.41 – 7.33 (m, 4H), 7.31 – 7.27 (m, 1H), 6.03 (dd, $J = 17.3, 10.6$ Hz, 1H), 5.15 – 5.08 (m, 2H), 2.67 – 2.54 (m, 2H), 2.25 – 2.13 (m, 2H), 1.95 – 1.81 (m, 2H), 1.76 – 1.58 (m, 2H) ppm. **¹³C NMR** (101 MHz, CDCl_3) δ 175.25, 143.31, 141.81, 129.01, 127.63, 125.95, 114.03, 85.94, 38.24, 37.13, 24.57, 23.14 ppm. **IR** (neat): ν (cm^{-1}) 3059, 2937, 2864, 1720, 1447, 1332, 1281, 1245, 1167, 997, 926, 759, 702, 680, 571. **HRMS** (ESI+, MeOH): m/z calcd. 239.1043 ($M + \text{Na}$)⁺, found: 239.1036.

Summary and General Conclusions

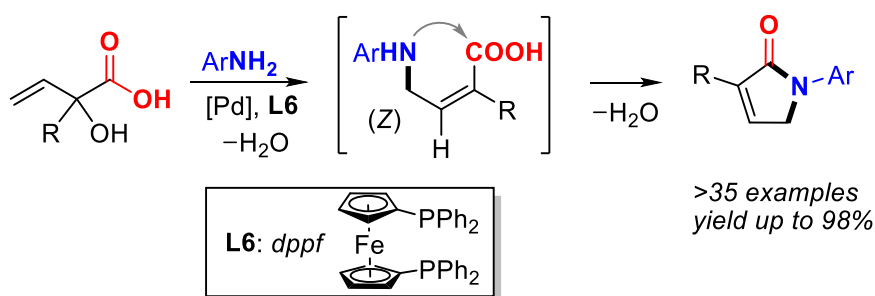
To conclude this doctoral dissertation, it is crucial to compare the initial hypotheses and the actual achievements. In line with the ongoing interest of Kleij group at ICIQ (Tarragona), this doctoral thesis initially aimed at the synthesis of challenging and valuable (heterocyclic) products by taking advantage of Pd-catalyzed stereo-controlled allylic substitution reactions. The key to the success achieved in the studied transformations has been a combination of a proper substrate design, reaction routes and rational ligand engineering, as this allowed for a high control over the chemo-, regio-, stereo-, and/or enantio-selectivity features of the involved conversions. In this regard, three types of allylic precursors (VCCs, carboxy-functionalized tertiary allylic alcohols and vinyl γ -lactones) with a different steric and electronic bias were examined/introduced, offering a tangible and modular way for target-oriented synthesis.

Based on the potential of VCCs in fine-chemical synthesis and “allylic chemistry” as explained in chapter 1, the work in the second chapter illustrates that Pd-catalyzed allylic substitution reactions provide a productive way for the asymmetric construction of sterically congested quaternary stereocenters, and more specifically for enantioenriched tertiary allylic aryl ethers using phenolic nucleophiles. By a judicious selection of the ancillary ligand, both regio- and enantio-control could be simultaneously exerted. Switching from a phosphoramidite to a mono-phosphine ligand, a complete inversion of the regio-selectivity was observed. Thus, proper ligand engineering effects were demonstrated in this allylic substitution process, providing potential for the construction of other types of sterically congested quaternary stereocenters.

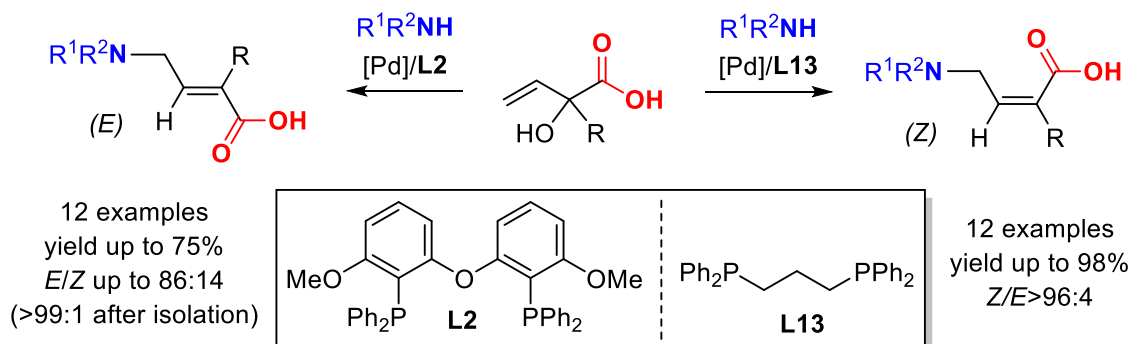


Inspired by previous work in our group concerning stereoselective allylic substitution reactions using VCCs as allylic surrogates, the work described in chapter 3 focused on the rapid construction of heterocyclic compounds by making use of a stereoselective allylic substitution step being part of a tandem process. Although allylic amination has been widely studied for C–N bond formation in natural product synthesis, its use as a key step in (unsaturated) lactam synthesis still remained unexplored.

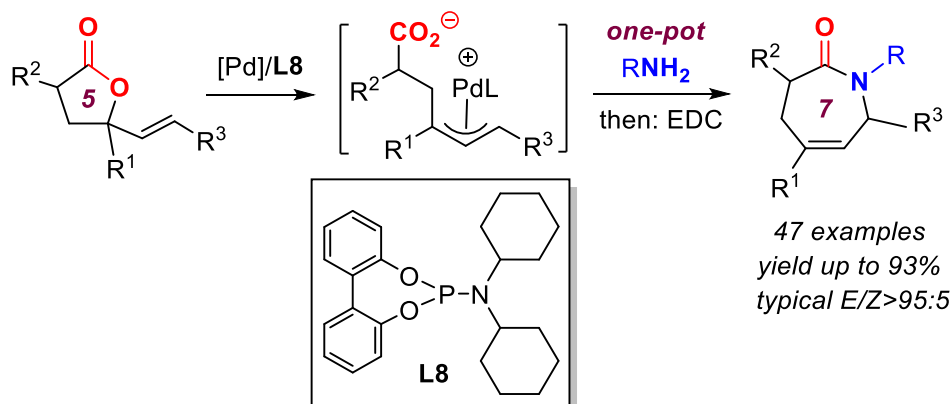
In this context, the formation of unsaturated amino acid intermediates with a defined double bond configuration was investigated by Pd-catalyzed stereoselective allylic amination of tertiary allylic alcohols functionalized with a –COOH group in the presence of primary amines, allowing the preparation of unsaturated lactam products in a formal domino process under ambient conditions. The *in situ* formed *Z*-configured γ -amino acid intermediate cyclizes to afford an α,β -unsaturated γ -lactam, releasing water as the only byproduct. Moreover, mechanistic studies suggested that the carboxyl group is crucial for this transformation, and acts both as an activating and stereodirecting functional group.



Considering the potentially isomerizable nature of the Pd(allyl) intermediate generated from our newly developed tertiary allylic alcohol substrate and Pd precursor, we decided to investigate the potential stereodivergent allylic amination in the presence of secondary amines. As described in chapter 4, the key to the observed stereochemical course was the presence of a suitable diphosphine ligand, allowing for selective formation of the *Z*- or *E*-configured α,β -unsaturated γ -amino acids. The experimental results highlight the crucial role of the supporting ligand and the diphosphine bite angle, which may influence the chelation mode of the ligand and the relative kinetics of the interconversion of the *syn* and *anti* Pd(allyl) intermediates versus the amination step.



Following this work on the successful use of VCCs, we designed a conceptually novel protocol involving a stereoselective amination/cyclization cascade process for the preparation of a series of unsaturated caprolactam derivatives derived from vinyl lactones as heterocyclic precursors. In the presence of a newly developed phosphoramidite ligand (**L8**), a highly stereocontrolled ring-opening/allylic amination manifold was achieved using vinyl γ -lactones as modular substrates under ambient conditions. The requisite cyclization step occurred readily in the presence of a suitable dehydrating agent and gave access to a series of caprolactams in an efficient one-pot, two-step sequence. Combined with the work focusing on unsaturated γ -lactam synthesis, the key to the high efficiency of our strategy is the chemo-, stereo- and regio-selective allylic amination step by a judicious choice of substrate, ligand and optimized reaction conditions. Such a platform provides a practical, catalytic domino process enabled by the “allylic substitution” step streamlining the rapid construction of larger or more complicated heterocycles. This allows for great potential in drug-development processes and the creation of new polyamide monomers.



Concluding this thesis, the overall results are consistent with our initial hypothesis that novel, multistep methodologies based on “stereoselective allylic substitution” can indeed allow for challenging small molecule synthesis. We have succeeded in Pd-catalyzed enantio-, stereo- and regio-selective allylic substitution protocols while creating new C–O and C–N bonds, which consequently has given access to important *N*-heterocycles such as functionalized (capro)lactams.

Three types of substrates and a series of ligands (>60) have been involved in this doctoral thesis, which demonstrates the importance of substrate design and ligand engineering for the success of cascade transformations. Therefore, the developed strategies in this thesis may provide great potential and impetus for the use of stereoselective allylic substitution as an integrated tool in the creation of (small) molecules with increased molecular complexity.



UNIVERSITAT
ROVIRA i VIRGILI



Institut
Català
d'Investigació
Química